Effects of maternal body weight on Wharton's Jelly mesenchymal stromal cells (Pilot study)

Badraiq, Heba Ghazi O

Awarding institution:
King's College London

Effects of Maternal Body Weight on Wharton's Jelly Mesenchymal Stromal Cells (Pilot Study)

Heba Ghazi Badraiq

Faculty of Life Science and Medicine

Division of Women's Health

King's College London

(2017)

Thesis is submitted for the degree of Doctor of Philosophy

Declaration

I, *Heba Ghazi Badraiq*, declare that this PhD thesis contains no material that has been submitted previously, in whole or in part, for the award of any other academic degree. Where information has been derived from other sources, I confirm that this has been indicated in the thesis.
The work presented in this PhD thesis is my own except for the following:

- Part of the statistical analysis was performed by the statistician Khadija Rantell.
- RT-PCR was performed by Dr. Aleksandra Cvoro.
- Western blotting was performed by Dr. Dusko Ilic.

When any experimental work was outsourced, the details are provided in the thesis text.

Publications

1- Isolation and expansion of mesenchymal stromal/stem cells from umbilical cord under chemically defined conditions. **Badraiq H**, Devito L, Ilic D. Methods Molecular Biology. 2015;1283:65-71.

2- Wharton's jelly mesenchymal stromal/stem cells derived under chemically defined animal product-free low oxygen conditions are rich in MSCA-1(+) subpopulation. Devito L, **Badraiq H**, Galleu A, Taheem D, Codognotto S, Siow R, Khalaf Y, Briley A, Shennan A, Poston L, McGrath J, Gentleman E, Dazzi F, Ilic D. Regenerative Medecine. 2014;9(6):723-32.

3- Induced pluripotent stem cell differentiation and three-dimensional tissue formation attenuate clonal epigenetic differences in trichohyalin. Petrova A, Capalbo A, Jacquet L, Hazelwood-Smith S, Dafou D, Hobbs C, Arno M, Farcomeni A, Devito L, **Badraiq H**, Simpson M, McGrath JA, Di WL, Cheng JB, Mauro TM, Ilic D. Stem Cell Development 2016 September15;25(18):1366-75.

4- Effects of maternal obesity on Wharton's jelly mesenchymal stromal cells. **Badraiq H**, Cvoro A, Galleu A, Simon M, Miere C, Hobbs C, Schulz R, Siow R, Dazzi F, Ilic D. Scientific Reports – **UNDER REVIEW**.

Acknowledgment

It has been a great honor to have had the opportunity to study a PhD at King's College London, in particular the Division of Women's Health. This PhD journey would not have been achieved without the support of a number of members and divisions.

Firstly, I would like to express a deep gratitude to the Saudi Arabian Cultural Bureau in London for their continuous guidance and support throughout my scholarship, from the early beginning to the late end. Special thanks go to Dr. Ghazi Makki, Ibrahim Al-Trairi, Amel Trabelsi and Dr. Faisal Aba Al-Khail.

Similarly, a deep gratitude to my supervisors: Dr. Dusko Ilic, who introduced me to the world of stem cells and epigenetics and offered me the opportunity to undertake this program and developed as a scientist; Dr. Richard Siow, who developed my lab skills from the beginning, advised and supported until the end of this journey.

Secondly, I would like to express my deepest sense of thankfulness to volunteers who donated their umbilical cords and made this study possible. Also my deepest sense of thankfulness to doctors, midwives, nurses and research assistants of the Division of Women's Health at St. Thomas Hospital. Special thanks go to Hannah Powles, Annette Briley, Prof. Andrew Shennan, Funso Adegoke and Prof. Lucilla Poston.

Furthermore, I would like to acknowledge all members of Biomedical Research Center at Guy's Hospital for their facilities. In Flow Cytometry facility, special thanks go to Dr. Susanne Heck, PJ Chana and Anna Rose. In Genomics facility, special thanks go to Dr. Alka Saxena and Rosamond Nuamah. Also, I thank all members of the Division of Cardiovascular Medicine, especially Dr. Sarah Chapple, and from the Department of Haemato-Oncology at King's College London, Prof. Francesco Dazzi and Dr. Antonio Galleu. Additionally, I would like to thank members at King's College, Dr. Eileen Gentleman and Dheraj Taheem from Department of Craniofacial Development and Stem Cell Biology. Also Dr. Reiner Schulz from Division of Genetics & Molecular Medicine.

In particular I would like to thank Cristian Miere for his support and friendship through the journey. I would like to thank Stefano Codognotto, Dr. Heema Hewitson, Sreekala

Sathyavruthan and Justo Gonzalez for their collegiality and also Ghazala Mirza and Viktoria Husz for their continues support through the journey.

In particular I would like to thank my friend and PhD partner Laila Noli, who made my journey easier and worthwhile since the bachelor degree, and most of all made me feel like having a sister in a country that is not my own. Educational achievement in my life is nothing if I do not have friend with whom to share the highs and lows.

A great deal of my gratitude goes to my dearest mother (Ameera Gazzaz) and father (Ghazi Badraiq) for their prayers, support, belief and encouragement. Also, my siblings nieces and nephew: Ghada, Nouf, Bader, Faris, Essam, Mohammed, Tala, Layan and Omar. Without continuous family support, I would not have been able to make it this far.

A big thank you to my extended family: uncles, aunts and cousins especially, Bodor, Laila, Abeer, Howida, Hattan, Husam, Bassam, Nada and Alaa for their support and care.

Finally, I appreciate all my dear friends: special thanks go to my childhood friend Aseel Khafaji; also, a big thank you to my close friends Abrar Madani, Nouf Nass, Ashjan Zainalabdeen and Nojoud Abokhamees for their extended support.

Most of all I fully appreciate my dear fiancé Alhasan Madani for entirely care, love and constant encouragement and support, for cheering me on and making me smile and laugh through the whole journey. Is so appreciated. Thank you.

Above all, I give glory to Allah for watching me through to completion.

Heba Ghazi Badraiq

December 2016

Table of Contents

Abstract

To investigate whether the maternal metabolic environment affects the DNA methylation of mesenchymal stromal/stem cells (MSCs) from umbilical cord (UC) Wharton's Jelly (WJ), potentially rendering them unsuitable for clinical use in multiple recipients, a pilot study was conducted on fourteen UCs obtained *post partum* from healthy non-obese (BMI=19-25; n=7) and obese (BMI≥30; n=7) donors receiving elective Caesarean sections.

The time of first WJ-MSCs outgrowth from UC explants was similar in samples from obese and non-obese donors. However, the cells from non-obese donors proliferated faster after 34 hours of culture than cells from obese donors. Differentiation into adipogenic, osteogenic and chondrogenic lineages was similar between obese and non-obese donor samples as demonstrated by tissue-specific staining and RT-PCR for lineage markers. However, WJ-MSCs from obese donors exhibited stronger immunosuppressive activity than those from non-obese donors.

Genome-wide DNA methylation of triple-positive (CD73+CD90+CD105+) WJ-MSCs sorted from the first passage of a mixed population of cells was assessed. Samples from the obese and non-obese donors clustered separately, and 5,767 of the analysed CpG sites (1%) exhibited different methylation. Sixty-seven genes were observed with at least one CpG site with a methylation difference ≥0.2 in four or more obese donors. These 67 genes were further refined based on a list of polymorphic CpG sites and segmental duplications. In 18 of the 67 genes with a different CpG methylation pattern, the CpG sites were in non-polymorphic regions. However, two genes (*DCAF6* and

ZNF714) resided in segmentally duplicated regions.

To determine whether methylation differences altered gene expression, the samples were analysed using a HumanHT-12 Expression BeadChip array and, of the 18 genes, only *PNPLA7* was significantly affected at the mRNA level, which was confirmed independently by RT-PCR and Western blotting.

Although the number of analysed donors was limited, the data suggest that an abnormal metabolic environment related to excessive body weight might alter the properties of WJ-MSCs used for cellular therapy.

Abbreviation

APC	allophycocyanin
BM	bone marrow
BMI	body mass index
bp	base pair
BRC	biomedical research centre
CD	cluster of differentiation
CFU-F	colony forming unit fibroblast
CNV	copy number variation
CpG	cytosin-phosphate-guanin site
DMEM	dulbecco's modified eagle's medium
DNA	deoxyribonucleic acid
DNMT	DNA methyltransferase
DNP	dinitrophenyl
ECM	extracellular matrix
ESC	embryonic stem cell
FACS	fluorescence-activated cell-sorting technique
FBS	fetal bovine serum
FITC	fluorescein isothiocyanate
FSC	forward scatter
GAG	glycosaminoglycan
gDNA	genomic DNA
GDM	gestational diabetes mellitus
GO	Gene Ontology
GVHD	graft-versus-host disease
HIV	human immunodeficiency virus
HLA	human leukocyte antigen
HSC	hematopoietic stem cell

IFN	interferon
IL	interleukin
ISCT	international society for cellular therapy
KEGG	kyoto encyclopedia of genes and genomes
LPA	lysophosphatidic acid
miRNA	microRNA
mRNA	messenger RNA
MSC	mesenchymal stromal/stem cell
NHS	national health service
NK	natural killer
PBMC	peripheral blood mononuclear cell
PBS	phosphate buffered saline
PBS-EDTA	PBS-ethylenediamine tetraacetic acid
PCR	polymerase chain reaction
PD	population doubling
PE	phycoerythrin
PHA	phytohaemagglutinin
RIN	RNA integrity number
RNA	ribonucleic acid
RNAi	RNA interference
RT-PCR	real-time polymerase chain reaction
SGA	small for gestational age
siRNA	small interfering RNA
SNP	single nucleotide polymorphism
SSC	side scatter
TNF	tumour necrosis factor
UC	umbilical cord
WHO	world health organization
WJ	wharton's jelly
1st exon	exon 1

3’UTR	3'-untranslated region
5'UTR	5'-untranslated region

Chapter 1

Introduction

1. Introduction

1.1 Mesenchymal Stromal/Stem Cells (MSCs)

Over the last few decades, researchers have taken a significant interest in understanding mesenchymal stem cells (MSCs). Their stem-like properties, including their ability to proliferate *in vitro* for many passages without displaying any senescence characteristics while remaining stable and undifferentiated, their differentiation potential under certain conditions, and their capability to commit to multiple lineages, have been a major focus of studies investigating therapies for tissue repair and regeneration (El Omar *et al.*, 2014; Wang *et al.*, 2008). More recently, researchers have identified additional properties of MSCs that have furthered the understanding of their involvement in tissue regeneration; their secretion of immunomodulatory and cytoprotective factors has been shown to beneficially contribute to the tissue regeneration process (Squillaro *et al.*, 2015).

In addition to such properties, other benefits of MSCs have received global attention, and many new investigators are extensively studying MSCs in the context of developing novel and effective cell-based therapeutic applications (Baksh *et al.*, 2004). The growing number of research studies is increasing the pace of advances in pre-clinical research; valuable findings have been reported from clinical trials of treatments for various diseases (Dominici *et al.*, 2006; Squillaro *et al.*, 2015). However, the outcomes from the ever-increasing number of publications are somewhat inconsistent; therefore, it is necessary for laboratories to adopt tighter standardization procedures to ensure that ambiguities are absent from publications (Dominici *et al.*, 2006). Other

remarkable attributes of MSCs that make them notable candidates for cell-based therapeutics include their ease of collection, safe use, and minimal associated ethical concerns (Ullah *et al.*, 2015).

MSCs are also known as mesenchymal stromal cells (MSCs); they have the potential to differentiate into multiple lineages and, therefore, are multipotent (Ilic & Polak, 2011). Although MSCs are often referred to as stem cells, the only attribute of stem cells they possess is the capacity for self-renewal, meaning that they maintain their identity after many cell divisions. However, they are not capable of giving rise to any type of cell found in the human body, unlike pluripotent stem cells (Nombela-Arrieta *et al.*, 2011). Thus, strictly speaking, MSCs do not fulfil the criteria of true stem cells. The term 'mesenchymal stem cell' has caused many disagreements as a result of these defining criteria of stem cells (Dominici *et al.*, 2006). The Greek word 'stroma' translates as 'bed', which anatomically refers to supportive tissue comprising connective tissue, endothelium and blood vessels; stroma is indicative of a structure, an organ or a gland that is distinct from the functional elements of an organ (Spraycar, 1995). Stromal cells are part of the stromal fraction that provides a physical support structure, which is mainly composed of collagen and adherent cells, such as fibroblastic, vascular and immune cells (Troyer & Weiss, 2008). Furthermore, stroma and stromal cells release signals and cues, such as growth factors and chemokines, which drive the maturation and differentiation of haematopoietic cells (Baksh *et al.*, 2004).

1.1.1 History of MSCs

In 1867, Cohnheim, a German biologist, was the first to discuss the presence of regenerative cells in the human body; he hypothesized that bone marrow (BM)-derived

fibroblasts were involved in wound healing (Cohnheim, 1867; Murray & Peault, 2015). Approximately a century later, Alexander Friedenstein discovered the presence of MSCs in BM. He also described a procedure to isolate them using plastic adherence in which extracted cells are plated at a low density and BM-MSCs rapidly adhere to the plate. By repeatedly washing the cells, BM-MSCs are easily separated from non-adherent cells, such as haematopoietic cells. Under favourable culture conditions, distinct colonies emerge from the BM, and each colony can be derived from a single precursor cell known as the colony-forming unit fibroblast (CFU-F) (Bianco *et al.*, 2001; Friedenstein *et al.*, 1974; Friedenstein *et al.*, 1976; Friedenstein *et al.*, 1966; Murphy *et al.*, 2013). In the 1980s, Friedenstein, Owen, and their colleagues utilized *in vitro* culture and transplantation in laboratory animals in either closed systems (diffusion chambers) or open systems (under the renal capsule or subcutaneously), to characterize the cells generating the physical stroma of BM (Bianco *et al.*, 2001; Friedenstein *et al.*, 1970; Friedenstein *et al.*, 1966; Owen, 1988). Long-term BM cultures were found to yield BM-MSCs; in addition, the cultures also exhibited osteogenic differentiation characteristics, specifically the ability to form bone, fat, cartilage and muscle cells *in vitro* as well as the capacity to regenerate ectopic bone, stroma and haematopoietic tissue *in vivo* upon re-transplantation (Murphy *et al.*, 2013; Murray & Peault, 2015). These properties are the hallmarks of this cell type and have been validated and undisputed from their first identification. Further characterization revealed that BM-MSCs were capable of differentiating into other cell populations of mesodermal origin, such as ligaments and tendons (Young *et al.*, 1998), cardiomyocytes (Makino *et al.*, 1999) and muscle (Wakitani *et al.*, 1995). Additionally, during the 1980s, Arnold Caplan proposed the mesengenic process as an adult marrow pathway that contains multipotent progenitor cells, in which MSCs differentiate into several mesodermal cell types that can differentiate along many lineages to

generate the end-stage differentiated cells that fabricate and maintain mature mesenchymal tissue (Caplan & Correa, 2011).

Later, in the 1990s, Caplan identified the first surface antigens expressed by MSCs, cluster of differentiation (CD)73 and CD105. He also showed an association between the differentiation characteristics of MSCs and the embryonic development of various mesenchymal tissues, leading him to coin the term 'mesenchymal stem cell' to describe MSCs (Caplan, 1991; Murphy *et al.*, 2013; Murray & Peault, 2015).

In the 21st century, many studies have shown that the differentiation potential of MSCs is not limited to tissues of mesodermal origin, and studies have been designed to determine whether MSCs can differentiate into progeny from other embryonic germ layers, i.e., to differentiate into ectodermal, mesodermal and endodermal lineage tissue types (Kobolak *et al.*, 2015). One study, designed by Munoz-Elias *et al.* (2004), showed that MSCs differentiated *in vitro* into presumptive neurons, which are cells of ectodermal origin. Moreover, they demonstrated that adult MSCs transplanted into embryonic rat brain *in vivo* exhibited a plastic ability to respond specifically to different microenvironments by expressing gene products and cell morphologies in a regionally and temporally specific manner. Other studies reported that MSCs can break the germ layer commitment and can differentiate into a wide range of ectodermal and endodermal tissue type lineages, including skin cells (Nakagawa *et al.*, 2005), lung cells (Ortiz *et al.*, 2003; Sato *et al.*, 2005), and hepatocytes and pancreatic islet cells (Schwartz *et al.*, 2002; Tang *et al.*, 2004). Although MSCs can develop into a broad range of cells, they are not considered true stem cells; however, they are functionally defined as non-haematopoietic, multipotent cells of 'mesenchymal' origin (Caplan, 2007; Kobolak *et al.*, 2015).

In 2008, Crisan *et al.* (2008) identified perivascular cells, principally pericytes, in multiple human organs. Caplan further established that all MSCs are derived from perivascular cells, and by cell sorting for pericytes (CD146, CD34, CD45 and CD56), he revealed that MSCs can be isolated from every vascularized tissue of the body (Caplan, 2008). He also hypothesized that MSCs are activated by the local micro-environment and react by secreting two sets of bioactive molecules. First, as the front of the MSCs enter the injury field, molecules inhibit interrogating immune cells from entering (the first line of defence against the establishment of autoimmune reactions). Second, at the rear of locally activated MSCs, another complex set of factors is secreted and helped establish a regenerative microenvironment. The functions of MSCs led Caplan to redefine the MSC as a medicinal signalling cell that functions as a drug store at the site of tissue injury or inflammation (Caplan, 2015). He suggested that a range of variables must be optimized before MSC-based therapy can be considered for cellular medicine (Caplan & Hariri, 2015).

1.1.2 Main criteria provided by the International Society for Cellular Therapy to define MSCs

The rapidly expanding collection of information and published data on MSCs highlighted the need to unify the definition of the basic characteristics of MSCs. Within the literature, the acronym MSC has been used to represent many cell types, including BM stromal cells, mesenchymal stem cells, and multipotent mesenchymal stromal cells, and this has resulted in confusion (Troyer & Weiss, 2008).

The International Society for Cellular Therapy (ISCT) distinguishes mesenchymal stromal cells from mesenchymal stem cells via *in vivo* characterization. For example,

after cell engraftment, the cell behaviour is monitored, and they are identified as mesenchymal stem cells if they self-renew and exhibit multipotent differentiation. Unfortunately, the surface markers that enable stem cells to be selected with certainty in BM isolates can be difficult to identify (Troyer & Weiss, 2008). Currently, neither a single definition nor a quantitative assay to help improve the identification of MSCs in mixed cell populations exists (Horwitz *et al.*, 2005; Ullah *et al.*, 2015). Moreover, these stem cells do not have well-defined growth conditions, such as low-glucose Dulbecco's modified Eagle's medium (DMEM) containing relatively high concentrations of foetal bovine serum (FBS) (10–20%); commercially available lots of FBS are variable, and this variability can affect the ability to maintain MSCs. Other complexities of differentiating MSCs arise from differences between individual donors, such as donor age; additional challenges include any changes in potency or phenotype occurring during *in vitro* expansion and limited MSC capability of expanding *in vitro* (Troyer & Weiss, 2008).

In 2006, the ISCT declared minimal criteria for defining MSCs. The ISCT proposed the following identification criteria as a basis for additional characterization of these cells by investigators. First, MSCs must be plastic-adherent when maintained in standard culture conditions (i.e., α minimal essential medium plus 20% FBS). Second, ≥95% of the MSC population must express CD105, CD73, and CD90, and MSCs must not express (≤2% positive) the haematopoietic stem cell (HSC) markers CD45, CD34, CD14, CD11b, CD79α or CD19 or human leukocyte antigen D-related (HLA-DR) surface molecules. Third, MSCs must have the ability to differentiate into osteoblasts, adipocytes, and chondroblasts *in vitro* (Dominici *et al.*, 2006; Kobolak *et al.*, 2015). These listed characteristics are valid for nearly all MSCs, although minor variations exist in MSCs that are isolated from different tissue origins (Ullah *et al.*, 2015).

However, since these criteria were published, several reports have suggested that

MSCs reside in almost all organs and are located specifically within the connective tissue of organs. Furthermore, in addition to isolating these cells by taking advantage of their adhesive feature, they can now be isolated using cell surface markers that known to be specific to the MSC phenotype (Kobolak *et al.*, 2015). Dominic and colleagues (2006) used immunological methods to elucidate MSC surface antigen expression. Their results formed the identification criteria for MSCs: the expressed cell surface markers should include CD105 (known as endoglin and originally recognized by the MAb (monoclonal antibody) SH2), CD73 (known as ecto-5'-nucleotidase and previously recognized by the MAb SH3 and SH4) and CD90 (also known as Thy-1). These researchers recognized that these criteria can be modified if novel surface markers are identified in the future. Moreover, because the basic criteria state that MSCs should not express haematopoietic antigens, they proposed that investigators should include a panel of antigens to exclude those cells most likely to be found in MSC cultures and then select those markers that work reliably in their laboratory for their characterization. Cells of haematopoietic origin, namely, macrophages and monocytes, are the most likely haematopoietic cells to be found in an MSC culture, and they express CD14 and CD11b prominently. CD45 is a pan-leukocyte marker, CD34 is a marker of primitive haematopoietic progenitors and endothelial cells, CD79α and CD19 are markers of B cells that may also adhere to MSCs in culture and remain vital through stromal interactions. HLA-DR molecules are only expressed on MSCs after the cells are stimulated by factors such as interferon gamma (IFN-γ).

1.1.3 Tissue sources of MSCs

Although the name for these stem cells (mesenchymal or multipotent stem cells) is still debated, there is a consensus describing them as MSCs (Kalaszczynska & Ferdyn,

2015). MSCs have been identified and successfully isolated from almost all tissue sources, both foetal and adult. The efficient isolation of MSC populations has mainly been reported from BM (Campagnoli *et al.*, 2001; Pittenger *et al.*, 1999). MSC populations have also been isolated from other tissues, including adipose (Wagner *et al.*, 2005; Zhang *et al.*, 2006; Zuk *et al.*, 2001), lung (Fan *et al.*, 2005; Hennrick *et al.*, 2007), heart (Chong *et al.*, 2011), and liver tissues (Campagnoli *et al.*, 2001); Wharton's Jelly (WJ) (Erices *et al.*, 2000; Hou *et al.*, 2009; Wang *et al.*, 2004); synovium (De Bari *et al.*, 2001); the placenta (Fukuchi *et al.*, 2004); amniotic fluid (In 't Anker *et al.*, 2003; Tsai *et al.*, 2004); foetal blood (Noort *et al.*, 2002); limb buds (Jiao *et al.*, 2012); endometrium (Cho *et al.*, 2004; Schuring *et al.*, 2011); menstrual blood (Allickson *et al.*, 2011); peripheral blood (Ab Kadir *et al.*, 2012; Kassis *et al.*, 2006); dental pulp (Gronthos *et al.*, 2000); salivary glands (Rotter *et al.*, 2008); corneal stroma (Branch *et al.*, 2012); skin and foreskin (Bartsch *et al.*, 2005; Riekstina *et al.*, 2008); skeletal muscle (Williams *et al.*, 1999); and perivascular areas (Kuznetsov *et al.*, 2001). Researchers have obtained MSCs from multiple tissues, and the main tissue sources exhibit properties that are either beneficial or disadvantageous in terms of multipotent properties (Table 1).

Table 1. Advantages and disadvantages of common MSC sources			
MSC source	**Advantages**	**Disadvantages**	**References**
BM	- Most studied and utilized	- Difficult to procure - Lack of suitable donors - Proliferation rate related to donor age - Invasive	(Nemeth & Mezey, 2015)
Adipose tissue	- Relatively accessible in the patient subpopulation	- Invasive - Requires digestive enzymes	(Chavez-Munoz *et al.*, 2013) (Toyserkani *et al.*, 2015)
UC	- Easy accessibility (clinical waste) - Non-invasive - Easy to isolate	- Explant or digestive enzymes needed - Heterogeneous population	(Kern *et al.*, 2006) (Pytlík, 2011) (Troyer & Weiss, 2008)
Placenta	- Easy accessibility (clinical waste) - Non-invasive	- Requires digestive enzymes - Heterogeneous population - Difficult to isolate	(Barlow *et al.*, 2008) (Brooke *et al.*, 2009)

1.1.4 Adult versus foetal MSCs

The successful therapeutic application of stem cells depends on the success of stem cell extraction and expansion, as well as their immunosuppressive properties. Some investigators have harvested human MSCs from foetal BM as well as adult BM, and they observed many behavioural differences between the foetal and adult MSCs. *In vitro*, foetal MSCs show greater expansion capacity, with no loss of phenotypic characteristics and faster doubling time than that of adult MSCs; these observed differences have been suggested to be due to the chromosomes in foetal MSCs having longer telomeres than the chromosomes of adult MSCs (Campagnoli *et al.*, 2001; Guillot *et al.*, 2007; Troyer & Weiss, 2008). The observed capabilities of foetal MSCs may result from their youth and lack of maturity; foetal MSCs have a different physiology that is likely due to their naive status (Gotherstrom *et al.*, 2005; Weiss &

Troyer, 2006). Adult MSCs exhibit immunosuppressive properties that do not seem to exist in foetal MSCs (Gotherstrom *et al.*, 2003; Troyer & Weiss, 2008). Moreover, they express class II human leukocyte antigen (HLA), which is absent in foetal MSCs (Gotherstrom *et al.*, 2005; Troyer & Weiss, 2008). Likewise, foetal MSCs appear to synthesize human leukocyte antigen G (HLA-G), which is absent in adult MSCs. HLA-G is a ligand for inhibitory receptors on natural killer (NK) cells and lymphocytes; it has been suggested to act as an immunosuppressor during pregnancy. Despite some differences in the expression profiles of these cell types, neither foetal nor adult MSCs appear to be innately immunogenic as they are not recognized by lymphocytes (Gotherstrom *et al.*, 2005). Furthermore, comparisons of the cytokine profiles of both MSC types have shown some differences. Similar observations have been reported regarding umbilical cord (UC) blood and adult peripheral blood (Troyer & Weiss, 2008).

1.2 MSC clinical trials

1.2.1 MSC biological properties to support clinical trials

The first-ever clinical trial using culture-expanded MSCs from BM was conducted by Dr. Hilary Lazarus in 1995; 15 patients who presented with haematologic cancer became the recipients of the therapy (Lazarus, 1995). Since then, several clinical trials have been conducted with over 2,000 patients to determine the feasibility and efficacy of using either autologous or allogeneic MSCs to treat various congenital and acquired diseases, including graft-versus-host disease (GVHD) (Squillaro *et al.*, 2015).

The effectiveness of MSCs for treating acute GVHD has been shown by Le Blanc and colleagues (2004) via the first transplantation of haploidentical MSCs in a 9-year-old child receiving treatment for therapy-resistant grade IV acute GVHD of the gut and liver. After 1 year, a remarkable clinical response without any complications was observed. Another example of an MSC-based application for the treatment of acute leukaemia was reported by Lee and colleagues (2002), who described a 20-year-old patient with myelogenous leukaemia; this patient received an allogenic HSC and MSC transplantation from the haploidentical father. The cells engrafted rapidly, and the patient did not exhibit signs of acute GVHD. After 31 months, a haematological response was observed to have occurred, and the patient showed a complete remission of the leukaemia. Recently, Zhao *et al.* (2015) was able to treat 47 patients with refractory acute GVHD; 28 patients out of 47 received the MSC treatment, and the rest were infused with saline. The overall response rate to the treatment was 75% in the MSC group and 42.1% in the non-MSC group. The authors concluded that the incidence and severity of chronic GVHD might be reduced via MSC-based treatment in acute GVHD patients.

MSCs have been shown to be promising candidates for the treatment of many types of immunological and non-immunological disorders. Several models implementing the beneficial properties of MSCs have arisen (Squillaro *et al.*, 2015; Wei *et al.*, 2013); specifically, such properties include their ability to i) differentiate, ii) secrete factors important for cell survival and proliferation, iii) modulate immune response, and iv) migrate to injury sites. These four aspects are combined and overlapped, and their exact roles in the therapeutic effects of MSCs have not yet been clearly defined (Wang *et al.*, 2012).

1.2.1.1 Differentiation potential

The multipotent characteristics of MSCs enable them to differentiate into cells of mesenchymal lineages, such as osteoblasts, chondroblasts, adipocytes, myocytes, and tenocytes, both *in vitro* and *in vivo*. MSCs obtained from a range of adult and birth-related tissues exhibit various differentiation characteristics (Table 2). MSCs have also been reported to transdifferentiate into non-mesodermal cell types similar to neuronal cells, hepatocytes, and pancreatic islet-like cell clusters that express insulin and glucagon (Chao *et al.*, 2008; Chen *et al.*, 2004). Furthermore, Kopen and colleagues (1999) were the first to show that MSCs injected into the central nervous system of newborn mice could adopt the morphological and phenotypic characteristics of astrocytes and neurons. These reports suggested that MSCs possess tremendous plasticity and can rapidly alter their phenotype via transdifferentiation, producing cells bearing the features and characteristics of different lineages (Squillaro *et al.*, 2015).

Type equation here.

Table 2. Properties of differentiation for MSCs from different sources.

MSC source	Multi-lineage differentiation ability reported in the literature (osteogenesis, chondrogenesis and adipogenesis)	Differentiation potential
BM-MSCs	Good ability for all three lineages	Charbord *et al.* (2011) described novel factors implicated in osteogenesis and adipogenesis. Johnstone *et al.* (1998) developed a culture system that facilitates the chondrogenic differentiation of postnatal marrow mesenchymal progenitor cells.
Synovial MSCs	Very good ability for all three lineages	Yoshimura *et al.* (2007) found that synovium-derived cells have the highest proliferation rate and chondrogenic potential after passage in rats, and similar results were observed in humans.
Adipose MSCs	Good ability for all three lineages	Heo *et al.* (2016) demonstrated that MSCs derived from BM and adipose tissue shared not only *in vitro* tri-lineage differentiation potential but also gene expression profiles.
Tendon MSCs	Very good ability for osteogenic and chondrogenic lineages	Rui *et al.* (2010) showed that tendon MSCs exhibited higher osteogenic differentiation than BM-MSCs.
Circulating MSCs	Fair ability for osteogenic and adipogenic lineages	Zvaifler *et al.* (2000) showed that circulating blood contains a small population of CD34 mononuclear cells that proliferate and differentiate into several lineages such as osteoblasts and adipocytes.
Placenta MSCs	Varied ability for all three lineages	Jeon *et al.* (2016) placental MSCs have a lower potential to undergo adipogenesis but have a higher potential to undergo osteogenesis than other MSCs.
Heart stromal MSCs	Good ability for all three lineages	Srikanth *et al.* (2013) showed that rat foetal cardiac MSCs, in addition to suitability for cardiovascular regenerative therapy, have the potential to differentiate into cells of all three germ layers.
Amniotic fluid MSCs	Fair ability for all three lineages	Pievani *et al.* (2014) found that amniotic fluid MSCs completely fail to differentiate into cartilage and show that their multipotent capacity is limited to osteogenic differentiation.
Chorionic villi MSCs	Fair ability for all three lineages	Barlow *et al.* (2008) found human placental MSCs derived from placental tissue (including chorion, amnion and desidua basalis) showed the potential for osteogenic and chondrogenic differentiation but were less able to differentiate into adipocyte lineages.

The transdifferentiation and differentiation properties of these cells have sparked innovative ideas for potential clinical applications. Their ability to differentiate into

epithelial-type cells holds much promise for tissue engineering and cellular therapy (Squillaro *et al.*, 2015). For example, Li and colleagues (2010) used the infusion of human adipose-derived MSCs and their transdifferentiation into renal tubular epithelium to recover tissue by repairing damaged cells and maintaining their structural integrity. Others have reported some related challenges; for example, MSCs have been observed to become trapped within the capillaries of lung tissues (Galderisi & Giordano, 2014; Lee *et al.*, 2009; Sohni & Verfaillie, 2013). Other studies have investigated animal models of lung injury that is inflicted by bleomycin exposure; these studies demonstrated that the MSCs engrafted into these lungs either differentiated into type I pneumocytes and type II epithelial cells or they seemed to bear features of all myofibroblasts (Kotton *et al.*, 2001; Ortiz *et al.*, 2003; Rojas *et al.*, 2005).

A significant point to consider is that the evidence of the benefits of MSCs to treat disease have been reported using *in vitro*-based studies; therefore, the assessment and interpretation of these results are limited. With this under consideration, recent studies have adopted *in vivo* approaches for studying many MSC features; aside from MSC differentiation potential, these studies have strived to understand other mechanisms of MSC action that contribute therapeutic effects (Squillaro *et al.*, 2015). In addition, more data have emerged, suggesting that the replacement of damaged cells by MSCs through specific differentiation may be just a small part of the process underlying the therapeutic effects of MSCs (Wang *et al.*, 2012).

1.2.1.2 Bioactive molecule secretion

Many studies have identified key findings that explain the successful use of MSCs for transplantation. These studies suggest that MSCs interact with their environment by secreting many types of active biological factors, such as cytokines, chemokines and

growth factors (Galderisi & Giordano, 2014). In turn, these molecules profoundly affect the dynamics of the local cellular microenvironment. Studies have shown that these biological factors may not only prevent cells in the vicinity from undergoing apoptosis but also stimulate their proliferation, thereby recovering sites of tissue injury. Other researchers have observed in their experiments that regardless of the number of MSCs implanted in injured tissues, the resulting cell numbers were too low to consider them to have significantly contributed to tissue recovery or wound healing (Wang *et al.*, 2011). However, other evidence has demonstrated the contrary, whereby once MSCs were infused into injured tissue, they exerted paracrine effects and interacted with local stimuli, such as inflammatory cytokines, the ligands of Toll-like receptors, and hypoxia. In this way, MSCs were observed to stimulate the cells to exhibit many growth factors that carry out several functions in tissue regeneration (Caplan & Dennis, 2006; Crisostomo *et al.*, 2008). Current knowledge highlights the need not only for comprehensively testing MSCs to ascertain their strategies for modulating their secretion of molecules with greater certainty but also for developing techniques to identify the important factors released by MSCs. Proteins secreted by MSCs include interleukin-6 (IL-6), IL-8, and monocyte chemoattractant protein-1 (MCP-1), which are known for their signalling role in the immune system, as well as transforming growth factor-β (TGF-β), which is known to suppress T-lymphocyte proliferation (Di Nicola *et al.*, 2002). Other important molecules that are secreted and known for their role in remodelling the extracellular matrix (ECM) include metallopeptidase inhibitor-2 (TIMP-2), fibronectin, periostin, collagen, decorin and metalloproteinase inhibitors. Growth factors and their regulators are also released, such as granulocyte-macrophage colony-stimulating factor (GM-CSF), bone morphogenetic protein 2 (BMP2), basic fibroblast growth factor (bFGF), insulin-like growth factor-binding protein 3 (IGFBP3), IGFBP4 and IGFBP7 (Galderisi & Giordano, 2014). The bioactive molecule vascular endothelial growth factor (VEGF) is known to enhance the proliferation of endothelial

cells and smooth muscle cells (Kinnaird *et al.*, 2004). IL-10, IL-1 receptor antagonist and prostaglandin-E2 are known to play anti-inflammatory roles (Foraker *et al.*, 2011; Gupta *et al.*, 2007; Nemeth *et al.*, 2009; Ortiz *et al.*, 2007). The secretory molecule cathelicidin antimicrobial peptide (LL-37) is known to function as an antimicrobial peptide, and it also reduces inflammation (Krasnodembskaya *et al.*, 2010). MSCs are thought to secrete angiopoietin-1 to restore epithelial protein permeability (Fang *et al.*, 2010). Matrix metallopeptidase-3 (MMP3) and MMP9 are known to mediate neovascularization (Kim *et al.*, 2007). In addition, keratinocyte growth factor is known to play a role in alveolar fluid transport (Lee *et al.*, 2009; Wang *et al.*, 2012).

Other studies have reported that the administration of MSC-conditioned medium may support the theory of paracrine effects; components of this conditioned medium may act as chemoattractants for recruiting other cells such as macrophages and endothelial cells to the site of tissue injury, thereby promoting the healing process (Chen *et al.*, 2008). A good example of this paracrine feature of MSCs has been shown by Takashashi and colleagues (2006). MSC-conditioned medium infused into hearts undergoing acute necrosis improved cardiac function by inhibiting the apoptosis of cardiomyocytes and controlled ischaemic injury by increasing capillary density; these effects stemmed directly from the preserved contractile capacity of the myocardium and the stimulated therapeutic angiogenesis of the infarcted heart. Van Poll and colleagues (2008) have reported evidence that MSC-conditioned medium provides trophic support to injured liver tissue by inhibiting hepatocellular death and inducing regeneration, thus enabling new methods for treating fulminant hepatic failure.

1.2.1.3 Immunomodulatory MSC effects

Liechty *et al.* (2000) was the first to recognize the immunomodulatory effects of MSCs upon *in utero* transplantation in sheep. Since then, numerous researchers have demonstrated, in both human and animal models, the ability of MSCs to treat various immune-related disorders (Wei *et al.*, 2013). Unfortunately, the mechanism of MSC immunomodulatory function remains to be elucidated. The most commonly accepted theory for this mechanism of action is based on cell-to-cell interactions and the ability of MSCs to release many immunosuppressive molecules (Squillaro *et al.*, 2015; Wang *et al.*, 2012).

Many studies have demonstrated the ability of MSCs to interact with a variety of immune cells as well as their ability to suppress responses by T cells, B cells, dendritic cells, macrophages and NK cells (Han *et al.*, 2012; Uccelli *et al.*, 2008). Moreover, MSCs have been shown to induce and regulate the capability of regulatory T cells, which are thought to expand and persist in the presence of MSCs (Ghannam *et al.*, 2010; Gonzalez *et al.*, 2009; Tasso *et al.*, 2012). When MSCs are injected *in vivo*, they are thought to function as catalysts for the expansion of antigen-specific regulatory T cells, indicating their potential to regulate important immunomodulatory functions (Tasso *et al.*, 2012). This makes them suitable for the treatment of autoimmune diseases and GVHD. For example, Popp and colleagues (2008) showed that donor-derived MSCs induced long-term allograft acceptance in a rat model of heart transplantation. Based on these findings, MSCs have been proposed to play a beneficial role in promoting tissue repair. In addition, the systematic use of MSCs has been suggested for treating subjects with damaged tissues or organs causing inflammation or inflammatory activities that are associated with diseases such as kidney failure, heart injury and rheumatoid arthritis (Squillaro *et al.*, 2015).

Recently, new findings have emerged that shed light on the immunomodulatory properties of MSCs. These findings propose that MSCs interact with their local environments by negatively regulating the immune response when major inflammation occurs and by stimulating the release of proinflammatory factors when levels of inflammatory cytokines are low (Bernardo & Fibbe, 2013; Galderisi & Giordano, 2014).

1.2.1.4 Homing efficiency

Another remarkable feature of MSCs is their ability to respond when injury occurs. Through a perfect combination of signalling molecules emitted from a site of injury and corresponding surface receptors, MSCs are able to locate and migrate to damaged tissue and subsequently engraft in the sites of inflammation. Many researchers have studied this homing ability of leukocytes to migrate to sites of inflamed tissue (Moser & Loetscher, 2001) in an effort to elucidate the roles of surface receptors and involved molecules that are known to be drivers of the homing mechanism. However, a clear explanation for how these MSCs are recruited to sites of injury has not yet been found. Other studies using MSCs have shown their capacity to home to sites of inflammation in damaged tissues, regardless of tissue type (Forte *et al.*, 2008; Horwitz *et al.*, 2002; Mahmood *et al.*, 2003); however, MSCs migrating towards inflammation in the lungs have been reported to become lodged in the lung microvasculature (Squillaro *et al.*, 2015).

Cell migration is thought to be regulated by and dependent on multiple signals ranging from growth factors to chemokines secreted by injured cells and/or responding immune cells (Spaeth *et al.*, 2008). Studies examining MSC homing have shown that the mechanism involves many trafficking-related molecules, such as chemokines, adhesion molecules and matrix metalloproteinases (Wei *et al.*, 2013), as well as

important signalling factors, such as stromal-derived factor 1 (SDF1), chemokine C-X-C motif receptor 4 (CXCR4) and hepatocyte growth factor and its receptor, the transmembrane tyrosine kinase (HGF-c-MET axes) (Neuss *et al.*, 2004; Shi *et al.*, 2007; Son *et al.*, 2006). These studies have shown that the migration process relies on the receptor CXCR4 and its binding partner, SDF1 chemokine C-X-C motif ligand 12 (CXCL12) (Sohni & Verfaillie, 2013). Wynn and colleagues (2004) have shown that CXCR4 is found in subpopulations of MSCs, which facilitates CXCL12-dependent homing and migration. Furthermore, BM-MSCs have been shown to express other molecules that are thought to be involved in the migration process, namely, chemokine C-C motif receptor 1 (CCR1), CCR4, chemokine C-X-C motif receptor 5 (CXCR5), CXCR6, CCR7, CCR9 and CCR10 (Sohni & Verfaillie, 2013). MSCs migrate by a coordinated process known as transendothelial migration, which involves adhering to vascular endothelial cells and then crossing the endothelial barrier (Schmidt *et al.*, 2006). The mechanism of adhesion between MSCs and the microvascular endothelium indicates coordinated rolling on and adhesion to endothelial cells mediated by the late antigen-4/vascular cell adhesion molecule-1 (VLA-4/VCAM-1) (Ruster *et al.*, 2006; Wang *et al.*, 2011). Furthermore, matrix metalloproteinases, such as matrix metallopeptidase-2 (MMP2) and membrane type 1 metalloprotease (MT1-MMP), have been shown to be important to the invasiveness of MSCs (Ding *et al.*, 2009; Ries *et al.*, 2007). Homing-related molecules can be up-regulated by inflammatory cytokines, such as tumour necrosis factor (TNF) and IL-1 (Ren *et al.*, 2010). This suggests that different inflammation states may promote specific and distinctive MSC engraftment and therapeutic actions (Wei *et al.*, 2013).

1.2.2 MSC clinical trials to date

Squillaro *et al.* (2015) report that the number of current and previously undertaken MSC-based clinical trials has doubled in the last few years. The majority of the trials are in phase I, which includes safety studies (n=109), phase I/II (n=185), or phase II, in which proof-of-concept for efficacy in human patients needs to be demonstrated (n=98). A few trials have reached phase II/III (n=17) or phase III (n=26), in which a newer treatment is compared with a standard or well-known treatment. Remarkably, phase I/II and phase II/III are mixtures of each other. The data show that when MSC-based trials are classified by disease type, the highest proportion of trials are studying bone and cartilage disease, followed by neurological disease, cardiovascular disease, GVHD, liver disease, diabetes, and haematological disease. The smallest proportion of clinical trials includes those studying treatments for Crohn's disease and lupus erythaematosus (Squillaro *et al.*, 2015).

Indeed, as of December 2016, the number of either completed or on-going MSC-based clinical trials registered in the official database of the United States National Institute of Health (U.S. National Institute of Health, 2016) under the search term 'mesenchymal stem cells' stood at 676; together, these trials covered a very wide range of therapeutic applications. These trials have and will provide information and evidence pertaining to the outcomes of MSC infusion and administration, and these results should support preliminary observations that the efficacy of MSC-based therapy can extend to diseases beyond the few that are currently targeted by therapeutic applications (Squillaro *et al.*, 2015). Presently, the main challenges facing the use of MSCs in clinical practice are issues such as donor heterogeneity, the lack of standardized procedures regulating *ex vivo* expansion that is known to affect MSC properties, immunogenicity and cryopreservation (Galderisi & Giordano, 2014; Galipeau, 2013).

1.2.3 MSC donor criteria

The guidelines recommended for the screening and testing for MSC donations are similar to those in place for other cell-based or tissue-based products. The purpose of these guidelines is both to determine who can be a donor and to protect the health and safety of recipients. According to the National Health Service (NHS) UC Bank, the use of health questionnaires is recommended to determine the status of a donor, such as whether a donor tested positive for hepatitis C antibody or hepatitis B surface antigen or whether female donors have had malaria within the last three years or a full course of anti-malaria treatment within the past six months. The viral testing of female donors who are at higher risk for or who have Human Immunodeficiency Virus (HIV) is also recommended (National Marrow Donor Program, 2016; NHS Blood and Transplant, 2016). Furthermore, donor age is an important factor to consider. It has been observed that BM from children contains a higher concentration of CFU-F precursors than does BM from adults (Baxter *et al.*, 2004). Moreover, an MSC donor should have no abnormalities or risks for abnormalities potentially involving MSCs, which may currently be difficult to assess. The guidelines also recommend that an extra blood sample be taken from each donor for testing in an effort to exclude any medical reasons that may prevent them from being a donor (Sharma *et al.*, 2014).

Wu and colleagues (2013) hypothesized that obesity has an inhibitory effect on the multipotent potential of MSCs. Their findings indicate that obesity affects MSCs by resulting in altered *in vitro* adipogenic and osteogenic potential;

furthermore, they suggest that increased body mass seems to promote bone formation and that the characteristics of stem cells resident in many tissues be significantly affected by obesity, such that their capacity for therapeutic applications becomes undermined. By the current definition of epigenetics, the issue of qualifying MSCs as universal donors should be reconsidered carefully, even more so when they are to be used for multiple recipients.

1.3 Umbilical Cord and Wharton's Jelly

1.3.1 UC formation and structure

The human UC is a flexible tube-like structure that is formed during pregnancy. It connects the developing embryo to the placenta and not only supplies the developing embryo with oxygen and nutrients from the mother but also removes waste products from the embryo (Sadler, 1990). The UC is formed by 22 days post coitum (dpc), when the body stalk and the extra-embryonic omphalomesenteric duct (an intermediate structure formed from the primary yolk sac and a precursor of the secondary yolk sac, or secondary yolk) become completely surrounded by the amnion; during this stage, extensions of the allantois also occupy the UC (Baergen, 2011). During the period from 28-40 dpc, the amniotic cavity starts to surround the connecting stalk and the embryo, pressing the stalk into a thin tube-like structure; the cavity then becomes surrounded by the amniotic epithelium. During this time, the allantois and yolk sac regress (Baergen, 2011; Subramanian *et al.*, 2015) (Figure 1). This newly formed UC continues to lengthen; it is essentially composed of the umbilical vessels surrounded by a connective tissue called WJ (Baergen, 2011). The main feature of the UC is its elasticity, which enables it to protect the umbilical vessels from compression, torsion, and bending and to avoid compromising the bi-directional blood flow between the mother and embryo (Kim *et al.*, 2013). A striking feature of the UC is its helical-like arrangement; most of the cords that have been examined in mothers exhibit counter-clockwise turns (Malpas & Symonds, 1966), and the veins and arteries within the cord are also arranged in a helical format. Both the helical coils and the mean length of the UC are used to calculate the umbilical coiling index (UCI), and these measurements are used to determine whether a foetus is at risk (Can & Karahuseyinoglu, 2007; Peng *et al.*, 2006; Trevisanuto *et al.*, 2007). At term, the UC is approximately 60-cm to 65-cm

long on average, approximately 1.5-cm in diameter, and approximately 40-g in weight (Can & Karahuseyinoglu, 2007; Di Naro *et al.*, 2001; Raio *et al.*, 1999).

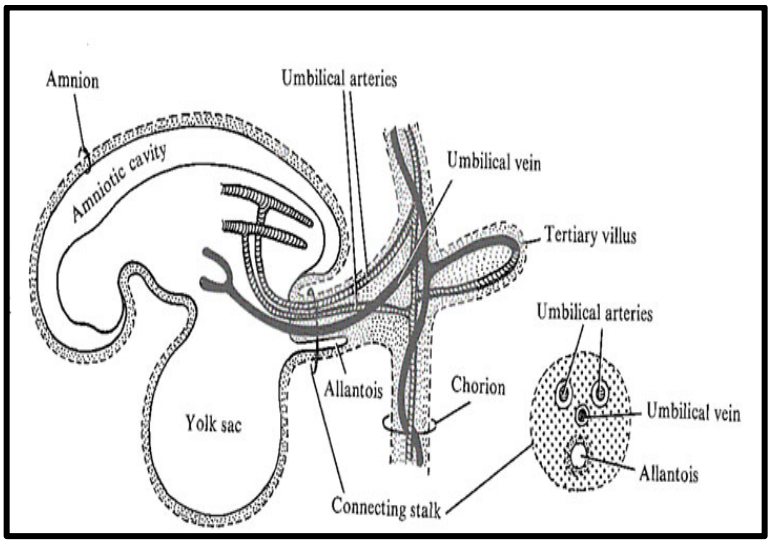

Figure 1. Simplified schematic of the developing UC at approximately day 20 post coitum. The connecting stalk progresses ventrally as a result of the cephalocaudal flexion of the embryo and fuses with the yolk sac stalk to form the UC. Reproduced from (Pansky, 1982).

The UC consists of two umbilical arteries and one umbilical vein, which are all embedded within the WJ (Figure 2). The UC is enveloped by a single or multiple layer(s) of squamous-cubic epithelial cells, which are thought to be derived from the amniotic epithelium. As this tissue grows to cover the surface layer of the UC, it also becomes contiguous with the placenta and developing embryo (Can & Karahuseyinoglu, 2007; Copland *et al.*, 2002; Mizoguchi *et al.*, 2004). The tissues of the human UC are compartmentalized into distinct regions, and the regions consist of unique tissue structures in terms of ECM component composition, including connective tissue fibres and proteins. The cellular characteristics of these regions show differences in both the number and nature of cells. The results of functional and immunohistochemical studies have led to the hypothesis that these regions may

originate from different pre-existing formations (Akerman *et al.*, 2002; Karahuseyinoglu *et al.*, 2007; Nanaev *et al.*, 1997; Sarugaser *et al.*, 2005; Takechi *et al.*, 1993). For example, myofibroblast cells of the WJ may have been derived from either the adjacent vascular smooth muscle cells or pre-existing fibroblasts (Can & Karahuseyinoglu, 2007). Can & Karahuseyinoglu (2007) reviewed and described six distinct zones in the UC. In order from the outermost to the innermost region, they are as follows: a) The amnion epithelium and UC epithelium comprise type IV and type VII collagen and are located in the epithelial basement membrane in term cord. b) The subamniotic stroma comprises collagen types I, III, and VI. c) Clefts form a spongy network of interlacing collagen fibres in a continuous, soft skeleton enclosing a wide system of interconnected cavities and canaliculi-like structures. This structure is thought to have a mechanical function that prevents any inconsistences of ground substance during any compression events that may arise. The remaining three zones include the following: d) WJ, e) the perivascular stroma, and f) vessels (Figure 2). Collagen can not be easily solubilized by organic or chemical substances; it builds strong ionic bonds with glycosaminoglycans and proteoglycans, and the structure of collagen is what allows it to fulfil its functions by providing the stroma with extraordinary strength (Can & Karahuseyinoglu, 2007; Sobolewski *et al.*, 1997).

Stem cells have been shown to be derived from distinct regions of the UC. The nomenclature used in the literature for the listed compartments has been unstandardized (Bongso & Fong, 2013; Jeschke *et al.*, 2011). Within these compartments, stem cell populations with various stem cell-like properties have been described (Conconi *et al.*, 2011). Various derivation protocols for isolating stem cells have been described by researchers in the literature. These protocols are not standardized, and at times, the variations in stem cell populations from different compartments have not been considered (Bongso & Fong, 2013). Recent studies have

demonstrated that MSCs isolated from the WJ, in particular, are preferred over those isolated from other UC compartments due to the simple and easily standardized isolation procedure, smaller non-stem cell populations; additional advantages include the large numbers of MSCs that can be generated with minimal manipulation, as well as the rich stemness characteristics and ability of these MSCs to proliferate with a broad differentiation potential (Subramanian *et al.*, 2015).

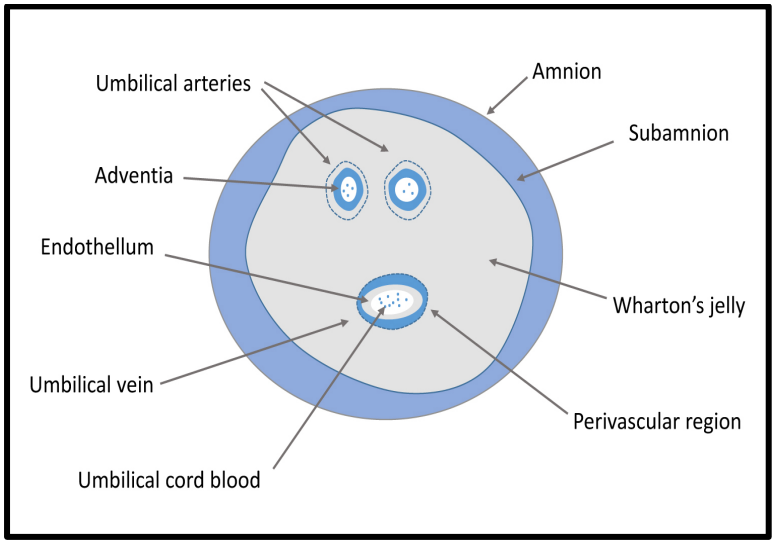

Figure 2. A cross-sectional diagram illustrating the compartments of the human UC, including the amnion, the subamnion, WJ, the perivascular region, the adventitia, the endothelium, and the UC blood and vessels.

1.3.1.1 UC-MSC versus embryonic stem cell surface markers

UC-MSCs are classified as perinatal stem cells. The term 'perinatal' refers to the period from immediately before (prenatal) to the period immediately after (postnatal) birth. These stem cells are considered to be valuable for their broad use in developing regenerative medicine strategies and for their impressive ability to modulate the

immune response (Aggarwal & Pittenger, 2005; Friedman *et al.*, 2007; Le Blanc & Ringden, 2005).

UC-MSCs share common surface markers with other MSCs, such as BM-MSCs. They adhere to and grow on surfaces such as plastic. Various techniques, namely, polymerase chain reaction (PCR), real-time polymerase chain reaction (RT-PCR), immunocytochemistry and microarray analysis, have been employed to identify UC-MSCs, which are identified by the presence of the surface markers CD105, CD90, and CD73. However, these markers are also present amongst MSCs from different sources (Can & Karahuseyinoglu, 2007; Dominici *et al.*, 2006). Additional identification of MSCs is based on their *in vivo* characterization; for instance, upon engraftment, MSCs self-renew and undergo multipotent differentiation (Troyer & Weiss, 2008). Studies have shown that they express certain embryonic stem cell (ESC) markers, e.g., HLA-1, albeit in low levels. Some reports in the literature have shown cultured UC cells to have inconsistent gene expression profiles. Sarugaser *et al.* (2005) demonstrated that HLA-1 expression in UC-MSCs was stable for up to five passages and that no HLA-1 expression could be detected in cells recovered after cryopreservation. In contrast, Weiss and colleagues (2006) did not find any changes in expression throughout a number of passages. One potential explanation for the variations in gene expression is differences in epigenetic factors, which may have been caused by varying culture conditions.

Many studies have reported that three specific transcription factors expressed in human ESCs are thought to play a central role in the events regulating pluripotency and self-renewal. These transcription factors include POU5F1 (OCT4), SRY-box 2 (SOX2) and NANOG homeobox (NANOG) (Carlin *et al.*, 2006; Chambers *et al.*, 2003; Mitsui *et al.*, 2003). It has been shown that down-regulation of NANOG induces the differentiation of human ESCs into extra-embryonic lineages (Hyslop *et al.*, 2005; Liu *et*

al., 2009). In addition, the expression of these three markers has been reported in cultured WJ-MSCs (Carlin *et al.*, 2006). Human UC-MSCs inherit some of the stemness properties of both ESCs and adult MSCs. Developmentally, the UC exists between the embryo and adult, and that is likely the reason behind UC-MSCs inheriting some ESC markers (Bongso & Fong, 2013; Pappa & Anagnou, 2009).

Liu and colleagues (2009) discussed increased MSC growth rate and enhanced colony formation due to an ectopic expression of NANOG, suggesting that an overexpression of NANOG maintained MSC stemness. In addition, this expression might function in mature MSCs in the same fashion as it does in ESCs, showing the capacity of NANOG to act as a key player in sustaining the pluripotency of stem cells. Furthermore, MSCs overexpressing NANOG have much higher capabilities for expansion and osteogenesis (Go *et al.*, 2008). Oct4 has been shown to be temporally expressed in the endoderm and neuroectoderm of developing embryos (Palmieri *et al.*, 1994; Reim & Brand, 2002). Furthermore, down-regulation of Oct4 in ESCs causes trophectoderm differentiation, while overexpression of the same marker causes differentiation into extra-embryonic mesoderm and endoderm (Niwa *et al.*, 2000), demonstrating that Oct4 is an important dose-dependent determinant of ESC pluripotency status. Liu's group (2009) demonstrated that overexpression of OCT4 in MSCs not only promoted proliferation rate but also enhanced colony formation, suggesting that overexpression of OCT4 plays a critical role in maintaining the stemness of MSCs.

Researchers have shown that the main three transcription factors (i.e., Nanog, Oct4 and Sox2) are expressed at high levels in ESCs and are markers of primitive stem cells. The down-regulation of all three transcription factors is correlated with the loss of pluripotency and the capacity for self-renewal (Chambers *et al.*, 2003; Mitsui *et al.*, 2003). It has been reported that stem cells isolated from postnatal sources, such as BM (Kucia *et al.*, 2005), vascular and perivascular space (Kim *et al.*, 2004; Romanov *et*

al., 2003; Sarugaser *et al.*, 2005), placental tissue (Fukuchi *et al.*, 2004; Yen *et al.*, 2005) and UC blood (Bodger, 1987; Erices *et al.*, 2000; Yang *et al.*, 2004), have more restricted differentiation potential, and these cells are not thought to be pluripotent. OCT4, SOX2 and NANOG are expressed in these cells but not at high levels (Carlin *et al.*, 2006). The results reported by Carlin and colleagues (2006) from research using porcine UC cells have been consistent with the interpretation that porcine UC cells represent a stem cell population that expresses OCT4, NANOG and SOX2 and that these factors are central regulators of gene transcription in primitive stem cells. All of these transcription factors have been reported to be occupying the promoters of over 2,000 human genes and co-occupying over 350 gene promoters (Boyer *et al.*, 2005). Some reports in the literature have concluded that these three transcription factors control pluripotency and self-renewal both individually and together in human ESCs.

In contrast, other studies by Fong and others (2007, 2011) using different characterization techniques have found low expression levels of the key pluripotency markers, such as NANOG, OCT4 and SOX2, in human WJ-MSCs. These results confirm the stemness of WJ-MSCs. These researchers hypothesized that this could be the reason why human WJ-MSCs do not produce teratomas when they are transplanted in an undifferentiated status. One explanation for the different expression levels of OCT4 that have been reported could be that in humans, there are two isoforms of POU5F1 (i.e., OCT4A and OCT4B), and POU5F1 becomes difficult to detect because only OCT4A is included in the maintenance of pluripotency, whereas OCT4B is expressed ubiquitously (La Rocca *et al.*, 2009; Lee *et al.*, 2006; Takeda *et al.*, 1992). Additionally, differences in cell isolation procedures and culture conditions may explain divergent results in the literature. These pluripotency markers are up-regulated in undifferentiated human ESCs and have been shown to maintain pluripotency in self-renewing human ESC populations (Zhao & Daley, 2008). The

reduced relative expression of these pluripotent markers in UC-MSCs would suggest that they are not as pluripotent as ESCs; nonetheless, the data suggest that UC-MSCs are notably multipotent (Taghizadeh *et al.*, 2011). Based on the findings that WJ-MSCs express common mesenchymal CD markers similar to those of other MSCs, they are typically considered to originate from mesenchymal or connective tissue (Karahuseyinoglu *et al.*, 2007). Furthermore, WJ-MSCs have been shown to express matrix receptors and not receptors of haematopoietic lineage, suggesting more similarities to MSCs (Fong *et al.*, 2007).

1.3.2 WJ description

Within the UC, between the amniotic epithelium and the umbilical vessels, lies WJ (Figure 2), which was initially described by Thomas Wharton in 1956 as a substance that is composed of a primitive mucus and connective tissue (Taghizadeh *et al.*, 2011; Wharton, 1656). In the 1990s, instead of discarding UCs, scientists re-examined the WJ stromal cells and ECM composition of the UCs. Two main drivers were behind these examinations. One driver was the search to detect potential structural alterations present in cases of pre-eclampsia, as ECM components of the WJ had been found to be altered and were associated with the 'premature ageing' observed in pre-eclampsia patients (Bankowski *et al.*, 2004; Bankowski *et al.*, 1996). The second driver was the cellular identification of UC stromal cells, which essentially resemble mesenchymal fibroblasts found elsewhere during *in utero* development (Can & Karahuseyinoglu, 2007).

WJ is known to be rich in proteoglycans, particularly hyaluronic acid, which is an important substance that retains water and maintains the elasticity of the UC. Another

major component of the ECM of WJ is the ground substance, which is mainly composed of glycosaminoglycans (GAGs). The total abundance of GAGs in WJ is twice as high as that contained in the arteries, the amount of sulphated GAGs (i.e., keratin, heparin, dermatan, chondroitin-4, and chondroitin-6 sulphate) is very low, and traces of heparin are present (Sobolewski *et al.*, 1997). Structurally, WJ does not contain any capillaries or lymphatics. The main function of WJ is to prevent any obstruction of the umbilical vessels, such as that caused by compression and torsion, and to prevent bending of the umbilical vessels so that not only is an uninterrupted supply of oxygen and nutrients, namely, glucose and amino acids, provided to the developing foetus but also the removal of carbon dioxide and other waste products from the placenta and the foetus is maintained (Can & Karahuseyinoglu, 2007; Taghizadeh *et al.*, 2011; Troyer & Weiss, 2008; Wang *et al.*, 2008).

WJ is known to contain primitive MSCs, and it has been shown that during the early stages of embryogenesis, before embryonic day 10.5, the MSCs migrate through the aorta-gonad-mesonephros (AGM) region of the developing cord. These MSCs are thought to be trapped in the connective tissue matrix during their migration. Through the early stages of embryogenesis, haematopoiesis occurs within the yolk sac and then in the AGM region. Colonies of early HSCs and MSCs migrate to the placenta via the developing UC between embryonic day 4 and embryonic day 12. A second migration of the HSCs and MSCs from the placenta occurs through the developing UC to the liver of the developing foetus, after which the cells finally engraft into the foetal BM, where they reside for the entire lifespan of the human. The colonies contain precursors of HSCs and primitive MSCs. The MSCs are thought to become embedded in the WJ quite early in embryogenesis, perhaps during the migration events, and to remain there for the entire gestation period (Wang *et al.*, 2008).

The formation of these perinatal stem cells during the early embryonic stages enables them to exhibit characteristics resembling those of ESCs as well as bear features of the somatic MSCs found in the BM (Taghizadeh *et al.*, 2011). This resemblance has been defined by the ISCT (Dominici *et al.*, 2006). Taghizadeh and colleagues (2011) define WJ stem cells as native stem cells that are found within the UC-ECM, and they define UC-MSCs as *in vitro* cell populations derived from WJ-MSCs.

Cells derived from WJ have a higher CFU-F frequency. Consequently, more MSCs may be found in the initial isolation from WJ than in those from BM or UC blood (Karahuseyinoglu *et al.*, 2007; Sarugaser *et al.*, 2005; Troyer & Weiss, 2008). Moreover, WJ-MSCs have greater expansion capability and grow faster *in vitro*, and they are thought to synthesize cytokines, such as GM-CSF and granulocyte colony-stimulating factor (G-CSF), that have not been shown to be synthesized by BM-MSCs (Lu *et al.*, 2006). Additionally, cells from WJ can go through greater numbers of passages before reaching senescence, and even though they have faster doubling times than those of BM-MSCs, they differentiate into adipocytes more slowly than do the MSCs derived from BM (Karahuseyinoglu *et al.*, 2007); this feature is thought to reflect the primitive nature of these MSCs (Troyer & Weiss, 2008). Along these lines, it is generally accepted that MSCs harvested from WJ, which is a young tissue, will be much more proliferative, immunosuppressive and even therapeutically active stem cells than the stem cells isolated from adult tissue sources, such as BM (Kim *et al.*, 2013). A remarkable feature of the cells isolated from WJ is that they maintain their growth potential even when they are harvested from UCs that have been stored for 48 hours (Carlin *et al.*, 2006). Additionally, these WJ-MSCs are able to maintain a normal karyotype, which is another confirmed marker used for stem cell characterization during primary, early and late passages (Fong *et al.*, 2007). Conversely, genomic mutations causing chromosomal instability are commonly observed in ESC lines

expanded *in vitro* (La Rocca *et al.*, 2009; Mantel *et al.*, 2007; Rao, 2006; Rebuzzini *et al.*, 2008).

1.3.2.1 WJ-MSCs fulfil MSC criteria

In 1991, McElreavey and colleagues reported WJ as an alternative source of stem cells, as they were successfully able to isolate and culture these cells (McElreavey *et al.*, 1991). A few years later, Wang *et al.* (2004) provided evidence that these WJ-derived stem cells could indeed be classified as MSCs. Since their first isolation, many advances have been made in not only optimizing their isolation but also enabling them to undergo differentiation (Kadner *et al.*, 2002; Kadner *et al.*, 2004; Mitchell *et al.*, 2003; Romanov *et al.*, 2003; Takechi *et al.*, 1993). Together with the discoveries that have been made and the milestones that have been reached, the use of WJ-derived stem cells should significantly impact the development of therapeutic, cell biology-based strategies for clinical applications (Kim *et al.*, 2013).

Wang and colleagues (2004) described MSC features to resemble those of fibroblasts when they are cultured *in vitro*; they also reported that upon stimulation, MSCs are successfully able to differentiate into cells from multiple lineages, such as osteoblasts, adipocytes and chondrocytes. Furthermore, their work provided additional phenotypic information; reportedly, MSCs expressed high levels of CD29, CD44, CD51, CD73 and CD105, which are also expressed by BM-MSCs. In addition, the MSCs did not express the haematopoietic markers CD34 and CD45. Many other reports have provided further details on the phenotypic features and characteristics of MSCs, including specific membrane molecules on MSCs that can be used for cell identification, such as CD90, CD146, CD166 and ganglioside 2 (Carlin *et al.*, 2006; Dominici *et al.*, 2006; Fong *et al.*, 2011; Wang *et al.*, 2004; Xu *et al.*, 2009). According to the ISCT, a cell must exhibit all three characteristics of MSCs, i.e., the morphology, immunophenotype

and differentiation potential of MSCs, to meet the criteria for identification (Dominici *et al.*, 2006). Currently, no specific marker for UC-MSCs has been identified; therefore, researchers are required to ensure that cells derived from UC tissues also meet the identification criteria for MSCs (Batsali *et al.*, 2013).

1.3.2.2 WJ-MSC isolation methods

Several isolation methods for the stem cell sources within the UC exist in the literature, and the experimental approaches that can be used vary considerably. Moreover, the cells isolated from the UC tend to be heterogeneous and contribute to the bias, particularly when researchers carry out protocol comparisons (Batsali *et al.*, 2013). However, all the methods reported demonstrate that the procedure is complex, and all the methods have been designed to ensure maximal cell recovery in as little time as possible. At the present, there are two main methods used for isolating WJ-MSCs; 'enzymatic digestion' and/or 'tissue explant' methods can be used, but none of the methods have been standardized (El Omar *et al.*, 2014; Han *et al.*, 2013; Klontzas *et al.*, 2015). Selected methods are briefly described here to illustrate the extent of the variations that exist among the practices.

One method involves scraping off the WJ, while keeping the blood vessels intact, to isolate stem cells from the scrapings. An alternative method includes removing the blood vessels first and then scraping off the WJ. The method described by Han and colleagues (2013) involves immersing a UC sample in a solution containing 0.2% collagenase enzyme at 37°C and incubating it for 16-20 hours to allow completion of the digestion reaction. Other groups have used collagenase enzyme alone or in combination with trypsin and/or hyaluronidase, which separates the stem cells from the WJ and perivascular mesenchyme; with this method, dissecting the UC into smaller

pieces with or without removing the blood vessels is optional (Fong *et al.*, 2010; Karahuseyinoglu *et al.*, 2007; Lu *et al.*, 2006; Sarugaser *et al.*, 2005; Tong *et al.*, 2011; Tsagias *et al.*, 2011; Wang *et al.*, 2004).

Other groups have avoided using enzymatic approaches because they have found that the enzymes damage cells, alter cell functions and reduce cell populations. These groups have developed explant methods by taking advantage of MSC properties, i.e., their ability to migrate and adhere to a plastic surface, from which cultures can subsequently be established (La Rocca *et al.*, 2009; Majore *et al.*, 2011; Mitchell *et al.*, 2003). A simple and rapid method to isolate UC-MSCs was developed by De Bruyn and colleagues (2011), whereby an UC is cut into longitudinal segments that are plated with the WJ facing down on the plastic surface; this method avoids both dissection and the use of enzymes. An explant method described by Ding and colleagues (2015) involves removing the UC vessels and manually mincing the remaining fragments until they are approximately 1-2 mm^3 in size. These fragments are then incubated for 7 days to allow stem cell outgrowth. One issue with this method is that the fragments become suspended in the medium, and variable numbers of MSCs are recovered. However, the enzymatic method generally yields consistent numbers of isolated MSCs.

A recent study demonstrated that expression patterns of the MSC markers CD73, CD90, and CD105 varied depending on whether an enzyme or an explant method was used for their isolation. The differences that have been identified highlight the importance of further work to establish precisely how the different methods used for isolation impact the cells (Salehinejad *et al.*, 2012). Hua *et al.* (2013) compared the two main methods for isolating WJ-MSCs and examined many variables, including primary culture duration, recovered cell number, and cell morphology, as well as immunophenotypic features and differentiation potential. They concluded that the optimal method for isolating MSCs is the protocol using 10-mm tissue explants.

One standardized and comprehensive procedure for the isolation, characterization and *ex vivo* expansion of MSCs is required so that investigation outcomes are more reliable, particularly regarding the exact source and homogeneity of the stem cell populations within the UC. Unfortunately, no consensus on a standard method has yet been reached among researchers. Therefore, it is nearly impossible to come to an agreement on the characteristics and biological properties of MSCs, which is an essential requirement for designing any translational clinical studies concerning the use of these cells.

1.4 Epigenetic and developmental reprogramming

In principle, the cells of a multicellular organism all carry an identical genotype, despite exhibiting broad morphological and functional diversity within the organism. Therefore, the identity and developmental potential of an individual cell is not only influenced by its genetic component but also by changes that do not involve changes in the deoxyribonucleic acid (DNA) sequence. Differential gene expression, an area of research known as 'epigenetics', is the process by which these changes are achieved. Mechanisms resulting in differential gene expression involve methylation, acetylation, ubiquitination, and other chemical interactions that either modify DNA itself or its packaging proteins, histones, or change micro-ribonucleic acid (miRNA) expression (Baccarelli & Bollati, 2009). The word 'epi' is derived from the Greek meaning 'over', 'above' or 'in addition to'; in this sense, epigenetic modifications can be regarded as another layer of information in addition to the genetic code. In 1942, Conrad Hal Waddington first defined epigenetics as 'the study of the interactions between genes and their products which bring phenotype into being' (Waddington, 2012). Epigenetics is now understood as 'the study of mitotically and/or meiotically heritable changes in gene expression that are not caused by changes in the DNA sequence but by biochemical modifications' (Bird, 2002). Epigenetics broadly connects genotype and phenotype by altering the final outcome of the genome in a stable manner without changing the underlying DNA sequences (Wu & Morris, 2001). Modifications to DNA and histone proteins can occur via covalent and non-covalent mechanisms that influence the overall chromatin structure. Epigenetic modifications are stable and heritable and thus can be transferred from one cell generation to the next (mitotic inheritance) as well as inter-generationally (meiotic inheritance). The heritability of epigenetic traits in plants from one generation to the next has been well documented (Cubas *et al.*, 1999). However, less evidence has been collected on the heritability of

epigenetic modifications between generations in mammals, although some studies have demonstrated environmentally induced epigenetic transgenerational inheritance of adult-onset disease phenotypes in F_3 generations (Guerrero-Bosagna & Skinner, 2012). For example, certain variations in nutrition are known to result in obesity in the F_3 generation as a result of epigenetic transgenerational inheritance (Waterland *et al.*, 2008). Thus, epigenetics is central to understanding both developmental plasticity and how the intrauterine environment affects short-term and long-term phenomena, including obesity.

1.4.1 Epigenetic mechanisms

The mechanisms by which epigenetic regulation exerts effects alter the physical accessibility of gene promoters and regulatory regions, thereby influencing expression. These mechanisms include DNA methylation, histone modification, chromatin-remodelling complexes, and RNA interference (RNAi) (Grewal & Elgin, 2007; Hake & Allis, 2006; Jenuwein & Allis, 2001; Reik *et al.*, 2001; Vaissiere *et al.*, 2008). DNA methyltransferases (DNMTs) and enzymes that either modify histones or remodel chromatin operate in conjunction with miRNA mechanisms to form a specific chromatin structure that results in specific genetic transcription (Figure 3). Epigenetic mechanisms are vital for development during normal embryogenesis and for the differentiation of individual cell lineages in adult organisms (Reik, 2007). Furthermore, epigenetic control directs cell fate during early development following fertilization, as dividing blastocysts increasingly develop trophectoderm and inner cell mass gene expression patterns.

Although almost every cell in the human body contains the same DNA sequences,

epigenetic marks promote gene expression in cells that are relevant for each tissue type. For example, a neuronal cell expresses genes necessary for the development of dendrites and axons. In a liver cell, epigenetic tags on those same genes result in tighter binding of the DNA, thereby silencing expression because the resulting gene-epigenetic tag structure is inaccessible to transcription machinery. Although they are stable, epigenetic mechanisms that enable the inheritance of gene expression states from one generation of cells to the next are not definitive; instead, they are flexible. Normal ageing can lead to changes arising in a stochastic manner; changes can also occur in response to environmental stimuli (Baccarelli & Bollati, 2009; Fraga *et al.*, 2005; Probst *et al.*, 2009). Thus, epigenetic changes facilitate genomic adaption to environmental factors and enable development towards a specific phenotype. This capacity to alter phenotype as a result of environmentally sensitive dynamic processes ensures that offspring will be more suited to the environment after birth, thereby allowing offspring to fulfil the ultimate biological imperative of reproduction as adult organisms.

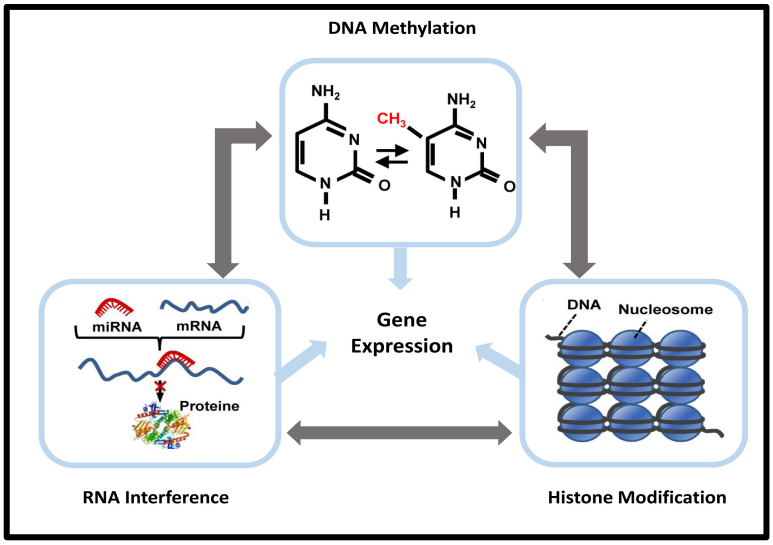

Figure 3. The three distinct mechanisms of epigenetic regulation are DNA methylation, histone modification, and RNAi. All described epigenetic mechanisms have a two-way, interdependent control relationship between them, creating multifaceted regulatory machinery. This figure was modified from (Barnes *et al.*, 2005; Morales Prieto & Markert, 2011; Ulrey *et al.*, 2005; Yeung *et al.*, 2005).

***DNA methylation*,** because methylation is the subject of study for this doctoral thesis, it is discussed in greater detail in section 1.4.2. Other epigenetic modifications are described below.

Histone modification is another major epigenetic mechanism that alters gene expression. Histone proteins are packaging proteins that organize and compact DNA into structural units called nucleosomes. Each nucleosome consists of a histone octamer composed of the four core histones, H2A, H2B, H3 and H4 (Bentley *et al.*, 1984). The core histone proteins can undergo various modifications, including phosphorylation, methylation, ubiquitination, sumoylation, and acetylation, among others. (Kouzarides, 2007; Ruthenburg *et al.*, 2007). A set of histone modifications, or a 'histone code', can mark the chromatin as active or inactive and thus has the potential to influence DNA transcription (Strahl & Allis, 2000). The most common histone modifications are histone acetylation and histone methylation. Acetylation occurs at the lysine residues of the N-terminus via histone acetyl transferases (HATs);

these residues can also be subjected to deacetylation via histone deacetylases (HDACs). Acetylation at the lysine residue removes the normal positive charge; this change reduces the affinity between the histone and DNA and allows the chromatin structure to open up, making the DNA more accessible for transcription (Ruthenburg *et al.*, 2007). Histone methylations are facilitated by histone methyl transferases (HMTs) and can either increase or decrease gene expression.

RNAi is a biological mechanism that is only found in eukaryotic cells. The effects of RNAi are exerted either via miRNA or through small interfering RNA (siRNA). RNAi contributes to the control over the activity and degree of gene expression. miRNAs are distinct from siRNAs in their biogenesis, rather than function, and differentiating between the various classes of small ribonucleic acid (RNAs) is becoming increasingly difficult. miRNAs are a class of small, non-coding RNAs consisting of approximately 23 nucleotides; the main function of miRNAs is to down-regulate gene expression via mechanisms such as translational regression, messenger RNA (mRNA) cleavage and deadenylation (Bartel, 2004). They are single-stranded products of an organism's own genome that are endogenously and purposefully expressed. In contrast, siRNAs are double-stranded and exogenous in origin, and they enter cells via vectors such as viruses or transposons. In addition, miRNAs are processed from stem-loop precursors with incomplete double-stranded character, whereas double-stranded siRNAs are excised from long, fully complementary strands (Tomari & Zamore, 2005).

1.4.2 DNA methylation

1.4.2.1 DNA methylation basics

the first recognized epigenetic modification, is mostly linked to transcriptional silencing

(60-90% of genes) (Nakao, 2001). In mammalian cells, DNA methylation involves the addition of a methyl group (-CH_3) to the 5^{th} carbon atom of the cytosine in cytosin-phosphate-guanin site (CpG) (Chen & Li, 2004), which is a reaction catalysed by DNMTs. DNMT3A and DNMT3B mainly execute *de novo* methylation of unmethylated CpG islands, and DNMT1 acts as a maintenance methyltransferase by ensuring the mitotic inheritance of the methylated patterns (Bestor, 2000). CpG islands predominantly occur in the promoter regions, the regulatory domains in the genome, as well as in the intergenic regions to some extent. DNA methylation can interfere with the transcriptional machinery; hence, it plays a crucial role in gene regulation and development (Bestor, 2000). In fact, studies have shown using mouse models that DNMT-knockout results in embryonic death (Fatemi *et al.*, 2005; Li *et al.*, 1992).

In mammals, methylation mainly occurs at the 5' position of the pyrimidine ring of the cytosine in the CpG dinucleotide sequence (Bird, 2002), which results in two methylated cytosine residues existing diagonally opposite to each other on different DNA strands (Suzuki & Bird, 2008). In mammalian genomes, 5-methylcytosine accounts for ~1% of all bases, although this varies slightly according to tissue type. Most CpG dinucleotides (75%) are methylated (Tost, 2010). The methylation of cytosines in alternative formations, such as CpNpG or CpA sequences, is common in plants and in some fungi. Furthermore, non-CpG methylation has been identified in mammalian ESCs (Gupta *et al.*, 2010; Lister *et al.*, 2009; Ramsahoye *et al.*, 2000), although its function is currently unknown.

CpGs reside along a gene in particular patterns, allowing for multiple forms of epigenetic control. For example, some CpGs lie in clusters known as CpG islands, and these are found in over 50% of genes in the vertebrate genome (Illingworth & Bird, 2009). CpG islands are important for determining whether a gene is expressed in a

specific cell type. According to Gardiner-Garden and Frommer (1987) or Takai and Jones (2002), depending on the parameters involved, a CpG island can occur when the G+C content is more than 50% (55%) and when the ratio of observed versus expected occurrence of CpGs is greater than 0.6 (0.65); in addition, CpG islands have a minimum size of 200 (500) base pairs (bp). Some CpGs occur less frequently and tend to appear at sites where transcription factors bind, which are sites that are likely to be especially important in developmental plasticity. CpGs generally occur at a lower frequency in the genome than those of other dinucleotides, which is a phenomenon that may be caused by the conversion of methylated CpGs to TpGs via spontaneous or enzymatic deamination (Jones, 2012). Compared with those of other transitional mutations, estimates of CpG mutation rates range from 10 to 50 times greater. This discrepancy is likely to have had an evolutionary impact via the depletion of this dinucleotide over time (Tost, 2010).

De novo DNA methylation and its maintenance require the activity of a family of DNMT enzymes. For example, DNA methylation during early embryogenesis is executed by DNMT3A and DNMT3B; hence, these enzymes are central to cell fate during mammalian embryonic development. Another member of the DNMT3 family, DNMT3L, has no DNMT activity. Rather, it serves a general stimulatory function for DNMT3A and DNMT3B. It is also a prerequisite for maternal genomic imprinting. Parental imprinting is a specific type of epigenetic control, whereby a gene is methylated and thus silenced if derived from one parent but not the other. Imprinted genes seem to be especially significant for placental function as well as certain aspects of brain function, and the loss of imprinting is associated with some diseases (Reik & Walter, 2001).

Historically, it was believed that DNA methylation is maintained exclusively by DNMT1, which adds methyl groups ($-CH_3$) to non-methylated daughter strands, thereby restoring hemimethylated DNA generated during DNA replication to a fully methylated

state. Consequently, the possibility of the inheritance of DNA methylation and its corresponding effects on gene expression from cell to cell arises. Because correctly maintaining DNA methylation is essential for embryonic development, imprinting, and X-inactivation, accurately understanding these processes is central to research on developmental epigenetics. Several recent studies have supplemented the collective understanding of the subject and have demonstrated that, in fact, all three DNMTs (i.e., DNMT1, DNMT3A and DNMT3B) are involved and cooperate in both *de novo* methylation and methylation maintenance (Handy *et al.*, 2011; Hermann *et al.*, 2004; Jones, 2012; Okano *et al.*, 1999; Portela & Esteller, 2010).

1.4.2.2 Key processes regulated by DNA methylation

Epigenetics research is challenging because of the wide range of different epigenetic modifications contributing towards epigenetic marks as well as the multiple environmental factors that can influence the epigenome. For the most part, environmental cues that influence long-term phenotypic variations are initiated during intrauterine and perinatal periods (Martinez-Frias, 2010). During the mammalian life cycle, two significant global epigenetics reprogramming events occur, which remove any epigenetic errors that have accumulated during a parent's lifetime; these events ensure the correct introduction of embryonic gene expression and establish new gender-specific imprints in the developing germ cells (Lange & Schneider, 2010; Reik, 2007). The first reprogramming event occurs in the primordial germ cells. Studies in mice have shown that global DNA methylation and histone modifications occur in primordial germ cells, where cell reprogramming is initiated in the developing embryo at approximately mid-gestation. Although most of the DNA methylation events return to somatic levels during late foetal stages or at birth, genomic imprints have already been

made at this stage in a sex-dependent manner (Hajkova *et al.*, 2008; Hajkova *et al.*, 2002; Sasaki & Matsui, 2008). The second reprogramming event occurs immediately following fertilization, and it continues until the blastocyst stage. Research has shown that complex histone modifications and DNA methylation events occur throughout the pre-implantation phase (Burton & Torres-Padilla, 2010).

These two genome-wide reprogramming events are the time points in the life cycle where the most widespread epigenetic changes occur. Some of these epigenetic marks are maintained throughout the lifetime of an individual. Hence, a suboptimal intrauterine environment can induce epigenetic changes that can persist into adult-hood, even in the absence of the original stimulus, and this persistence carries the potential to pass changes on to the next generation. Unlike epigenetic changes in adult cells or tissues, changes in gametes or early embryos can effectively influence the whole body (Martin *et al.*, 2011). Hence, according to the early origins hypothesis proposed by Barker and Hales, suboptimal intrauterine conditions during crucial periods of foetal growth could cause permanent changes via foetal programming in metabolism, hormone production and structures that can affect vulnerability to major diseases in adult life (Hales *et al.*, 1991). Indeed, cellular differentiation, tissue deposition, organ size and high-level neuro-endocrine control systems are all affected by developmental control factors, such as nutrition. Thus, scientists exploring the mechanisms of inheritance and evaluating an individual's risk of developing diseases such as obesity are interested in studying the programming events that occur before conception as well as during embryo development.

1.5 Obesity

Currently, obesity is one of the most important medical and global health problems, and it is defined by the World Health Organization (WHO) as a condition of excessive body fat accumulation to an extent that can cause detrimental health defects (World Health Organization, 2000). Obesity affects all genders and ages but is highly prevalent in women. Once considered a problem for affluent countries, this condition is now on the rise in countries of all economic backgrounds (World Health Organization, 2011). An economic boom in the Arabian Gulf region invariably also led to an increased incidence of nutritional health conditions and associated diseases. In Saudi Arabia, the prevalence of obesity in individuals from 15-64 years old was 66.2% in men and 71.4% in women. In the younger population, consisting of individuals from 18-30 years old, the prevalence of obesity was almost double for women than it was for men, at 18% and 10%, respectively (Ng *et al.*, 2011). A WHO survey conducted in 2010 among high-income populations showed that 33% was obese (men 28.6% and women 39.1%) (World Health Organization, 2011) and that the body mass index (BMI) had steadily been increasing in both genders over the previous several years (Figure 4). In the Arabian Gulf states, differences in obesity prevalence between genders can be due to multiple factors, such as marriage and childbirth. Additional explanations could include cultural norms for women, such as high-fat diets, 'plumpness' being considered beautiful and indoor lifestyles with limited access to vigorous activities being preferred (Ng *et al.*, 2011). According to WHO records, in 2014, the prevalence of obesity amongst 18+ adults from both sexes was 28.1%, particularly in the United Kingdom (World Health Organization, 2014).

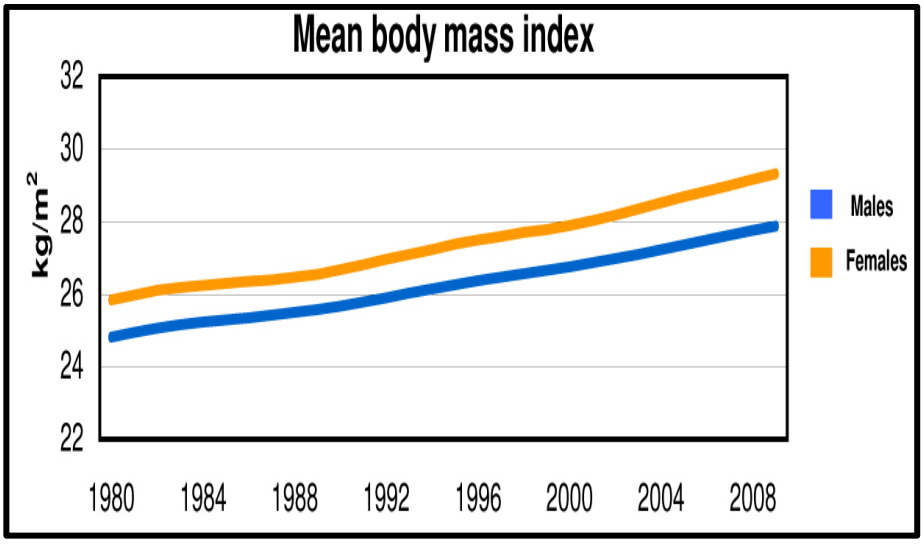

Figure 4. A steady increase in BMI was observed during the period from 1980-2008 in both sexes among high-income populations in Saudi Arabia (World Health Organization, 2011).

Obesity is one of the greatest global health challenges, particularly because it increases the risks of other chronic diseases, such as type 2 diabetes, hypertension, cardiovascular diseases, musculoskeletal disorders and some types of cancer. Therefore, with worldwide obesity more than doubling since 1980, this poses a significant threat to quality of life in general and places strain on healthcare budgets (World Health Organization, 2015). Hence, there is a strong need for a deeper understanding of the complex pathophysiology and factors contributing to this disease to facilitate the use of more effective intervention, prevention and treatment options and to reduce the worldwide burden of this disease. Obesity is a multifactorial disease with key elements that have been identified, including genetic factors and environmental factors that have been found to contribute to the cause and progression of the disorder (Day & Loos, 2011). Although candidate gene studies and genome-wide association studies (GWAS) have revealed several genetic loci associated with this disorder, the portion of obesity variation explained by these genetic variants is quite small (Hebebrand *et al.*, 2010; Sandholt *et al.*, 2012). The emerging field of epigenetics

paves a new path for understanding causes of complex diseases, such as obesity.

Adiposity can be measured using a diverse array of methods; some are as basic as only using a tape measure, and other methods involve the use of complex equations and expensive equipment. The most basic and commonly used method for measuring body fat is the BMI, which is a ratio of weight to height that is calculated as weight in kg divided by height in m^2 (kg/m^2) (Hu, 2008). BMI is an indirect measure of adipose tissue, as it does not distinguish between body fat and lean body mass. Furthermore, BMI does not take into account factors such as the greater muscle loss that occurs with age in women than in men or the higher fat content that tends to be observed in women than in men who have the same BMI; these factors often lead to misclassifications. However, several studies have shown that BMI has a strong correlation with body fat levels and obesity-related comorbidities, as measured by most accurate methods (Mei *et al.*, 2002; Sun *et al.*, 2010).

Due to simplicity, the use of anthropometric measurements, such as BMI, is considered to be one of the favoured methods for assessing obesity in both clinical settings and population studies. Because BMI is only a screening tool and not a diagnostic tool, determining whether excess weight imposes a health risk in individuals with a high BMI can be accomplished by a healthcare professional for verification via more accurate methods (World Health Organization, 2000). Although BMI is always calculated the same way, its interpretation depends on the gender, ethnicity and age of each individual (Prentice & Jebb, 2001). The WHO classifies a BMI ≤18.5 as underweight, a BMI from 18.6-24.99 kg/m^2 as normal, a BMI from 25-29.99 kg/m^2 as overweight and a BMI ≥ 30 kg/m^2 as obese (World Health Organization, 2000).

1.6 The link between epigenetics and obesity

The foetal programming hypothesis suggests that limited intrauterine nutrition can cause the foetus to programme its metabolism to anticipate a similar environment in adult life; hence, the foetus prepares for an adult life of limited nutrition, as well.

The uterine environment is under strict placental control, and by directly regulating foetal nutrient supply and growth, it plays an important role in foetal programming. The placenta constitutes the active interface between the maternal and foetal blood supplies. The placenta mediates the supply of nutrients to the foetus, secretes hormonal mediators of maternal and foetal physiology and acts as a modulator of developmental plasticity (Jansson & Powell, 2007).

Developmental plasticity refers to the set of changes that occur during development in response to variations in environmental cues, especially via the uterine environment or during infancy. Developmental plasticity is a normal biological and physiological function, and it allows for the foetus to develop appropriately according to environmental conditions. Having the capacity to alter phenotype according to the environment increases the probability of survival through to adulthood and reproduction. However, developmental plasticity requires an accurate prediction of the environment into which the offspring will be born and risks developmental mismatch. This means that an abundant nutritional diet postnatally can result in a metabolic imbalance or mismatch leading to a metabolic syndrome. However, studies using animal models have shown that both over-nutrition and under-nutrition during the gestational period can lead to similar metabolic disorders in adult life. Thus, the fact that opposite diet stresses lead to similar outcomes suggests the involvement of a common mechanism in both pathways (Li *et al.*, 2010).

Obesity is a metabolic disorder, and much attention has been focused on foetal programming as a facilitator of predisposition to this disorder in later life. Obesity has become a global concern and is one of the greatest public health challenges in the world. It is a multifactorial disorder comprising both genetic and environmental factors, and it can cause predisposition to many chronic diseases, including type 2 diabetes, hypertension, coronary heart disease and some types of cancer (Day & Loos, 2011). Numerous epidemiological studies have shown that over-nutrition, under-nutrition, stress or exposure to certain chemicals during gestation or lactation can lead to obesity (Bruce & Cagampang, 2011; Morris, 2009). Studies indicate that maternal obesity can lead to increased foetal insulin production and fat deposition (Gluckman *et al.*, 2008). Additionally, a considerable amount of data suggests that obese mothers confer a greater risk to their children of developing metabolic disorders, even during childhood (McIntyre *et al.*, 2012). Interestingly, it has also been shown that under-nutrition or famine during gestation and early infancy is associated with obesity in the adult offspring (Ravelli *et al.*, 1976). Although details of the exact mechanisms involved have remained limited, several animal studies have gained insight into some mechanisms involved; most importantly, these studies have established a link between the early-life programming and altered body composition and metabolism of adult offspring.

A study by Burdge *et al.* (2007) demonstrated that feeding a protein-restricted diet to rats during pregnancy in the F_0 generation increased the expression of peroxisome proliferator-activated receptor alpha *(Pparα)* and glucocorticoid receptor 1 *(GR1)*. The study also found increased expression of the corresponding hepatic target genes, acyl-CoA oxidase *(AOX)* and phosphoenolpyruvate carboxykinase *(PEPCK)*, in the F_1 and F_2 offspring. This increase in expression coincided with reduced methylation of the *Pparα* and *GR1* promoters in the liver, which was induced in the F_1 offspring by the maternal protein-restricted diet and was, interestingly, passed on to the F_2 generation.

This study demonstrated the transmission of a modified metabolic phenotype caused by changes in the prenatal environment to both the first-generation and second-generation offspring as a heritable epigenetic mark. *Pparα* is a ligand-activated transcriptional activator that regulates the expression of genes crucial for lipid and lipoprotein metabolism. Another investigation by Drake *et al.* (2005) used a model of rats exposed to dexamethasone, which is a poor substrate for 11β-hydroxysteroid dehydrogenase type 2 (11β-HSD 2) that leads to exposure of the foetus to high levels of glucocorticoids. The exposed rats showed reduced birth weight associated with high hepatic *PEPCK* activity, which was constant in the first-generation male offspring. The study also demonstrated that even in the absence of the initial stimulus, the reduced birth weight and high *PEPCK* activity were also transmitted to the second-generation male offspring.

Studies involving humans have also suggested a causal link between epigenetics and obesity. A human study of two cohorts involving screening the methylation status of 68 candidate genes from UC-derived DNA revealed that elevated methylation at Retinoid X receptor-α *(RXRA)* strongly correlated with increased adiposity in late childhood and was subsequently associated with maternal carbohydrate consumption (Godfrey *et al.*, 2011). The methylation of endothelial nitric oxide synthase *(eNOS)* was associated with increased adiposity in one cohort. The hyper-methylation of CpG islands in both *eNOS* and *RXRA* and the hypo-methylation of superoxide dismutase 1 *(SOD1)* were strongly correlated with fat distribution. These findings not only confirmed that the early pregnancy environment can affect offspring adiposity but also indicated that epigenetic measurements in neonates such as these are more accurate indicators of later obesity than the conventional measures, such as body weight and BMI. Another independent study by Relton *et al.* (2012), involving the use of peripheral blood for DNA methylation profiling in two cohorts, revealed associations between altered gene expression and

childhood body composition and size. Several genes involved in the cell cycle and proliferation, including cyclin-dependent kinase inhibitor 1C *(CDKN1C)* and nidogen-2 *(NID-2)*, showed differential methylation and expression levels.

Research has also indicated that when maternal fat intake is increased during pregnancy and lactation, the proportion of polyunsaturated fatty acids (PUFAs) in the liver of the adult offspring is changed. This observation was accompanied by a varied epigenetic regulation of fatty acid desaturase 2 *(FADS2)*, which encodes Δ6 desaturase, an enzyme involved in the rate-limiting step of PUFA synthesis (Hoile *et al.*, 2013). The high-fat diet induced an increased methylation of specific CpG sites in the promoter region of *FADS2*, which was associated with a reduced expression of this gene in the offspring (Hoile *et al.*, 2013; Kelsall *et al.*, 2012). Apart from being vital components of the cell membrane, PUFAs are further metabolized into more highly unsaturated fatty acids that are utilized in the synthesis of lipid second messengers (Burdge & Calder, 2006).

In addition to maternal diet and other environmental factors that are likely to exert heritable, epigenetic effects in the offspring, paternal factors can also exert an influence. The testes are formed during early development, and the germ cells from which sperm ultimately differentiate are sequestered during foetal development; thus, it is likely that epigenetic changes can also occur in paternal sperm from conception of the father through to the production of sperm in adult life. Because spermatogenesis occurs over 2-3 months, environmental factors affecting the father during this time and immediately prior to conception can result in changes to the sperm that can also affect the offspring. For example, evidence suggests that epigenetic inheritance of paternal origin can result in offspring having a greater risk for obesity (Drake & Liu, 2010).

1.6.1 Global methylation and Obesity

Global methylation is an overall measure of cytosine methylation in the genome. However, for ease of measurement, the methylation status of repetitive elements, such as Alu and long interspersed nucleotide elements (LINE1), which make up approximately 50% of the genome, is frequently used as a substitute to represent the overall genome methylation; these metrics have been found to correlate well with the overall genomic cytosine methylation (Weisenberger *et al.*, 2005). The importance of epigenetic alterations in human pathology was first identified in cancer (Laird & Jaenisch, 1996). Global hypo-methylation or reduced global methylation has been associated with cancer causation and progression, and because epigenetic modifications are typically reversible, thereby allowing a malignant cell to revert to a more normal state, epigenetic marks have become valuable targets for chemotherapy (Huang *et al.*, 2011). In contrast, less is known about the impact of global methylation on other human diseases, such as obesity. Although numerous studies have been conducted to investigate the association between global methylation and obesity, the results have been inconsistent; some studies have demonstrated that both global hyper-methylation and global hypo-methylation are associated with increased BMI, which is the most commonly employed method of measuring obesity. In a study based on 323 women, hypo-methylation of Alu elements was associated with increased BMI (Jintaridth *et al.*, 2013). Similarly, another study conducted in women found that reduced methylation of LINE1 elements was associated with increased risk for both obesity and insulin resistance. However, one limitation of this study is that the association was observed in women with lower levels of the dietary methyl donor folate (Piyathilake *et al.*, 2013). In contrast, in a study consisting of both men and women of Samoan origin, LINE1 methylation in peripheral blood showed a significant positive association with BMI (Cash *et al.*, 2011). Similarly, in a study conducted in Singapore

also including both men and women, a positive association was found between global methylation in peripheral blood leukocytes and BMI (Kim *et al.*, 2010). Another study demonstrated that global methylation levels in the placenta were higher in obese women than those in non-obese women (Nomura *et al.*, 2014). Because there is no consistent pattern of association between global methylation and obesity shown by the studies that have performed to date, it is difficult to determine what global methylation changes might occur in obesity. Multiple factors, including gender, ethnicity and lifestyle choices, such as tobacco use and diet, have been found to influence the methylation levels of the whole genome (Zhang *et al.*, 2011). Therefore, even though some studies have taken these factors into account, all the confounding factors are often not known, which may account for the inconsistent results between studies. The relationship between obesity and DNA methylation might be better understood by investigating the global methylation status of native cells, particularly from early passages, and this is the area of interest.

1.7 Objectives

Historically, UCs have been considered clinical waste and were generally discarded after birth. Recently, UCs have been recognized as a rich source of MSCs that can be used for therapeutic applications, although it has been suggested that an abnormal metabolic environment during pregnancy might induce epigenetic changes that globally alter gene expression in UC tissues, rendering them unsuitable for cellular therapy. Metabolic diseases, such as obesity, might affect the stem cell niche or the properties of MSCs, but no experimental evidence has demonstrated this effect in WJ-MSCs.

The overall goal of this study was to determine the effects of an abnormal metabolic environment on WJ-MSCs using UCs from healthy obese donors. The objectives of the study were to

1. Determine the optimal WJ-MSC isolation method (enzymatic versus explant).
2. Determine the cell behaviours, such as initial outgrowth and cell proliferation, of WJ-MSCs in tissue culture.
3. Determine the expression of MSC surface markers.
4. Determine the effect of obesity on the differentiation potential of WJ-MSCs into three mesodermal lineages: adipocytes, chondrocytes and osteoblasts.
5. Determine the effect of obesity on the immunomodulatory properties of WJ-MSCs.
6. Determine differences in the global DNA methylation profile of WJ-MSCs from obese and non-obese donors.
7. Determine differences in the gene expression profile of WJ-MSCs from obese and non-obese donors.

Chapter 2

Materials and Methods

2. Materials and Methods

2.1 Patient selection

Human UC samples were collected at the time of delivery from mothers who had provided consent (REC reference 12/NE/0371). The UC samples were collected from full-term infants who were delivered by elective Caesarean section at Guy's and St. Thomas' NHS Foundation Trust.

WJ samples were chosen based on their suitability for the investigation, which is looking at the impact of obesity and its contribution to an abnormal maternal metabolic environment during pregnancy. This study further investigates whether the interaction with such an abnormal metabolic environment during pregnancy changes the DNA methylation profile of MSCs. Any significant outcomes could be clinically relevant and could potentially render MSCs from such donor types unsuitable for clinical use in multiple recipients. During their first-trimester prenatal check-up at the clinic, healthy mothers were classified as obese if they had a BMI >30 kg/m^2, and healthy mothers with a BMI from 19-25 kg/m^2 were classified as non-obese. The total number of UCs recovered from the mothers after childbirth was 14 (n=7, non-obese; n=7, obese). All deliveries were without complications; the babies and mothers were healthy, with no apparent abnormalities. The placentas and UCs were assessed by midwives for any abnormalities, and all tissues were confirmed to have a normal appearance. The majority of the participating women did not smoke or drink during pregnancy. Only one woman in the healthy obese group (subject O2) was a smoker and reported smoking

one to four cigarettes per day during her pregnancy.

All women who were classified as non-obese had Caucasian ethnicity and were aged between 35 and 43 years. The obese group comprised three women who were of Caucasian origin (aged 34, 35 and 39), two Black-African women (aged 34 and 38) and two Black-Caribbean women (aged 28 and 35); a summary of the patient information is shown in Table 3.

Table 3. Non-obese and obese donor age, BMI and ethnicity (N=non-obese, O=obese).

Non-obese				Obese			
Donor	**Age**	**BMI**	**Ethnicity**	**Donor**	**Age**	**BMI**	**Ethnicity**
N1	43	24	Caucasian	**O1**	39	36	Caucasian
N2	35	21	Caucasian	**O2**	35	30	Caucasian
N3	36	22	Caucasian	**O3**	34	39	Caucasian
N4	35	21	Caucasian	**O4**	34	30	Black-African
N5	38	25	Caucasian	**O5**	38	45	Black-African
N6	39	23	Caucasian	**O6**	28	41	Black-Caribbean
N7	39	23	Caucasian	**O7**	35	35	Black-Caribbean

2.1.1 Sample size justification

Because no *a priori* information was available from any publications to assist with sample size estimates, a sample size of twelve per group was considered appropriate for this pilot investigation and justified to be sufficiently large to provide feasibility for the estimate of variance and precision. Others can use the sample size information from this study to formally calculate a sample size for future studies (Julious, 2005).

The anticipated recruitment rate was two subjects per month in each group from a single site (Guy's and St. Thomas' NHS Foundation Trust).

The target recruitment for this study was not met for several reasons. Despite efforts made to obtain consent by involving midwives and providing patient leaflets explaining the aims of the study, most women were very reluctant to consent to participate in the study; women who belonged to the healthy obese group were particularly reluctant. Some women simply declined to participate without giving a reason. There were also challenges in identifying healthy obese participants because most obese women had other co-morbidities that kept them from meeting the study eligibility criteria. Moreover, there was a high demand for the participants to participate in other research projects. I was therefore permitted limited time to recruit participants, resulting in one-day-per-week access to participants at the hospital. The most common reasons for not consenting to participate in the study were as follows:

- Subject already participating in other study
- Religious beliefs
- Misconceptions regarding genetic testing
- Plan to bank UCs for future use

The participant consent process did not offer any monetary incentives, such as gift vouchers or a prize draw, for the subjects, nor any financial recompense for their time. The lack of rewards for potential participants for our study was an oversight on our part and may have contributed to a low recruitment rate compared with other studies that had offered such compensation for their participants.

The study timeline allowed six months for the recruitment of participants to allow sufficient time for meeting other milestones, such data collection, processing, analysis

and results dissemination. The study timeline also included four weeks to process each cord after collection.

2.2 Isolation and culture of WJ-MSCs from UCs (enzymatic versus explant) and assessment of initial outgrowth and proliferation rate

WJ-MSCs can be isolated and expanded from UCs using two different approaches: an enzymatic digestion method (Fong *et al.*, 2007) or an explant method (La Rocca *et al.*, 2009). In this study, I applied both isolation methods to each cord and proceeded with the isolation method that resulted the most successful outcome. After identifying the optimal isolation method, the first outgrowth and proliferation rates were assessed, and differences and similarities were compared for obese and non-obese donors.

2.2.1 Enzymatic protocol versus explant protocol for WJ-MSC isolation

The first five cords (N1, N2, O1, O2, and O3) that were collected were used to determine the optimum isolation method for WJ-MSCs from UCs. Both explant and enzymatic digestion procedures were used in parallel for isolation and culturing of WJ-MSCs from each UC. Once the optimal isolation and expansion method was determined, it would be used for the remaining UCs that are expected to be processed during the course of this thesis.

After the UC samples were retrieved, they were kept in phosphate-buffered saline (PBS) supplemented with 10-µg/ml gentamycin and 0.25-µg/ml amphotericin B (Life Technologies, UK). The samples were then processed within 2-4 hours from the time they were collected as described below. Each UC was cut into equal halves; one half

of the cord was processed using the enzymatic digestion method, and the other half was processed using the explant method.

The isolation of WJ-MSCs from UCs using the enzymatic digestion method followed the procedure reported by Fong *et al.* (2007) and her group. The UC was washed to remove any blood and then cut into 2-cm segments. Each segment was cut into very fine pieces under aseptic conditions using a pair of scissors. The resulting pieces from the five cords (N1, N2, O1, O2, and O3) were placed in separate 100-mm Petri dishes (Corning, UK) containing enzymatic solution and incubated for different durations (60 minutes, 90 minutes, 120 minutes, 150 minutes and 180 minutes) on a gentle rocking platform (Eppendorf, UK) at 37°C. The enzymatic solution was composed of 2-mg/ml collagenase type I, 2-mg/ml collagenase type IV and 100-IU/ml hyaluronidase (all from Sigma-Aldrich, UK) in DMEM containing 4.5-g/L glucose and L-glutamine (Life Technologies, UK).

The next stage of the enzymatic method included the use of DMEM containing the UC, which was transferred to a 15-ml Falcon tube (Fisher Scientific, UK) and re-suspended using a 10-ml sterile pipette (Dutscher Scientific, UK). The tube was centrifuged (Thermo Scientific) at 1,200 rpm for 5 minutes, after which the supernatant was discarded, and the cell pellet was repeatedly washed by re-suspending it in fresh DMEM. After the washes, the pellet was re-suspended in fresh DMEM supplemented with 10% FBS (HyClone, New Zealand), 10-µg/ml gentamycin and 0.25-µg/ml amphotericin B in a T25 flask (25-cm^2) (Falcon, UK) and maintained in an incubator (Thermo Scientific) at 5% O_2, 5% CO_2 and 37°C. Cell growth was assessed visually for three weeks and controlled by changing the medium three times a week.

The other half of the UC segment was processed using the explant method. Under sterile conditions and using aseptic techniques, each UC segment was initially washed with PBS to remove the blood. The samples were dissected into 3-cm-long segments

and then further dissected into fragments approximately 1-cm^2 in size, which were inspected to confirm that they were free of blood vessels. Then, 10 small fragments were seeded on a 100-mm Petri dish with the WJ side of each fragmented UC facing down on the plastic and they were left exposed to air for 10 minutes to facilitate the attachment. The explanted fragments were grown in 15-ml of DMEM containing 4.5-g/L glucose and L-glutamine supplemented with 10% FBS and gentamycin/amphotericin B solution. The Petri dish was then placed in an incubator with 5% O_2 and 5% CO_2 at 37°C (Badraiq *et al.*, 2015). The culture medium was replaced with fresh medium two to three times a week, and cell growth was assessed visually and controlled for three weeks.

2.2.2 Assessment of initial out growth and proliferation rate of the UC received from obese and non-obese donors using the explant method

The explant method was selected as the preferred isolation method for this study. The initial growth of fibroblast-like cells was visually assessed in samples from both non-obese and obese donors using light microscopy (Olympus).

The cells had reached confluence (80-90%) in the explanted cords after 3 weeks; colonies of cells were visible, and the cord segments were floating in the medium. The culture medium containing the floating cord pieces was decanted, and then, the adherent cells were ready for harvesting. The adherent cells were rinsed once with PBS containing ethylenediamine tetraacetic acid (PBS-EDTA) (Lonza, UK) and were subsequently detached by exposing them to 5-ml of a solution containing the adherent cell dissociation product TrypLE (Life Technologies, UK) for approximately 5 minutes in

an incubator set at 37°C with 5% CO_2 to allow the solution to become activated and to cause the adherent cells to detach from the plastic surface. Light microscopy was used to confirm that the cells had detached from the surface. Once the cells were observed to be floating, an equal volume of wash solution only containing DMEM was immediately added to inactivate the TrypLE. The cells were then collected in a tube and were centrifuged for 5 minutes at 12,000 rpm. The supernatant was eluted, and the pelleted cells were gently re-suspended in fresh medium and mixed thoroughly to eliminate aggregates and to produce a uniform suspension. The total population recovered was determined by cell counting; 10-µl of the cell suspension from each tube was collected and loaded below a coverslip that sits firmly on the chamber of a haemocytometer instrument (Hausser). The slide was then examined under a microscope, and the number of cells present in the four corner squares of the grid was counted using a cell counter. The total cell counts were calculated using the following formula:

$$\text{Total cells/ml} = \frac{\text{Total cells counted} \times \text{dilution factor} \times 10{,}000 \text{ cells/ml}}{\text{Number of squares}}$$

At this point, the cells were assigned a population doubling stage figure of 0 (PD0). The PD time was calculated using the formula PD=[log(A/B)]/0.301, where A is the number of harvested cells, and B is the number of cells seeded onto the plate. The cells from PD0 were re-plated in a T75 flask (75-cm^2) (Falcon, UK) for further expansion in an incubator with 5% O_2 and 5% CO_2 at 37°C. When the cells reached confluence (80-90%), they had reached stage PD1 and were harvested and re-suspended for cryopreservation in a medium that consisted of FBS supplemented with 10% dimethyl sulphoxide (DMSO) (Sigma-Aldrich, UK) for cryopreservation. The cells were aliquoted

into cryotubes (Thermo Scientific, UK) and placed in a freezing container (Sigma-Aldrich, UK) at -80°C for 24 hours; the cells were then transferred into liquid nitrogen for longer term storage until future use (Badraiq *et al.*, 2015). The proliferation rate (PD time), which represents the ability of cells to double their population, was evaluated between PD1 and PD2 for the two groups.

The statistical analysis methods used to describe and compare the growth and proliferation rates between obese and non-obese groups are described in the statistical analyses section (2.3.4).

2.3 Comparison of the properties of WJ-MSCs derived from obese and non-obese subjects

Once WJ-MSCs had been recovered from cords collected from obese and non-obese subjects with the explant method, properties such as immunophenotypic properties, differentiation properties and immunomodulatory properties were evaluated and comparatively analysed for similarities and differences between the two groups.

2.3.1 Immunophenotypic comparative analysis of WJ-MSCs isolated from obese and non-obese subjects

Cell surface epitope profiles were analysed using flow cytometry to compare WJ-MSCs isolated from obese and non-obese donors. Cells from PD2 of fourteen different WJ-MSC cultures were harvested, as described previously (section 2.2.2). The supernatant was aspirated before re-suspending the cell pellet in cold PBS containing 10% FBS.

Cell suspension aliquots (100-µl, approximately 1×10^6 cells) were prepared. Antibodies listed in Table 4 (Miltenyi Biotec and BD Biosciences, UK) were added to the cell suspensions at a final concentration of 1:50. The cells were gently vortexed (Whirlimixer, UK) and then incubated for 10 minutes at 4°C in the dark. In addition, separate WJ-MSC aliquots not stained with antibodies were prepared to serve as a negative control; these samples were used to determine the WJ-MSC population gate. Four compensation bead tubes (Miltenyi Biotec, UK) were prepared in parallel; one tube contained blank beads as a negative control, and the other three individual tubes each contained anti-human Igκ beads conjugated with fluorescein isothiocyanate (FITC), phycoerythrin (PE) and allophycocyanin (APC) as positive controls. All four

bead tubes were incubated for 10 minutes in the dark at room temperature. After the incubation step, the stained cells, unstained cells and the beads were washed once with 1,000-µl of cold PBS/10% FBS. The PBS was decanted, and the cells and beads were then re-suspended in 500-µl of PBS/10% FBS per tube and were analysed on a FACSCanto™ II using DIVA software (BD Biosciences, Biomedical Research Centre (BRC) Flow Cytometry Core, King's College London). To confirm that specific CD45 and CD34 markers were being detected, a Kasumi cell line (acute myeloid leukaemia cells) was used as a positive control for flow cytometry, and clinical-grade BM-MSCs were also used as a positive control to confirm the antibodies identified by MSC flow cytometry (Devito *et al.*, 2014).

The flow cytometry analysis was based on the MSC profile that was determined by the forward scatter (FSC), known to correlate with cell size and shape. The side scatter (SSC) correlates with cell granularity. Because the FSC and SSC differ for each cell type, the combination helps improve the identification of the different cell types. Following staining and cytometry, the differences between the non-obese and obese groups were compared for each marker. The statistical analysis methods used to describe and compare the proportions of positive markers between obese and non-obese groups are described in the statistical analysis section (2.3.4).

Table 4. Antibodies used for cell surface epitope profiles and isotypes for flow cytometry.

MSC Markers	Isotype
CD90-FITC	Mouse IgG1
CD73-PE	Mouse IgG1
CD105-APC	Mouse IgG1
CD44-FITC	Mouse IgG1
CD29-APC	Mouse IgG1κ
CD56-APC	Mouse IgG1
CD45-FITC	Mouse IgG2a
CD34-PE	Mouse IgG2a
CD271-FITC	Mouse IgG1
Anti-MSCA-1	Mouse IgG1

2.3.2 The differentiation properties of WJ-MSCs from obese and non-obese donors

The ISCT describes the minimal criteria that are required to positively identify MSCs; one of the elements includes the ability of these cells to differentiate into adipocytes, osteoblasts and chondrocytes (Dominici *et al.*, 2006). Therefore, the cells recovered from the donors were evaluated to determine whether they met the criteria set for MSCs by the ISCT. MSCs from all donors differentiated into adipocytes, chondrocytes and osteoblasts under differentiation conditions; furthermore, their commitment towards differentiation between obese and non-obese groups was also compared. Firstly, cells were differentiated, and they were then tested for the presence of targeted gene expression using RT-PCR and stained to confirm their differentiation state. For

both gene expression and staining experiments, undifferentiated cells from all fourteen cell lines were included in the assays as a control.

2.3.2.1 Adipogenesis differentiation

The StemPro® adipogenesis differentiation kit (Gibco, UK) was designed for the adipogenic differentiation of MSCs. In these experiments, it was used to induce the adipogenesis of cells from obese and non-obese donors and to compare the ability of the cells from both groups for their level of commitment towards adipogenicity.

Once WJ-MSCs cultures had reached 70-80% confluence using standard medium, the cells were washed gently with PBS-EDTA and detached using TrypLE solution, as described previously in section 2.2.2. The collected cells were re-plated onto a 4-well plate (Thermo Fisher, UK) for the staining procedure and on a 6-well plate (Thermo Fisher, UK) for the gene expression assay. The cells were incubated in DMEM supplemented with 10% FCS with 5% O_2 and 5% CO_2 at 37°C. After 2 days, the medium was replaced with complete StemPro adipogenesis differentiation medium. The adipogenic medium was changed every 3-4 days. The active components and their concentrations in the kit that were used to promote adipogenic differentiation were proprietary information of the manufacturer and hence, were unknown.

After incubation for 14 days under differentiation conditions, the cells cultured for the staining procedure were washed with PBS and fixed with 4% formaldehyde solution (Sigma-Aldrich, UK) for 30 minutes at room temperature. After fixation, the cells were washed twice with PBS and incubated for 30 minutes in a 1:100 dilution of LipidTOX™ green neutral lipid stain (Invitrogen, UK). LipidTOX™ green neutral lipid stain detects cellular lipids. After incubation, the cells were washed twice with PBS and then mounted in Vectashield Mounting Medium supplemented with 1.5-µg/ml 4',6-diamidino-2-phenylindole (DAPI) (Vector Labs, UK). The cells were then visualized using an

epifluorescence microscope (Nikon ECLIPSE 50i) for qualitative analysis, and three black and white images were chosen for each line. The signals in the images were quantified using ImageJ64 software by calculating the percentage of cellular lipids per cell to obtain the total surface area of LipidTOX™ positive droplets per number of nuclei in one field. For each of the lines, I screened on average about 900 cells per each of the three fields.

For the gene expression assay, cells were also collected from 6-well plates after 14 days of culturing under differentiation conditions. RNA was extracted using an RNeasy mini kit (Qiagen, UK) according to the manufacturer's instructions; all necessary reagents were provided in the kit. Briefly, 600-µl of RLT buffer was added to the well for direct cell lysis. The cells were collected into 1.5-ml micro-centrifuge tubes (Ambion, UK), and the mixtures were vortexed for 1 minute, resulting in a homogenous solution; this step confirmed adequate cell lysis. The cell lysates were washed with 600-µl of 70% ethanol (Sigma-Aldrich, UK) and mixed thoroughly by pipetting. The lysates were carefully transferred to the RNeasy spin columns that had been placed in 2-ml collection tubes and were centrifuged in a bench-top micro-centrifuge (Eppendorf) at 10,000 rpm for 15 seconds. The collection tubes containing the flow-through were discarded, and the spin columns containing the RNA bound to the silicon filter were retained. Then, 700-µl of RW1 buffer was added on top of the RNA bound filter, and the columns were centrifuged at 10,000 rpm for 15 seconds; then, the columns were transferred to new 2-ml collection tubes. The RNA-bound filters were washed with 500-µl of RPE buffer and were centrifuged at 10,000 rpm for 15 seconds. A further washing step was performed by adding another 500-µl of RPE buffer and re-centrifuging the column at 10,000 rpm for 2 minutes, making sure the flow-through was discarded after each spin. The collection tubes were replaced with new tubes to prevent carryover from RPE buffer, and the columns were dried further by an additional centrifugation

step at the maximum speed of 14,000 rpm for 1 minute. Finally, the RNeasy spin columns were placed in sterile 1.5-ml micro-centrifuge tubes, and 40-µl of RNeasy-free water was added directly to the spin column membrane to elute the RNA; then, the columns were centrifuged at 10,000 rpm for 1 minute. The spin columns were discarded at this stage because the eluted RNA had been recovered in the micro-centrifuge tubes. The concentration of the extracted RNA samples was determined using a Qubit fluorometer (Invitrogen; the device was provided by BRC Genomics Core, King's College London), and the RNA samples were stored at -80°C until use.

For the Qubit RNA quantification assay, the Qubit® RNA BR assay kit (Life Technologies, UK) was used. A working solution was prepared by diluting Qubit RNA BR reagent in Qubit RNA BR buffer to 1:200; both solutions were from the reagent kit. The final volume in either the standard or sample tube was 200-µl for the assay. Two standard tubes were individually prepared by mixing 190-µl of the working solution with 10-µl of standard-1 solution in tube 1 and 10-µl of standard-2 solution in tube 2. Next, sample tubes were prepared by combining 199-µl of working solution with 1-µl of sample. The tubes containing the diluted RNA samples were then vortexed for 2-3 seconds and incubated at room temperature for 2 minutes. The standard curve for the assay was generated by taking a reading first from standard-1 and then from standard-2; thereafter, RNA in the tubes was quantified using the Qubit fluorometer.

Next, 1000-ng of RNA was used for cDNA synthesis (Bio-Rad, UK). For optimal cDNA synthesis, each 20-µl reaction should have 1000-ng of RNA, 4-µl of 5× iScript reaction mix, and 1-µl of iScript reverse transcriptase prepared to a total 20-µl volume with nuclease-free water (Table 5). The reaction mix was incubated in a thermocycler (G-Strom) using the following conditions: 5 minutes at 25°C, 30 minutes at 42°C, 5

minutes at 85°C and held at 4°C. The resulting synthesized cDNA from each RNA sample was kept at -20°C until further use.

Table 5. The required mixture composition of RNA samples from adipocytes for the cDNA protocol (N=non-obese, O=obese).

Sample number	RNA volume for 1000-ng (µl)	5× iScript Reaction mix (µl)	iScript reverse Transcriptase (µl)	Water (µl)	Total (µl)
N1	3.1	4	1	11.9	20
N2	5.4	4	1	9.60	20
N3	4.2	4	1	10.8	20
N4	3.3	4	1	11.7	20
N5	3.6	4	1	11.4	20
N6	3.0	4	1	12.0	20
N7	2.4	4	1	12.6	20
O1	2.3	4	1	12.7	20
O2	2.9	4	1	12.1	20
O3	4.1	4	1	10.9	20
O4	5.7	4	1	9.30	20
O5	5.0	4	1	10.0	20
O6	4.6	4	1	10.4	20
O7	4.7	4	1	10.3	20

The RT-PCR assay using the synthesized cDNA was performed on the Roche LightCycler 480 RT-PCR instrument (Roche), 2X SYBR green master mix (Roche, UK) was included in the reaction. Primer pairs for adipogenesis target gene, fatty acid binding protein-4 (*FABP4)* (Table 8). A 10-µl reaction was prepared for each sample by adding 90-ng/µl of cDNA, 10-µM of each forward and reverse primers for the gene of

interest, 2X SYBR green master mix and nuclease-free water to reach to a final volume of 10-µl. After that, the reaction mix was placed in a thermocycler for a pre-incubation step for 5 minutes to denature the components. The amplification step consisted of 45 cycles at 95°C for 10 seconds, 10 seconds at 60°C and 10 seconds at 72°C, followed by a dissociation curve run consisting of a 3-step procedure at 95°C for 5 seconds, 65°C for 60 seconds, and a gradual increase in temperature at a rate of 0.11/second up to 97°C. Next, the tubes were cooled at 40°C for 30 seconds. Undifferentiated WJ-MSCs were also included as a control in parallel with the assay. The data were collected and analysed using the comparative threshold cycle method with TATA-box binding protein *(TBP)* and glucuronidase beta *(GUSB)* as reference genes (Table 8).

The statistical analysis methods used to describe and compare adipogenicity between obese and normal groups are described in the statistical analysis section (2.3.4).

2.3.2.2 Chondrogenesis differentiation

The StemPro® chondrogenesis differentiation kit (Gibco, UK) was used for the chondrogenic differentiation of MSCs. In this experiment, the kit was used to induce chondrogenesis of cells from obese and non-obese donors and to compare the ability of the cells from both groups to commit towards chondrogenicity.

Briefly, once the WJ-MSCs reached confluence, the cells were washed and detached. Again, the collected cells were re-plated onto a 4-well plate and a 6-well plate for different purposes. For staining purposes, a micro-mass culture was generated by seeding 3-µl droplets of cell suspension in the centre of the well of a 4-well plate. After cultivating the micro-mass culture for 2 hours in 5% O_2 and 5% CO_2 at 37˚C, warmed complete StemPro chondrogenesis medium was added to the culture. For gene

expression purposes, the cells were re-plated as usual in 6-well plates and incubated in DMEM/10% FCS. After 48 hours, the medium was replaced with complete StemPro chondrogenesis differentiation medium. For both cultures, the chondrogenic medium was changed every 2-3 days. The names and concentrations of the active components in the kit that promote chondrogenic differentiation were proprietary information of the manufacturer and were not available.

After incubation for 14 days under differentiation conditions, the cells designated for staining were washed and fixed. After fixation, the cells were washed and incubated for 30 minutes with Alcian blue solution pH 1.0 (Abcam, UK). Blue staining indicates proteoglycan synthesis by chondrocytes. The cells were washed with PBS after the staining step and then left for drying. The cells were then visualized, and images were captured using a fluorescence microscope (Zeiss Axioskop) for qualitative analysis.

The sample preparation for gene expression followed the same method as explained in section (2.3.2.1). After 14 days under differentiation conditions, the cells were collected from 6-well plates, RNA was extracted, and the eluate that was recovered was quantified. Then, cDNA synthesis was performed for the RT-PCR assay (Table 6). Primer pairs for the chondrogenesis target gene, collagen type XI alpha 1 chain *(COL11A1)*, are reported in Table 8. RNA was extracted, and cDNA was synthesized from differentiated cells; cDNA resulting from undifferentiated cells was included as a control for the RT-PCR.

The statistical analysis methods used to describe and compare chondrogenicity between obese and normal groups are described in the statistical analysis section (2.3.4).

Table 6. The required mixture composition of RNA samples from chondroocytes for the cDNA synthesis protocol (N=non-obese, O=obese).

Sample number	RNA volume for 1000-ng (µl)	5× iScript Reaction mix (µl)	iScript reverse Transcriptase (µl)	Water (µl)	Total (µl)
N1	1.9	4	1	13.1	20
N2	3.1	4	1	11.9	20
N3	7.1	4	1	7.90	20
N4	2.5	4	1	12.5	20
N5	4.2	4	1	10.8	20
N6	4.4	4	1	10.6	20
N7	3.7	4	1	11.3	20
O1	3.4	4	1	11.6	20
O2	2.2	4	1	12.8	20
O3	2.6	4	1	12.4	20
O4	3.7	4	1	11.3	20
O5	4.7	4	1	10.3	20
O6	6.3	4	1	8.70	20
O7	3.4	4	1	11.6	20

2.3.2.3 Osteogenesis differentiation

The StemPro® Osteogenesis differentiation kit (Gibco, UK) was selected for the osteogenic differentiation of MSCs. The kit was designed to induce osteogenesis of cells from obese and non-obese donors and to compare the ability of the cells from both groups and their level of commitment towards osteogenicity.

Once WJ-MSCs reached confluence, the cells were washed and detached. The collected cells were re-plated onto a 4-well plate and a 6-well plate, then incubated in DMEM/10% FCS. After 2 days, the medium was replaced with complete StemPro osteogenesis differentiation medium. Fresh osteogenic medium was replaced in the

plates every 3-4 days. The active components and their concentrations in the kit that were used to promote osteogenic differentiation were proprietary information of the manufacturer, and hence, were unknown.

After incubation for 21 days under differentiation conditions, the cultured cells underwent fixation for staining purposes. After fixation, the cells were washed with PBS and then incubated for 30 minutes with Alizarin Red staining solution (Sigma, UK). Calcium deposits were an indication of successful differentiation of MSCs into osteoblasts. After incubation, the cells were washed to remove excess stain and then dried to remove excess water. The cells were qualitatively analysed and visualized under a fluorescence microscope, and cell images were captured.

For the gene expression procedure, the cells were collected 21 days after being subjected to differentiation conditions. RNA was extracted from the cells, quantified and then used to synthesize cDNA (Table 7), as explained previously (in section 2.3.2.1). RT-PCR was performed using primer pairs for the osteogenesis gene runt related transcription factor 2 *(RUNX2)* (Table 8). RNA was extracted, and cDNA was synthesized from undifferentiated cells; the resultant cDNA was included as a control for the procedure.

The statistical analysis methods used to describe and compare osteogenicity between obese and normal groups are described in the statistical analysis section (2.3.4).

Table 7. The required mixture composition of RNA samples from osteoblasts for the cDNA protocol (N=non-obese, O=obese).

Sample number	RNA volume for 1000-ng (µl)	5× iScript Reaction mix (µl)	iScript reverse Transcriptase (µl)	Water (µl)	Total (µl)
N1	2.7	4	1	12.3	20
N2	4.8	4	1	10.2	20
N3	2.5	4	1	12.5	20
N4	6.0	4	1	9.00	20
N5	3.3	4	1	11.7	20
N6	2.9	4	1	12.1	20
N7	5.0	4	1	10.0	20
O1	5.2	4	1	9.80	20
O2	3.3	4	1	11.7	20
O3	3.4	4	1	11.6	20
O4	3.0	4	1	12.0	20
O5	3.8	4	1	11.2	20
O6	1.6	4	1	13.4	20
O7	2.5	4	1	12.5	20

Table 8. Primer sequences for differentiation (Life Technologies, UK).

FABP4-F	5'-AGCACCATAACCTTAGATGGG-3'	Adipogenesis
FABP4-R	5'-CGTGGAAGTGACGCCTTTCA-3'	
COL11A1-F	5'-CCAGCGTCTGTTGGTTCAGT-3'	Chondrogenesis
COL11A1-R	5'-CAGCTTCCCCTTTCTCTCCT-3'	
RUNX2-F	5'-TTACTTACACCCCGCCAGTC-3'	Osteogenesis
RUNX2-R	5'-TATGGAGTGCTGCTGGTCTG-3'	
TBP-F	CAGCGTGACTGTGAGTTGCT	Reference gene
TBP-R	TGGTTCATGGGGAAAAACAT	
GUSB-F	AAACGATTGCAGGGTTTCAC	Reference gene
GUSB-R	CTCTCGTCGGTGACTGTTCA	

2.3.3 The immunomodulatory properties of WJ-MSCs from obese and non-obese subjects

The immunomodulatory activities of WJ-MSCs isolated from obese group were assessed and compared with the immunomodulatory activities of WJ-MSCs isolated from the control group.

T75 flasks were coated with CellStart (Invitrogen, UK) to enhance cell attachment before being used for expanding the WJ-MSCs from the fourteen donors. The cells were cultured using MezenGro®, a xeno-free medium (StemRD, USA), for two weeks or until the cells reached 80-90% confluence. Rho-associated kinase p160ROCK (ROCK inhibitor) (Santa Cruz Biotechnology, UK) was used during the sub-culturing to enhance the survival rate of the WJ-MSCs. When the cells reached confluence, they were harvested with TrypLE, washed with DMEM only and counted using a haemocytometer. A total of 1×10^6 diluted cells was recommended for the proliferation assay for every 1-ml of Roswell Park Memorial Institute (RPMI) medium supplemented with 10% FBS and 10,000-U/ml penicillin and 10,000-µg/ml streptomycin (Life Technologies, UK). Human peripheral blood mononuclear cells (PBMCs) were isolated from leukocyte cones, which were purchased from The National Blood Service (Colindale). The leukocyte cones were diluted 1:1 with PBS and layered on Histopaque (Sigma-Aldrich, UK) for density gradient separation.

The proliferation assay was conducted using a 96-well plate (Costar, UK) with a total volume of 200-µl of RPMI/10% FBS, penicillin and streptomycin per well. The WJ-MSCs were serially diluted, plated and incubated overnight. The PBMCs were then stained using violet dye from a CellTrace cell proliferation kit (Life Technologies, UK) using a working concentration of 1-µM cell suspension. Next, the cells were incubated at 37°C for 10 minutes and washed twice; the first wash used FBS, and the second

wash used RPMI. Subsequently, a total of $5x10^5$ stained PBMCs were added to each well of WJ-MSCs to obtain co-cultures with MSC:PBMC ratios increasing from 1:5 to 1:80. The PBMCs were then stimulated with 5-µg/ml phytohaemagglutinin (PHA) (Sigma-Aldrich, UK). BM was run in parallel as a reference and guide for the immunosuppression of the WJ-MSCs. Cultures of stimulated PBMCs without MSCs were used as a positive control, whereas non-stimulated PBMCs were used as a negative control. The cells were incubated in 5% CO_2 at 37°C for 72 hours. After 3 days, the cells were collected and washed once with PBS; thereafter, proliferation was measured using flow cytometry.

PBMC proliferation was assessed according to the pattern and distribution of the peak of the cells that were labelled with violet dye. Non-stimulated PBMCs were used as a guide for gating the proliferation. With increasing dilutions, the pattern of the peak from stained cells also increases. The relative proliferation at each MSC:PBMC ratio was then calculated as a percentage of the proliferation obtained in the positive control, according to the following formula: A/Bx100, where A is the proliferation at one specific MSC:PBMC ratio, and B is the proliferation of the positive control. The percentage of inhibition was then calculated by subtracting the percentage of proliferation from 100 (maximum inhibition). The statistical analysis methods used to describe and compare the immune response between obese and non-obese groups are described in the statistical analysis section (2.3.4).

2.3.4 Statistical analysis

Continuous data were summarized using mean, standard, median and range. Categorical data were summarized using count and percentages.

I used the Mann-Whitney U test (Sedgwick, 2012) to compare the sample distributions between two independent groups (obese and non-obese donors) with respect to numerical outcome. This test is the non-parametric equivalent to the two-sample t-test for comparing the mean between two independent groups with respect to a numerical outcome. I used the Wilcoxon rank test (Sedgwick, 2014) to compare the difference in outcomes relating to the same donor. This is the non-parametric equivalent to the paired t-test.

Non-parametric tests do not make any assumption regarding data distribution and are valid when the data follow a normal distribution. Non-parametric methods use the rank of the data rather than the actual values. These methods are particularly useful when sample size is small (less than 12 subjects per group) because it is not possible to ascertain the data distribution, and the distribution test will lack sufficient power to provide meaningful results. Unlike the case when the sample size is large, even if the data do not follow the normal distribution, the results from the parametric test would still be valid.

The Mann-Whitney U and Wilcoxon rank tests only provide p-values to confirm or reject the null hypotheses. However, to quantify the uncertainty around the estimates of the difference between the two groups or within subjects, the 95% confidence intervals are required. The 95% confidence interval represents the range of values within which the true population parameters, e.g., the mean, would lie. Generally, the computation of the confidence interval is based on normal approximation (asymptomatic inference). Asymptomatic theory is very convenient when available; however, in small samples, the results may be inaccurate. Therefore, I used Bootstrap as a re-sampling method (Bland & Altman, 2015) to obtain valid confidence intervals in this situation, as it improves the precision of asymptotic approximations in small samples. This method

estimates standard errors for the difference and confidence interval without making any assumption regarding the probability distribution of the data. The 95% confidence intervals were derived using 1000 replications.

I used the Poisson regression model (Gardner *et al.*, 1995) to model the association between obesity status and growth days. This model is based on count data, i.e., the number of growth days.

I used the Kaplan-Meier method (Bland & Altman, 1998) to compare the median time to doubling by obesity status. This is a standard method for the analysis of time to event data. I first considered the ‘event’ as the doubling of the cell counts within a time less than or equal the overall median doubling time; in this case, it was 34 hours. I also looked at the difference in the Kaplan-Meier curves for an `event' that occurred within the first 24 hours. The medians of the time to doubling of the cells were compared between the groups using the log-rank test (Sedgwick & Joekes, 2013).

I used either the Chi-square or Fisher's exact test (Altman, 1990) to compare the distribution of categorical variables, for example immunophenotypic markers, between two independent groups (obese and non-obese donors). The Chi-square test compares the observed frequency in each response category to the frequency I would expect if the null hypothesis of no association were true. When the expected frequencies are small (less than 5), Fisher's exact test can be used instead.

All statistical analyses were performed in Stata V11.2. No adjustment was made to the p-values as a result of multiple testing. All hypothesis testing is considered exploratory.

2.4 Sample preparation and analysis for the DNA methylation study

DNA was extracted from triple-positive (CD73, CD90 and CD105) WJ-MSCs from obese and non-obese donors, quantified and subjected to bisulfite conversion. Successful bisulfite conversion was confirmed using PCR with methylation-specific primers. Then, bisulfite-converted DNA was processed using Human Methylation 450K BeadChip (Illumina, UK) to determine whether obesity had any effects and changes on their methylation profiles; the methylation profiles of MSCs from the obese donors were compared with the profiles of MSCs obtained from the control group.

2.1.1 WJ-MSC sorting and extraction analysis from obese and non-obese lines

According to the ISCT, CD73, CD90 and CD105 are the most commonly used markers for MSC detection (Dominici *et al.*, 2006). Cells that were positive for all three markers were selected using the fluorescence-activated cell-sorting technique (FACS) to confirm a pure MSC population. The samples were prepared using the same method that was used for flow cytometry (Section 2.3.1). In brief, WJ-MSCs were suspended in cold PBS/10% FBS. The cells were incubated with antibodies in the dark for 10 minutes at 4°C and were then washed and re-suspended in 2-ml of PBS/10% FBS per tube. Negative and positive controls were tested in parallel for FITC, PE and APC. A BD FACSAria™ II/III Cell Sorter (BD Biosciences, BRC Flow Cytometry Core service provider, King's College London) was used by a BRC Core staff member to identify the population of interest. The sorting was also based on the MSC profile that was

determined using both FSC and SSC. After the cell sorting was complete, the cell suspension was centrifuged at 12,000 rpm for 5 minutes, the supernatant was aspirated, and the pellet was re-suspended in PBS to a final volume of 200-µl.

Genomic (g) DNA was extracted from the cells using a QIAamp DNA mini kit (Qiagen, UK) according to the manufacturer's instructions; all necessary reagents were provided in the kit. In brief, 20-µl of Qiagen proteinase K was added to each cell suspension. Then, 200-µl of AL buffer was added, and the mixtures were vortexed for 15 seconds, resulting in a homogenous solution, which confirmed adequate cell lysis. Subsequently, the samples were incubated at 56°C for 10 minutes for optimal DNA yield after lysis; the tubes were then briefly centrifuged in a bench-top micro-centrifuge to collect any drops of DNA from inside the lid. The cell lysates were washed with 200-µl of 100% ethanol and were mixed thoroughly by being vortexed for 15 seconds. The lysates were carefully transferred to the QIAamp mini spin columns and centrifuged at 8,000 rpm for 1 minute. The collection tubes containing the flow-through were discarded, and the spin columns containing the DNA bound to the silicon filter were placed in new 2-ml collection tubes. The spin columns were washed with 500-µl of AW1 buffer and were centrifuged at 8,000 rpm for 1 minute; then, the columns were placed in new 2-ml collection tubes. The QIAamp mini spin columns with bound DNA were washed further with 500-µl of AW2 buffer and were then centrifuged at the maximum speed for 3 minutes. To prevent carryover from AW2 buffer, the collection tubes were replaced with new tubes, and the columns were dried further by an additional centrifugation step at the maximum speed for 1 minute. Finally, the QIAamp columns were placed in sterile 1.5-ml micro-centrifuge tubes, and 200-µl of AE elution buffer was added. To promote optimal gDNA yield, the columns were incubated at room temperature for 5 minutes and then centrifuged at 8,000 rpm for 1 minute. The spin columns were discarded at this stage because the eluted DNA had been recovered in the micro-centrifuge tubes.

The concentration of the extracted gDNA samples was determined using a Qubit fluorometer. For Qubit DNA quantification assay, the Qubit® dsDNA BR assay kit (Life Technologies, UK) was used, and the same procedure was followed as described in section (2.3.2.1). The DNA samples were stored at -20°C until use.

2.1.2 Bisulfite conversion of DNA from all donors

The EZ DNA Methylation™ kit (Zymo Research, UK) was developed to enable a simple and accurate gDNA bisulfite conversion procedure. This procedure is based on an interaction between sodium bisulfite and cytosine, where unmethylated cytosine is converted to uracil, and methylated cytosine remains protected and unchanged.

After the gDNA was extracted, it was ready for bisulfite conversion. The manufacturer's instructions recommend that the amount of input DNA used for optimal bisulfite conversion should range from 200-ng to 500-ng. In this experiment, between 400-ng and 500-ng of gDNA from each of the fourteen samples was used for the reaction; three technical replicates were included in the bisulfite conversion reaction.

The procedure was performed as recommended by the EZ DNA Methylation™ kit manufacturers. Exactly 5-µl of M-dilution buffer was added to each gDNA sample that ranged between 400-ng and 500-ng. Distilled water was used to adjust the final volume to 50-µl, and the solution was thoroughly mixed by either pipetting the solution or flicking the tube (Table 9). Then, the mixture was incubated for 15 minutes at 37°C. During the incubation, fresh CT conversion reagent was prepared; 750-µl of water and 210-µl of M-dilution buffer were added to one reagent tube and vortexed for 10 minutes at room temperature. One hundred microlitres of the prepared reagent was added to the tubes containing gDNA and mixed thoroughly by pipetting. The tubes were then

incubated in a G-Storm thermocycler using the following conditions: 95°C for 30 seconds and 50°C for 60 minutes, both for 16 cycles, followed by a hold at 4°C.

After a 16-hour incubation, the samples were placed on ice for 10 minutes. Zymo-spin™ IC columns were placed in collection tubes, and 400-µl of M-binding buffer was then added. The samples were loaded into the corresponding columns, the caps were closed securely, and the solutions were mixed several times by gently inverting the tubes, which were then centrifuged for 30 seconds at full speed. The flow-through was discarded. One hundred microlitres of M-wash buffer was then added to the tubes containing samples, which were then centrifuged for 30 seconds at full speed using a bench-top micro-centrifuge. Two hundred microlitres of M-desulphonation buffer was added to each sample, and then the samples were incubated at room temperature for 15-20 minutes, followed by centrifugation at maximum speed for 30 seconds. The tubes were washed twice with 200-µl of M-wash buffer and were centrifuged for 30 seconds at maximum speed. Finally, the column was placed into a new 1.5-ml micro-centrifuge tube, and 12-µl of M-elution buffer was added directly to each column matrix. The DNA was eluted from the tubes containing matrix by centrifugation at maximum speed for 30 seconds. The eluted bisulfite-converted gDNA samples were stored at -20°C for later use.

Table 9. The required mixture composition (water, gDNA volume and M-dilution buffer) of samples for the bisulfite conversion protocol (N=non-obese, O=obese).

Sample number	DNA volume (µl) of 400-ng to 500-ng	M-dilution buffer concentration (µl)	Water (µl)	Total (µl)
N1	14.5	5	30.5	50
N2	4.5	5	40.5	50
N3	6.7	5	38.3	50
N4	10.2	5	34.8	50
N5	7.9	5	37.1	50
N6	7.2	5	37.8	50
N7	12.5	5	32.5	50
O1	6.4	5	38.6	50
O2	5.4	5	39.6	50
O3	4.9	5	40.1	50
O4	5	5	40	50
O5	3.7	5	41.3	50
O6	15.2	5	29.8	50
O7	6.6	5	38.4	50

2.1.3 Verification of complete bisulfite conversion

Two sets of primers, i.e., methylated and un-methylated, were designed to amplify the methylated and un-methylated copies of the differentially methylated regions of *MEG3* in the bisulfite-converted DNA (Sigma-Aldrich Oligo, UK). These primers were used to independently determine the successful completion of the gDNA bisulfite conversion; primers sequences and sizes descriptions are shown in Table 10 (Murphy *et al.*, 2003).

In this experiment, three technical replicates of bisulfite-converted and non-converted gDNA samples obtained from the same donor were tested for conversion efficiency.

Each PCR reaction was performed in a total volume of 25-µl, comprising 1× PCR buffer, 0.2-mM dNTPs, 0.5-µM of each primer, 2-U of Taq polymerase, and 1-µl of converted or non-converted gDNA, and H_2O was added to obtain a final volume of 25-µl (all reaction components were obtained from Zymo Research, UK). The conditions used for the PCR reaction are shown in Table 11.

The amplified products were loaded in plastic tubes and placed in an Agilent 2200 TapeStation electrophoresis system (Agilent Technologies). This system is available for researchers to use by the service providers BRC Genomics Core at King's College London. The run was set up as follows. The DNA ladder was prepared and loaded alongside the samples to size the fragments after electrophoresis. The D1000 reagents kit (Agilent Technologies, UK) was used for the electrophoresis, 3-µl of D1000 buffer was added to 1-µl of D1000 ladder in a 0.2-ml tube. One microlitre of the amplified sample was added to individual 0.2-ml tubes, and then 3-µl of D1000 buffer was added to the tube. The tubes were vortexed (IKA MS 3 basic, UK) at 2,000 rpm for 1 minute. After the tubes were vortexed, they were centrifuged for 1 minute to ensure that the mixture reached the bottom of the tubes. At this stage, the sample tubes and the D1000 ready to use screen tape (Agilent Technologies, UK) were loaded onto the TapeStation instrument, and the automated processing had started. Samples migrated through the channels of the screen tape. Once the process had completed, the resulting bands along with their sizes were visible in images. The sizes of each PCR product indicate either a successful or an unsuccessful bisulfite conversion.

Table 10. Primer sequences and product sizes in bp.		
Methylated-F	GTT AGT AAT CGG GTT TGT CGG C	160-bp
Methylated-R	AAT CAT AAC TCC GAA CAC CCG CG	
Un-methylated-F	GAG GAT GGT TAG TTA TTG GGG T	120-bp
Un-methylated-R	CCA CCA TAA CCA ACA CCC TAT AAT CAC A	

Table 11. PCR cycling conditions.		
Temperature	**Time**	**Cycle number**
94°C	3 minutes	1 cycle
94°C 70°C 72°C	30 seconds/step	5 cycles
94°C 65°C 72°C	30 seconds/step	5 cycles
94°C 60°C 72°C	30 seconds/step	35 cycles
72°C	5 minutes	1 cycle

2.1.4 DNA methylation study using Infinium Human Methylation 450K BeadChips

The Infinium Human Methylation 450K BeadChip consists of 485,764 cytosine positions from regions across the human genome; 99.3% of the sites are CpG dinucleotides, whereas 0.7% of the sites, corresponding to 3,343 positions, are more related to CNG targets. Regarding the distribution of CpG sites among chromosomal locations, the CpG sites can be found in all 23 human chromosomes. In particular, the Y chromosome contains the fewest positions (0.08%), while chromosome 1 contains the most CpG positions (9.6%). Regarding the relation between CpG sites and content and the surrounding context, 36.3% of CpGs are located in open seas, 30.9% are in islands, 23% are in shores, and 9.7% are in shelves. The functional genomic distribution of the CpG sites consists of 41% in proximal promoters, 30.9% in gene bodies, 24.6% in intergenic regions, and 3.16% in 3'-untranslated regions (3'UTRs)

(Sandoval *et al.*, 2011).

Generally, the beads on the chip are designed to represent 99% of the Reference Sequence genes, with an average of 17 CpG sites per gene region distributed across the promoter, 5'-untranslated region (5'UTR), exon 1 (1st exon), gene body, and 3'UTR from the whole genome. Ninety-six percent of CpG islands are also represented, including island shores and the regions flanking them. Each beadchip accommodates twelve samples for interrogation; therefore, a total of four beadchips were used to test 45 samples. The experimental design for testing the methylation status of the samples involved processing all fourteen samples in triplicate on the array. Additionally, three blank samples (without template DNA) were processed on the array. Four microlitres of bisulfite-converted gDNA, which had been obtained from processing each DNA sample and was stored under -20°C conditions, was provided to the service providers of the BRC Genomics Core facility at King's College London. The service provision covered the process steps described by the Infinium HD methylation assay protocol guide (Document # 15019519 v01). Additionally, built-in controls were used to evaluate the quality performance of each step in the assay for all samples. The results were provided in a raw data output for data analysis.

2.1.4.1 Infinium Human Methylation 450K BeadChip principle

To prepare the bisulfite-converted DNA for amplification, the samples were first denatured and neutralized (Figure 5.A). Through an overnight incubation step, the denatured DNA was isothermally amplified; the whole-genome amplification reaction generated a sufficient amount of each DNA sample by increasing the sample by several thousand fold (Figure 5.B). Using a controlled enzymatic process, the amplified DNA products were fragmented; an end-point fragmentation process was used to

prevent over-fragmentation of the DNA (Figure 5.C). The fragmented DNA was precipitated with isopropanol and collected via centrifugation at 4°C (Figure 5.D). The precipitated DNA samples were re-suspended in hybridization buffer (Figure 5.E). At this stage, the re-suspended DNA samples were denatured at 95°C for 20 minutes and allowed to cool at room temperature for 30 minutes before being individually loaded onto each beadchip stripe for hybridization. The beadchips were incubated in the Illumina hybridization oven (48°C) overnight to allow for hybridization of the samples onto the Infinium Human Methylation 450K BeadChips, and the DNA samples annealed to locus-specific 50-mers during hybridization (Figure 5.F). After a series of washing steps were performed to eliminate non-specifically hybridized and un-hybridized DNA (Figure 5.G), the beadchips were ready for the subsequent staining and extension steps (Figure 5.H). The DNA fragments that had annealed specifically on the beads during the hybridization step were used as templates for the single-base extension reaction of the oligos on the beadchips. After the extension reaction, a series of staining steps allowed the incorporation of fluorescent dye labels onto the beadchips; label detection enabled the determination of the methylation status of the queried CpG sites. An Illumina iScan system was used to scan the beadchips (Figure 5.I). The scanner recorded high-resolution images of the light emitted from the fluorophores after using a laser to excite the fluorophores of the single-base extension products on the beads.

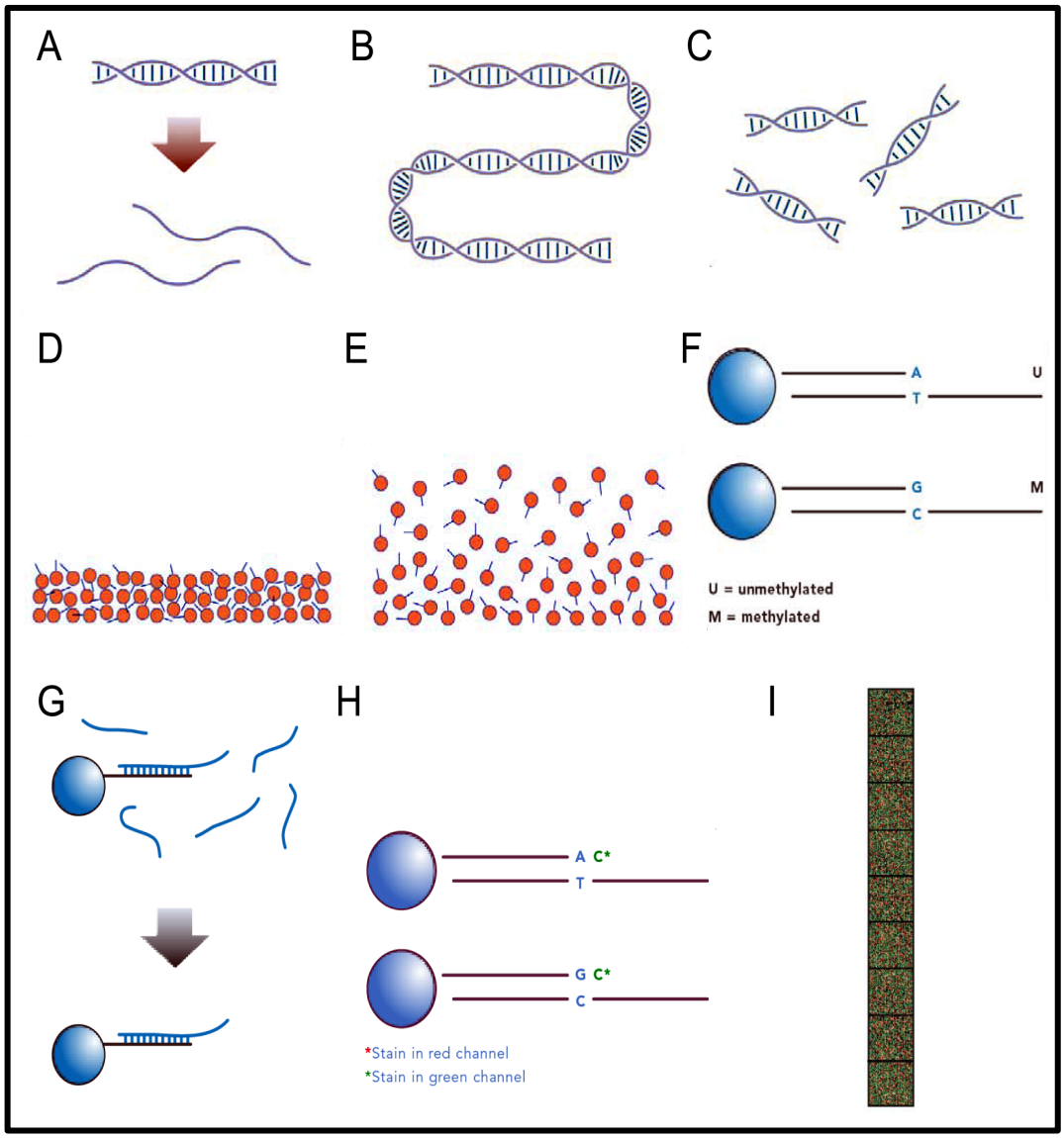

Figure 5. Principle of processing Infinium Human Methylation 450K BeadChips. **A.** Denaturing and neutralizing bisulfite-converted DNA. **B.** Incubating DNA for amplification. **C.** Fragmenting DNA. **D.** Precipitating DNA. **E.** Re-suspending DNA. **F.** Hybridizing to beadchip. **G.** Washing beadchip. **H.** Extending and staining beadchip. **I.** Imaging beadchip. Adapted from the Infinium HD assay methylation protocol guide (Document # 15019519 v01).

2.1.4.2 Quality control principles of the Infinium Human Methylation 450K BeadChip

The controls test the key aspects of the protocol to ensure that the data generated are high quality; outcomes from sample-independent and sample-dependent controls were generated for all 42 gDNA samples.

The controls test for reaction efficiency at the critical steps of the protocol, including dinitrophenyl (DNP) and biotin staining, extension of the nucleotide bases on beads (probes), target removal, hybridization, CpG site detection, non-polymorphic controls, bisulfite conversion I and II, specificity controls 1 and 2 and negative controls.

Purpose of sample-independent controls:

The DNP and biotin staining control, determined the sensitivity and efficiency of the staining reaction. The intensities were captured for evaluation through the red and green channels during scanning.

The extension control, used a hairpin probe to measure the extension efficiency of single base nucleotides (i.e., A, T, C and G). The ideally matched probes (A and T) were expected to produce a high-intensity signal that is shown in the red channel, whereas the mismatched probes (C and G) were expected to result in a low signal visible in the green channel.

The target removal control, measured the efficiency of the stripping of the DNA after the hybridization step on the beads had occurred and after the DNA had acted as a template for the single base extension reaction to occur. Its efficiency was monitored in the green channel of the scanner; it should result in a low signal.

The hybridization control, was designed to give an overall evaluation of the Infinium assay performance by using synthetic targets to probes on the array to enable perfect matches at three concentration levels, low (0.2-pM), medium (1-pM) and high (5-pM). This control was measured in the green channel. The intensity from these targets should be low, medium and high, respectively.

Purpose of sample-dependent controls:

The CpG site detection control, was implemented by detecting CpG sites with p-values between 0.01 and 0.05.

The non-polymorphic controls, enabled the evaluation of overall assay performance from amplification to detection by querying bases (A, T, C and G) in non-polymorphic regions of the genome across samples. C and G were monitored in the green channel, while A and T were monitored in the red channel.

The bisulfite conversion I and II controls, were sample-dependent controls used to confirm successful and complete sample conversion. For bisulfite conversion I, converted C probes matched the converted sequence and extended; in the case of incomplete conversion, the U probes extended instead. For bisulfite conversion II, the A base was incorporated, and the probe was observed with high intensity in the red channel; in the case of unconverted gDNA, the G base was incorporated, and the probe yielded a high-intensity signal in the green channel.

Specificity controls 1 and 2, were both designed to observe the allele-specific extension of probes I and II. Three of each G/T mismatch controls were present on the array to evaluate perfect matches and mismatches and to identify any unspecific detection of methylation signal over un-methylated background.

The negative controls, were designed to monitor the assay background. The probes on the array were permutated bisulfite-converted sequences that did not contain CpGs and, therefore, were not able to hybridize to DNA. There were approximately 600 of these probes on the array, and they were expected to show background-level intensities.

2.1.4.3 Statistical analysis of the data

Array data analysis was performed using GenoSplice (www.genosplice.com, France). The data were normalized for adjustment of type-II bias using the Beta-MIxture Quantile dilation (BMIQ) method (Teschendorff *et al.*, 2013) from the Chip Analysis Methylation Pipeline (ChAMP) R package (Morris *et al.*, 2014). The 450K array contains 65 single nucleotide polymorphism (SNP) probes that do not interrogate methylation, and these were filtered out. In addition, probes having a detection p-value above 0.01 were filtered out; thus, a total of 1,921 probes were removed from the analysis. The remaining 483,591 probes were included for the analysis. The CpGassoc R package (Barfield *et al.*, 2012) and MethLAB software (Kilaru *et al.*, 2012) were used for the differential methylation analysis together with information provided in the Human Methylation 450 v1.2 Manifest File for CpG annotations. T-statistics were calculated using logit-transformed beta values to help stabilize the variance (Du *et al.*, 2010). The T-statistic measures the size of the difference relative to the variation in the sample data. The logit transform, log (beta/(1-beta)), is equivalent to the log ratio of the methylated signal to the unmethylated signal. Multiple tests were performed using the q-values, which are adjusted p-values that take the false discovery rate (FDR) into account. The q-value was obtained using an optimized FDR method (Storey, 2002).

A comparative analysis using the averaged data obtained from the three replicates of all the obese donors versus the averaged data obtained from the three replicates of the non-obese donors were performed. Thereafter, the genes with at least one CpG site showing a methylation difference ≥0.20 in four or more obese donors were filtered based on the list of polymorphic CpG sites (Chen *et al.*, 2013) and segmental duplication (Kent *et al.*, 2002). The methylation data outcomes have been deposited in the Gene Expression Omnibus under the accession number GSE74167.

2.5 Copy number variation analysis for segmentally duplicated genes

To confirm that the two segmentally duplicated genes, zinc finger protein 714 (*ZNF714*) and *DDB1*- and *CUL4*-associated factor 6 (*DCAF6*), were present in multiple locations in all donors from both groups, Copy Number Variation (CNV) analysis was made possible by TaqMan Copy Number Assays.

The same gDNA that was extracted from fourteen donors (obese and non-obese) in section (2.4.1) was used for this experiment. A 20-ng aliquot of gDNA was constituted in a volume of 4-µl. Probes for *ZNF714* and *DCAF6* were designed and synthesized by the manufacturer to be used for the copy number assay. RNase P was selected as a reference gene assay. Each 20-µl reaction contained 4-µl of gDNA, 10-µl of TaqMan genotyping master mix, 1-µl of TaqMan copy number assay (either *ZNF714* or *DCAF6* in two different reactions), 1-µl of TaqMan copy number reference assay RNase P, and 4-µl of nuclease-free water (all reagents from Thermo Fisher Scientific, UK). Then, the reaction mix was incubated in a thermocycler for 10 minutes at 95°C for 1 cycle followed by 15 seconds at 95°C and 60 seconds at 60°C for 40 cycles. Additionally, a no-template control was included to show the background fluorescence and to allow for the detection of contamination. Copy number was calculated by Applied Biosystems Copy CallerTM Software v2.0.

2.6 Sample preparation and analysis for gene expression array analysis

Microarray gene expression analysis was performed on all fourteen donors to compare the global gene expression profiles of the obese and non-obese donors and to identify any significant changes that could affect gene expression levels. Then, the gene expression level was analysed in the 16 genes that have been highlighted in the experiments performed to this point. These 16 genes have significant differences in DNA methylation of one or more CpG sites not located in polymorphic regions. Briefly, WJ-MSCs from both groups were cell-sorted (CD73, CD90 and CD105), RNA was extracted and quantified, and the integrity of the recovered RNA was evaluated. The RNA was then used for whole-genome gene expression direct hybridization assay.

2.6.1 WJ-MSC sorting, RNA extraction, quantification and qualification analysis

WJ-MSCs that were triple positive for the markers CD73, CD90 and CD105 were selected using FACS. The samples from fourteen donors were prepared and sorted using the same methods that were used for preparation and sorting in section (2.4.1). RNA was extracted from the cells, the concentration of the extracted RNA samples was determined using a Qubit fluorometer, and the RNA samples were stored at -80°C until use. For RNA extraction and quantification assays, I followed the same procedures that were detailed in section 2.3.2.1.

To ensure that highly accurate data were obtained, only good-quality RNA was used for the gene expression array protocol. The quality was determined by obtaining an

RNA integrity number (RIN) score for each sample; the RIN score was determined using the Agilent 2100 Bioanalyzer (Agilent Technologies, instrument was provided by BRC Genomics Core, King's College London). The RNA quality of the samples was tested with the Agilent RNA 6000 Nano kit (Agilent Technologies, UK).

The main steps of the protocol are briefly described. The RNA ladder was prepared by heat denaturation for 2 minutes at 70°C and then immediately cooled on ice. The gel was prepared next by allowing it to equilibrate at room temperature for at least 30 minutes; a 550-µl aliquot of gel matrix was placed into a spin filter, and the spin filter was placed into a micro-centrifuge to spin for 10 minutes at 4,000 rpm. Next, a 65-µl aliquot of the filtered gel was transferred to a 0.5-ml tube. Following this step, the gel-dye mix was prepared by adding 1-µl of dye concentrate to the 65-µl aliquot of filtered gel tube, and the mix was vortexed thoroughly and visually inspected to ensure proper mixing of gel and dye. The gel-dye mix vial was centrifuged at 14,000 rpm for 10 minutes at room temperature.

Then, a 9-µl aliquot of the gel-dye mix was collected from the filtered gel-dye mix vial and pipetted in the RNA Nano chip at the bottom of the well-marked G on the chip. The chip with gel-dye mix was placed in a chip priming station; the purpose of the priming is to ensure that the gel spreads evenly across the wells in the chip. Next, the timer was set to 30 seconds, and the plunger was set and checked that it was at 1-ml on the chip priming station. The latch of the station was closed until a click was heard, ensuring that the priming station was closed correctly. The plunger of the syringe was secured down under the clip and held there for exactly 30 seconds; the plunger was released by triggering the clip release mechanism. The plunger was checked to ensure that it moved back up at least to the 0.3-ml position on the syringe. After waiting for 5 seconds, the plunger was gently pulled up manually to the 1-ml position. The latch of the chip priming station was opened, and the chip was placed on the bench-top. Then, 9-µl of the gel-dye mix was pipetted in each of the wells marked gel-dye mix. Next, a 5-

µl aliquot of RNA 6000 Nano marker was pipetted straight into the well marked with the ladder symbol and into each of the 12 wells for the samples. The RNA ladder was kept on ice during use; 1-µl of ladder was pipetted into the well marked with the ladder symbol, and 1-µl from each sample, which was also kept on ice, was pipetted into each of the sample wells. The chip was immediately placed horizontally in the adapter of the IKA vortex mixer (Agilent Technologies) and was vortexed for exactly 60 seconds at 2,400 rpm; the chip was ready for processing without any delay on the Bioanalyzer instrument.

2.6.2 Gene expression array for obese and non-obese

The new HumanHT-12 v4.0 Expression BeadChip (Illumina, UK) provides a comprehensive solution for viewing gene activity in samples and is designed to support flexible usage across a wide-spectrum of experiments, including large-scale studies that include human whole-genome gene expression profiling for applications, such as differential expression analysis, disease classification, expression-based quantitative trait loci studies, and pathway analysis.

The content on the array was carefully selected by Illumina to ensure it was of high quality and that it provided genome-wide transcriptional coverage of well-characterized genes, gene candidates, and splice variants. The array targets more than 47,000 probes, ensuring that >99.98% of the bead types are present on any given HumanHT-12 array. Therefore, five probes may be represented with only 0, 1, or 2 copies on each HumanHT-12 array. Probes were derived from National Center for Biotechnology Information Reference Sequence (NCBI RefSeq) Release 38, as well as other sources, such as the legacy UniGene content.

RNA from the samples was stored under -80°C conditions, ready to be processed on the global gene expression array with the aim to compare the data outcomes from

obese and non-obese groups. Each HumanHT-12 v4 Expression beadchip enables twelve samples to be processed, and each kit provides two beadchips. The experimental design for testing the gene expression of the samples required processing all fourteen samples in triplicate from obese and non-obese donors. Therefore, two kits were used, as they were sufficient for processing all fourteen samples in triplicate. Some statistical considerations for the analysis were based on the data outcomes from the DNA methylation microarray experiment.

After confirming that the RNA quality was high, 5-µl aliquots containing 500-ng of each sample were provided to the service providers of the BRC Genomics Core facility at King's College London. BRC Genomics provided the standard off-the-shelf Epicentre TargetAmp Nano-g Biotin RNA labelling kit (Epicentre, UK) and the RNeasy MinElute clean-up kit (Qiagen, UK) that are recommended by Illumina for labelling the RNA sample prior to committing it to hybridization on the expression beadchip.

The instructions described by the Whole-Genome gene expression direct hybridization assay guide (Part # 11322355 Rev. A) were applied for the process of the arrays. The assay contained built-in controls that evaluated the quality performance of the main steps in the assay for all samples. The raw data output generated after scanning the beadchip was analysed by GenoSplice.

2.6.2.1 Nano labelling for the Illumina expression beadchip process and the whole-genome gene expression direct hybridization assay principle

First-strand cDNA Synthesis: the Poly(A) RNA contained in a total RNA sample was reverse transcribed into cDNA. The reaction was primed from an oligo(dT)-primer

containing a phage T7 RNA Polymerase promoter sequence at its 5′ end. First-strand cDNA synthesis was catalysed by SuperScript III Reverse Transcriptase and performed at an elevated temperature to reduce RNA secondary structure. Second-strand cDNA Synthesis: the cDNA produced from earlier step was converted to double-stranded cDNA containing a T7 transcription promoter in an orientation that generated anti-sense RNA (aRNA; also called cRNA) during the subsequent *in vitro* transcription reaction. *In vitro* transcription of Biotin-aRNA: high yields of Biotin-aRNA (Biotin-cRNA) were produced in a rapid *in vitro* transcription reaction that utilized the double-stranded cDNA produced previously as the template (Figure 6A). Then, the aRNA was cleaned up and purified.

The labelled RNA strand was hybridized to the bead on the beadchip containing the complementary gene-specific sequence (Figure 6B). Beadchips were removed from the overnight hybridization and then washed (Figure 6C). Analytical probes were bound to the hybridized beadchip, which allowed for differential detection of signals when the beadchips were scanned (Figure 6D). The Illumina HiScan or iScan system or bead array reader measured fluorescence intensity at each addressed bead location. The intensity of the signals corresponds to the quantity of the respective transcript in the original sample (Figure 6E).

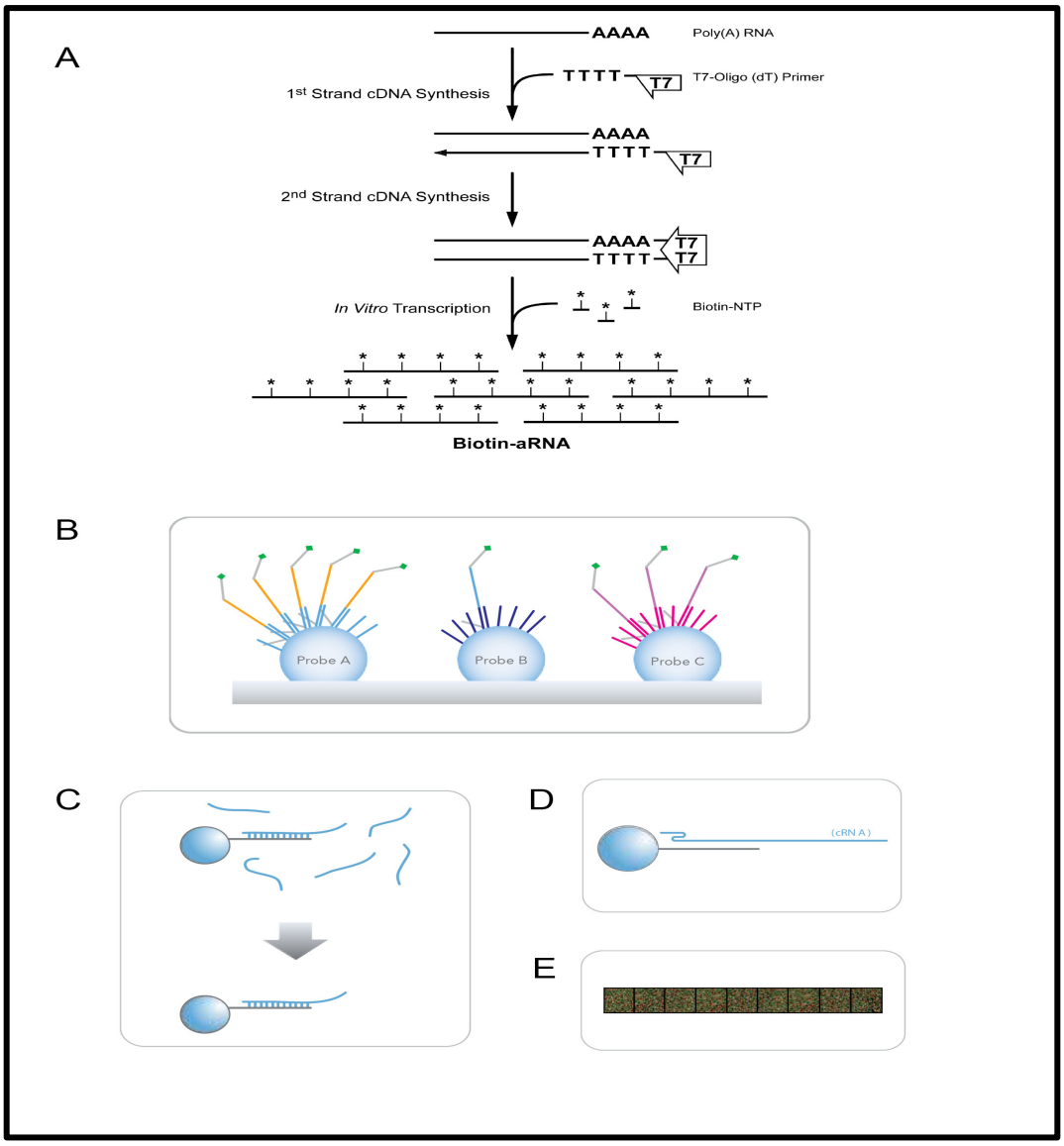

Figure 6. Principle of processing the Illumina HumanHT-12 v4 Expression beadchip. **A.** Sample labelling protocol in which total RNA is converted to double-stranded cDNA to generate labelled cRNA. **B.** Hybridizing strand to beadchip. **C.** Washing beadchip. **D.** Binding probes to beadchip. **E.** Imaging beadchip. Adapted from the TargetAmp-Nano labelling kit for Illumina expression beadchip (Lit. # 269 • 5/2013-EPILIT269 Rev. A) and the whole-genome gene expression direct hybridization assay guide (Part # 11322355 Rev. A).

2.6.2.2 Gene expression array quality control

This section describes the system controls that were used for the platform. Control categories are built in the direct hybridization assay system. These controls test the main aspects of the protocol, ranging from the biological specimen, sample labelling,

hybridization, and signal generation. The performance of the controls was monitored by uploading the data on the Genomestudio application.

Hybridization controls (high stringency), these controls test the hybridization of the single-stranded assay products to the immobilized beads. The controls consist of 50-mer oligos labelled with Cy3 dye included in the hybridization reagent. They should generate a signal independent of both the RNA sample and the success of the sample preparation reactions. The expected signal for all samples was expected to be roughly the same value because the hybridization control is sample independent.

Background control, this control consisted of approximately 800 probes of random sequences selected to have no corresponding targets in the genomes. The mean signal of these probes defined the system background and facilitated checking for any non-specific binding or cross hybridization. The signal value was expected to be lower than 150.

Gene intensities, the intactness of the biological specimens was monitored by housekeeping gene controls. There were fourteen probes in total, two probes for each housekeeping gene. These genes should be expressed in any cellular sample; however, the average gene intensity will vary with different gene expression products, due to the properties of the species.

Number of genes detected, the number of genes with a detection p-value of 0.05 and 0.01 or less was a good indicator of the robustness of the assay.

2.6.2.3 Statistical analysis

For global gene expression between obese and non-obese donors in triplicate:

- The data normalization was performed using the R packages ‘illuminaio’ and

'limma'.

- The quality control analysis was performed using the R package 'limma'.
- The hierarchical clustering analysis was performed with R using the complete linkage method and Euclidean distance.
- The data were further analysed according to the Kyoto Encyclopaedia of Genes and Genomes (KEGG) database, the Reactome database and the Gene Ontology (GO) analysis.

A comparison of obese and non-obese donor networks related to *PNPLA7* when detecting signalling cascades and interaction between *PNLPA7* and other genes:

- GeneMANIA (genemania.org).
- String V10.0 (string-db.org).

2.7 Confirmation of a significant difference in *PNPLA7* between obese and non-obese donors

The data generated from the gene expression arrays showed a significant difference in the mRNA expression level of only one gene, patatin-like phospholipase domain-containing 7 (*PNPLA7)*, between obese and non-obese donors. *PNPLA7* gene expression data from the arrays were confirmed using RT-PCR. *PNPLA7* protein expression level was determined using Western blot analysis.

2.7.1 Testing *PNPLA7* using RT-PCR

RT-PCR was used to validate the findings from the array data that showed a significant difference in mRNA expression levels of *PNPLA7* between obese and non-obese groups. WJ-MSCs from obese and non-obese groups were collected, RNA was extracted and quantified, and cDNA was synthesized (Table 12) as explained previously in section (2.3.2.1). RT-PCR was performed using SYBR green master mix with primers designed for the targeted gene (*PNPLA7*) in obese and non-obese donors (Table 13). Sample preparation and conditions for RT-PCR were followed as previously described in section (2.3.2.1). The data were collected and analysed using the comparative threshold cycle method using *TBP* and *GUSB* as reference genes (Table 8). The statistical analysis methods used to describe and compare gene expression levels between obese and normal groups are described in the statistical analysis section (2.3.4).

Table 12. The required mixture composition of RNA samples of WJ-MSCs for the cDNA protocol (N=non-obese, O=obese).					
Sample number	**RNA volume for 1000-ng (µl)**	**5× iScript Reaction mix (µl)**	**iScript reverse Transcriptase (µl)**	**Water (µl)**	**Total (µl)**
N1	2.7	4	1	12.3	20
N2	1.5	4	1	13.5	20
N3	2.0	4	1	13.0	20
N4	3.0	4	1	12.0	20
N5	1.2	4	1	13.8	20
N6	2.2	4	1	12.8	20
N7	1.7	4	1	13.3	20
O1	2.0	4	1	13.0	20
O2	1.8	4	1	13.2	20
O3	4.2	4	1	10.8	20
O4	1.7	4	1	13.3	20
O5	2.1	4	1	12.9	20
O6	3.3	4	1	11.7	20
O7	1.1	4	1	13.9	20

Table 13. Primer sequences of *PNPLA7* (Life Technologies, UK).	
PNPLA7-F	5'-CACTCTTGGGGACTGTGGTT-3'
PNPLA7-R	5'-CGGCCGTAAAACATCACTTT-3'

2.7.2 Western blot analysis for *PNPLA7*

A Western blot analysis was prepared to validate the protein expression levels of *PNPLA7* in the obese and non-obese groups.

WJ-MSCs pellets ($1x10^6$ cells) were lysed in in 400-µl of RIPA buffer (Thermo Scientific, UK), supplemented with cOmplete protease inhibitor cocktail (Roche, UK). The lysate

was homogenized by passing it ten times through a 29-G needle (Sigma-Aldrich, UK) and was sonicated twice every 10 seconds with a sonicator (Fisher sonic dismembranator model 300) at 35% of capacity. Fifteen microlitres of lysate were mixed with 5-µl of LDS Sample Buffer (Life Technologies, UK), boiled for 5 minutes, chilled on ice, spun briefly in a bench-top micro-centrifuge and loaded at 15-µl/well in a 4-12% SDS polyacrylamide gel (Life Technologies, UK). The proteins were separated in MOPS SDS Running Buffer (Life Technologies, UK) at a constant current of 20-mA using Novex XCell SureLock® Mini-Cell system (Life Technologies) that was connected with a 1000/500 constant voltage power supply (Bio-Rad). The molecular weight of the proteins was determined using Bolt™ BenchMark™ Pre-Stained Protein Ladder (Life Technologies, UK). The gel was equilibrated in Transfer Buffer (Life Technologies, UK) for 10 minutes. The proteins were transferred from the gel to the 0.2-µm pore size nitrocellulose membrane (Life Technologies, UK) overnight in transfer buffer at a constant current of 25-mA.

The membrane was washed in TBST buffer (Thermo Fisher Scientific, UK) for 10 minutes and blocked for 20 minutes in 5% bovine serum albumin (Sigma-Aldrich, UK) in TBST. The membrane was then incubated with rabbit anti-PNPLA7 antibody (Sigma-Aldrich, UK) at a dilution of 1:1000 (20-ng/ml) in TBST on a rocking platform at room temperature for one hour. The membrane was washed three times every 10 minutes in TBST and then incubated with HRP-conjugated donkey anti-rabbit IgG (H+L) cross-absorbed secondary antibody (Thermo Scientific, UK) diluted at 1:2500 (20-ng/ml) on a rocking platform at room temperature for 30 minutes. The membrane was washed again three times every 10 minutes in TBST. The protein was detected with an enhanced chemiluminescent Pierce® ECL Western Blotting Substrate (Thermo Scientific, UK). The images were detected and recorded using Intelligent Dark Box LAS-3000 (Fujifilm).

The membrane was washed in TBST for 10 minutes, stripped in Restore™ Western Blot Stripping Buffer (Thermo Scientific, UK) on a rocking platform at room temperature for 15 minutes and washed again for 10 minutes in TBST. The membrane was then incubated with a loading control HRP-conjugated mouse anti-actin antibody BA3R (Thermo Scientific, UK) for 1 hour and then washed three times every 10 minutes in TBST and exposed to Pierce® ECL Western Blotting Substrate. The images were detected and recorded using Intelligent Dark Box LAS-3000. Actin, used as housekeeping protein for the analysis. The statistical analysis methods used to describe and compare the protein levels between the obese and normal groups are described in the statistical analysis section (2.3.4).

Chapter 3

Results

3. Results

The genome-wide effect of obesity on DNA methylation was evaluated in WJ-MSCs isolated from UCs collected immediately after delivery. The WJ-MSCs were isolated from mothers who exhibited healthy pregnancies; the mothers were categorized into obese and non-obese groups based on whether they presented with high (>30) or normal (19-25) BMI, respectively. The cells from UCs were isolated and cultured using the explant method, and their properties were evaluated. The genome-wide DNA methylation and gene expression profiles were assessed and compared between two groups.

3.1 Isolation and evaluation of WJ-MSCs

First, this chapter describes the outcomes of method used to isolate WJ-MSCs from UCs. Second, it presents the assessment results of the initial observations of the outgrowth and proliferation rates of WJ-MSCs from fourteen donors (obese n=7 and non-obese n=7). Third, the biomarker expression profiles of the panel of MSC markers in the obese and non-obese groups are evaluated. Fourth, WJ-MSCs from both groups are evaluated for their differentiation potential. Lastly, the effect of obesity on immune response is assessed for WJ-MSCs from obese donors and compared with the results from the control group.

To eliminate any technical errors and minimize variability among samples, all fourteen UCs were processed under similar conditions using sterile techniques from the day of collection until the end stage of the experimental procedure. Moreover, UC collection was conducted under tightly controlled conditions. The conditions for UC processing in the laboratory were standardized, and freshly prepared medium was used to culture samples in an incubator with a constant temperature of 37°C and provision of gases, including 5% O_2 and 5% CO_2.

3.1.1 Assessment of WJ-MSCs isolated from UCs using an explant procedure versus enzymatic digestion

The UCs collected from the first five donors were cut in a half and one part was subjected to enzymatic digestion, whereas the other was cut in smaller pieces and cultured as explants to isolate MSCs from WJ. The cultures obtained using the enzymatic method retained a high number of red blood cells from the initial day of processing. Very few cells were found attached to the surface of the dish in these cultures, and the cultures could not be expanded further (Figure 7). Cultures obtained using the explant method had present haematopoietic cells on the day of the procedure and they could be removed by changing medium. These cultures showed mostly adherent cells that mainly exhibited a fibroblastic morphology (Figure 7). The explant method for MSCs isolation was therefore easier, faster, and better for isolation of adherent cells that were homogenous than the enzymatic digestion method.

After processing, isolating and expanding the MSCs of WJ from five cords using the explant and enzymatic methods, the remaining samples were processed solely using the explant method. Therefore, the explant method was used for the isolation and expansion of MSCs from WJ throughout this project.

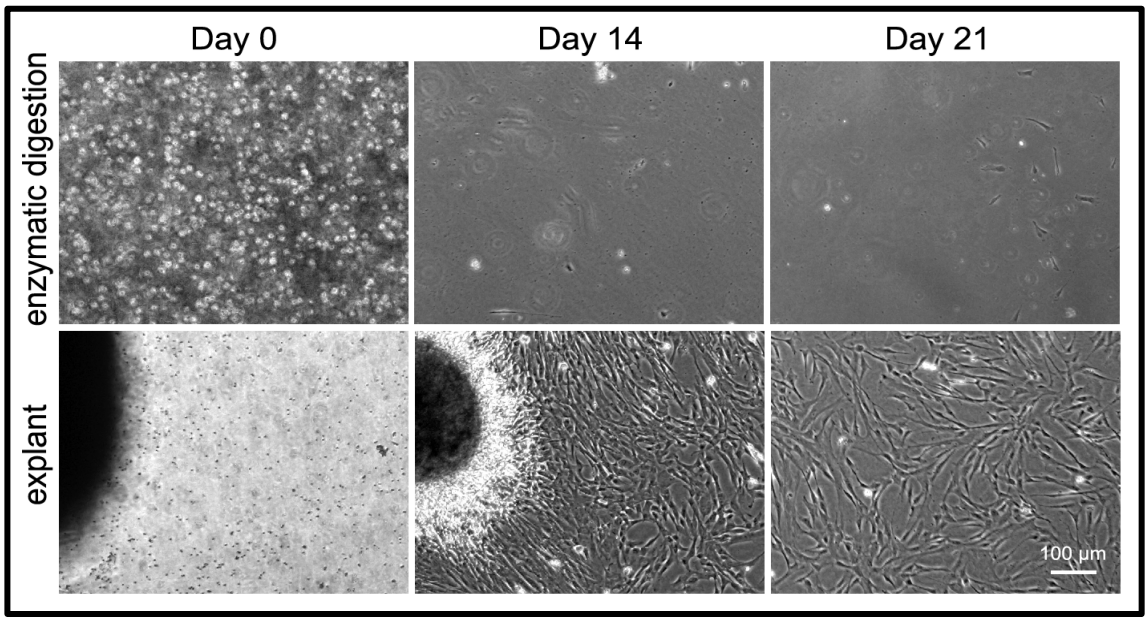

Figure 7. On day 0, haematopoietic cells were present in cultures obtained from the enzymatic and explant methods. On day 14, more fibroblast-like cells were present in cultures obtained from WJ explants than in cultures obtained using the enzymatic procedure. On day 21, a network of fibroblast-like cells was visible in the explant cultures, whereas few attached cells were present in the culture obtained using the enzymatic method.

3.1.2 Assessment of the initial outgrowth and proliferation rates of explants from WJ-MSCs from obese and non-obese donors

The WJ portions of the UCs collected from all donors were sectioned into 10 small fragments on individual plates. Each fragment was approximately 1-cm^2 in size. The

cultures containing WJ-MSCs were monitored at regular intervals to determine the start of outgrowth. The cells from obese and non-obese cords exhibited a predominantly fibroblast-like phenotype; they were spindle shaped and had a relatively high nuclear-to-cytoplasmic ratio (Figure 8).

The WJ-MSCs from the control groups showed an initial outgrowth on day 7 for donors N1 and N3 and on day 10 for donors N4, N6, and N7. Initial outgrowth for donors N5 and N2 was observed on days 9 and 11, respectively. In contrast, the cultures that were grown using explants from the obese group an initial outgrowth was evident on day 8 from donors O3 and O6 and on day 12 from donors O2 and O5. Donors O1 and O4 showed initial outgrowth on days 9 and 11, respectively. The explant culture from donor O7 was the slowest to establish and expand, showing the initial outgrowth on day 14 (Table 14, Figure 9A).

The mean (± standard deviation) time to the first observation of outgrowth was 9.1 (±1.5) days in the non-obese donors and 10.5 (±2.2) days in the obese donors. However, the difference between the obese and non-obese groups in terms of the initial outgrowth of the cells was not significant (p-value 0.220, Mann-Whitney test) (Figure 9B and Table 15). Analysis based on the Poisson model showed that the rate of initial outgrowth in the non-obese group was earlier than in the obese group but still not significant. The 95% confidence interval of the incidence rate ratio was 1.15 (0.827 to 1.61; p=0.395).

The proliferation rate of the WJ-MSC cultures from each group type was assessed between PD1 and PD2 using the PD formula. In the non-obese group, it took 25.2 hours for the cells from donor N3 and 24 hours for the cells from donor N4 to double their populations; it took 33.1 and 32 hours for the cells from donors N2 and N7, respectively, to double their populations. The cells from donor N1 took 25.9 hours, and

the cells from donor N6 took 53.3 hours. Of the cells in the non-obese group, those from donor N5 displayed the longest doubling time, at 71.6 hours. In the obese group, the cells from donors O1, O3, O6 and O7 doubled their populations after 55.4, 28.5, 75 and 48 hours, respectively. The cells from donors O4 and O5 each took 34.2 hours to double their populations, and the cells from donor O2 displayed the longest doubling time, at 96 hours (Table 16).

The median (range) PD time of the WJ-MSCs between PD1 and PD2 was 32 (24 to 71.6) hours in the non-obese group and 48 (28.5 to 96) hours in the obese group. The overall median time to doubling was 34.2 (24 to 96) hours. These results suggest that the PD time of cells from the non-obese group was somewhat shorter than that of cells from the obese group; however, the difference was not significant (p-value 0.084, Mann-Whitney test).

However, the Kaplan-Meier test was used to compare the cell doubling time in both groups in the first 34 hours (overall median PD time). The difference in the time taken to double within the first 34 hours between the groups was significant (p-value 0.048, log-rank test). Thus, the results suggest that the population doubling time of the cells from the non-obese group was significantly shorter than that of the cells from the obese group (Figure 9C).

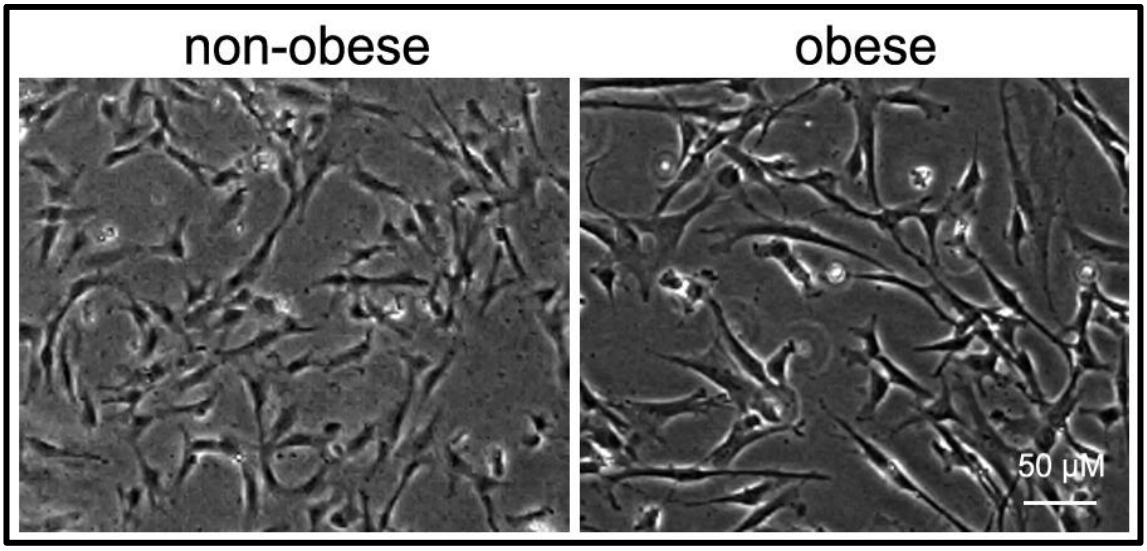

Figure 8. Fibroblast-like cells proliferated from non-obese (n=7) and obese (n=7) WJ explants are morphologically indistinguishable under phase-contrast microscopy.

Table 14. Number of days prior to initial outgrowth and expansion of WJ-MSCs from explant cultures (O=obese and N=non-obese) (n=14).

Non-obese	First outgrowth (days)	Obese	First outgrowth (days)
N1	7	**O1**	9
N2	11	**O2**	12
N3	7	**O3**	8
N4	10	**O4**	11
N5	9	**O5**	12
N6	10	**O6**	8
N7	10	**O7**	14

Table 15. Time of observation of initial outgrowth from explant cultures of obese and non-obese cords.

Group	Mean (standard deviation)	Median (minimum, maximum)	p-value (Mann-Whitney test)
Normal (n=7)	9.14 (1.57)	10.0 (7.0, 11.0)	0.220
Obese (n=7)	10.5 (2.29)	11.0 (8.0, 14.0)	
Total (n=14)	9.85 (2.03)	10.0 (7.0, 14.0)	

Table 16. Time (hours) required for the cells to double in population between PD1 and PD2 (O=obese and N=non-obese) (n=14).

Non-obese	Proliferation rate (hours)	Obese	Proliferation rate (hours)
N1	25.9	**O1**	55.4
N2	33.1	**O2**	96.0
N3	25.2	**O3**	28.5
N4	24.0	**O4**	34.2
N5	71.6	**O5**	34.2
N6	53.3	**O6**	75.0
N7	32.0	**O7**	48.0

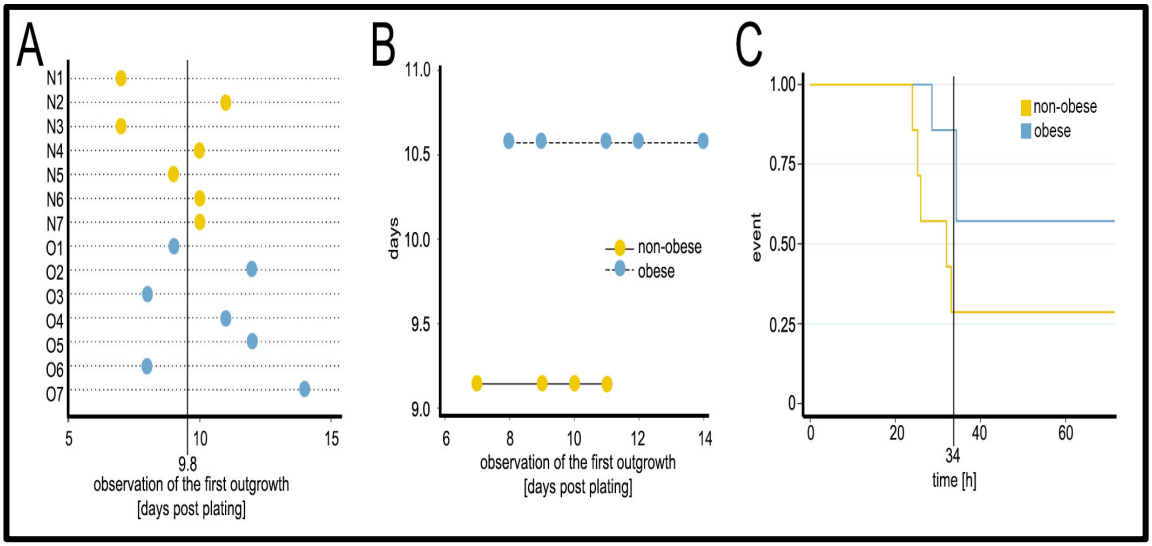

Figure 9. A. Total mean (days) prior to the first outgrowth of MSCs from WJ explants (observed microscopically) from all fourteen donors. **B.** Mean (days) prior to the first outgrowth of MSCs from WJ explants in obese and non-obese donors; no significant differences were observed between the cells in the two groups (p-value 0.220, Mann-Whitney test). **C.** Cells from non-obese donors showed a significant faster doubling time than cells from obese donors after 34 hours (p-value 0.048, log-rank test).

3.1.3 Biomarker detection in WJ-MSCs from obese and non-obese lines using flow cytometry

Flow cytometry was used to determine and compare the cell surface biomarker expressed in the WJ-MSC populations grown *in vitro* from the obese and non-obese donor groups. Cells that were collected for biomarker identification at the PD2 stage. Clinical-grade BM-MSCs, served as a positive reference for MSC markers, Kasumi cells served as a positive control for haematopoietic cell surface markers, unstained MSCs were used for gating assessment, and beads were used for manual compensation.

The flow cytometer was used to gate and assess unstained cells for the phenotypic expression of the following markers: CD90, CD73, CD105, CD44, CD29, CD271,

MSCA-1, CD56, CD45 and CD34. MSC marker CD90 was expressed in 94.8%, 95.2%, 94.5%, 97.2% and 95.2% of the gated cell populations from donors N2, N3, N4, N5 and O6, respectively. In the cells from donors N6, N7, O1 and O2, CD90 expression was slightly lower (77.2%, 78.9%, 73% and 72%, respectively). CD73 expression was highest in the cells from donor O2, at 99.4%, and lowest in the cells from donor O3, at 88%. CD105 expression ranged from 93.1% to 99.1%. Likewise, expression of the cell surface marker CD44 was observed in majority of the cells (range: 92.6% to 99.7%). CD29 expression levels were the highest in WJ-MSCs from all donors, but the WJ-MSC population from donor N7 showed the lowest CD29 expression level, at 99.4%. The cell surface marker CD56 showed the greatest variation in expression across the cell lines; 40.3% of the donor O3 cell population expressed CD56, while the majority, 80.6%, of the donor N6 cell population expressed CD56. CD56 expression levels in the remaining cell lines fell between these extremes (Tables 17 and 18).

Overall, the flow cytometric data analysis of the surface markers identified from the cells showed similar expression properties of the following main MSC markers in the non-obese and obese groups: CD90 (p-value 0.249, Mann-Whitney test), CD73 (p-value 0.949, Mann-Whitney test) and CD105 (p-value 0.608, Mann-Whitney test). In addition to, CD29 (p-value 0.268, Mann-Whitney test) and CD44 (p-value 0.482, Mann-Whitney test). One exception was CD56, the surface marker CD56 expression was significantly lower in the obese group than in the non-obese group (p-value 0.025, Mann-Whitney test) (Table 19, Figure 10). Both groups were negative for CD271 and MSCA-1 and for the haematopoietic cell surface markers CD45 and CD34 (Table 19).

Table 17. MSC marker panel showing the expression levels (percentages) of CD markers on the surfaces of WJ-MSCs from non-obese donors.

CD Marker	N1	N2	N3	N4	N5	N6	N7
CD90	85.8	94.8	95.2	94.5	97.2	77.2	78.9
CD73	98.9	97.8	94.8	95.3	99.0	98.9	90.5
CD105	95.2	99.1	98.6	95.5	99.0	96.5	99.1
CD44	96.4	98.9	96.6	94.9	99.7	98.6	95.1
CD29	99.6	99.9	99.8	99.9	99.9	99.7	99.4
CD271	0.00	0.00	0.00	0.00	0.00	0.00	0.00
MSCA-1	0.00	0.00	0.00	0.00	0.00	0.00	0.00
CD56	53.8	77.5	83.6	80.1	79.2	80.6	63.2
CD45	0.00	0.00	0.00	0.00	0.00	0.00	0.00
CD34	0.00	0.00	0.00	0.00	0.00	0.00	0.00

Table 18. MSC marker panel showing the expression levels (percentages) of CD markers on the surfaces of WJ-MSCs from obese donors.

CD Marker	O1	O2	O3	O4	O5	O6	O7
CD90	73.0	72.0	83.3	89.7	81.9	95.2	86.6
CD73	97.7	99.4	88.0	95.7	92.6	96.6	95.4
CD105	93.1	99.0	97.4	98.7	96.4	98.9	97.1
CD44	99.5	99.4	92.6	97.9	97.5	99.0	97.1
CD29	99.9	99.8	99.9	99.9	99.8	99.8	99.9
CD271	0.00	0.00	0.00	0.00	0.00	0.00	0.00
MSCA-1	0.00	0.00	0.00	0.00	0.00	0.00	0.00
CD56	51.6	65.6	40.3	62.1	53.9	55.4	75.3
CD45	0.00	0.00	0.00	0.00	0.00	0.00	0.00
CD34	0.00	0.00	0.00	0.00	0.00	0.00	0.00

Table 19. Comparison of the proportion of individual surface markers identified in WJ-MSCs according to obesity status.
+Confidence intervals obtained using the normal approximation to the binomial distribution

CD Marker	Median proportion (%)		p-value (Mann-Whitney test)	95% confidence interval (%)+
	Non-obese	Obese		
CD90	94.5	83.3	0.249	-5.9 (-6.0 to -5.9)
CD73	95.3	95.7	0.949	-0.11 (-0.13 to -0.09)
CD105	98.6	97.4	0.608	-0.34 (-0.35 to -0.32)
CD44	96.6	97.9	0.482	0.4 (0.38 to 0.41)
CD29	99.8	99.9	0.268	0.11 (0.10 to 0.11)
CD56	79.2	55.4	0.025	16.2 (-16.3 to -16.2)
CD271	00.0	00.0	0.00	0
MSCA-1	00.0	00.0	0.00	0
CD34	00.0	0.00	0.00	0
CD45	00.0	00.0	0.00	0

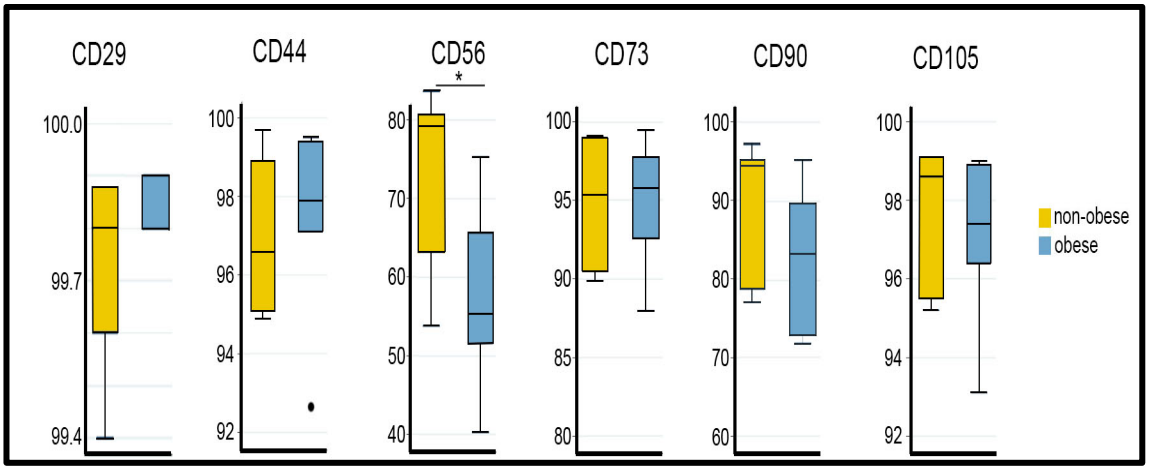

Figure 10. Expression of positive markers (CD90, CD73, CD105, CD44 and CD29) on the surfaces of WJ-MSCs from normal BMI (n=7) and high BMI (n=7) groups, levels did not differ significantly. CD56 was an exception, showing a significant difference between both groups (p-value 0.025, Mann-Whitney test).

3.1.4 Differentiation potential of WJ-MSCs from obese and non-obese donors

The WJ-MSCs isolated from obese mothers were tested to determine whether they exhibited differentiation potentials similar to or different from those of WJ-MSCs isolated from non-obese mothers. I compared differentiation propensity of WJ-MSCs from the obese and non-obese donors towards the adipogenic, chondrogenic and osteogenic lineages. The potential of the cells to commit to all three differentiation pathways was analysed to identify any differences between obese and non-obese donor cells.

3.1.4.1 Differentiation of WJ-MSCs into adipocytes

MSCs are multipotent and, by definition, can differentiate into cells of mesodermal origin. Researchers have demonstrated that diet-induced obesity alters MSC differentiation potential. Cells from both donor groups were differentiated into adipocytes to determine their adipogenic propensity.

After the cells had been cultured for 14 days, fat droplets positively stained for LipidTOX indicated that the cells had undergone adipogenesis (Figure 11A). The undifferentiated cells and differentiated cells from all fourteen donors were then assessed for the level of the adipogenic-specific marker *FABP4*.

The mean (± standard deviation) of the *FABP4* mRNA expression level was higher in differentiated cells 56.5 (± 34.7) than in undifferentiated cells 0.23 (± 0.12) (Table 20). The differences between the differentiated and undifferentiated cells were significant (p-value 0.001, Wilcoxon signed rank test) and confirmed the adipogenic state of the cells (Figure 11A).

The levels of *FABP4* mRNA in differentiated cells from individual obese and non-obese donors were also compared. Generally, *FABP4* mRNA levels varied within the samples from the same group as well as between samples from the obese and control groups. The highest *FABP4* mRNA expression level in cells from the non-obese group, 57.2, was obtained for N6, and the highest level in cells from the obese group, 118.6, was obtained for subject O4; the lowest *FABP4* mRNA level in the obese group, 24, was from O7, and the lowest value in the normal group, 11.7, was from donor N5. Overall, the mean (± standard deviation) *FABP4* mRNA expression level was higher in the obese group 75.5 (± 39.5) than in the non-obese group 37.6 (± 14.8) (Table 21). However, the differences between the obese and non-obese groups were not significant (p-value 0.110, Mann-Whitney test) (Figure 11A). Analysis based on the Bootstrap model showed that the incidence rate ratio at the 95% confidence interval was -48.1 (-82.9 to 11.7).

A second semi-quantitative analysis was performed by calculating the total surface area of LipidTOX-positive droplets per number of nuclei in one field to obtain the percentage of cellular lipid per cell. Generally, the percentage of cellular lipid per cell showed variations within the samples from the same group as well as between the obese and control groups. The highest percentage of lipid content found in either of the groups was 3.9% from donor N7. The lipid percentages in cells from donors N1, N2, O3 and O7 were close to the percentage found in donor N7 (3.6%, 3.7%, 3.4% and 3.7%, respectively). The percentage of lipid content did not differ greatly between the obese donors; donor O1 showed 2.6%, and donor O4 showed 2.5%. Similar ranges of lipid percentages were observed in both groups; donors N3, O6, N5, N6 and O2 showed lipid contents of 1.8%, 1.6%, 1.4%, 1.3% and 1.2%, respectively. The lowest percentages of lipid content were found in cells from donor O5 in the obese group and in cells from donor N4 in the non-obese group; these cells had 0.7% and 0.6% lipid

content, respectively. Overall, the mean (± standard deviation) lipid percentage of cells from the obese group was 2.2% (± 1.1), and the mean lipid percentage of cells from the non-obese group was 2.3% (± 1.3). The cells from the two groups showed no significant difference in cellular lipid percentage per cell (p-value 0.907, Mann-Whitney test) (Figure 12 and Table 22). Analysis based on the Bootstrap model showed that the mean lipid percentage in cells that had differentiated into adipocytes was similar in the obese and non-obese groups. The 95% confidence interval of the incidence rate ratio was 0.68 (-2.22 to 1.44).

Although the differentiation of cells from obese and non-obese donors into adipogenic lineages was successful, the results did not show any significant differences between the samples.

Table 20. Summary of mRNA levels by differentiation status using an adipogenic-specific marker (*FABP4)*.

Group	Mean (standard deviation)		Median (minimum, maximum)		p-value (Wilcoxon signed rank test)
	Undifferentiated cells	Differentiated cells	Undifferentiated cells	Differentiated cells	
Normal (n=7)	0.21 (0.12)	37.6 (14.8)	0.17 (0.10, 0.46)	35.7 (11.7, 57.2)	0.001
Obese (n=7)	0.25 (0.12)	75.5 (39.5)	0.20 (0.11, 0.40)	83.8 (24.0, 118)	
Total (n=14)	0.23 (0.12)	56.5 (34.7)	0.18 (0.10, 0.46)	46.6 (11.7, 118)	

Table 21. Summary of mRNA levels by obesity status using an adipogenic-specific marker (*FABP4)*.

Group	Mean (standard deviation)	Median (minimum, maximum)	p-value (Mann-Whitney test)
Normal (n=7)	37.6 (14.8)	35.7 (11.7, 57.2)	0.110
Obese (n=7)	75.5 (39.5)	83.8 (24.0, 118)	
Total (n=14)	56.5 (34.7)	46.6 (11.7, 118)	

Table 22. Summary of the average percentage of cellular lipid by obesity status in cells from normal and obese donors.

Group	Mean% (standard deviation)	Median% (minimum, maximum)	p-value (Mann-Whitney test)
Normal (n=7)	2.37 (1.32)	1.86 (0.65, 3.91)	0.749
Obese (n=7)	2.28 (1.10)	2.55 (0.77, 3.70)	
Total (n=14)	2.18 (1.26)	1.86 (0.15, 3.91)	

3.1.4.2 Differentiation of WJ-MSCs into chondrocytes

The WJ-MSCs obtained from obese and non-obese donors were differentiated into chondrocytes to determine their chondrogenic propensity.

After the cells were cultured for 14 days, round cells with a centrally located nucleus and a shiny ring in the cytoplasm around the nucleus were detected in the cultures, indicating that the cells had undergone chondrogenesis. This shiny ring is collagen, a specific protein synthesized by chondrocytes. Differentiated cells from all obese and non-obese donors were observed to be positively stained for Alcian blue (Figure 11B). Generally, Alcian blue staining of cultured cells is indicative of a high content of cartilage-specific proteoglycans in induced cultures. The staining was more intense

and uniform in the centres of the cultures and its intensity decreased and became irregular towards the outer rim of the cultures, suggesting a higher content of cartilage-specific proteoglycans in the inner region of the cultures.

After the cells were cultured for 14 days, undifferentiated cells and differentiated cells from all fourteen donors were assessed for the levels of the chondrogenic-specific marker *COL11A1*. The mean (± standard deviation) expression level of *COL11A1* mRNA was higher in differentiated cells 10.3 (± 4.94) than in undifferentiated cells 1.92 (± 0.74) (Table 23). The differences between the differentiated and undifferentiated cells were significant (p-value 0.001, Wilcoxon signed rank test), confirming the chondrogenic differentiation state of the cells (Figure 11B).

The expression of the chondrogenic-specific marker *COL11A1* by differentiated cells from obese and non-obese donors was compared. The highest mRNA expression levels in the differentiated cells from non-obese and obese donors were 21.4 (N2) and 11.6 (O2), respectively. The lowest expression levels were found in cells from donor N4 in the non-obese group (8.1) and in cells from donor O5 in the obese group (2.9). Overall, the mean (± standard deviation) *COL11A1* gene expression level was higher in the non-obese group 12.9 (± 5.42) than in the obese group 7.77 (± 2.84) (Table 24). The data show that the observed differences in the mRNA expression level of *COL11A1* in chondrogenic cells differentiated from cells obtained from obese and non-obese donors were not significant (p-value 0.063, Mann-Whitney test) (Figure 11B). Analysis based on the Bootstrap model showed that 95% confidence interval of the incidence rate ratio was 3.13 (-1.36 to 11.7).

Although the differentiation into chondrogenic lineages was successful, it did not reveal significant differences between samples from obese and non-obese donors.

Table 23. Summary of mRNA levels by differentiation status using a chondrogenic-specific marker *(COL11A1)*.

Group	Mean (standard deviation)		Median (minimum, maximum)		p-value (Wilcoxon signed rank test)
	Undifferentiated cells	Differentiated cells	Undifferentiated cells	Differentiated cells	
Normal (n=7)	2.18 (0.68)	12.9 (5.42)	2.07 (1.33, 3.24)	10.3 (8.16, 21.4)	0.001
Obese (n=7)	1.66 (0.76)	7.77 (2.84)	1.65 (0.57, 2.71)	7.21 (2.96, 11.6)	
Total (n=14)	1.92 (0.74)	10.3 (4.94)	1.96 (0.57, 3.24)	8.97 (2.96, 21.4)	

Table 24. Summary of mRNA levels by obesity status using a chondrogenic-specific marker *(COL11A1)*.

Group	Mean (standard deviation)	Median (minimum, maximum)	p-value (Mann-Whitney test)
Normal (n=7)	12.9 (5.42)	10.3 (8.16, 21.4)	0.063
Obese (n=7)	7.77 (2.84)	7.21 (2.96, 11.6)	
Total (n=14)	10.3 (4.94)	8.97 (2.96, 21.4)	

3.1.4.3 Differentiation of WJ-MSCs into osteoblast-like cells

The cells from all donors were differentiated into osteoblasts to determine whether the WJ-MSCs from obese and non-obese donors exhibit similar osteogenic propensity.

After the cells were cultured for 21 days, the cultures from both obese and non-obese donors were positively stained by Alizarin red indicating the presence of calcium deposits due to bone formation (Figure 11C).

The undifferentiated and differentiated cells from all fourteen donors were assessed for the levels of the osteogenic-specific marker *RUNX2*. The mean (± standard deviation) of the mRNA expression level of *RUNX2* was higher in differentiated cells 19.7 (± 11.6) than in undifferentiated cells 0.10 (± 0.09) (Table 25). The differences between the differentiated and undifferentiated cells were significant (p-value 0.001, Wilcoxon signed rank test), confirming that the cells had undergone osteogenesis (Figure 11C).

Next, the levels of mRNA for the osteogenic-specific marker *RUNX2* in differentiated cells from obese and non-obese donors were compared. The data showed that the mRNA expression level of *RUNX2* in the non-obese group was highest in cells from donors N2 (25.8) and lowest in cells from donor N4 (8.63), whereas the highest and lowest expression levels in cells from the obese group were found in donors O7 and O5, at 53.0 and 9.18, respectively. Overall, the mean (± standard deviation) of the *RUNX2* expression level was higher in the obese group 23.0 (± 15.1) than in the non-obese group 16.5 (± 6.14) (Table 26). Non-significant differences (p-value 0.482, Mann-Whitney test) in the mRNA expression levels of *RUNX2* were found in the osteogenic cells differentiated from the obese and non-obese groups (Figure 11C). Analysis based on the Bootstrap model showed that the 95% confidence interval of the incidence rate ratio was 0.54 (-15.4 to 10.4).

Although the analysis of the differentiation of WJ-MSCs into osteogenic lineages was successful, it did not show significant differences between samples from obese and non-obese donors.

Table 25. Summary of mRNA levels by differentiation status using an osteogenic-specific marker *(RUNX2)*.

Group	Mean (standard deviation)		Median (minimum, maximum)		p-value (Wilcoxon signed rank test)
	Undifferentiated cells	Differentiated cells	Undifferentiated cells	Differentiated cells	
Normal (n=7)	0.57 (0.67)	16.5 (6.14)	0.22 (0.002, 0.18)	15.8 (8.63, 25.8)	0.001
Obese (n=7)	0.15 (0.10)	23.0 (15.1)	0.11 (0.09, 0.38)	15.3 (9.18, 53.0)	
Total (n=14)	0.10 (0.09)	19.7 (11.6)	0.09 (0.002, 0.38)	15.6 (8.63, 53.0)	

Table 26. Summary of mRNA levels by obesity status using an osteogenic-specific marker *(RUNX2)*.

Group	Mean (standard deviation)	Median (minimum, maximum)	p-value (Mann-Whitney test)
Normal (n=7)	16.5 (6.14)	15.8 (8.63, 25.8)	0.482
Obese (n=7)	23.0 (15.1)	15.3 (9.18, 53.0)	
Total (n=14)	19.7 (11.6)	15.6 (8.63, 53.0)	

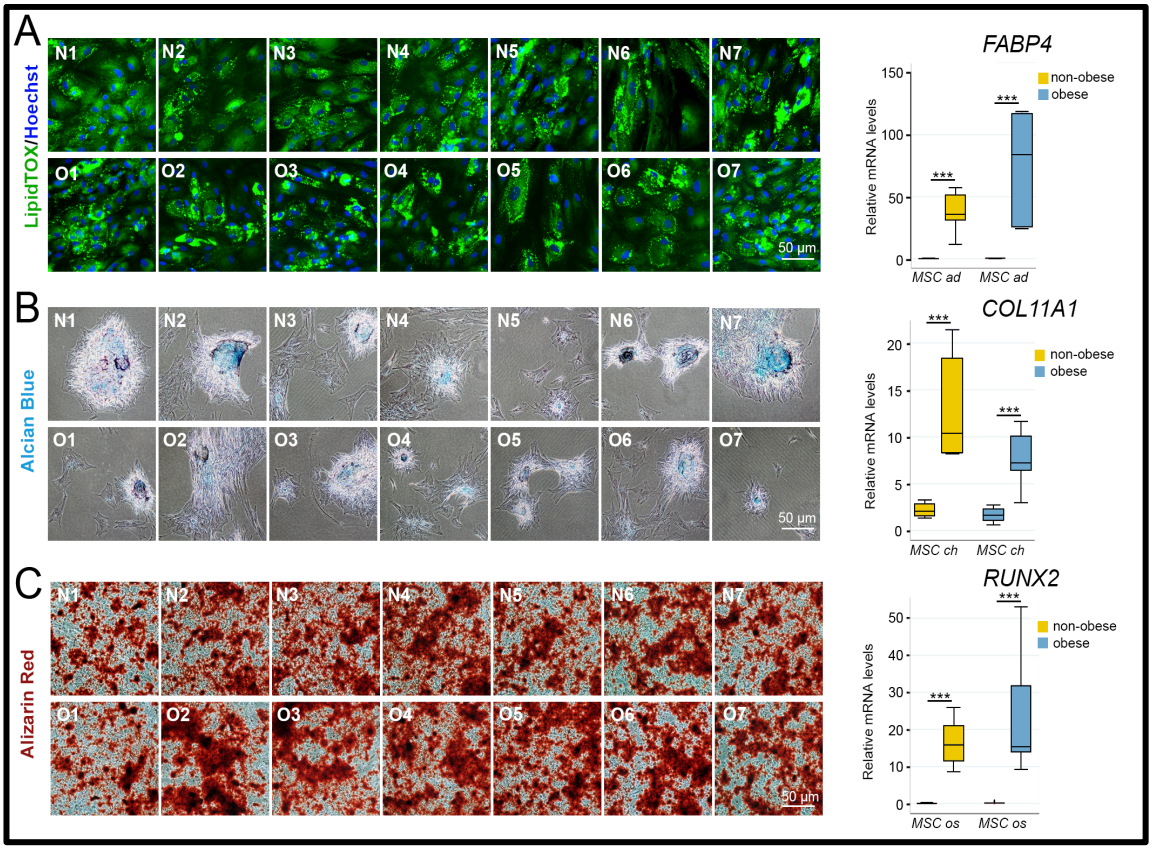

Figure 11. A. Directed adipogenic differentiation of WJ-MSCs from obese and non-obese donors conducted *in vitro* resulted in the formation of intracellular lipid droplets that were visualized with a fluorescent LipidTOX stain with the presence of *FABP4* in adipogenic differentiated cells. **B.** Direct chondrogenic differentiation of WJ-MSCs from obese and non-obese donors conducted *in vitro* resulted in the formation of cartilage-specific proteoglycans that were visualized with Alcian blue with the presence of *COL11A1* in chondrogenically differentiated cells. **C.** Direct osteogenic differentiation of WJ-MSCs from obese and non-obese donors conducted *in vitro* resulted in the presence of calcium deposits that were visualized with Alizarin red in the presence of *RUNX2* in osteogenically differentiated cells.

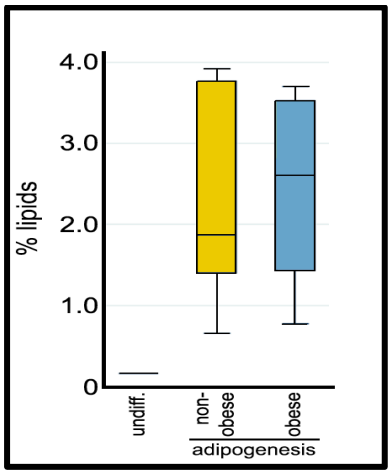

Figure 12. Quantitative analysis of the average cellular lipid (percentage) in each sample group showed no differences between adipogenically differentiated MSCs from obese and non-obese donors (p-value 0.749, Mann-Whitney test).

3.1.5 Effect of obesity on WJ-MSC immunomodulatory properties

The immunomodulatory test was performed to investigate the immune response properties of WJ-MSCs to determine whether they were affected by an abnormal metabolic environment. The immunomodulatory effects of WJ-MSCs from the fourteen non-obese and obese donors, were compared by adding WJ-MSCs to cultures containing PBMCs that had been stimulated by PHA. BM-MSCs were used as a reference for this experiment. Co-cultures were prepared at several different MSC:PBMC ratios. After 3 days of co-culture, the WJ-MSCs were found to inhibit the proliferation of stimulated PBMCs at all tested MSC:PBMC ratios.

Co-culture with WJ-MSCs inhibited the proliferation of PBMCs in response to PHA. The inhibition by cells from the obese and non-obese groups was not significantly different at an MSC:PBMC co-culture ratio of 1:5, with an average inhibition of 75.5% for non-obese and 82.7% for obese cell lines. Interestingly, when MSCs and PBMCs were co-cultured at ratios of 1:10, 1:20 and 1:40, the data indicated significant differences between the obese and control groups in the degree of inhibition of PBMC proliferation in response to PHA (defined here as the 'immune response'). At the 1:10 ratio, WJ-MSCs from the obese group showed greater inhibition of the immune response (88.4%) than WJ-MSCs from the control group (58.7%). At the 1:20 ratio, WJ-MSCs from the obese cell lines also demonstrated greater inhibition of the immune response (79%) than WJ-MSCs from the non-obese cell lines (37.7%). At the 1:40 ratio, WJ-MSCs isolated from donors with high BMI still showed a greater inhibition of the immune response (53%) than cells from donors with normal BMI (28.3%). Finally, at the 1:80 ratio, WJ-MSCs from obese donors inhibited PHA-induced proliferation of PBMCs by a non-significantly higher amount (20.4%) than their counterparts from the control group (7.4%) (Table 27 and Figure 13).

In conclusion, the WJ-MSCs derived from obese donors demonstrated significantly higher immune activity than the WJ-MSCs derived from non-obese donors. The corresponding p-values at 1:10, 1:20 and 1:40 MSC:PBMC co-culture ratios were 0.008, 0.012, and 0.047, respectively (Mann-Whitney test). The differences in immune activity for the ratios 1:5 and 1:80 were, however, not significant (p-value>0.05, Mann-Whitney test) (Table 27).

Table 27. Comparison of the immune activities of WJ-MSCs derived from obese and non-obese donors at WJ-MSC:PBMC ratios of 1:5, 1:10, 1:20, 1:40 and 1:80.

Ratio	Mean % (standard deviation)			Median % (minimum, maximum)			p-value (Mann-Whitney test)
	Non-obese (n=7)	Obese (n=7)	Total (n=14)	Non-obese (n=7)	Obese (n=7)	Total (n=14)	
1:5	75.5 (24.2)	82.7 (16.0)	79.1 (20.1)	85.2 (36.7, 99.5)	89.6 (58.0, 99.3)	87.4 (36.7, 99.5)	0.565
1:10	58.7 (27.0)	88.4 (18.5)	73.5 (27.0)	69.9 (22.1, 91.2)	93.9 (46.6, 97.7)	86.4 (22.1, 97.7)	0.008
1:20	37.7 (22.2)	79.0 (21.3)	58.3 (29.9)	43.2 (11.4, 68.0)	89.9 (36.5, 96.0)	61.4 (11.4, 96.0)	0.012
1:40	28.3 (20.9)	53.0 (21.0)	40.7 (23.9)	20.4 (7.45, 63.4)	61.7 (19.3, 78.5)	39.1 (7.45, 78.5)	0.047
1:80	7.47 (7.94)	20.4 (16.3)	13.9 (14.0)	7.62 (-1.81, 18.4)	17.9 (-8.24, 37.1)	13.7 (-8.24, 37.1)	0.110

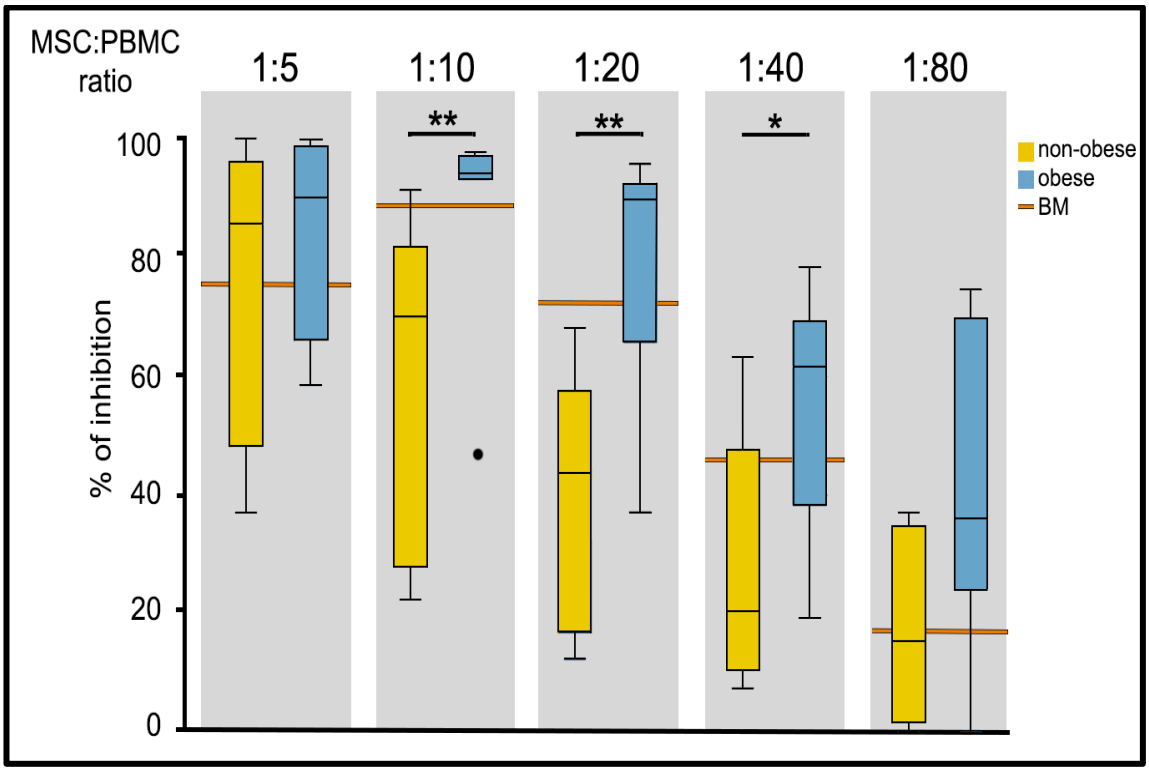

Figure 13. The immunomodulatory potential of WJ-MSCs showed higher immune activities in cell lines from obese donors than in cell lines from non-obese donors at the following MSC:PBMC ratios: 1:10, 1:20 and 1:40 (n=14). A representative immunomodulatory outcome is shown for 1:5 and 1:80 MSC:PBMC ratios with no significant differences were observed between the immune response of cells from obese and non-obese donors. BM was used as a control.

3.2 Analysis of WJ-MSC DNA methylation

The effects of obesity on genome-wide DNA methylation of WJ-MSCs were examined using methylation BeadChip arrays on a dedicated Illumina microarray platform. The methylation data produced after scanning the arrays were analysed using Illumina's GenomeStudio package and GenoSplice. The methylation assay was conducted specifically using WJ-MSCs from early passages that expressed common MSC markers, including CD90, CD73 and CD105. These WJ-MSCs were sorted from a triple-positive population using FACS. DNA was extracted from the sorted cells, and an aliquot of the eluted DNA was prepared for the bisulfite conversion reaction. A PCR assay designed to test bisulfite conversion efficiency, containing methylation-specific primers, was performed using the bisulfite-converted DNA. Successfully converted DNA was used for the DNA methylation assay. Illumina 450K Methylation BeadChips were used for genome-wide methylation. In total, 45 separate reactions were attempted (fourteen obese and non-obese samples that were tested in triplicate and three reactions that did not contain any DNA template). These 45 reactions were processed in one batch to minimize variations from any batch effects, allowing better evaluation of the potential biological relevance of DNA methylation differences among the samples.

3.2.1 WJ-MSC sorting and gDNA extraction and quantification

WJ-MSCs that were triple positive for CD90, CD73 and CD105 were sorted from the fourteen lines that had been obtained from UCs. The pre-sorting conditions for sorting for the triple-positively stained WJ-MSCs are shown in Figure 14.

WJ-MSCs were collected after sorting the cells from all fourteen lines, including obese and non-obese cell lines. The recovered gDNA was eluted in 200-µl of elution buffer and quantified using the Qubit fluorometer. The resulting values are shown in Table 28.

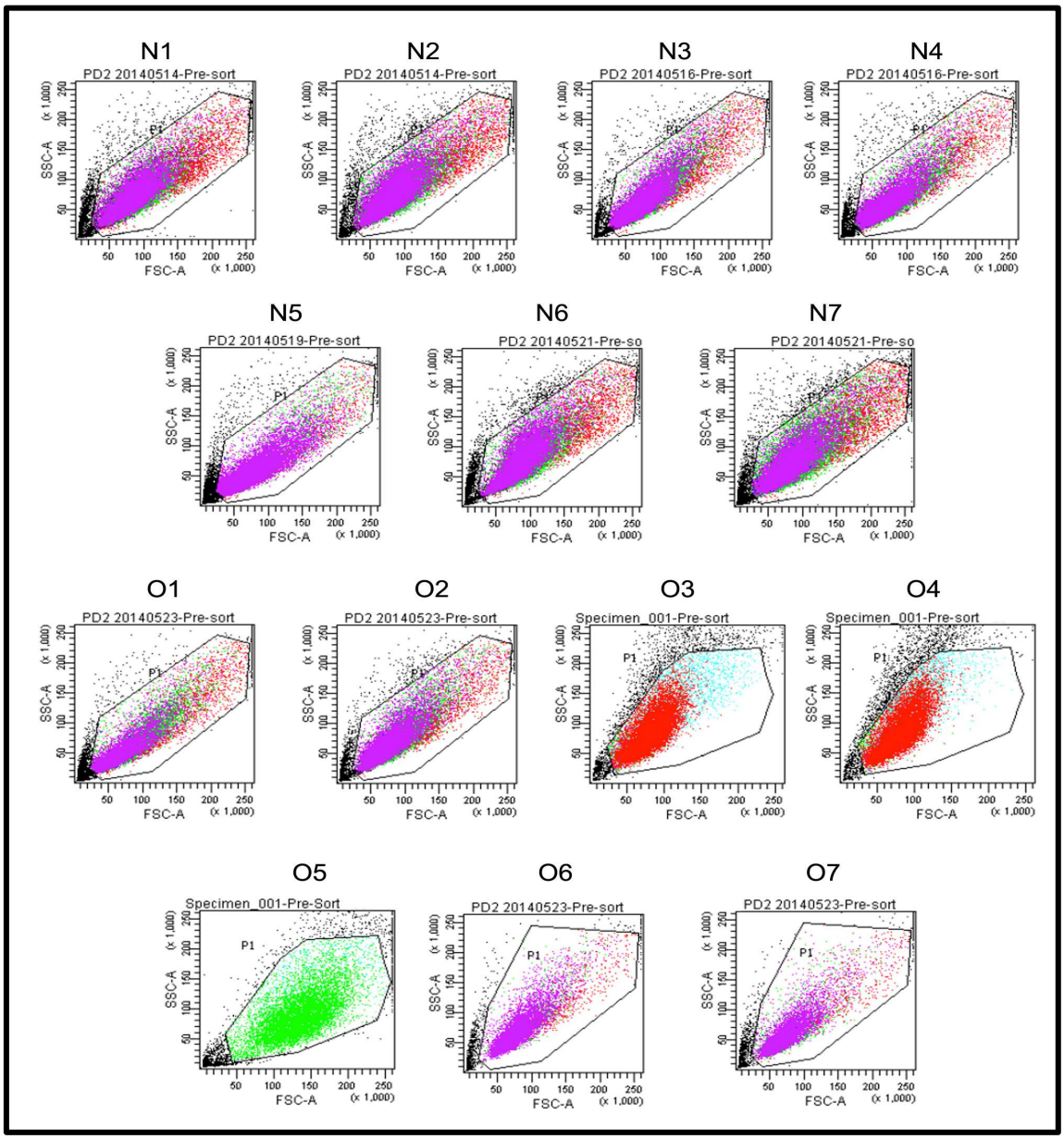

Figure 14. Pre-sorting of WJ-MSC populations stained with fluorescent antibodies (FITC-CD90, PE-CD73 and APC-CD105) from obese and non-obese donors. From left to right, the 1st row shows pre-sorting of WJ-MSCs from non-obese donors N1, N2, N3 and N4; the 2nd row corresponds to N5, N6 and N7 cell populations; the 3rd row corresponds to cell populations from obese donors O1, O2, O3 and O4; and the 4th row corresponds to cell populations from obese donors O5, O6 and O7.

Table 28. DNA yield after using the DNA extraction protocol. Measurements were determined using a Qubit instrument; N=non-obese (n=7), O=obese (n=7).

Donor number	DNA concentration (ng/µl)
N1	34.6
N2	91.9
N3	74.5
N4	48.9
N5	62.9
N6	69.3
N7	40
O1	78.2
O2	92
O3	101
O4	100
O5	135
O6	32.7
O7	75.2

3.2.2 Assessment of bisulfite conversion efficiency of the gDNA samples

Bisulfite treatment of the obese and non-obese samples was performed. For each reaction, 400-ng to 500-ng of gDNA was used, as recommended by Illumina. The ultimate purpose of this procedure was to reveal the absence or presence of methyl groups at cytosine residues across the genome. During the treatment process, unmethylated cytosine residues were converted into uracil residues, whereas cytosine residues that were methylated were protected from the conversion reaction. Subsequent downstream processes that use the elution from the bisulfite treatment, such as the whole-genome amplification step of the Illumina Infinium methylation procedure, delete all epigenetic information present on the DNA. Therefore, it was important to conserve the epigenetic status of the DNA in the bisulite-converted form. To accomplish this, the converted uracils/unconverted cytosines in the DNA samples were successfully whole-genome amplified. The amplified DNA was used for the Illumina Infinium methylation assay protocol. Infinium Human Methylation 450K BeadChips were selected for the assay. The data generated from scanning the arrays were used to infer the methylation status of the DNA.

The bisulfite-converted DNA was recovered in 12-µl of elution buffer. The efficiency of the conversion was determined by using PCR to test for false-positive methylation signals that may have resulted from the incomplete conversion of cytosine into uracil. Complete conversion of bisulfite-treated gDNA was determined by testing the amplified samples for the presence of specific band sizes on a pre-prepared automated electrophoresis gel. The primers that were designed to specifically amplify unmethylated copies of the *MEG3* DMR produced a 120-bp band, while the primers designed for amplifying methylated copies of the *MEG3* DMR produced a 160-bp band in the same reaction. Additional control reactions included unconverted DNA as a

template for every cell line. As expected, none of these controls produced any bands. Therefore, the specificity of both sets of primers for bisulfite-converted DNA was confirmed by the expected band sizes of the 120-bp and 160-bp PCR products. A negative control (H_2O) that did not include any DNA template was also included in the PCR as a contamination indicator (Figure 15). At this stage, the samples were assumed to be completely converted and the 42 samples were considered ready for further processing using the Infinium Human Methylation 450K BeadChip kit.

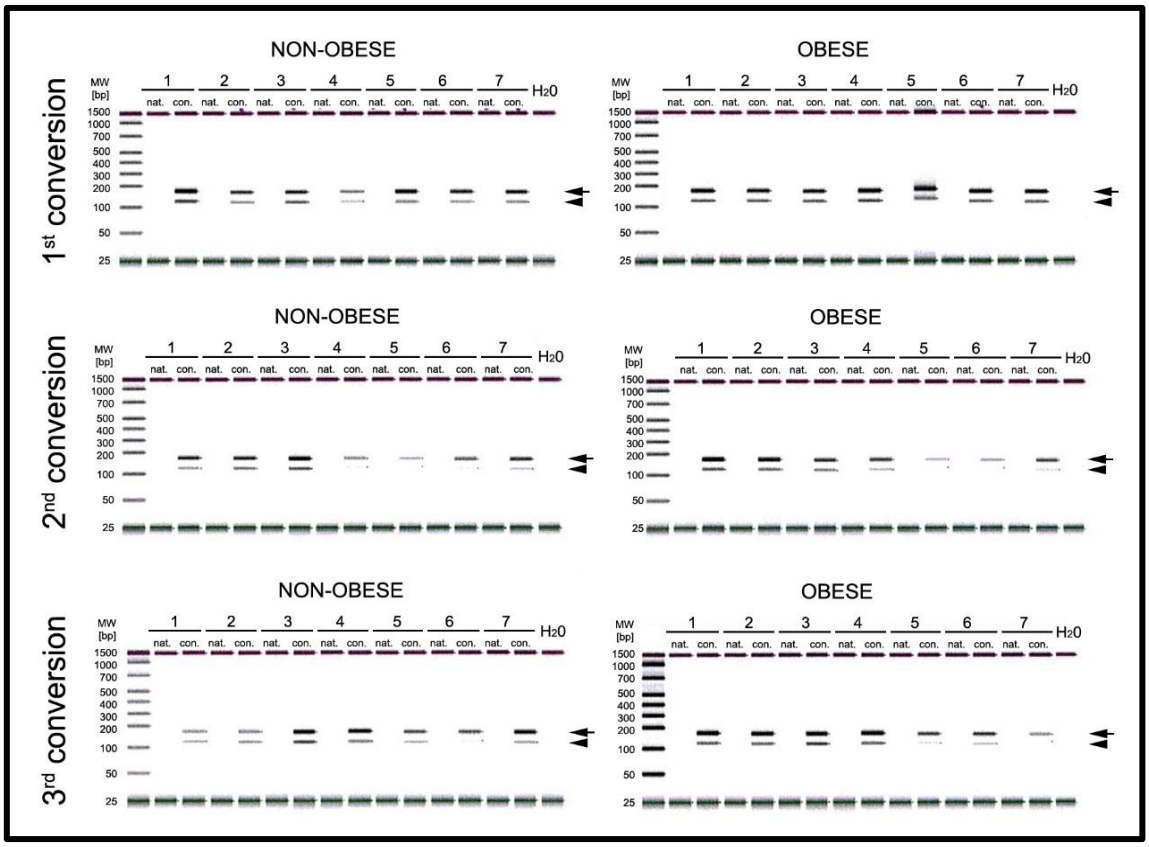

Figure 15. PCR results from the conversion reactions. Each sample from non-obese 1-7 (n=7) and obese 1-7 (n=7) donors was bisulfite converted and tested by PCR in triplicate (1st conversion, 2nd conversion and 3rd conversion). Each sample was amplified separately using converted and non-converted DNA templates and electrophoresed on the gel. The converted (con.) version showed two bands (120-bp and 160-bp); as expected, the native (nat.) version showed no bands. The use of H_2O, which served as a negative control, yielded no bands.

3.2.3 Quality control analysis of the methylation BeadChip array data

The controls provided in the Illumina methylation system assess the quality of the key parameters in its workflow, specifically, DNP and biotin staining, extension, target removal, hybridization, detected CpG sites, non-polymorphic controls, bisulfite conversion, specificity and negative controls. The data showed that the controls performed well. More importantly, the data generated from the sample-dependent control assays showed that the samples were of good quality and that the bisulfite conversion reaction was successful. The following diagrams (Figures 16-26) show the control dashboard that was produced by the GenomeStudio software (version 2011.1) and the data for each sample; each spot on the plots represents a single sample.

3.2.3.1 Sample-independent controls

The staining control reaction is monitored by assessing specific beads on the array that are known to have biotin and DNP attached; the efficiency of the staining step is evaluated in the green and red channels, where both the background intensity and the signal intensity can be seen (Figure 16). As expected, in the red laser channel, the average value for DNP high staining signal intensity was greater than 3,000 (6,031), and the average DNP background staining intensity value was 55; the latter value was low, as expected. In the green channel, the DNP signal was 70 for the high-intensity control and 76 for the DNP background control; these low values were expected because red signals should not be detected in the green channel.

In the green channel, the biotin high-intensity control value should be greater than 3,000, and it was 10,328. The biotin background intensity control in the green channel should be lower than 1,000; the observed background intensity value was 40, indicating that the staining reaction was efficient. In the red laser channel, the biotin background and biotin high staining signal intensities were less than 1,000, with values of 48 and 112, respectively. This staining control was independent of the hybridization and amplification steps.

Channel	Intensity	Expected Value	Average values	Results
Green	DNP high	<1000	70	Passed
Green	DNP background	<1000	76	Passed
Green	Biotin (high)	>3000	10328	Passed
Green	Biotin (bkgd)	<1000	40	Passed
Red	DNP high	>3000	6031	Passed
Red	DNP background	<1000	55	Passed
Red	Biotin (high)	<1000	112	Passed
Red	Biotin (bkgd)	<1000	48	Passed

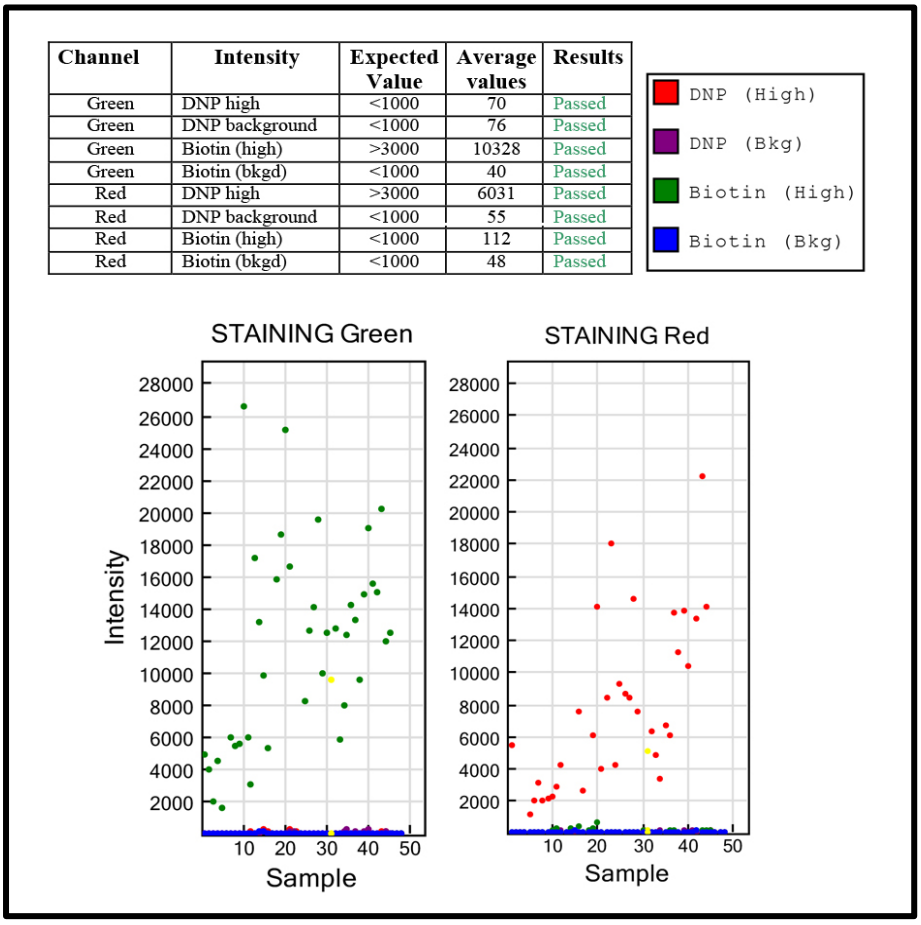

Figure 16. Staining control assessment using DNP and biotin in the green and red channels

Extension controls assess how well each nucleotide (A, T, C and G) was incorporated during the extension of hairpin probes that reside on the array. These controls are monitored in both the green (C, G) and red (A, T) channels; a high intensity indicates a successful extension. In the green channel, A and T intensities were less than 2,000, while C and G intensities were greater than 20,000. In the red channel, the A and T nucleotide extension intensities were greater than 20,000 and those of C and G were less than 2,000, indicating that all four nucleotides were extended successfully, as shown in Figure 17.

Channel	Intensity	Expected Value	Average value	Results
Green	A	<2000	545	Passed
Green	T	<2000	472	Passed
Green	C	>20000	30512	Passed
Green	G	>20000	29480	Passed
Red	A	>20000	24115	Passed
Red	T	>20000	26279	Passed
Red	C	<2000	1762	Passed
Red	G	<2000	1596	Passed

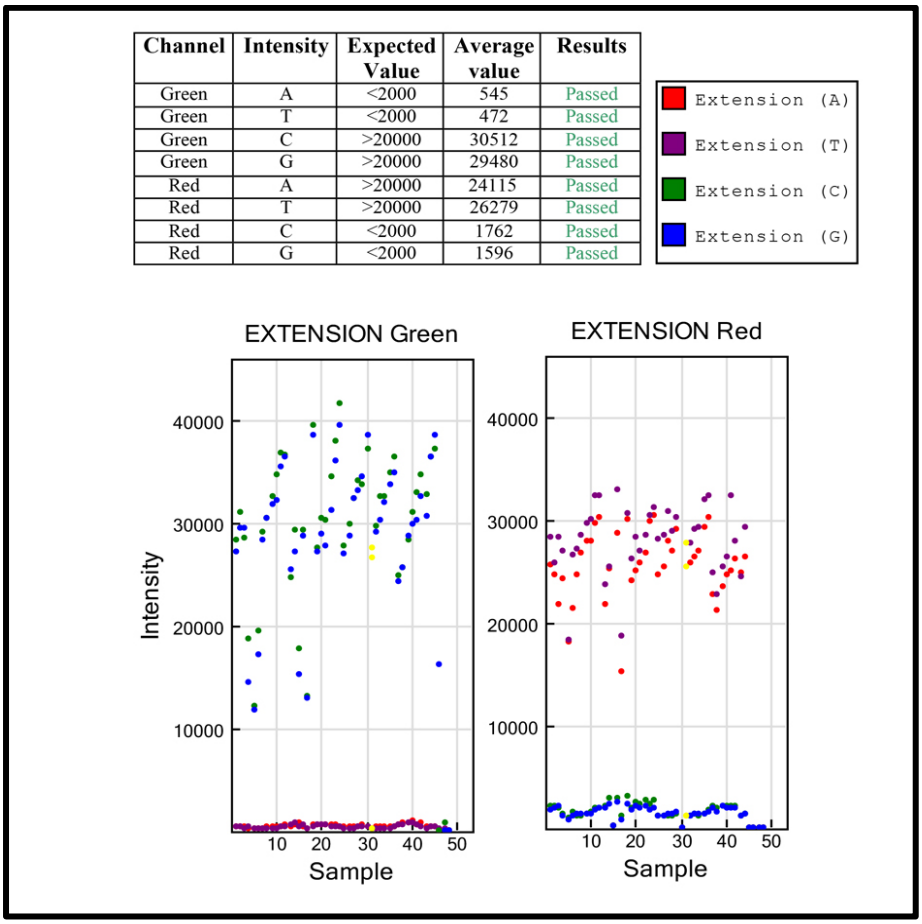

Figure 17. Extension control for each nucleotide in the green and red channels.

Target removal controls evaluate the efficiency of the stripping step after the extension reaction has occurred. The control oligonucleotides differ from the oligonucleotides used in the bead array for the samples, where the sample DNA (target) is used as a template for the extension reaction; the control oligonucleotides are extended using the probe sequence as a template, and this generates labelled targets. The target removal controls are present in the hybridization buffer. Their performance was monitored in the green channel and was expected to result in low signal intensity (<1,200) compared with that of the hybridization controls; this result would indicate that the targets were efficiently removed after extension (Figure 18).

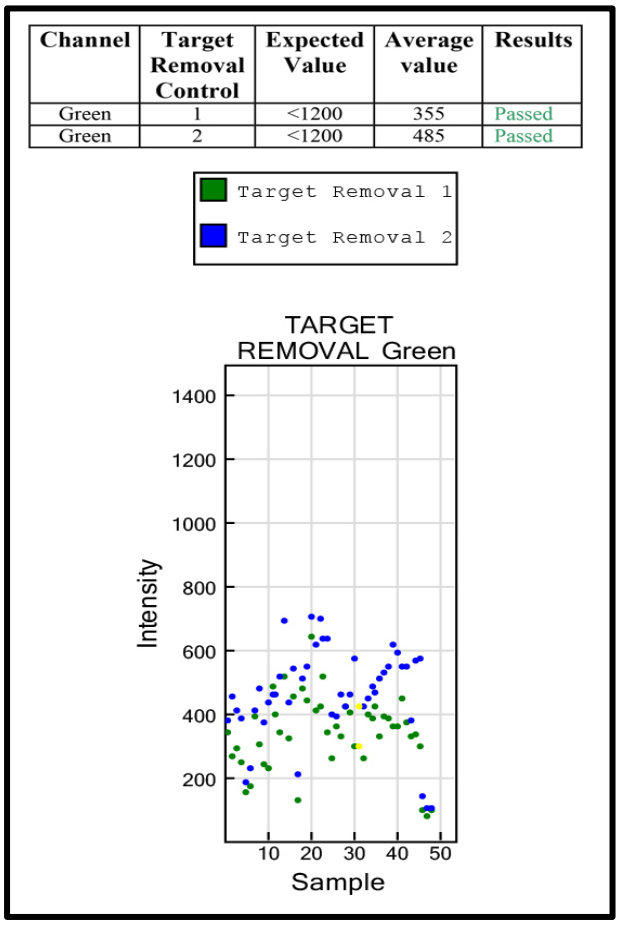

Figure 18. Target removal control assessment using the green channel only.

Hybridization controls examine the overall performance of the entire assay using synthetic targets and are independent of the amplified target (sample). These controls are spiked into the hybridization solution at three concentrations: high (5-pM), medium (1-pM), and low (0.2-pM). The signal intensities should correspond to the concentrations of the synthetic targets, and their signals are observed in the green channel. The signal intensity values were within the ranges expected from three different target concentrations; the signal intensities were 8,446, 16,436 and 27,350 for the low, medium, and high concentration levels, respectively (Figure 19).

Channel	Hyb control concentration	Expected Value	Average value	Results
Green	Low	<10000	8446	Passed
Green	Medium	<20000	16436	Passed
Green	High	>20000	27350	Passed

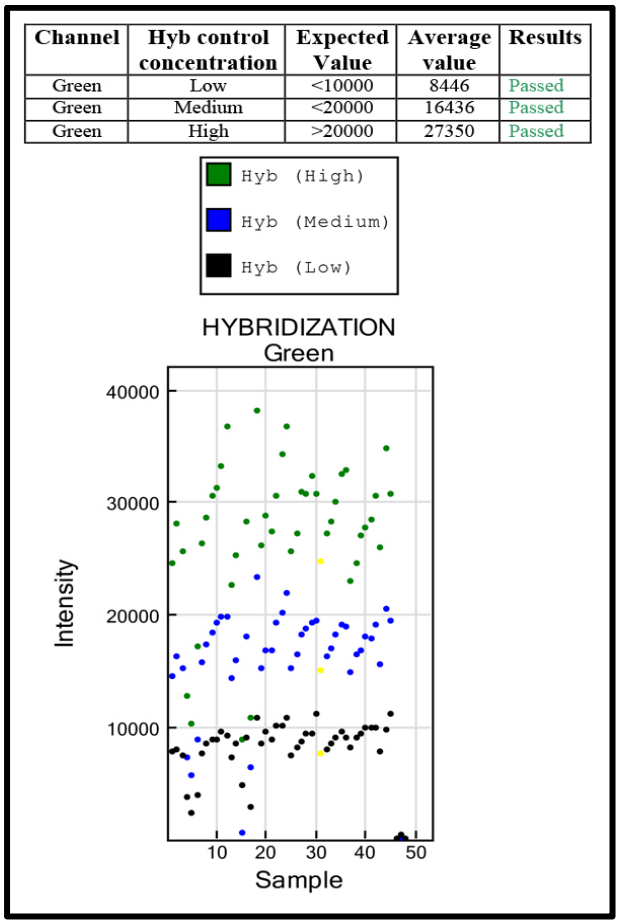

Figure 19. Hybridization control evaluation in the green channel.

3.2.3.2 Sample-dependent controls

Non-polymorphic controls evaluate the overall performance of the assay from the amplification step to the detection step by querying a specific base in the non-polymorphic region of the bisulfite-converted gDNA. This control enables the comparison of assay performance across different regions of the sample DNA. The non-polymorphic controls are designed to query each nucleotide (i.e., A, T, C, and G). The target control with the C base queries the whole-genome-amplified DNA strands generated from the converted strands. The signal intensities for nucleotides A and T in the red channel were expected to be greater than 5,000; the signal intensity values obtained were 9,066 for A and 11,410 for T. The signal intensities for these nucleotides were less than 2,000 in the green channel, as expected. However, the signal intensities from nucleotides C and G were 13,087 and 9,153, respectively, in the green channel, whereas values from the red channel for these particular nucleotides were less than 2,000, as expected. This control confirmed that the assay was successful across both polymorphic and non-polymorphic regions of the genome (Figure 20).

Channel	Nucleotide	Expected Value	Average value	Results
Red	A	>5000	9066	Passed
Red	T	>5000	11410	Passed
Red	C	<2000	525	Passed
Red	G	<2000	688	Passed
Green	A	<2000	828	Passed
Green	T	<2000	971	Passed
Green	C	>5000	13087	Passed
Green	G	>5000	9153	Passed

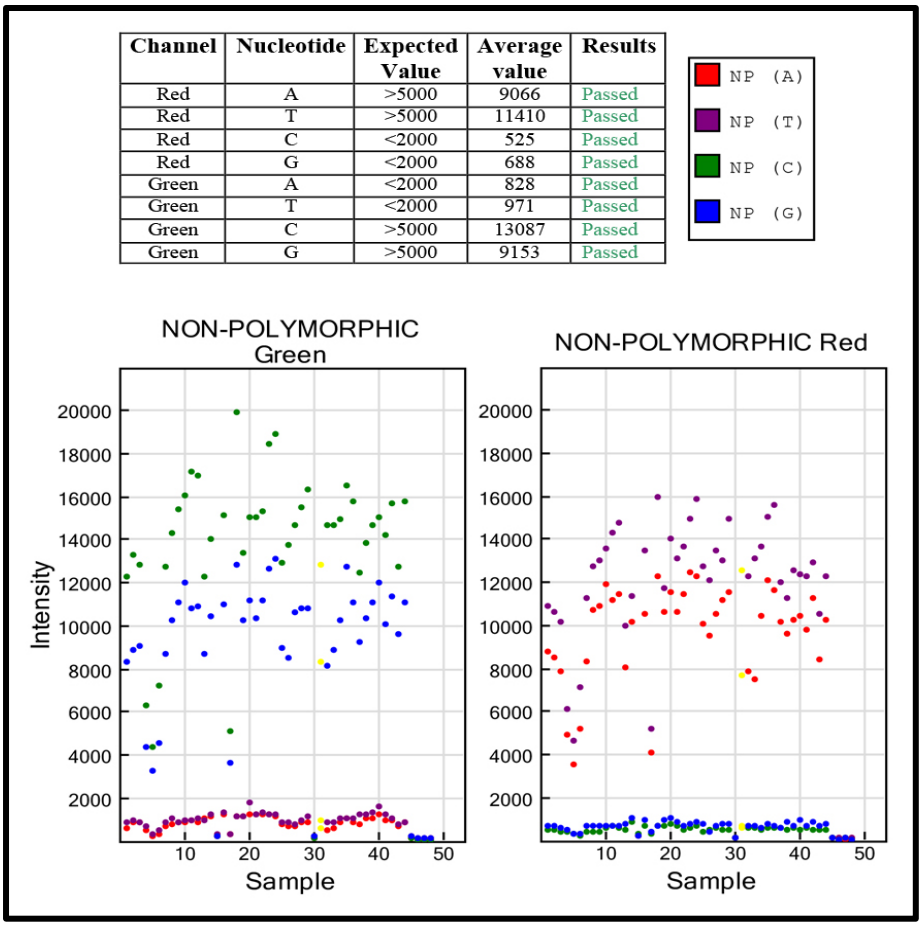

Figure 20. Non-polymorphic control for each nucleotide assessment using the green and red channels.

The detected CpG sites represent the number of CpG sites detected at p-values <0.01 and <0.05 in the tested samples (Figure 21).

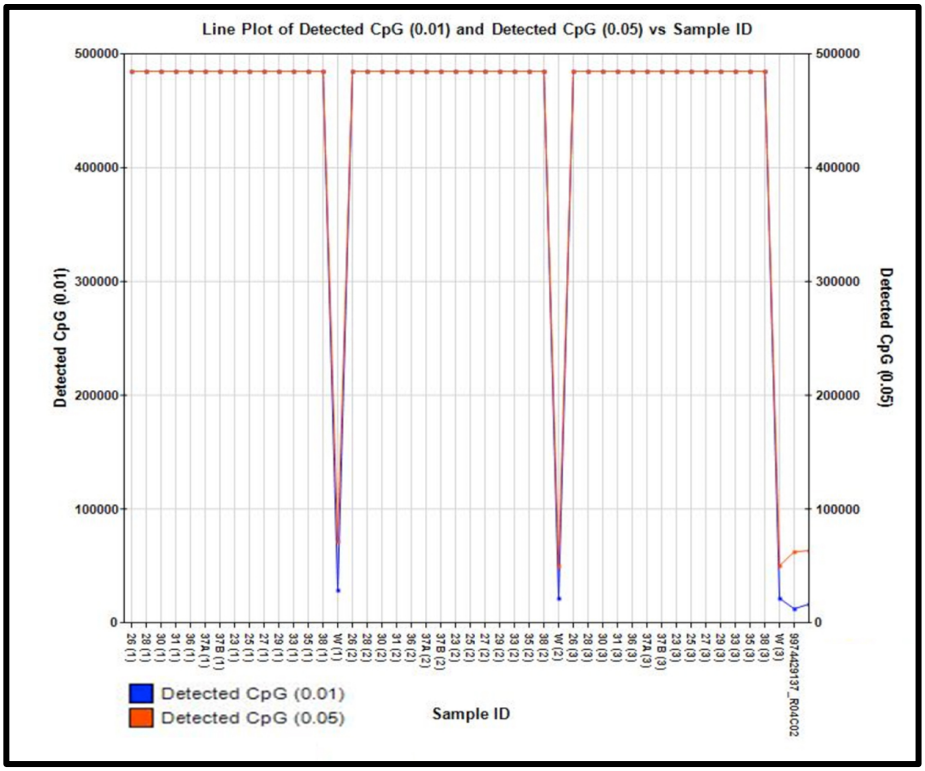

Figure 21. Line plot of CpG sites detected at p-values of 0.01 and 0.05 for 'no DNA template' samples and 'DNA template' samples (n=45).

Bisulfite conversion I and II controls evaluate the efficiency of bisulfite conversion using the Infinium I and II probe designs and allele-specific single base extension. In the bisulfite conversion I control reaction, the converted C probes match the converted sequence and are extended in the case of successful conversion; in unconverted DNA samples, the unconverted U probe is extended instead. The performance of the bisulfite conversion controls C1, C2 and C3 were assessed in the green channel, and controls C4, C5 and C6 were evaluated in the red channel because all conversion control values must be greater than 5,000, the results are shown in Figure 22. The signal intensities from the unconverted U controls (i.e., U1, U2, U3, U4, U5 and U6) were evaluated in both the green and red channels and were expected to be less than 1,000 (Figure 22). In the bisulfite conversion II control, if the A base was incorporated into the four (1-4) probes, the signal intensities would be over 5,000 and would be observed in the red channel, indicating successful bisulfite conversion. In contrast, the signals from the four probes (1, 2, 3 and 4) would be elevated in the green channel with values less than 3,000 (the observed values were 1,628, 594, 1,442 and 540, respectively) if the G base was incorporated across an unconverted cytosine, indicating an unconverted DNA sample (Figure 23).

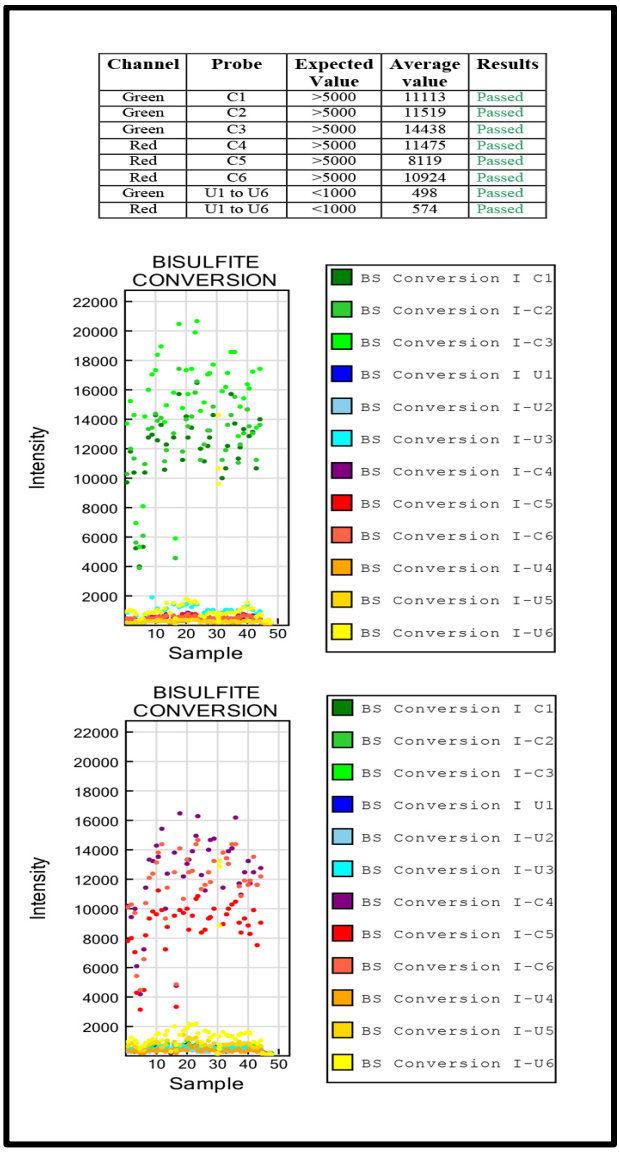

Figure 22. Bisulfite conversion I control evaluation using the green and red channels.

Channel	Probe	Expected Value	Average value	Result
Green	1	<3000	1628	Passed
Green	2	<3000	594	Passed
Green	3	<3000	1442	Passed
Green	4	<3000	540	Passed
Red	1	>5000	10278	Passed
Red	2	>5000	10747	Passed
Red	3	>5000	7162	Passed
Red	4	>5000	9796	Passed

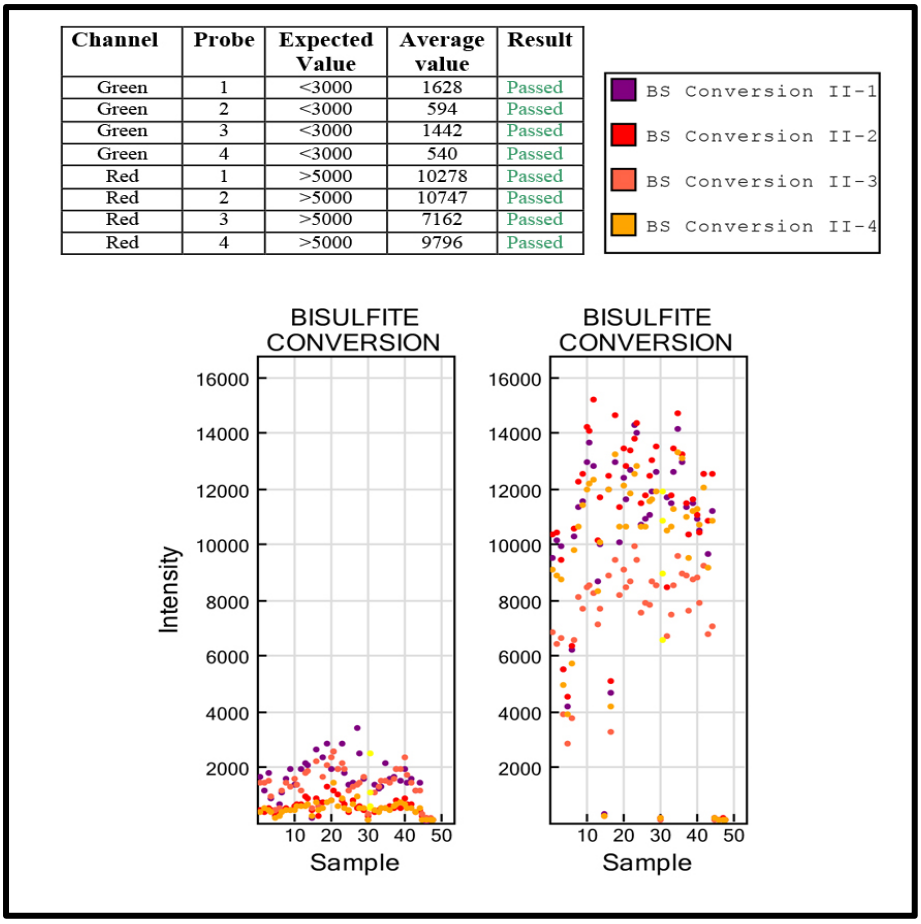

Figure 23. Bisulfite conversion II control evaluation using the green and red channels.

Specificity I and II controls are used to monitor the potential non-specific primer extension of the Infinium I and II assay probes. The Infinium specificity I control queries probes for the methylated and unmethylated state of each CpG locus. The G/C match corresponds to the methylated status of the interrogated C, while the A/T match corresponds to the unmethylated status of the interrogated C. The G/T mismatch controls test for non-specific detection of methylation signals over unmethylated background. Perfect match controls correspond to A/T matches that give high signals, and mismatch controls correspond to G/T mismatches that give weak signals. The performance of G/T mismatch controls was monitored in the green and red channels (Figure 24). The specificity II controls consist of three probes (specificity 1, specificity 2 and specificity 3); these probes assess the potential non-specific detection of methylation signals over the unmethylated background; the A base must be incorporated across from the non-polymorphic T base. These probes were expected to yield high intensities (>5,000) in the red channel. The average values of probes 1, 2, and 3 were 10,006, 7,463 and 8,951, respectively; these outcomes were as expected. The three probes would give an elevated signal in the green channel in the event of non-specific incorporation of the G base (Figure 25).

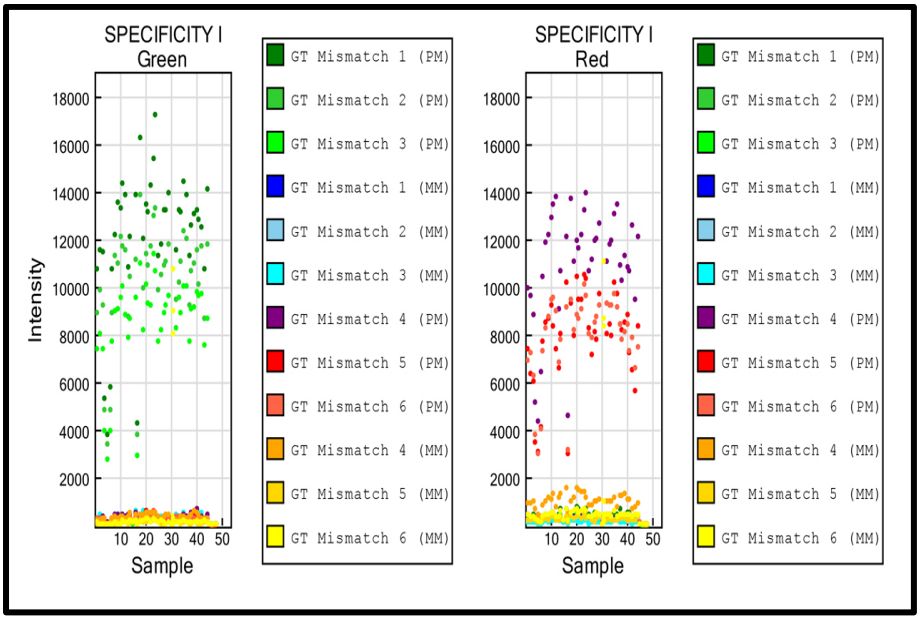

Figure 24. Specificity control I assessment using the green and red channels.

Channel	Probe	Expected Value	Average value	Results
Green	1	<3000	482	Passed
Green	2	<3000	426	Passed
Green	3	<3000	385	Passed
Red	1	>5000	10006	Passed
Red	2	>5000	7463	Passed
Red	3	>5000	8951	Passed

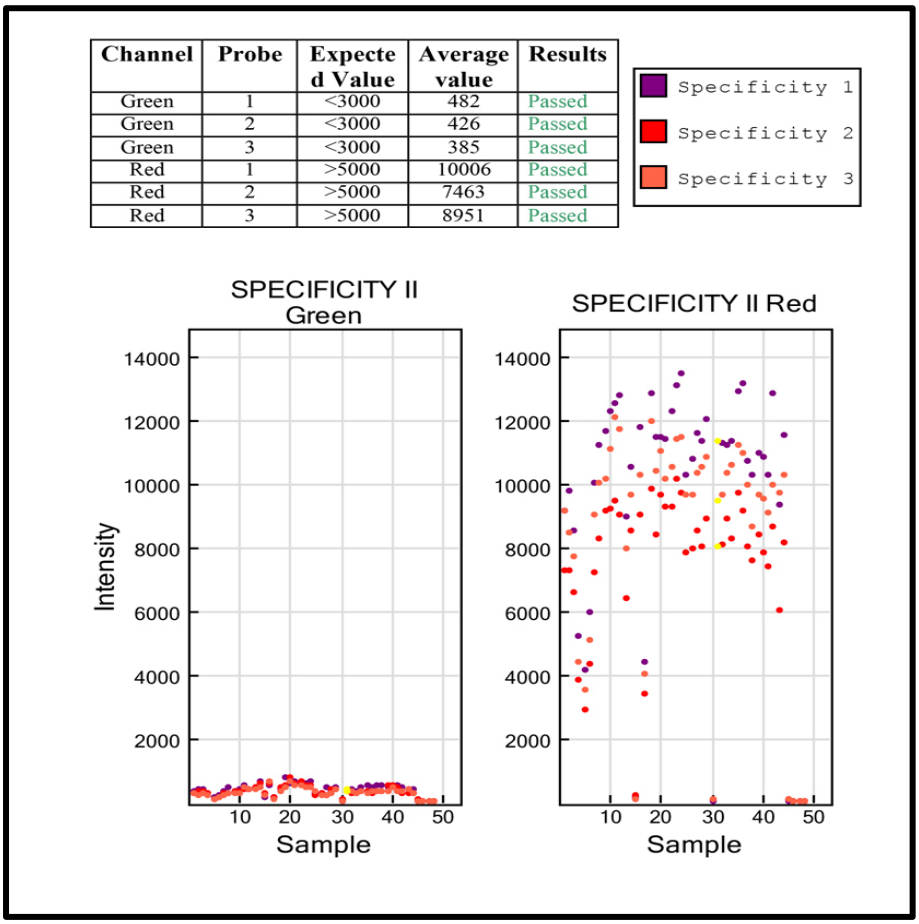

Figure 25. Specificity control II assessment using the green and red channels.

Negative controls are random sequences that are not expected to hybridize to the DNA template; they are used to assess the specificity of the reaction. In particular, they are useful for assessing the bisulfite-converted gDNA because the chemical treatment reduces the sequence complexity. This type of control is also a particularly useful measure for analysing the background, especially for cross-hybridization and non-specific extension. The green and red channels were used to monitor the performance of the negative controls (Figure 26).

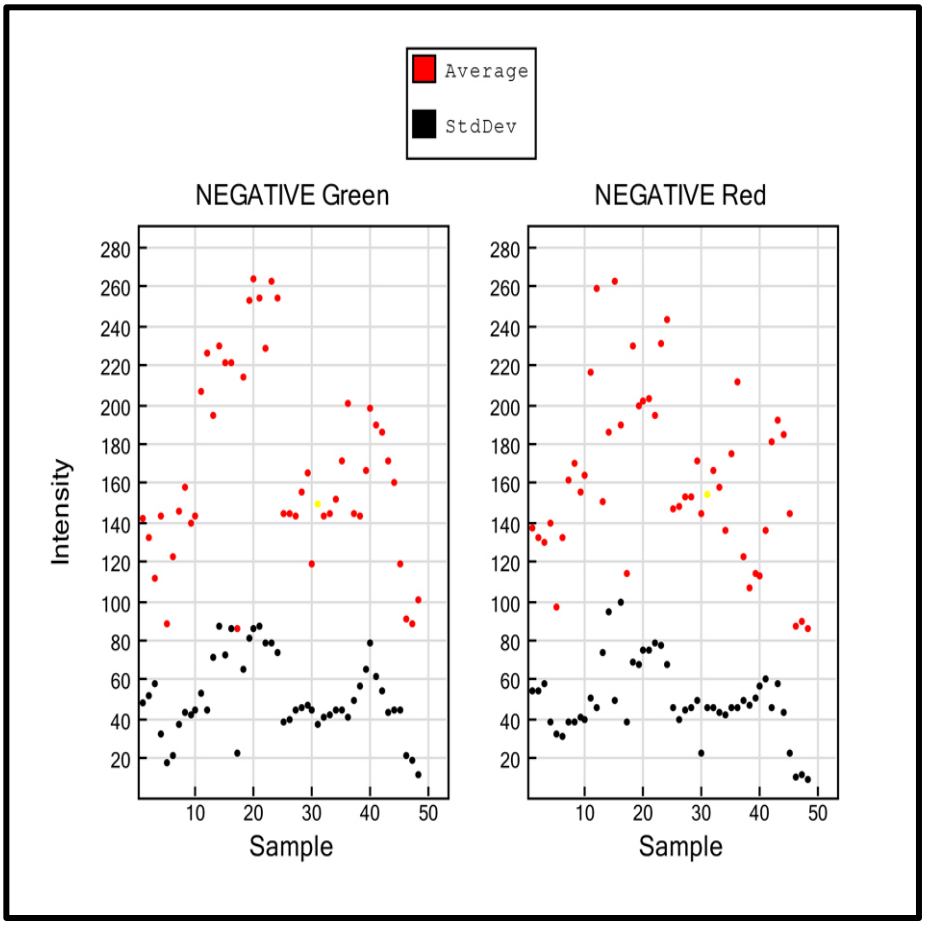

Figure 26. Negative control performance measured using the green and red channels.

3.2.4 Genome-wide effect of obesity on DNA methylation

Bisulfite-converted gDNA obtained from WJ-MSCs was tested on Illumina 450K methylation BeadChips to assess the impact of obesity and to detect changes resulting from obesity on the pattern of genome-wide DNA methylation. The experimental design ensured that the entire sample set would be tested in one batch. All fourteen lines were tested in triplicate, and three assays that did not contain any DNA were also included. All the samples were processed in one batch according to the Illumina Infinium methylation protocol. The robustness of the technique was confirmed by the fact that the values for all of the samples were within the quality control parameters. The data set generated for the methylation analyses was approximately 5-GB in size. The data analysis was performed using GenoSplice.

Methylation data analysis of WJ-MSCs isolated from obese and non-obese donors showed that the hierarchical clusters of differentially methylated samples from each group clustered in clearly separate groups according to their beta values (Figure 27A). Moreover, the results obtained using triplicate samples of each cell line immediately clustered together when principal component analysis (PCA) was applied (Figure 27B). A comparison analysis between the averages of all obese samples with those of all non-obese samples identified 1% of differentially methylated CpG sites, indicating that changes were observed in 5,767 CpG sites. Further analysis of the sites identified as differentially methylated showed that 41% (2,373) of these CpG sites were significantly hypomethylated and 59% (3,394) were significantly hypermethylated (Figure 27C). A Manhattan plot displaying the significance of the associations by chromosomes indicates that altered methylation states were distributed across all chromosomes (Figure 27D).

From the standpoint of functional distribution, the majority of CpG sites that were significantly differentially methylated were located in gene body regions; 38% (1,284) of these CpG sites were hypermethylated, and 31% (748) were hypomethylated. The intergenic sites also contained many CpG sites that were significantly differentially methylated; 29% (984) of these were hypermethylated, and 34% (801) were hypomethylated. A minority (2%) of CpG sites referenced to loci in the 1st exons were hypermethylated, corresponding to 71 CpG sites, and a total of 3% of CpG sites in 1st exons and 3'UTRs were hypomethylated, corresponding to 82 and 67 CpG sites, respectively (Figure 28). Based on the CpG content and the surrounding context, the majority of CpG sites that showed significant differential methylation were isolated CpGs in the genome, defined as being in open sea regions; of these, 43% (1,450) were hypermethylated and 47% (1,119) were hypomethylated. The minority of differentially methylated CpG sites occurred in the shelves; 12% (406) of these CpG sites were hypermethylated, and 8% (181) were hypomethylated (Figure 28). With respect to chromosomal location, chromosome 1 harboured the majority of the hypermethylated or hypomethylated CpG sites and chromosome Y contained the fewest (Figure 28). This outcome reflects the distribution of CpG sites across the chromosomes; chromosome 1 is the largest and contains the most (46,867) CpG sites, and chromosome Y is the smallest chromosome and contains the fewest (416) CpG sites.

Subsequently, the genes associated with the significantly differentially methylated CpG sites were identified and analysed by comparatively analysing the data from the obese and non-obese donor groups; in this data, each donor was represented by the average of three replicates. The average difference ranged from 1% in donors O3 and O4 to 5% in donor O2. Donor O5 was an exception, with 32% of differentially methylated CpG sites. An investigation of the background of this particular obese patient revealed no

clear explanation for the high percentage of differentially methylated CpG sites in these cells (Figure 29). Among the CpG sites that exhibited differences in their methylation profiles, three donors (O6, O2 and O3) predominantly exhibited hypomethylation at 56%, 80% and 81% of these sites, respectively, whereas four donors (O5, O4, O1 and O7) predominantly exhibited hypermethylation at 53%, 59%, 65%, and 70% of these sites, respectively (Figure 29).

Next, the data from the obese donors were examined with the specific aim of identifying CpG sites with methylation profiles that might be influenced by an abnormal metabolic environment. The selection criterion chosen was that a particular CpG site with a significantly differentially methylated profile was detected from four or more obese donors. Differentially methylated CpG sites with changes equal to or greater than 20% and shared among four or more obese donors were detected in 67 genes. Six out of the seven obese donors shared 3 differentially methylated genes (*NTM*, *SIM2* and *STT3A*), five out of the seven obese donors shared 22 differentially methylated genes, and four out of the seven obese donors shared 42 differentially methylated genes (Table 29). However, of these 67 genes, only three had more than one significantly differentially methylated CpG site: *MAD1L1* had two sites, *TRIM10* had four sites, and *ZNF714* had five sites (Table 30). Four of the seven donors had CpG sites in *MAD1L1* and *TRIM10* that were significantly differentially methylated, and five of the seven donors had CpG sites in *ZNF714* that were significantly differentially methylated (Table 30).

The 67 genes were further filtered based on the list of polymorphic CpG sites and segmental duplication. Filtering based on the list of polymorphic CpG sites aimed to eliminate any false interpretations due to genotype polymorphisms. It was important to determine whether any of these genes is segmentally duplicated because these genes are known to have long, nearly identical DNA sequences approximately 1-kb in length

and these genes normally occur in multiple locations as result of duplication events and usually only one copy is functional, which may lead easily to misinterpretation of the results. Among the 67 genes filtered, 65 had probes targeting polymorphic CpGs (Table 31) and two genes were segmentally duplicated (*DCAF6* and *ZNF714*).

Further statistical analysis of the list of 67 genes was performed to determine whether differentially methylated CpG sites were located in polymorphic regions. If they were, they could be excluded. After the 67 genes were further filtered, the list was narrowed to 18 genes whose differentially methylated CpG sites were in non-polymorphic regions (Figure 30A). Most of the differentially methylated CpGs were located in the body (85.61%), whereas promoter areas (TSS1500, TSS200 and 5'UTR) and the 1st exon accounted for 12.53% of the differentially methylated sites (Figure 30B).

The statistical power for detecting 20% methylation in this data set for 21 versus 21 samples (7 non-obese versus 7 obese donors, each in triplicate; Figure 27) was approximately 99%. The same was true of the 3 versus 21 samples comparison (1 obese versus the average of 7 non-obese donors, each in triplicate; Figure 29). The sample size used for the analysis was small; however, taken together, the array data suggest that maternal obesity might have a lasting effect on the DNA methylation profile of WJ-MSCs isolated from UC explants and cultured *in vitro* for at least one passage.

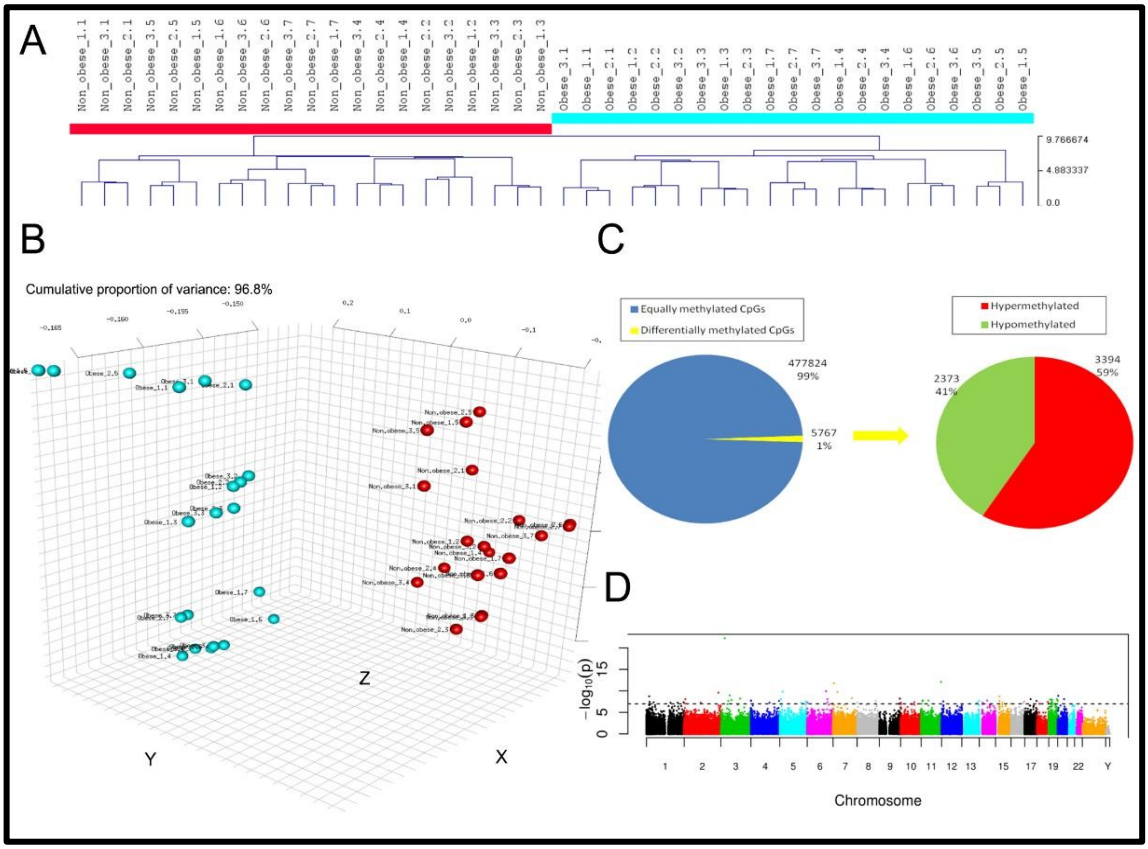

Figure 27. A. Hierarchical clustering analysis of obese verses non-obese samples based on epigenome-wide DNA methylation showed that each group clustered separately. **B.** PCA yielded separate clusters of obese and non-obese samples. **C.** The results showed that 1% of CpGs sites were differentially methylated in non-obese and obese donors, 41% of the CpG sites were hypomethylated and 59% of the CpG sites were hypermethylated. **D.** Changes in methylation patterns were observed to be distributed across all chromosomes.

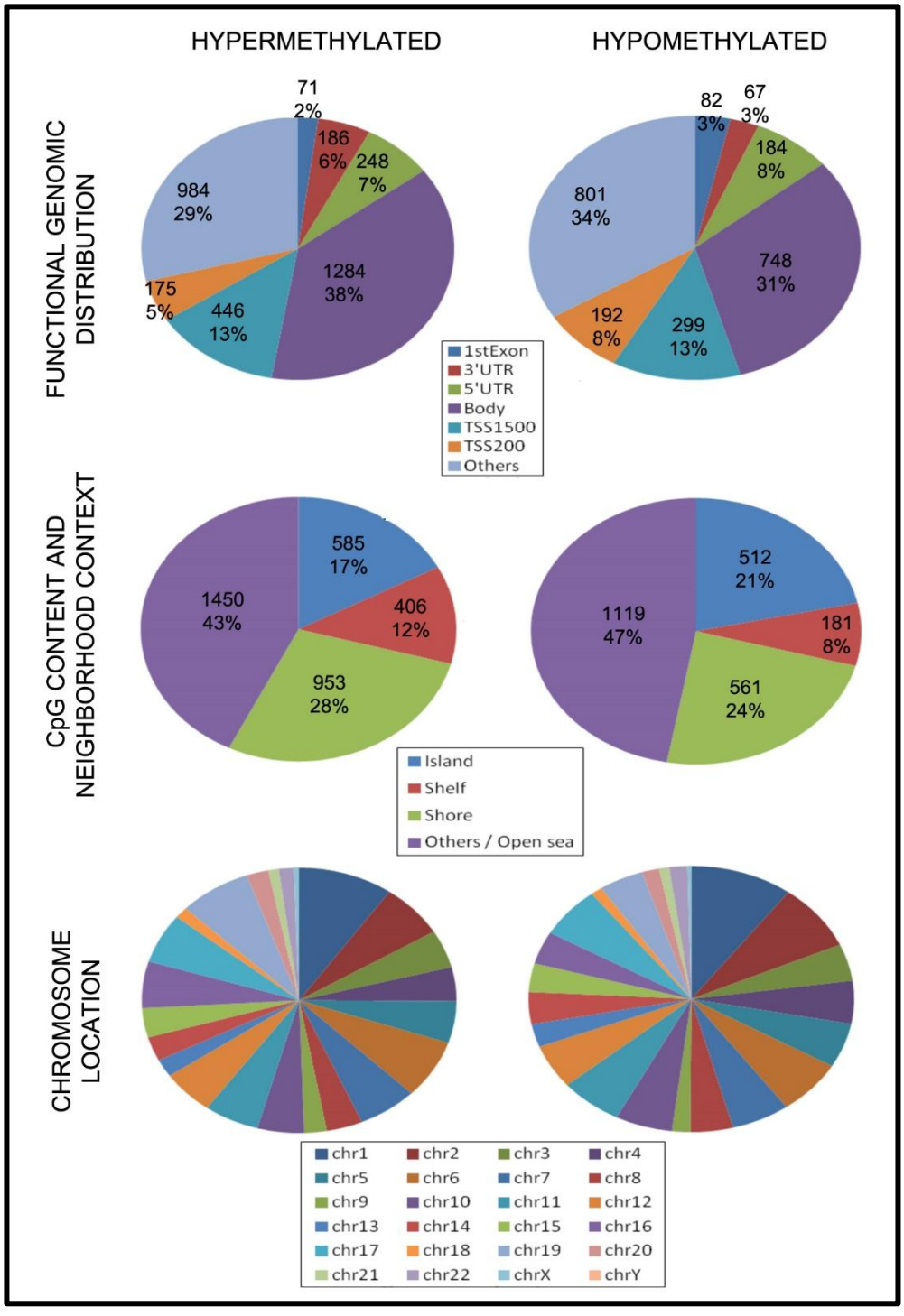

Figure 28. DNA methylation status according to the genomic environment. In the context of functional genomic distribution, hypermethylated and hypomethylated CpG sites were similar. Similar findings were obtained in the context of CpG content and the surrounding environment. Differential methylation states were distributed across all chromosomes, with chromosomes 1, 2 and 6 harbouring the most hypermethylated and hypomethylated CpG sites.

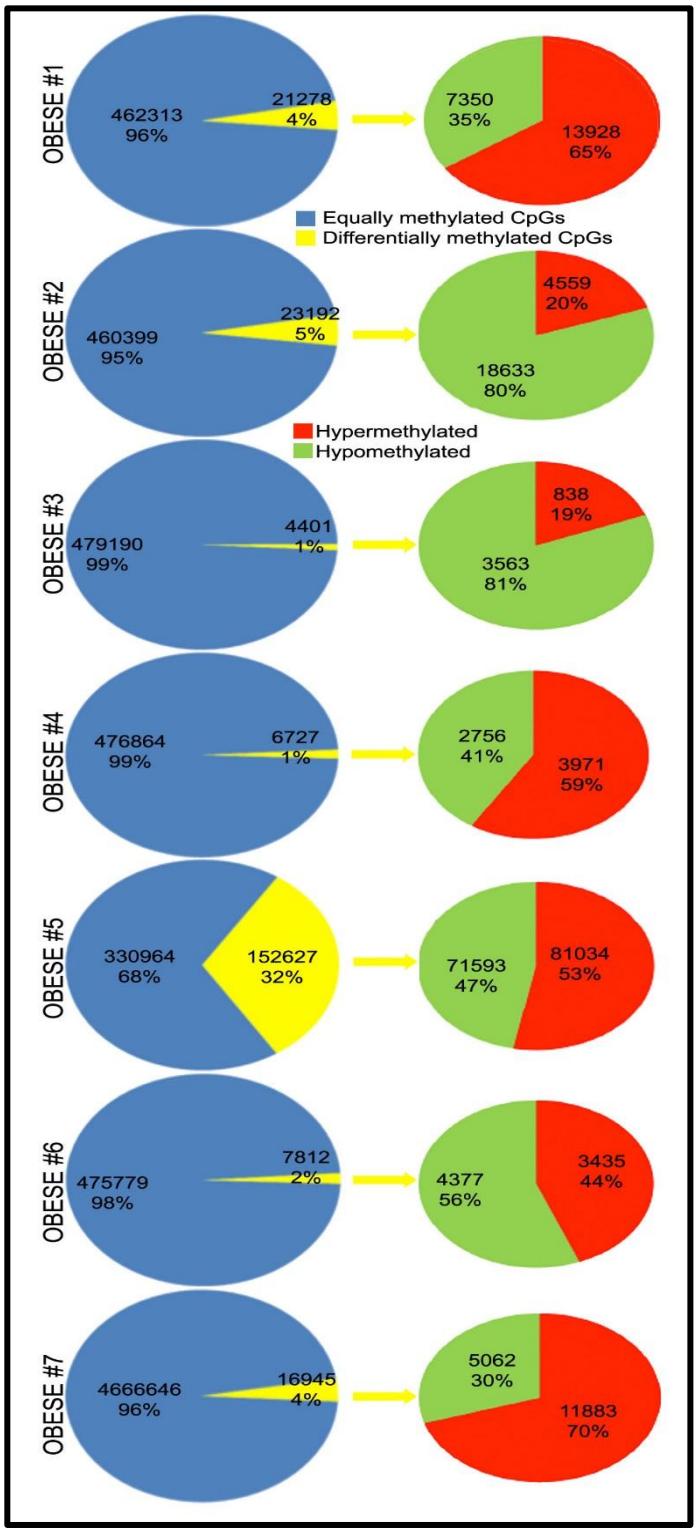

Figure 29. CpG sites that were found to be differentially methylated based on the average of three technical replicates from obese donors and the average of all non-obese donors. Significant alteration of DNA methylation was observed in 1-5% of all CpG sites in 6 of 7 donors, and 32% of the CpG sites were differentially methylated in the samples from obese donor number 5.

A

Gene Name	Number of CpG sites	Not significant sites (less than 4 donors with methylation difference ≥ 0,20)		Significant sites (4 or more donors with methylation difference ≥ 0,20)		
		Number of sites	Number of sites present in polymorphic CpG list	Number of sites	Number of sites present in polymorphic CpG list	Number of sites not present in polymorphic CpG list
AHRR	83	82	23	1	0	1
ARHGEF10	81	80	19	1	0	1
C2orf69	4	3	1	1	0	1
CHST11	16	15	3	1	0	1
CYP2E1	17	16	1	1	0	1
DCAF6	1	0	0	1	0	1
EYA4	36	35	4	1	0	1
HOOK2	14	13	2	1	0	1
MAD1L1	305	303	55	2	1	1
MTRR	3	2	1	1	0	1
PNPLA7	20	19	4	1	0	1
SDK1	113	112	29	1	0	1
SEPT8	11	10	1	1	0	1
SERPINE2	12	11	2	1	0	1
SIM2	39	38	2	1	0	1
TMEM44	16	15	5	1	0	1
TRIM10	36	32	3	4	1	3
ZNF714	5	0	0	5	0	5

B

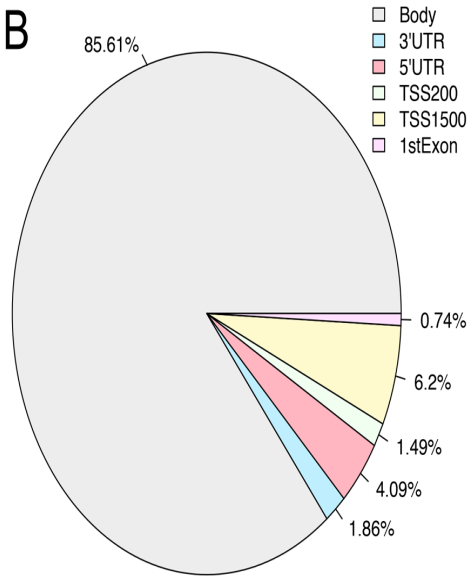

Figure 30. A. List of 18 genes that are differentially methylated but are not present in polymorphic regions. **B.** Proportion of the locations of CpG sites in the 18 genes.

Table 29. List of 67 genes associated with significantly differentially methylated CpG profiles in the specified numbers of donors

4 donors	5 donors	6 donors
AGPAT9	*ADAMTS16*	*NTM*
AHRR	*C14orf119*	*SIM2*
ARHGAP22	*C8orf12*	*STT3A*
ARHGEF10	*CARS2*	
BRDT	*CDH4*	
C2orf69	*CDKL1*	
CHST11	*CTBP1*	
CLIP2	*KCNS3*	
CYP2E1	*MTRR*	
DENND3	*MYO10*	
DCAF11	*NDUFS6*	
DCAF6	*NPSR1*	
DOCK2	*NRGN*	
EYA4	*PDHA2*	
GALNT9	*PTGFRN*	
GHRL	*RADIL*	
GPR37	*RPL13AP3*	
GRID2	*SDK1*	
HLA-DPA1	*THUMPD1*	
HOOK2	*TMEM44*	
IGSF21	*TOP1MT*	
ITGB2	*ZNF714*	
KCTD5		
LAMB1		
LILRA6		
MAD1L1		

NEK9		
OTOF		
PNPLA7		
SEPT8		
SERPINE2		
SLC23A2		
TGFBR3		
TM2D2		
TNS1		
TRIM10		
TRPC5		
WDR27		
ZDHHC14		
ZNF117		
ZNF670		
ZNF783		
42 genes	**22 genes**	**3 genes**

Table 30. List of 75 methylation CpG sites in 67 genes for which the methylation difference was greater than or equal to 20% in cells from four or more obese donors. Three genes had more than one CpG site (highlighted in blue). The total number of CpG sites that were differentially methylated per obese donor is shown.

Methylation Site Coordinate (hg18)	Gene Name	Beta value of average obese samples							Number of donors with methylation difference of at least 0.20
		O1	O2	O3	O4	O5	O6	O7	
chr5:5353241	*ADAMTS16*		X	X	X	X	X		**5**
chr4:84680531	*AGPAT9*			X		X	X	X	**4**
chr5:468575	*AHRR*				X	X	X	X	**4**
chr10:49329565	*ARHGAP22*			X	X		X	X	**4**
chr8:1780022	*ARHGEF10*				X	X	X	X	**4**
chr1:92190586	*BRDT*	X		X		X	X		**4**
chr14:22637857	*C14orf119*	X	X	X			X	X	**5**
chr2:200483703	*C2orf69*	X	X		X			X	**4**
chr8:11289019	*C8orf12*	X	X	X		X	X		**5**
chr13:110091847	*CARS2*		X		X	X	X	X	**5**
chr20:59933973	*CDH4*	X	X	X	X		X		**5**
chr14:49872721	*CDKL1*	X			X	X	X	X	**5**
chr12:103522661	*CHST11*	X	X			X		X	**4**
chr7:73341172	*CLIP2*			X		X	X	X	**4**
chr4:1205099	*CTBP1*			X	X	X	X	X	**5**
chr10:135193238	*CYP2E1*	X	X			X	X		**4**
chr14:23657478	*DCAF11*	X	X	X				X	**4**
chr1:166292176	*DCAF6*		X	X		X	X	X	**4**
chr8:142208369	*DENND3*		X			X	X	X	**4**
chr5:169062072	*DOCK2*	X	X	X		X			**4**

chr6:133829849	*EYA4*	X		X		X	X		**4**
chr12:131369514	*GALNT9*				X	X	X	X	**4**
chr3:10303490	*GHRL*	X	X		X	X			**4**
chr7:124182603	*GPR37*	X				X	X	X	**4**
chr4:94785174	*GRID2*		X	X		X		X	**4**
chr6:33145618	*HLA-DPA1*	X	X		X		X		**4**
chr19:12737947	*HOOK2*	X		X		X		X	**4**
chr1:18557174	*IGSF21*		X	X		X		X	**4**
chr21:45173924	*ITGB2*	X		X	X		X		**4**
chr2:17926797	*KCNS3*	X			X	X	X	X	**5**
chr16:2686545	*KCTD5*		X		X		X	X	**4**
chr7:107429006	*LAMB1*				X	X	X	X	**4**
chr19:59433522	*LILRA6*		X	X		X		X	**4**
chr7:2049055	*MAD1L1*	X	X			X		X	**4**
chr7:2065930	*MAD1L1*	X	X			X		X	**4**
chr5:7930198	*MTRR*	X	X		X	X	X		**5**
chr5:16948511	*MYO10*		X	X	X		X	X	**5**
chr5:1862712	*NDUFS6*		X		X	X	X	X	**5**
chr14:74660649	*NEK9*		X		X	X		X	**4**
chr7:34878610	*NPSR1*	X	X		X	X	X		**5**
chr11:124119166	*NRGN*		X		X		X	X	**4**
chr11:131284679	*NTM*	X	X		X	X	X	X	**6**
chr2:26555585	*OTOF*	X			X	X	X		**4**
chr4:96979968	*PDHA2*		X	X	X	X		X	**5**
chr9:139476578	*PNPLA7*		X	X	X			X	**4**

chr1:117288792	*PTGFRN*		X	X	X		X	X	**5**
chr7:4821932	*RADIL*	X	X	X		X	X		**5**
chr14:55302821	*RPL13AP3*		X		X	X	X	X	**5**
chr7:4211169	*SDK1*	X	X		X		X	X	**5**
chr5:132141954	*SEPT8*				X	X	X	X	**4**
chr2:224605669	*SERPINE2*				X	X	X	X	**4**
chr21:37002144	*SIM2*	X		X	X	X	X	X	**6**
chr20:4931091	*SLC23A2*				X	X	X	X	**4**
chr11:124984572	*STT3A*	X	X	X	X	X		X	**6**
chr1:91976255	*TGFBR3*	X		X	X			X	**4**
chr16:20657544	*THUMPD1*		X	X	X	X	X		**5**
chr8:38967115	*TM2D2*			X	X	X		X	**4**
chr3:195800933	*TMEM44*	X	X		X	X		X	**5**
chr2:218479852	*TNS1*			X	X	X	X		**4**
chr8:144470710	*TOP1MT*		X		X	X	X	X	**5**
chr6:30230523	*TRIM10*			X	X	X		X	**4**
chr6:30230502	*TRIM10*			X	X	X		X	**4**
chr6:30230572	*TRIM10*			X	X	X		X	**4**
chr6:30230544	*TRIM10*			X	X	X		X	**4**
chrX:111044937	*TRPC5*				X	X	X	X	**4**
chr6:169599375	*WDR27*			X	X		X	X	**4**
chr6:157745134	*ZDHHC14*				X	X	X	X	**4**
chr7:64088861	*ZNF117*		X	X	X	X			**4**
chr1:245285114	*ZNF670*	X	X		X			X	**4**
chr19:21056736	*ZNF714*	X	X		X	X		X	**5**

chr19:21057204	*ZNF714*	X	X		X	X		X	**5**
chr19:21057261	*ZNF714*	X	X		X	X		X	**5**
chr19:21057104	*ZNF714*	X	X		X	X		X	**5**
chr19:21056822	*ZNF714*	X	X		X	X		X	**5**
chr7:148608580	*ZNF783*			X		X	X	X	**4**
Total number of CpG sites per obese donor		**35**	**44**	**35**	**54**	**59**	**46**	**58**	

Table 31. List of 65 genes that had probes targeting polymorphic CpG regions.

ADAMTS16	*GPR37*	*RADIL*
AGPAT9	*GRID2*	*RPL13AP3*
AHRR	*HLA-DPA1*	*SDK1*
ARHGAP22	*HOOK2*	*SEPT8*
ARHGEF10	*IGSF21*	*SERPINE2*
BRDT	*ITGB2*	*SIM2*
C14orf119	*KCNS3*	*SLC23A2*
C2orf69	*KCTD5*	*STT3A*
C8orf12	*LAMB1*	*TGFBR3*
CARS2	*LILRA6*	*THUMPD1*
CDH4	*MAD1L1*	*TM2D2*
CDKL1	*MTRR*	*TMEM44*
CHST11	*MYO10*	*TNS1*
CLIP2	*NDUFS6*	*TOP1MT*
CTBP1	*NEK9*	*TRIM10*
CYP2E1	*NPSR1*	*TRPC5*
DENND3	*NRGN*	*WDR27*
DCAF11	*NTM*	*ZDHHC14*
DOCK2	*OTOF*	*ZNF117*
EYA4	*PDHA2*	*ZNF670*
GALNT9	*PNPLA7*	*ZNF783*
GHRL	*PTGFRN*	

3.3 Copy number variation analysis of segmentally duplicated genes

Copy number analysis of the ligand-dependent coactivator of nuclear receptors *DCAF6* revealed that donors have variable copy numbers of this gene. A number of *DCAF6* copies displayed variations within the samples from the same group as well as between the obese and control groups. Four donors from the obese and non-obese groups (N2, N6, N7 and O4) had one copy of *DCAF6*, five donors (N1, N3, N4, N5 and O1) two copies and five donors from the obese group (O2, O3, O5, O6 and O7) had three copies of *DCAF6* (Figure 31A). All donors that displayed a significant difference in *DCAF6* methylation had three copies of the gene (asterisks), which can explain the differences detected in the array. Indeed, *DCAF6* mRNA expression levels did not show any significant differences among individual donors (Figure 31B) or between the obese and control groups (Figure 31C).

Analysis revealed that all fourteen donors had two copies of the *ZNF714* gene, including the five donors in whom all five CpG sites were differentially methylated (asterisks) (Figure 31D). *ZNF714* mRNA expression levels, however, showed no differences within the samples from the same group (Figure 31E) and no variation between the obese and non-obese groups (Figure 31F). These results suggest that the methylation of these sites *per se* did not affect gene expression.

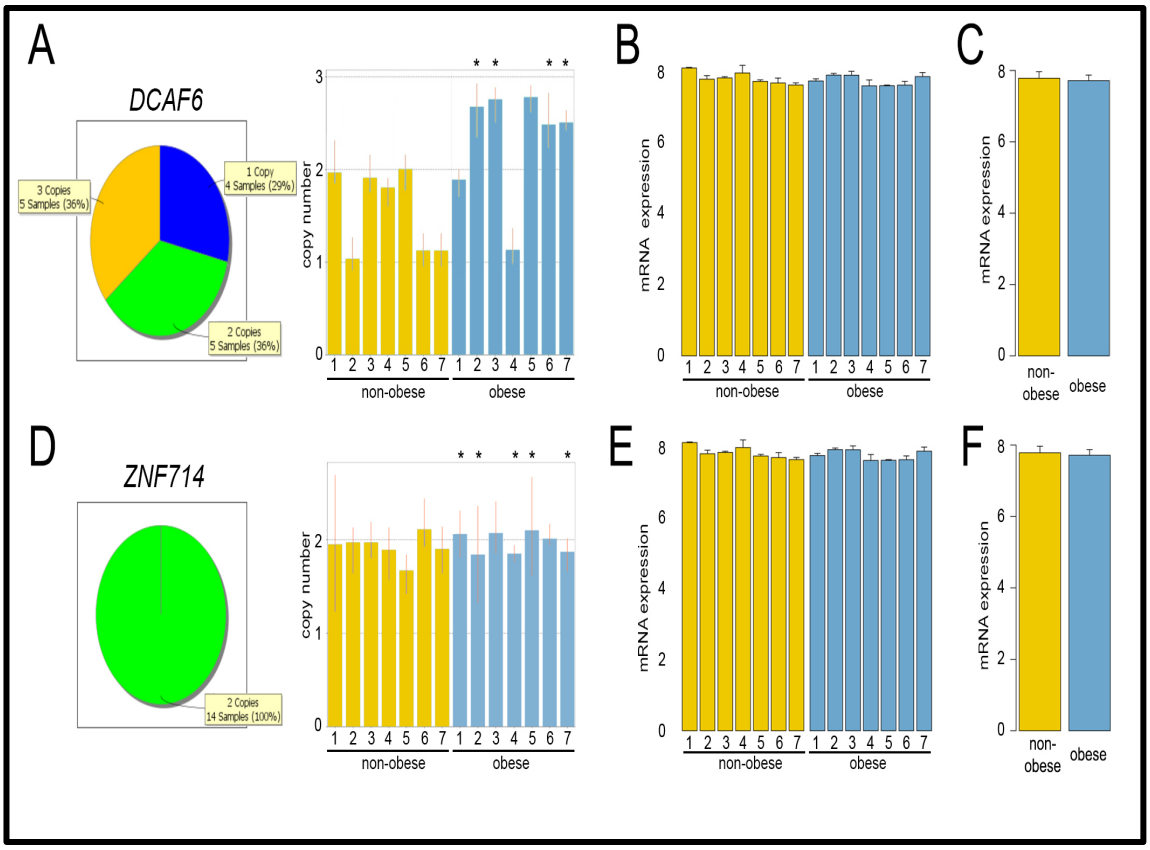

Figure 31. A. *DCAF6* showed variation in copy number among the samples. **B.** *DCAF6* gene expression was similar among fourteen samples. **C.** There was a non-significant difference in *DCAF6* expression level between the obese and non-obese groups. **D.** *ZNF714* was present in two copies in all samples. **E.** *ZNF714* showed no variation in all fourteen samples. **F.** A non-significant difference in *ZNF714* expression was observed in the obese and non-obese groups.

3.4 Gene expression array analysis between obese and non-obese donors

A gene expression array was used to determine whether the difference in DNA methylation between obese and non-obese donors affected the expression of any of the 18 genes in all donors from both groups. The gene expression assay was determined, same as the DNA methylation, in CD90, CD73 and CD105 triple-positive population of WJ MSC sorted by FACS. RNA was extracted from all the sorted cells, quantified and checked for the quality. Illumina HumanHT-12 v4 Expression BeadChips were used for gene expression assessment. All fourteen samples from obese and non-obese donors were run in triplicates. The reactions were processed in one batch to minimize variations due to batch effects and to better evaluate the potential biological relevance of any gene expression differences apparent in the samples from the obese group. Global gene expression was analysed in all samples from obese and non-obese donors.

3.4.1 WJ-MSC sorting, RNA extraction, quantification and qualification analysis

WJ-MSCs that were triple positive for CD90, CD73 and CD105 were sorted from the fourteen lines that had been obtained from UCs. The pre-sorting conditions for sorting for the triple-positively stained WJ-MSCs are shown in Figure 32.

The mRNA was quantified using Qubit (Table 32). mRNA quality was evaluated in all samples and all samples had high RIN scores indicating a good quality (Table 32, Figure 33).

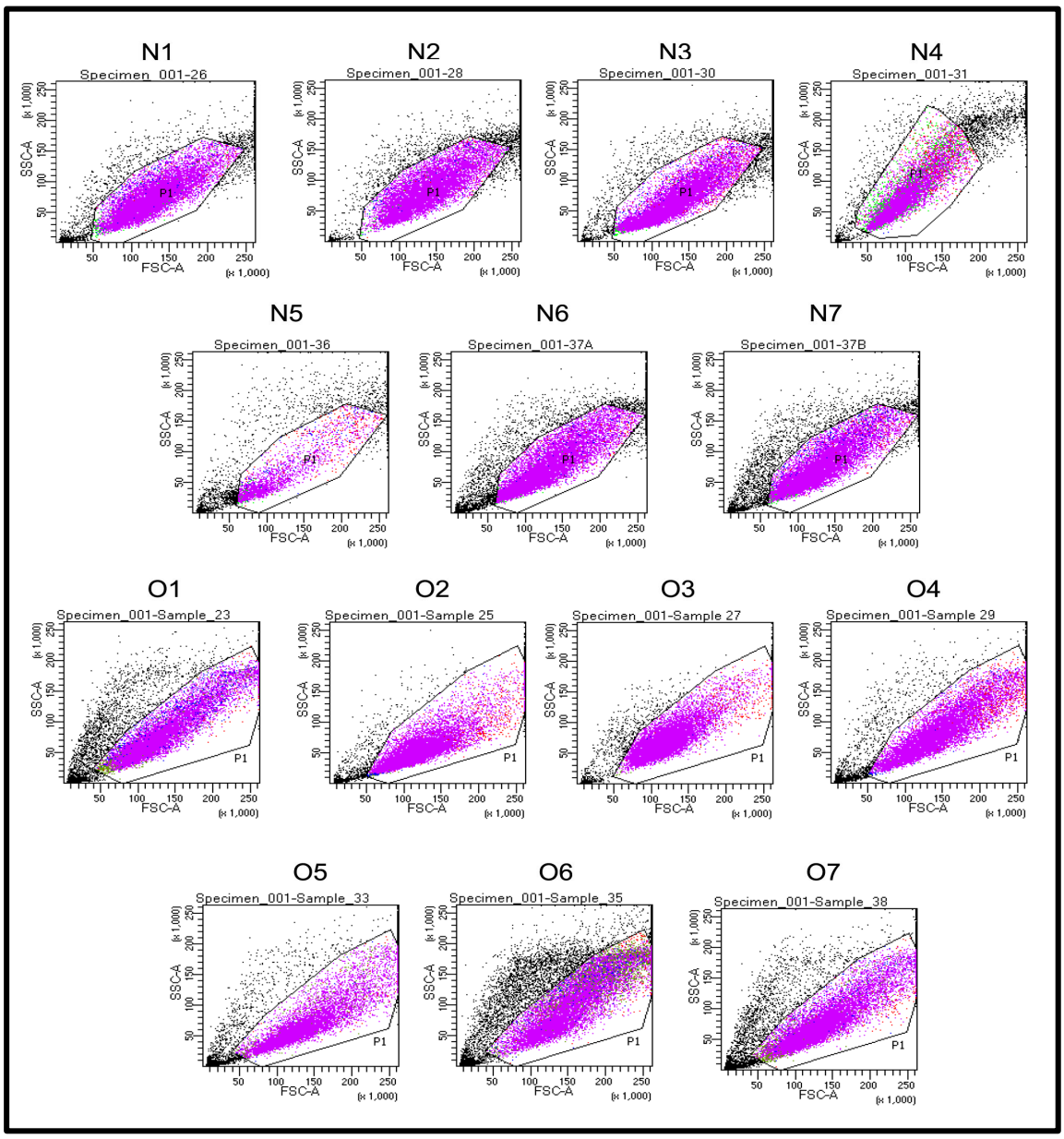

Figure 32. WJ-MSC pre-sorting of populations of cells from obese and non-obese donors after staining with fluorescent antibodies (FITC-CD90, PE-CD73 and APC-CD105). From left to right, the 1st row corresponds to pre-sorted WJ-MSCs from non-obese donors N1, N2, N3 and N4. The 2nd row corresponds to N5, N6 and N7 cell populations. The 3rd row corresponds to cell populations from obese donors O1, O2, O3 and O4, and the 4th row corresponds to cell populations from obese donors O5, O6 and O7.

Table 32. Quantification and qualification of RNA recovered after RNA extraction. Measurements were obtained using a Qubit and Bioanalyzer instruments (N=non-obese (n=7); O=obese (n=7)).

Donor number	RNA concentration (ng/µl)	RIN score
N1	366	10
N2	384	10
N3	270	10
N4	81.8	10
N5	262	10
N6	266	7.9
N7	688	10
O1	612	10
O2	732	9.9
O3	718	10
O4	294	10
O5	384	9.9
O6	188	10
O7	982	10

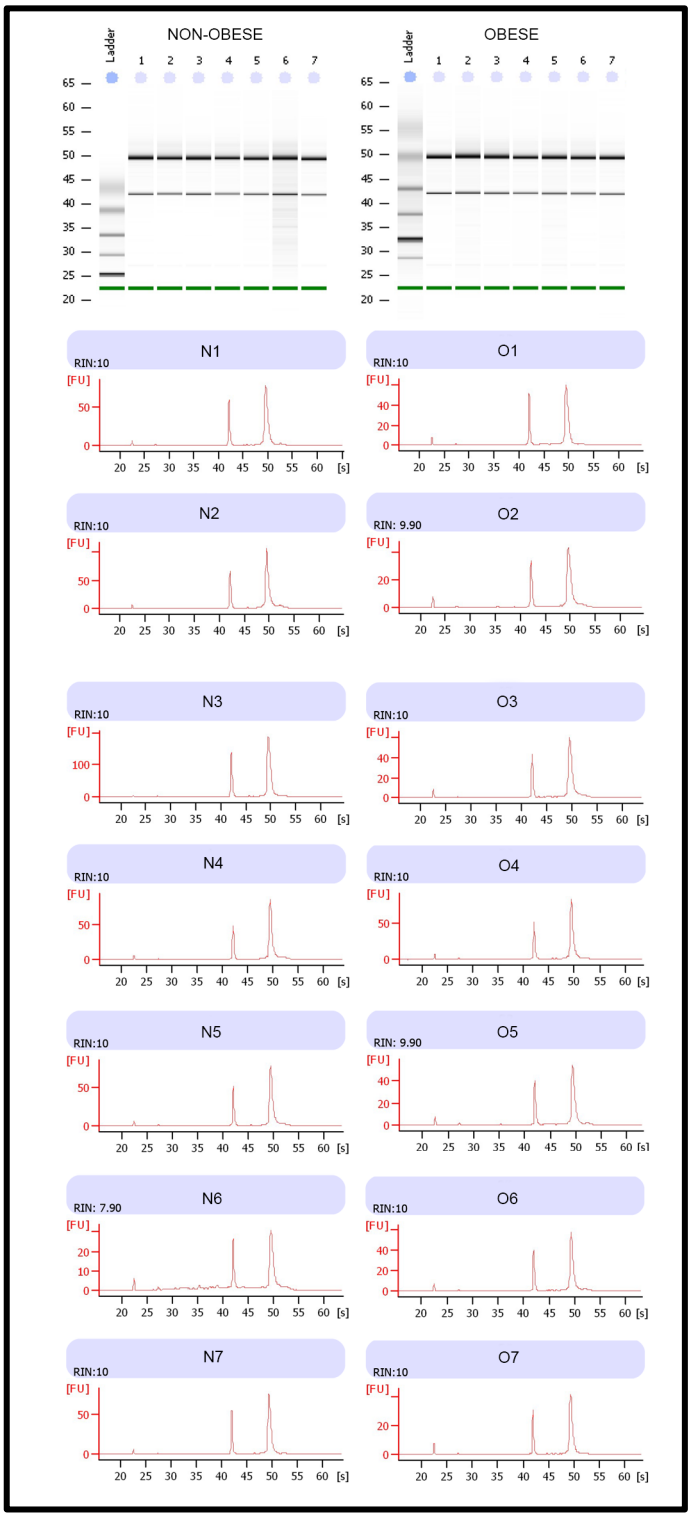

Figure 33. Good-quality mRNA was demonstrated using a bioanalyzer in all non-obese (n=7) and obese samples (n=7).

3.4.2 Quality control analysis of the gene expression BeadChip array data

The controls provided in the Illumina gene expression system assess the quality of the key parameters in its workflow, specifically, hybridization controls, background, gene intensities, and number of genes detected. The following diagrams (Figures 34-37) show the control dashboard that was produced with GenomeStudio software and the data for each sample; each point on the plots represents a sample.

Hybridization controls (high), test the hybridization of single-stranded assay products to the array beads. The signals for all samples should be consistent; the hybridization control is independent of the samples. All signal intensity values generated from the samples fall consistently within the high range, indicating that the hybridization reaction performed well. Almost half of the samples have signal intensity values between 20,000 and 30,000; the other half of the samples have values above 30,000 (Figure 34).

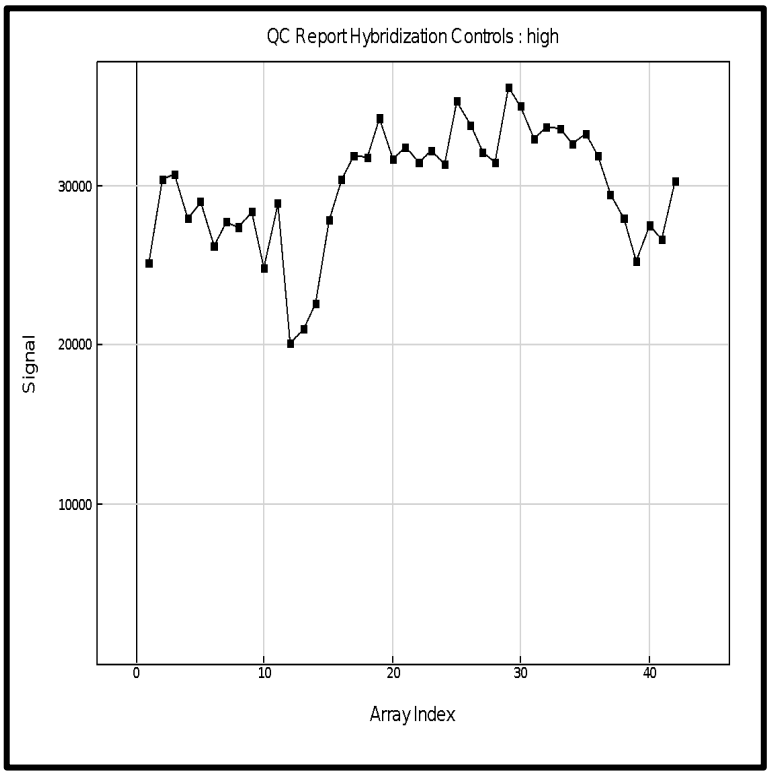

Figure 34. Hybridization controls in all 42 samples.

Background probes, the mean signal intensity of these probes defines the system background; it consists of probes of random sequence that were selected to have no corresponding targets in the genomes. The signal intensities of all samples are less than 150, indicating good performance (Figure 35).

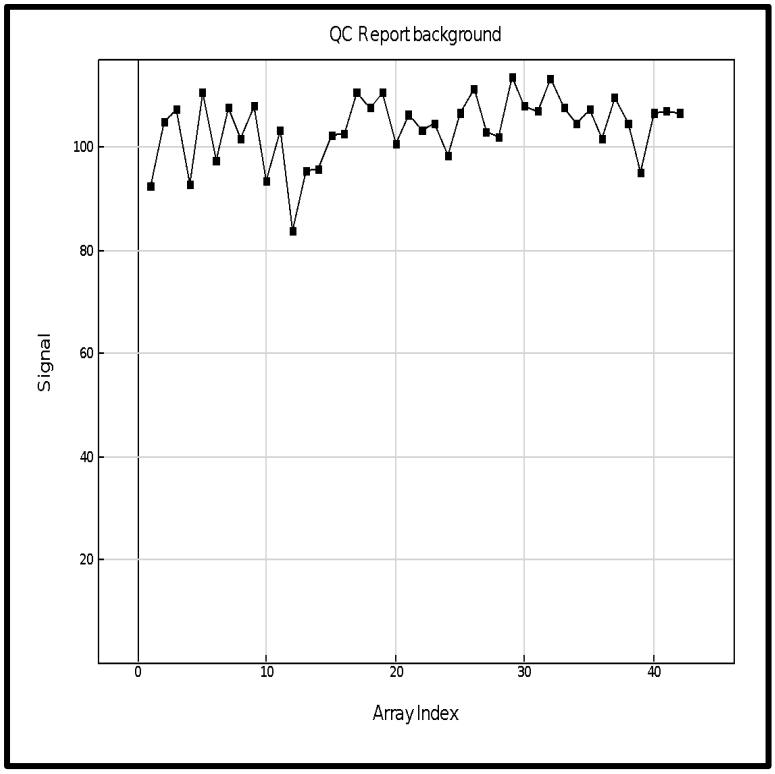

Figure 35. The signal intensities of all 42 samples are less than 150.

Gene intensity metric, This metric permits comparisons of the expression of housekeeping genes with the expression of genes of interest; all other genes located on each array should be compared with the background metric. Housekeeping genes should produce a higher-intensity signal than the background control. These values are shown for all samples. In the housekeeping gene control, the signal intensities ranged from 6,000 to 14,000. In the all gene control, the signal intensity was much lower than in the housekeeping gene control, ranging from 200 to 500. These values are in keeping with the expected values (Figure 36).

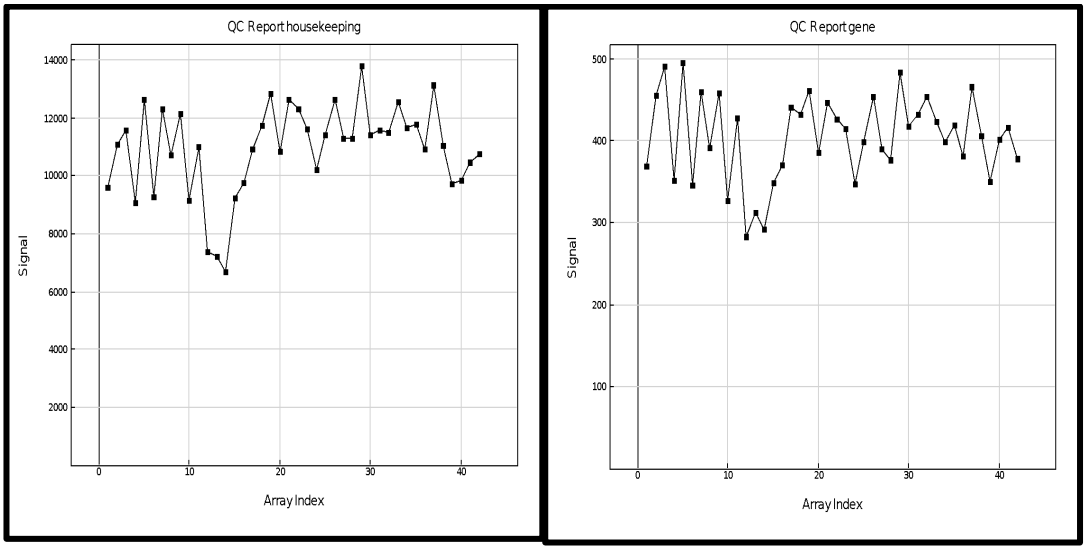

Figure 36. Signal intensities of housekeeping genes and all genes in 42 samples.

Number of genes detected, the number of genes with a detection p-value of 0.05 and 0.01 or less. All samples showed a high number and a similar number of detected transcripts, indicating good performance (Figure 37).

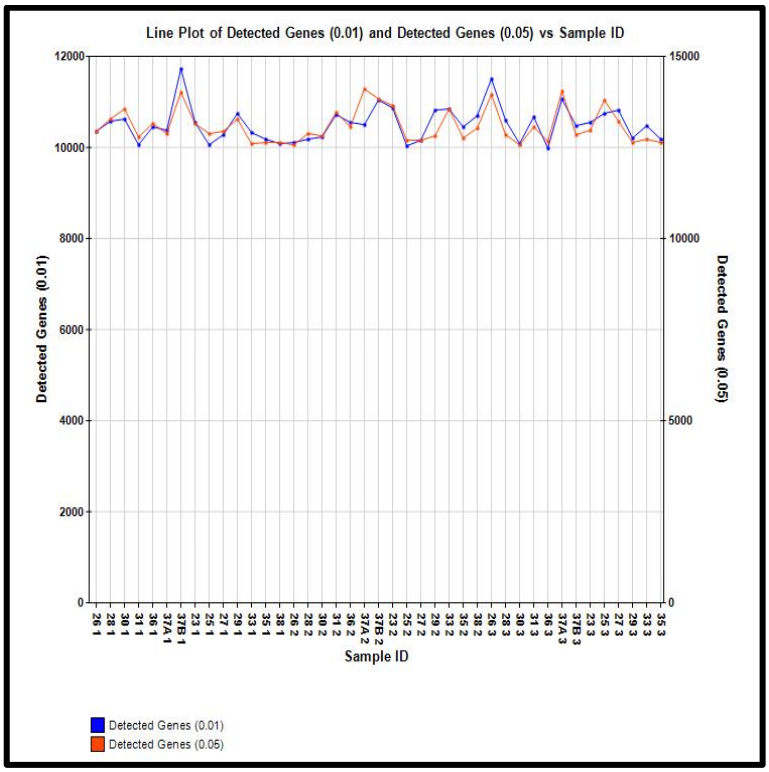

Figure 37. Number of genes detected with confidence in all genes in 42 samples.

3.4.3 Effect of obesity on gene expression

The entire sample set, including triplicates of fourteen lines, was processed in one batch according to the protocol described in the Illumina manual and the robustness of the technique was confirmed by establishing the performance of the quality control parameters. The data set generated for the gene expression analyses was approximately 1-GB in size. The data were analysed using GenoSplice. The effect of obesity on the expression of 16 individual genes was assessed. In addition, the effect of obesity on global gene expression in all samples was assessed.

To determine whether differences in methylation of the CpG sites led to different levels of gene expression, data from the whole transcriptome array were analysed. This analysis identified 244 regulated genes that showed a fold change ≥1.5 and had uncorrected p-values ≤0.05 (Figure 38). Six of the seven samples from obese donors clustered together, whereas one donor, subject O3, clustered with the non-obese group (Figure 39).

According to the KEGG database, the putative pathways involved are metabolism, cytochrome P450 (6.7% of genes), extracellular matrix-receptor interaction (6.0% of genes) and haematopoietic cell lineage (4.7% of genes). The REACTOME database suggested that pathways related to the mitotic cell cycle (3.9% of genes) and metabolism of proteins (1.8% of genes) are involved. GO analysis found that among the ten most significant biological processes involved, nine are linked to the cell cycle; this might explain our finding that the cells from non-obese donors proliferate much faster than the cells from obese donors. Four of the most significant cellular components involved are directly or indirectly linked to extracellular matrix signalling, which matches the predictions of the KEGG database (Figure 40).

Among the remaining 16 genes that displayed significant differences in the methylation of CpG sites in the two groups, only one, *PNPLA7*, displayed significant differences in mRNA expression level in the obese and non-obese groups, suggesting a possible association (Figure 41).

Probe_Id	Symbol	FC	P.Value
ILMN_2186216	GOLPH4	5.75	4.85E-05
ILMN_1693338	CYP1B1	4.26	8.04E-10
ILMN_1830462	XYLT1	3.88	6.22E-05
ILMN_1726448	MMP1	3.20	2.54E-04
ILMN_1669046	FOXQ1	3.18	1.24E-04
ILMN_2210519	HAPLN1	3.02	2.60E-06
ILMN_1707727	ANGPTL4	2.66	3.79E-05
ILMN_1770228	KRT34	2.60	3.58E-04
ILMN_2352023	RIPK5	2.57	1.99E-05
ILMN_1716264	ANKRD1	2.57	1.11E-04
ILMN_1782305	NR4A2	2.55	6.51E-08
ILMN_1730645	TMEFF2	2.43	2.63E-03
ILMN_2339955	NR4A2	2.40	2.64E-10
ILMN_1678812	HAPLN1	2.36	1.03E-04
ILMN_1666733	IL8	2.35	2.79E-03
ILMN_2184373	IL8	2.24	2.69E-03
ILMN_2113490	NTN4	2.22	5.43E-05
ILMN_1658483	IL1A	2.20	1.19E-06
ILMN_1775042	WDR69	2.15	1.41E-05
ILMN_1765578	TIPARP	2.15	1.11E-13
ILMN_1799569	LOC440895	2.06	3.71E-08
ILMN_1844593	---	2.05	1.48E-04
ILMN_2374865	ATF3	2.05	1.71E-07
ILMN_1798177	CHURC1	2.03	4.48E-04
ILMN_1658660	ACTC1	2.01	1.53E-02
ILMN_1676663	TNFRSF11B	2.01	6.30E-03
ILMN_1762255	GSTM1	2.01	3.10E-02
ILMN_1682636	CXCL2	1.98	1.41E-05
ILMN_1720829	ZFP36	1.97	3.20E-09
ILMN_1711838	SLC25A24	1.95	1.06E-03
ILMN_3271179	LOC100128775	1.95	2.42E-05
ILMN_2124585	GREM1	1.94	5.05E-07
ILMN_2139970	ALDH1A3	1.94	2.51E-06
ILMN_2132982	IGFBP5	1.93	2.57E-03
ILMN_1723116	AMFR	1.93	2.37E-02
ILMN_3305475	LOC729708	1.91	5.11E-04
ILMN_1690397	DYNC1I1	1.91	1.73E-05
ILMN_2395139	SERPINB7	1.90	1.79E-02
ILMN_1807439	ALDH1A3	1.87	6.14E-05
ILMN_1709800	POMZP3	1.87	8.23E-04
ILMN_1710284	HES1	1.87	2.36E-07
ILMN_1723035	OLR1	1.86	7.72E-03
ILMN_1751776	CKAP2L	1.86	8.47E-03
ILMN_1748840	CALB2	1.86	3.23E-03
ILMN_1775501	IL1B	1.84	3.71E-03
ILMN_2063168	MALL	1.83	1.58E-03
ILMN_1747650	BMP6	1.82	2.74E-06
ILMN_1787186	NOV	1.82	3.00E-04
ILMN_2400407	CNTN1	1.82	3.55E-03
ILMN_1699421	ANXA10	1.81	1.13E-03
ILMN_2174189	DKK1	1.81	1.73E-06
ILMN_1767685	SERPINB7	1.81	2.39E-02
ILMN_1651354	SPP1	1.80	1.35E-04
ILMN_1686116	THBS1	1.80	2.85E-04
ILMN_1805377	ZP3	1.78	3.75E-03
ILMN_1775268	HECW2	1.78	2.19E-05
ILMN_1660718	GABBR2	1.77	1.39E-02
ILMN_1716382	LOC387882	1.77	7.75E-06
ILMN_1746888	PCOLCE2	1.75	6.55E-05
ILMN_1725314	GBP3	1.75	3.07E-07
ILMN_1798952	KDELR3	1.75	4.36E-06
ILMN_1714880	LIMS3	1.74	1.66E-08
ILMN_1737205	MCM4	1.74	2.55E-04
ILMN_1786628	LOC653355	1.74	1.60E-04
ILMN_2249282	TIPRL	1.73	3.26E-05
ILMN_2376953	KCNK2	1.72	2.58E-04
ILMN_1728009	TMEM171	1.72	1.44E-03
ILMN_1766675	CDH6	1.72	7.14E-03
ILMN_1790761	POSTN	1.71	2.18E-03
ILMN_1789991	MARCH4	1.70	4.58E-04
ILMN_2196328	POSTN	1.70	7.83E-03
ILMN_2189027	LIPG	1.69	2.01E-02
ILMN_1714730	UBE2C	1.68	2.20E-02
ILMN_3245116	GOLIM4	1.67	9.01E-09
ILMN_1794522	EIF5A	1.67	1.91E-03
ILMN_2349459	BIRC5	1.67	1.76E-02
ILMN_2068104	TFPI2	1.66	1.30E-04
ILMN_1662970	ZP3	1.66	6.11E-03
ILMN_1739645	ANLN	1.66	2.47E-02
ILMN_1695475	SEMA3C	1.65	1.27E-05
ILMN_1685079	TELO2	1.65	1.05E-02

Probe_Id	Symbol	FC	P.Value
ILMN_1750324	IGFBP5	1.64	7.15E-03
ILMN_1656501	DUSP5	1.64	3.25E-03
ILMN_1788107	IL11	1.64	1.28E-06
ILMN_1795344	GOLPH4	1.64	7.65E-08
ILMN_1784300	TUBA4A	1.63	1.91E-04
ILMN_1683450	CDCA5	1.63	1.64E-02
ILMN_1692056	HS3ST3A1	1.63	5.97E-04
ILMN_1675453	HHIP	1.63	2.01E-04
ILMN_1755657	RASIP1	1.63	5.32E-03
ILMN_2221006	RAD21	1.63	3.23E-04
ILMN_1742789	LPXN	1.63	7.30E-04
ILMN_3240520	ELTD1	1.63	7.03E-05
ILMN_1689037	LIPG	1.62	1.41E-02
ILMN_2285568	NAAA	1.62	1.34E-05
ILMN_1653719	ITGBL1	1.62	1.38E-04
ILMN_1651237	CDT1	1.62	1.28E-02
ILMN_1792356	DPYSL4	1.61	1.51E-02
ILMN_1763390	ISL1	1.61	3.00E-03
ILMN_1678669	RRM2	1.61	3.20E-02
ILMN_2163873	FNDC1	1.61	4.03E-03
ILMN_1717541	CNTNAP3	1.61	1.16E-04
ILMN_1667594	KLF10	1.61	3.98E-06
ILMN_1658494	C13orf15	1.61	3.53E-06
ILMN_1717706	PLK2	1.60	6.17E-04
ILMN_1663787	KLK3	1.60	7.20E-05
ILMN_1739001	TACSTD2	1.59	1.22E-03
ILMN_2202915	FAR2	1.59	6.34E-03
ILMN_1761968	PPP1R14A	1.59	2.50E-03
ILMN_2189869	FCF1	1.59	1.64E-03
ILMN_1747911	CDC2	1.59	2.19E-02
ILMN_1703906	HJURP	1.58	2.47E-02
ILMN_1771149	MRPL19	1.58	4.83E-04
ILMN_2301083	UBE2C	1.58	4.77E-02
ILMN_3240433	GSTT2B	1.58	2.16E-02
ILMN_1687213	C8orf13	1.57	3.28E-03
ILMN_2327994	AZIN1	1.57	4.11E-02
ILMN_1765701	LOC399942	1.56	1.73E-03
ILMN_1673673	PBK	1.56	4.90E-02
ILMN_2409220	HMMR	1.56	4.40E-02
ILMN_2413158	PODXL	1.56	4.45E-02
ILMN_3248511	FAM167A	1.56	4.31E-03
ILMN_2412860	MCM4	1.55	2.77E-03
ILMN_2051373	NEK2	1.55	3.56E-02
ILMN_2144426	HIST2H2AA3	1.55	1.35E-05
ILMN_2173291	CYP4B1	1.55	8.16E-03
ILMN_1676336	AADACL1	1.55	2.57E-02
ILMN_1716265	PGM2L1	1.55	7.77E-08
ILMN_1800540	CD55	1.55	7.22E-06
ILMN_1784454	ITGB1	1.55	1.77E-06
ILMN_1809590	GINS2	1.54	3.12E-02
ILMN_2073184	S1PR5	1.54	2.47E-04
ILMN_1680955	AURKA	1.54	2.72E-02
ILMN_1695414	ASF1B	1.54	3.95E-02
ILMN_1772821	KIAA1671	1.54	1.08E-02
ILMN_1700413	MAFF	1.53	9.33E-03
ILMN_1709683	RASSF2	1.53	9.15E-04
ILMN_1682599	GPRC5A	1.53	4.42E-03
ILMN_2406815	LRRC17	1.53	2.08E-03
ILMN_1715458	PCDH10	1.53	1.00E-04
ILMN_2050911	SLC22A4	1.53	2.69E-10
ILMN_2413650	STIL	1.52	1.03E-02
ILMN_1673998	SSTR1	1.52	1.83E-04
ILMN_2069745	SSTR1	1.52	5.12E-04
ILMN_2189870	FCF1	1.52	1.89E-02
ILMN_1695978	LINGO2	1.51	7.06E-03
ILMN_1738589	MGLL	1.51	8.83E-03
ILMN_1751576	TEK	1.51	4.82E-07
ILMN_2143155	KIF11	1.51	4.14E-02
ILMN_2048591	LRRN3	1.51	1.77E-02
ILMN_2167915	DSEL	1.51	6.19E-04
ILMN_3238676	ULBP2	1.51	2.98E-04
ILMN_3230300	LOC729143	1.50	6.85E-06
ILMN_1737728	CDCA3	1.50	3.86E-02
ILMN_1717990	CALD1	1.50	3.31E-02
ILMN_1667081	CCND2	2.69	1.68E-02
ILMN_1701424	LAMC2	2.63	1.10E-04
ILMN_2196479	XRN2	2.62	5.08E-06
ILMN_1655867	HRASLS	2.54	3.47E-07
ILMN_2067656	CCND2	2.41	4.89E-02
ILMN_1767556	C10orf10	2.35	3.63E-05
ILMN_1745994	GAS7	2.27	6.63E-03

Probe_Id	Symbol	FC	P.Value
ILMN_1664464	PTGDS	2.12	1.21E-02
ILMN_1760990	SH3GL3	2.00	3.02E-05
ILMN_1789639	FMOD	1.97	1.03E-02
ILMN_1781400	SLC7A2	1.94	1.11E-02
ILMN_1686920	CCDC58	1.93	9.93E-03
ILMN_2384745	PSG4	1.89	3.00E-02
ILMN_1761425	OLFML2A	1.87	4.70E-04
ILMN_1653824	LAMC2	1.87	3.57E-04
ILMN_1668592	STON1	1.86	2.73E-03
ILMN_2404850	RPL14	1.84	4.33E-05
ILMN_2053103	SLC40A1	1.82	3.13E-03
ILMN_2181892	BEX2	1.81	7.02E-03
ILMN_2336609	SYTL2	1.79	6.72E-08
ILMN_2406501	SOD2	1.79	2.69E-03
ILMN_1674285	LOC401233	1.78	4.64E-02
ILMN_1676984	DDIT3	1.75	4.37E-06
ILMN_2390853	CTSH	1.74	2.39E-03
ILMN_2367883	GEM	1.69	8.73E-06
ILMN_1665107	ITGB1BP1	1.69	1.06E-03
ILMN_1715647	VANGL2	1.68	1.35E-02
ILMN_1709094	LIFR	1.68	3.94E-05
ILMN_2201596	CYTL1	1.67	6.51E-03
ILMN_1693270	SUSD2	1.67	1.98E-03
ILMN_1740842	SALL2	1.66	6.86E-06
ILMN_1677092	GEM	1.66	2.53E-05
ILMN_1746376	SCARA3	1.65	5.44E-04
ILMN_1809147	FAM118A	1.64	1.22E-03
ILMN_1695606	EFNB3	1.64	2.29E-05
ILMN_1672743	ZNF334	1.64	7.09E-04
ILMN_1797893	PFAAP5	1.63	8.70E-12
ILMN_1703955	FBXO32	1.63	3.98E-03
ILMN_1662587	PNPLA7	1.62	2.37E-06
ILMN_1812795	RUNX1T1	1.62	3.57E-03
ILMN_1758128	CYGB	1.62	1.28E-07
ILMN_1725338	CLDN23	1.62	2.53E-04
ILMN_2073592	CAND2	1.62	6.86E-05
ILMN_2384122	GPR56	1.61	2.19E-04
ILMN_2153679	TBC1D3B	1.61	1.59E-04
ILMN_1718046	ARNT2	1.60	3.92E-04
ILMN_1772612	ANGPTL2	1.60	7.02E-03
ILMN_1797728	HMGCS1	1.59	1.25E-06
ILMN_1811767	INHBE	1.59	2.00E-02
ILMN_2336781	SOD2	1.59	6.45E-03
ILMN_1718766	MT1F	1.59	3.75E-03
ILMN_1695271	RPP25	1.58	1.63E-03
ILMN_1776157	Sep-04	1.58	4.27E-03
ILMN_3233229	SNHG7	1.58	1.37E-07
ILMN_2224290	ZNF322B	1.58	1.57E-05
ILMN_1778087	ANXA8	1.57	1.25E-02
ILMN_1653794	C6orf160	1.57	3.89E-02
ILMN_3226181	NUDT7	1.57	7.04E-06
ILMN_1658504	CHKA	1.57	2.66E-06
ILMN_1714335	RDH10	1.56	2.98E-03
ILMN_2159152	TP53TG3	1.56	2.38E-06
ILMN_1654966	SCARA3	1.56	2.96E-03
ILMN_1772459	RPS23	1.56	1.53E-02
ILMN_1725889	AFF2	1.56	5.29E-03
ILMN_3234837	PKDCC	1.55	2.57E-04
ILMN_3246060	LOC654433	1.55	8.80E-04
ILMN_1731374	CPE	1.55	4.24E-02
ILMN_1678422	DHX58	1.55	3.10E-07
ILMN_1716843	ELOVL2	1.55	3.50E-05
ILMN_3241692	LOC100129668	1.55	2.80E-02
ILMN_3243924	P2RX6	1.55	9.04E-05
ILMN_2159453	STXBP2	1.54	7.07E-03
ILMN_1846922	---	1.54	2.99E-04
ILMN_1809496	COPG2	1.53	1.65E-03
ILMN_1680874	TUBB2B	1.52	2.09E-03
ILMN_1784364	STARD5	1.52	2.54E-02
ILMN_3241957	LOC100133930	1.52	8.07E-06
ILMN_1754538	C10orf58	1.52	7.41E-03
ILMN_1764769	VWA5A	1.52	2.92E-03
ILMN_1738147	NES	1.52	3.29E-04
ILMN_1814657	TFAP4	1.52	7.62E-06
ILMN_1757636	C5orf35	1.52	3.64E-03
ILMN_1716733	MYOM2	1.51	5.71E-04
ILMN_2326512	CASP1	1.51	8.76E-05
ILMN_1702320	JAKMIP2	1.51	1.55E-02
ILMN_1794612	UBA7	1.51	2.07E-08
ILMN_1734445	LOC91461	1.51	9.60E-04
ILMN_1690523	LRRC20	1.50	6.79E-05
ILMN_1784428	MGC57346	1.50	6.29E-04

Figure 38. List of 244 regulated genes with significantly different transcriptome level between two groups.

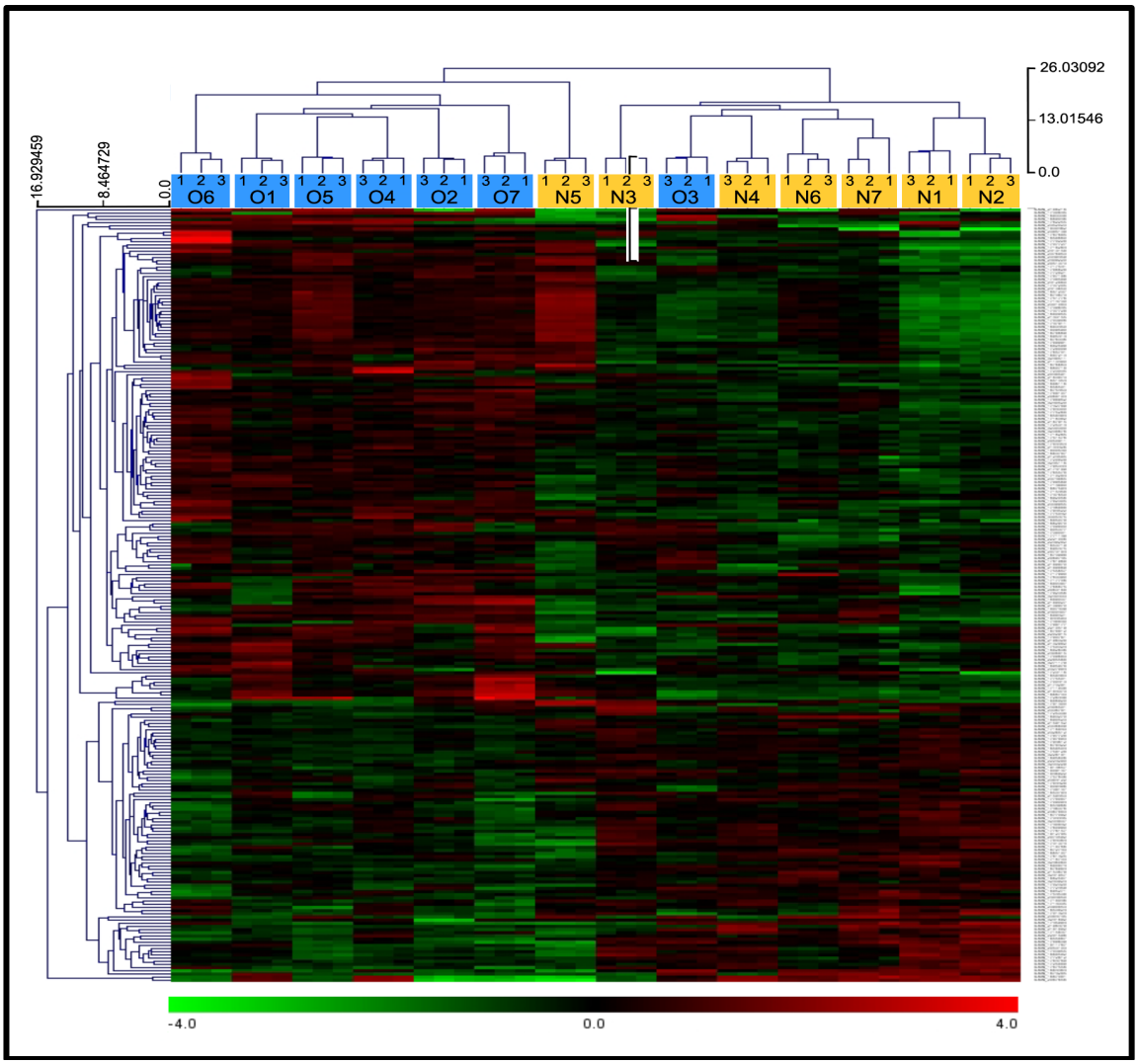

Figure 39. All obese samples clustered together within the obese group except sample O3, which clustered with the non-obese group.

Link to KEGG Pathway	Pathway Description (KEGG)	Nb Genes in Pathway	Nb Regulated Genes (Up / Down)	P-Value (All)	P-Value (Up)	P-Value (Down)	Min P-Value
hsa00980	Metabolism of xenobiotics by	60	4 (4/0)	NA	1.75E-02	NA	1.75E-02
hsa04512	ECM-receptor interaction	84	5 (4/1)	3.47E-02	4.18E-02	NA	3.47E-02
hsa04640	Hematopoietic cell lineage	86	4 (4/0)	NA	4.44E-02	NA	4.44E-02

Link to REACTOME Pathway	Pathway Description (REACTOME)	Nb Genes in Pathway	Nb Regulated Genes (Up / Down)	P-Value (All)	P-Value (Up)	P-Value (Down)	Min P-Value
REACT_152	Cell Cycle, Mitotic	304	12 (11/1)	1.03E-03	4.05E-04	NA	4.05E-04
REACT_17015	Metabolism of proteins	217	4 (0/4)	NA	NA	1.61E-02	1.61E-02

Term Type	GO ID with Link	Go Term	Nb Genes in Term	Nb Regulated Genes (Up / Down)	P-Value
cellular_component	GO:0005576	extracellular region	2010	44 (32/12)	1.68E-05
cellular_component	GO:0044421	extracellular region part	960	27 (22/5)	2.47E-05
biological_process	GO:0000280	nuclear division	220	12 (11/1)	5.53E-05
biological_process	GO:0007067	mitosis	220	12 (11/1)	5.53E-05
biological_process	GO:0000087	M phase of mitotic cell cycle	224	12 (11/1)	6.52E-05
biological_process	GO:0048285	organelle fission	229	12 (11/1)	7.93E-05
biological_process	GO:0007049	cell cycle	776	23 (18/5)	1.02E-04
biological_process	GO:0000278	mitotic cell cycle	370	15 (13/2)	1.13E-04
biological_process	GO:0022402	cell cycle process	565	18 (14/4)	3.34E-04
cellular_component	GO:0031012	extracellular matrix	345	13 (10/3)	5.17E-04
biological_process	GO:0042221	response to chemical stimulus	1281	29 (19/10)	8.76E-04
molecular_function	GO:0005102	receptor binding	886	22 (16/6)	1.02E-03
biological_process	GO:0022403	cell cycle phase	414	14 (12/2)	1.15E-03
molecular_function	GO:0005125	cytokine activity	195	9 (9/0)	1.69E-03
biological_process	GO:0000279	M phase	329	12 (11/1)	1.69E-03
molecular_function	GO:0030247	polysaccharide binding	154	8 (6/2)	1.83E-03
molecular_function	GO:0001871	pattern binding	154	8 (6/2)	1.83E-03
biological_process	GO:0007346	regulation of mitotic cell cycle	152	8 (8/0)	2.05E-03
molecular_function	GO:0005515	protein binding	8154	112 (74/38)	2.07E-03
biological_process	GO:0048731	system development	2330	43 (28/15)	2.11E-03
biological_process	GO:0010564	regulation of cell cycle process	114	7 (7/0)	2.19E-03
biological_process	GO:0050793	regulation of developmental process	674	18 (15/3)	2.32E-03
biological_process	GO:0051301	cell division	295	11 (9/2)	2.47E-03
biological_process	GO:0045766	positive regulation of angiogenesis	26	4 (4/0)	3.34E-03
biological_process	GO:0007155	cell adhesion	700	18 (14/4)	3.42E-03
biological_process	GO:0022610	biological adhesion	701	18 (14/4)	3.47E-03
biological_process	GO:0042493	response to drug	216	9 (5/4)	3.89E-03
biological_process	GO:0007275	multicellular organismal development	2865	49 (32/17)	4.29E-03
biological_process	GO:0009991	response to extracellular stimulus	220	9 (6/3)	4.35E-03
cellular_component	GO:0005615	extracellular space	685	17 (14/3)	4.38E-03
biological_process	GO:0009888	tissue development	665	17 (14/3)	4.91E-03
molecular_function	GO:0005539	glycosaminoglycan binding	140	7 (6/1)	5.13E-03
biological_process	GO:0048856	anatomical structure development	2527	44 (28/16)	5.50E-03
biological_process	GO:0051726	regulation of cell cycle	331	11 (10/1)	5.57E-03
biological_process	GO:0045765	regulation of angiogenesis	63	5 (5/0)	6.27E-03
biological_process	GO:0007399	nervous system development	1088	23 (11/12)	8.10E-03
biological_process	GO:0007096	regulation of exit from mitosis	12	3 (3/0)	8.29E-03
biological_process	GO:0031667	response to nutrient levels	197	8 (5/3)	8.44E-03
biological_process	GO:0043933	macromolecular complex subunit organization	710	17 (10/7)	9.00E-03
cellular_component	GO:0000267	cell fraction	1083	22 (12/10)	9.68E-03
cellular_component	GO:0005578	proteinaceous extracellular matrix	320	10 (8/2)	1.00E-02

Figure 40. Gene expression data analysis according to the KEGG database, the REACTOME database and GO analysis.

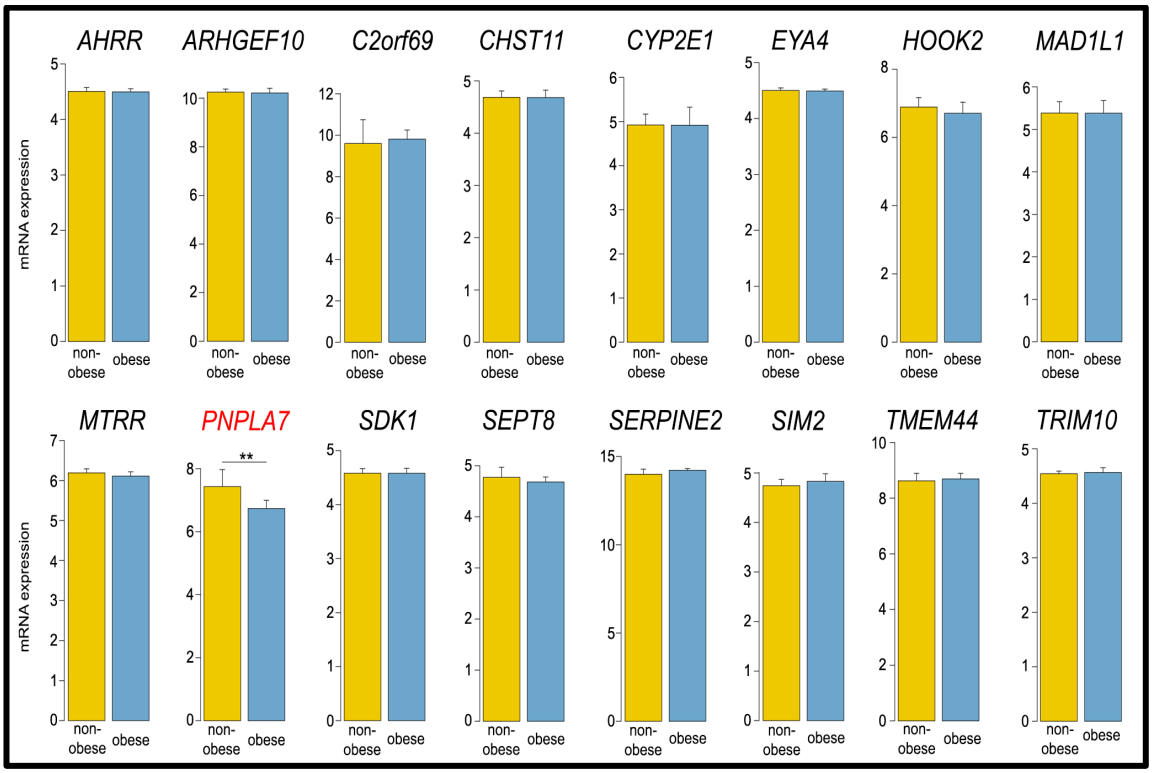

Figure 41. The mRNA expression levels of 16 genes showed no differences in the obese and non-obese groups. The single exception was the *PNPLA7* gene, which showed lower expression in the obese group than in the non-obese group.

3.4.3.1 *PNPLA7* is down-regulated in samples from obese donors

The transcriptome array data were validated using *PNPLA7*-specific RT-PCR (Figure 42A). There is indeed a significant difference between the two groups (p-value 0.001, Mann-Whitney test). The mean (± standard deviation) of the gene expression level was 20.6 (± 2.55) in the non-obese group and 4.3 (± 2.16) in the obese group (Table 33). Analysis based on the Bootstrap model showed that the 95% confidence interval of the incidence rate ratio was 0.18 (0.15 to 0.21).

Searches of interaction networks using GeneMANIA and String V10.0 were conducted to detect any possible known signalling cascades and any possible interactions between *PNLPA7* and other genes. According to GeneMANIA, *PNPLA7* has predicted interactions with 14 genes, including *PRKAR2A* and *ATP7B* (Figure 42B). The experiments revealed that *PNPLA7* interacts with *MAPK11*, *MAPK14* and *PEMT* according to String (Figure 42C). However, no significant differences were found in the expression levels of any of the genes pinpointed by either of the two programmes.

PNPLA7 is an integral component of lysosomal, mitochondrial, nuclear and endoplasmic reticulum membranes and is involved in metabolic and developmental processes. Western blot analysis did indicate that the difference between the two groups is maintained at the protein level (Figure 42D). Overall, the mean (± standard deviation) value of *PNPLA7* was lower 0.36 (±0.01) in the obese group than in the non-obese group 0.39 (± 0.01) (Table 34). The data show that significant difference (p-value 0.006, Mann-Whitney test) at the protein level was present between the obese and non-obese groups. Actin, used as housekeeping protein, showed no significant difference between the obese and non-obese group (Figure 42D).

Table 33. Summary of expression of mRNA level by obesity status using *PNPLA7*.			
Group	**Mean (standard deviation)**	**Median (minimum, maximum)**	**p-value** (Mann-Whitney test)
Normal (n=7)	20.6 (2.55)	21.6 (16.1, 23.8)	0.001
Obese (n=7)	4.35 (2.16)	3.95 (1.15, 8.18)	
Total (n=14)	12.4 (8.73)	12.1 (1.15, 23.8)	

Table 34. Summary of value of protein level by obesity status using *PNPLA7*.			
Group	**Mean (standard deviation)**	**Median (minimum, maximum)**	**p-value** (Mann-Whitney test)
Normal (n=7)	0.39 (0.01)	0.39 (0.36, 0.41)	0.006
Obese (n=7)	0.36 (0.01)	0.35 (0.34, 0.38)	
Total (n=14)	0.37 (0.02)	0.37 (0.34, 0.41)	

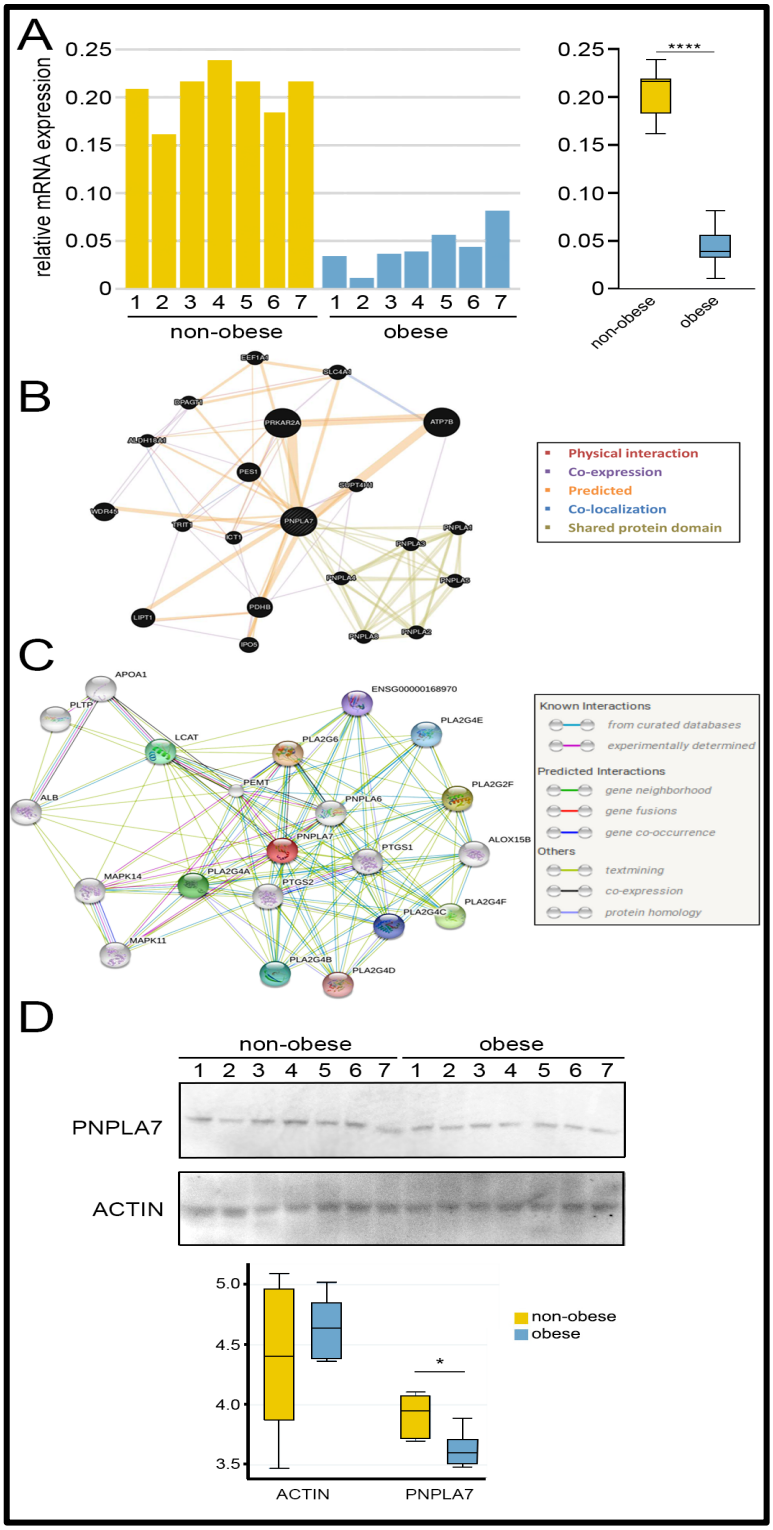

Figure 42. A. *PNPLA7* expression levels in all fourteen samples from obese and non-obese donors were assessed using RT-PCR. **B.** Interaction networks between *PNLPA7* and other genes were identified using GeneMANIA. **C.** Interaction networks between *PNLPA7* and other genes were identified using String. **D.** Western blot data demonstrate lower expression of *PNPLA7* at the protein levels in the obese group compared to the non-obese group.

Chapter 4

Discussion

4. Discussion

Numerous studies have demonstrated that epigenetic modifications are affected by environmental factors and that these external cues can modulate the establishment and maintenance of these modifications, including DNA methylation. Epigenetic modifications cause changes in gene expression that have profound effects on development and health. Furthermore, epigenetic variation in foetal tissue may be the underlying mechanism of metabolic disease programming through interactions between the uterine environment and gene expression.

Despite these observations, it is important to consider that adult obesity does not always give rise to a disease state, and the threshold level of body fat at which an individual is at an increased risk for health complications is subject to individual variation. There is now a recognized phenomenon, demonstrated by numerous epidemiological studies, known as the “obesity paradox”, whereby individuals falling in the overweight to mildly obese category have a reduced risk for a range of diseases including stroke, cancer, hypertension and heart disease (Hainer & Aldhoon-Hainerova, 2013). The correlation between disease and weight increases only at the severely obese stage. However, there is growing evidence to suggest that maternal obesity confers suboptimal developmental potential to the foetus, although the “obesity paradox” could suggest that there may be a degree of individual variation in terms of the effects of maternal obesity on foetal development. In other words, if mildly obese states confer some level of protection to adults in terms of all-cause and cardiovascular mortality and risk increases only in severely obese individuals, a plot of the relative risk

of mortality against BMI would show a U-shaped or J-shaped curve (Flegal *et al.*, 2005). The molecular mechanism of the "obesity paradox" phenomenon is unknown; therefore, it is possible that there may not be a linear relationship between increasing maternal BMI and unhealthy foetal development (Hainer & Aldhoon-Hainerova, 2013).

The research discussed here focuses on maternal obesity, but studies have also shown that paternal obesity induces aberrant methylation patterns in sperm that could represent a mechanism by which obese phenotypes are transmitted to the next generation from the father (Donkin *et al.*, 2016). Significant differences were found in the epigenome of obese men compared with that of their normal-weight counterparts, with epigenetic modifications found in more than 9,000 genes, including the fat mass and obesity-associated gene *(FTO)*, which is linked to obesity. Further studies are currently investigating the transgenerational inheritance of these modifications. In this thesis, studies and discussions have not accounted for the potential involvement of paternal factors in genome-wide methylation of WJ-MSCs or other relevant tissue types.

As discussed in the introduction of this thesis, studies that have investigated the effects of obesity on DNA methylation have been largely restricted to analysing the promoter regions of genes. Nevertheless, these studies present substantive evidence that obesity results in aberrant DNA methylation patterns that are likely to have significant metabolic and inflammatory consequences in the body. Recent advances in array-based technologies have enabled researchers to assess the molecular effects of obesity in MSCs. With the availability of the Illumina 450K beadchip array, genome-wide DNA methylation pattern analysis with a high coverage of promoters, 5' UTRs, 1st exons, gene bodies and 3' UTRs is now possible.

Consequently, several recent studies have been published on obesity and genome-

wide DNA methylation using MSCs that will provide a basis for the discussion in subsequent sections of this chapter. These studies highlight the level of interest in this subject because of the potential impact of MSCs on human health; additionally, these studies support the theories and results presented herein.

The purpose of this pilot study was to investigate the effects of obesity on epigenome-wide DNA methylation using the Human Methylation 450K BeadChip array. WJ-MSCs from the UCs of infants born to normal BMI and high BMI healthy pregnant mothers were analysed. The underlying hypothesis proposed that metabolic diseases, including obesity, trigger the methylation of specific genes and that these environmentally induced epigenetic alterations may help elucidate the stem cell niche and endogenous properties of MSCs.

4.1 Effect of obesity on the properties of WJ-MSCs

The results of this study demonstrate that WJ-MSCs can be isolated from obese and non-obese UCs under sterile conditions with minimal tissue processing using explant method. Various protocols allow for the isolation of WJ-MSCs (Fong *et al.*, 2007; La Rocca *et al.*, 2009), but technical limitations, such as the requirement of harsh enzymatic treatment, can result in cell damage and a relatively low yield. However, an alternative method that was first demonstrated by La Rocca *et al.* (2009) mitigates these effects. The explant method capitalizes on the specific properties of MSCs that enable these cells to migrate and adhere to plastic surfaces. It provides an optimal protocol for WJ-MSC isolation and shows improved scores in relation to the time of primary culture, cell number, cell morphology, immunophenotype, and differentiation potential over alternative methodologies for the isolation of WJ-MSCs, such as the

enzymatic method (Hua *et al.*, 2013). Therefore, the protocol chosen for this study involved the isolation of WJ-MSCs without using enzymes, which removed the possibility of cell damage (De Bruyn *et al.*, 2011). We cultured small pieces of UC tissue explants in an appropriate microenvironment that supports the outgrowth of cells from tissue (Badraiq *et al.*, 2015; Devito *et al.*, 2014). Moreover, the explant procedure is simple and non-invasive, generates a homogenous cell population and does not involve any enzymatic treatments, which are considered to be damaging to cells (Majore *et al.*, 2011).

The results of this study showed that the explant method for the isolation of WJ-MSCs from UCs in our hands was more effective and convenient than other isolation methods. It produced a higher number of isolated cells and required a shorter time for primary culture. Additionally, the cost of explant cultivation was lower and the cell cultures consisted of a purer cell population (Figure 7). This outcome has also been demonstrated by another study (Hua *et al.*, 2013). Thus, the results indicated that the method of isolation may have a significant influence on the growth capacity of isolated cell populations. Therefore, it is crucial that a range of methods should be tested and optimized before committing to the method. Notably, the current existing data are conflicting with regard to the heterogeneity of stem cell cultures and the isolation procedure used. However, this study confirmed the observations of other researchers that cultures using the explant method are homogenous in the early passages (Majore *et al.*, 2011).

Explants from both groups (obese and non-obese) were cultured in standard DMEM supplemented with 10% FBS and had a mean initial outgrowth period of 9.1 (±1.5) days for non-obese and 10.5 (±2.2) days for obese patients, which are comparable to the results of others (Devito *et al.*, 2014). There was no significant difference between

the two groups with regard to the initial outgrowth period (Figure 9B). WJ-MSCs from non-obese and obese explants also exhibited similar proliferation and expansion rates; specifically, the median PD times were 32 (24 to 71.6) hours and 48 (28.5 to 96) hours, respectively. These cells were tested to compare the time required for the cell number to double within both groups during the first 34 hours (the overall median PD time). The differences in the time required for doubling between the groups were statistically significant and the results suggest that the cell population doubling was slower in the obese group than in the non-obese group after 34 hours of culture (Figure 9C). To understand whether this is a general rule or a pure coincidence, we would need to test more samples. Molecular mechanisms behind this phenomenon are at this stage still elusive and any discussion would be speculative. Collectively, the data suggest that there are no growth rate differences in WJ-MSCs from obese and non-obese donors at their initial outgrowth stage. However, the number of cells from obese donors doubled at a slower rate than the cells from the non-obese group within the first 34 hours

WJ-MSCs are identified as MSCs if they are phenotypically positive for the surface markers CD90, CD73 and CD105 and negative for the haematopoietic cell surface markers CD34 and CD45, according to the ISCT guidelines (Dominici *et al.*, 2006). The cultures from normal BMI and high BMI donors exhibited similar expression patterns, and p-value was not significant for the MSC markers CD90, CD73, CD105, CD29 and CD44 (Figure 10). MSCs from obese and non-obese donors showed an absence of haematopoietic markers. However, the cultures from the two BMI groups showed different expression levels of CD56. Cells from the high BMI group exhibited a lower expression of CD56 than normal BMI cells (Figure 10). The CD56 expression level findings in this study were similar to those of previous studies in our group using the same cell type (Devito *et al.*, 2014). Data from other studies indicated that this marker is primarily expressed in NK cells, muscle cells and neural cells. Moreover, this marker

is expressed in a small subset of CD271^{bright} BM-MSCs (Battula *et al.*, 2009). This study also showed that CD56 is expressed on the cell surface of WJ-MSCs.

Neither of the cell lines expressed MSCA-1 when cultured in the presence of serum. MSCA-1 is conditionally expressed in the CD271^{bright} BM-MSC population when containing only CFU-Fs (Busser *et al.*, 2015) and has also been identified in WJ-MSCs that were cultured in xeno-free medium (Devito *et al.*, 2014). Another MSC marker, CD271, a nerve growth factor receptor, is known to be absent in WJ-MSCs but has been proposed to be present in BM-MSCs (Alvarez-Viejo *et al.*, 2015; Busser *et al.*, 2015; Ishige *et al.*, 2009). In another study, WJ-MSCs were shown to have <5% CD271 expression levels irrespective of testing using various supporting culture conditions (Devito *et al.*, 2014). However, in this study none of the cell lines from either group expressed CD271. This lack of expression could be due to the effect of the use of different FBS batches or differences between individual donors. In summary, my study demonstrated that WJ-MSCs from high BMI donors exhibit similar MSC surface marker expression pattern to MSCs from normal BMI donors.

WJ-MSCs from both obese and non-obese donors were also tested to determine their differentiation capacity, in particular, their capacity to commit to the adipogenic, chondrogenic and osteogenic lineages. Under normal conditions, MSCs are non-haematopoietic, multipotent cells with the capacity for multi-lineage differentiation. Indeed, WJ-MSCs are a potential source of stem cells for regenerative medicine purposes because of these properties and their capacity for self-renewal and immunomodulation (Ali *et al.*, 2015). Some researchers have hypothesized that the properties of adult stem cells may be altered as a result of obesity (Wu *et al.*, 2013). Their results support the proposed hypothesis that obesity changes the properties of stem cells according to the cell source. These effects are thought to be mediated by elevated free fatty acids (FFAs) and potentially other cytokines involved in obesity-

associated pathways. Therefore, it is important to test the impact of maternal obesity specifically on the capacity of WJ-MSCs to differentiate into adipocytes. WJ-MSC cultures from all samples were treated concurrently in adipogenic differentiation medium subsequent to the differentiation procedure, and LipidTOX staining was applied to detect the presence of fat droplets (Figure 11A). The results showed an insignificant difference in the mean lipid percentage between the obese group and the normal BMI group (2.2% (±1.1) and 2.3% (±1.3), respectively) (Figure 12). Furthermore, the differentiated cells were tested for the presence of an adipogenic-specific marker *(FABP4),* and the data showed similar values for the *FABP4* mRNA expression level in the samples from obese and non-obese donors (Figure 11A). Overall, the results showed that MSCs from both lean and obese mothers have the same ability to differentiate into adipocytes in a suitable microenvironment and under the same experimental conditions.

UC-derived cell differentiation into cartilage-forming cells is likely supported with the structural properties of UC tissue. The human UC is very rich in hyaluronic acid, a native component of articular cartilage (Can & Karahuseyinoglu, 2007). In my experimental work, WJ-MSC samples from obese and non-obese groups were exposed to chondrogenic differentiation medium for 14 days. Alcian blue positive staining confirmed the presence of cartilage-specific proteoglycans in the induced cultures (Figure 11B). Furthermore, the differentiated cells were tested positive for the presence of the chondrogenic-specific marker *(COL11A1)* and the data showed similar levels of the mRNA *COL11A1* expression in samples from obese and non-obese donors (Figure 11B). Overall, the results showed that MSCs from both lean and obese mothers had a similar ability to differentiate into chondrocytes in a suitable microenvironment and under the same experimental conditions.

The potential of MSCs to differentiate into adipogenic and chondrogenic lineages has

been studied and discussed extensively by several groups, and the results have generally been consistent. However, the literature shows widely different outcomes with regard to the osteogenic capacity of UC-derived cells. Some investigators describe an osteogenic potential comparable to that of BM-MSCs (Diao *et al.*, 2009; Hou *et al.*, 2009) or even higher (Baksh *et al.*, 2007). Other investigators have shown that cells collected from the human UC are poorly osteogenic and that only some of them are capable of undergoing osteogenic differentiation (Girdlestone *et al.*, 2009; Majore *et al.*, 2011; Suzdal'tseva *et al.*, 2007). The WJ-MSC samples from all fourteen donors were treated with osteogenic differentiation medium. Following the differentiation treatment, Alizarin red staining was applied to detect calcium deposits (Figure 11C). Furthermore, the differentiated cells were tested for the presence of an osteogenic-specific marker (*RUNX2),* and the data showed similar *RUNX2* mRNA expression levels in obese and non-obese donors (Figure 11C). Overall, the results showed that, in our hands, MSCs from both lean and obese mothers had the same ability to differentiate into osteoblasts in a suitable microenvironment and when the same experimental conditions were used. Although we did not compare directly osteogenic potential of WJ-MSC isolated in our laboratory with osteogenic potential of other type of MSC, low levels of *RUNX2* in differentiated cells in comparison with studies with other cells suggested that indeed their osteogenic potential might be relatively low (Girdlestone *et al.*, 2009; Majore *et al.*, 2011; Suzdal'tseva *et al.*, 2007).

A particularly interesting observation from this study is that WJ-MSCs from obese donors have a considerably greater immunosuppressive potential than equivalent cells from non-obese donors at certain doses (Figure 13). Obesity is typically associated with meta-inflammation or low-grade chronic inflammation triggered by metabolic cells as a result of excess nutrients and energy (Egger & Dixon, 2010; Gregor & Hotamisligil, 2011). This inflammatory response is distinct from that arising from assault, injury, or

infection and in association with insulin resistance, it is a combination common in several diseases, including hepatitis C, HIV, rheumatoid arthritis and obesity. Obese adipose tissue secretes inflammatory cytokines that inhibit insulin signalling, damage metabolic homeostasis, and contribute to the altered metabolic environment that imposes stress on a developing foetus. Thus, the consensus opinion is that the immunosuppressive capability of MSCs is not constitutive; rather, it arises as a result of exposure to an inflammatory uterine microenvironment (Ren *et al.*, 2008). The immunomodulatory state of MSCs is dynamic and driven by various factors, one of which is the aforementioned inflammatory environment. MSCs derived from BM mice that were not exposed to inflammatory cytokines do not exhibit immunosuppression; rather, this property is specifically induced following exposure to a combination of pro-inflammatory cytokines (Ren *et al.*, 2008). These cytokines elicit their response by triggering the expression of various chemokines and inducible nitric oxide synthase (iNOS) by MSCs. Thus, the induction of immunosuppression in MSCs via the effects of chemokines or nitric oxide (NO) requires exposure to pro-inflammatory cytokines. The mechanism of immunosuppression in response to chemokines and NO is still unknown. It is possible that the significant up-regulation of iNOS and several leukocyte chemokines in response to cytokines may affect immune cells, including T-cells, B-cells and antigen-presenting cells, and MSCs, thus allowing the high levels of NO to suppress immune cell function. Several inflammatory cytokines, including TNF-α and IL, are increased in the tissues of obese individuals (Gregor & Hotamisligil, 2011). Based on this study on WJ-MSCs, the inflammatory cytokines and chemokines that are likely to be elevated as a result of the altered metabolic state of obese donors, such as TNF-α, may induce WJ-MSCs from obese pregnant women to secrete elevated levels of various immunomodulatory factors, thereby exerting a stronger inhibitory effect on the proliferation of PHA-stimulated PBMCs. Purified PBMCs are used *in vitro* to assess a range of lymphocyte functions, including proliferation and mitogenic stimulation (Panda

& Ravindran, 2013). The stimulation of PBMCs leads to an up-regulation of various cell surface receptors and transcription factors and PHA-stimulated PBMCs are used in this assay to assess immunomodulation.

4.2 Effects of obesity on DNA methylation

Several human and animal studies have documented the epigenetic modifications that alter gene expression as a result of stress conditions in the uterine environment during prenatal development (Barua & Junaid, 2015; Curley *et al.*, 2011; Li *et al.*, 2010; Sasaki *et al.*, 2013; Vaiserman, 2015). Perinatal stress may lead to neuroendocrine disruptions that can impact a range of outcomes later in life, including an increased risk of cardio-metabolic disease. Additionally, increasing evidence indicates that epigenetic changes are subject to transgenerational inheritance.

Poor intrauterine growth, which results in babies born small for gestational age (SGA), is known to be caused by several prenatal stressors. For example, insufficient vitamin B12 intake during pregnancy can lead to elevated maternal plasma homocysteine and is associated with SGA infants (Hogeveen *et al.*, 2012). Low maternal plasma vitamin E levels can also result in SGA babies (Dreyfuss *et al.*, 2001). The molecular mechanisms that give rise to SGA babies can be identified via the epigenetic analysis of WJ-MSCs. MSCs from SGA newborns, for example, were shown to exhibit an altered expression of the early growth response 1 *(EGR-1)*-dependent gene network, which is involved in the regulation of cell proliferation and oxidative stress (Sukarieh *et al.*, 2014). Furthermore, intrauterine growth restriction (IUGR) is associated with an increased risk for metabolic diseases, such as type 2 diabetes, obesity and cardiovascular disease.

Maternal obesity gives rise to an altered metabolic environment *in utero* that could be a stressor to the developing foetus. In fact, maternal obesity is associated with the differential expression of multiple genes (Carty *et al.*, 2014). When the total RNA was isolated from samples of whole blood and subcutaneous fat and gene expression was profiled using Illumina microarray technology, researchers identified differential expression between lean and non-lean (overweight and obese) donors. In the whole blood samples, six genes were differentially expressed between the two groups: angiopoietin-like protein *(ANGPTL)*, cytochrome c oxidase subunit VIIa polypeptide II *(COX7A2)*, eukaryotic translation initiation factor 3 subunit A *(EIF3A)*, 6-pyruvoyltetrahydropterin synthase *(PTS)*, CDGSH iron sulphur domain 1 *(CISD1)* and glutaredoxin *(GLRX)*. Furthermore, when gene expression was analysed in subcutaneous fat, *COX7A2* expression was decreased in obese and overweight women compared with that in lean women. The overweight and obese groups exhibited similar expression patterns. Differences between the two sample types (whole blood and subcutaneous fat) are a result of specific environmentally induced expression patterns of each tissue type. *COX7A2* encodes a mitochondrial protein that is important in steroidogenesis and oxidative stress regulation; thus, changes in its expression as a result of a higher BMI could explain the inflammation-induced pregnancy complications in obese women.

Although the number of samples I analysed was limited in this study, as this was a small patient cohort, I was still able to detect significant differences between non-obese and obese pregnancies in terms of cell proliferation, immunomodulatory properties, DNA methylation and gene expression of WJ-MSCs. In addition, the possibility that the effects of an abnormal *in utero* environment are reversible and lost during *in vitro* expansion cannot be excluded. The data from my limited cohort suggest that the effects of maternal obesity on DNA methylation are not constitutive, although the

possibility that major differential methylation cannot yet be detected in second-passage and third-passage WJ-MSCs cannot be ruled out. Consideration must also be given to tissue specificity in relation to obesity-induced epigenetic changes and differing methods of complex data set analysis when interpreting the results of this study.

The results of another study showed that specific changes in global methylation in placental tissues were positively correlated with maternal gestational diabetes mellitus (GDM), preeclampsia and obesity. This association did not hold for UC blood, and there was no correlation between global methylation in the placenta and the UC (Nomura *et al.*, 2014). Numerous other studies have demonstrated that global methylation occurs least in the placenta (Ehrlich *et al.*, 1982; Gama-Sosa *et al.*, 1983). Global methylation levels in placental tissues are approximately 10% lower than those in UC blood (Nomura *et al.*, 2014). The difference in global methylation between the placental tissues in women suffering from GDM, preeclampsia and obesity found in the study by Nomura *et al.* (2014) was relatively small (approximately 3–5%). In contrast to our methodology, methylation was analysed in that study using the LUMA platform. In terms of UC blood, there was no significant difference in the methylation of samples between different study groups (i.e., women with or without GDM, preeclampsia and obesity). Interestingly, global methylation in the placental samples was highest in the obese group. The results also demonstrated an association between global DNA methylation in the placenta and particular maternal, pregnancy and newborn phenotypes. For example, higher methylation in the placenta was associated with a decreased head circumference and body length, indicating that of the three conditions tested, obesity is likely to have the greatest impact on the phenotype of an infant (Nomura *et al.*, 2014). These results suggest a possible mechanism for the impact of the uterine environment on foetal development and health. Given that IUGR is linked to

an increased risk for a range of later-life diseases, these results also provide further evidence for the Barker hypothesis, whereby the origins of adult diseases can be associated with foetal environmental exposure (Barker, 1998; 2004). This study also raises questions about the relationship between placental health, foetal growth and brain development and function (Nomura *et al.*, 2014).

The placenta controls the uterine environment by regulating the maternal-foetal interface, thus coordinating embryonic development. Understanding the mechanisms by which maternal obesity impacts obstetric outcomes and infant phenotypes, particularly with regard to differences in the epigenetic landscape of WJ-MSCs in obese individuals, is of particular interest. Data from Nomura *et al.* (2014) and this thesis suggest that methylation patterns may be tissue-specific, which is important in understanding the molecular mechanisms involved. Studies have shown the placenta to be the least methylated organ in the human body (Ehrlich *et al.*, 1982; Gama-Sosa *et al.*, 1983). Nomura *et al.* (2014) proposed that differences in tissue methylation could be explained by the fact that genes may be permanently methylated and confined in heterochromatic areas of the already specialized UC blood cells. Thus, they may be less susceptible to alterations in the uterine environment that are triggered by maternal metabolic changes. However, the cellular heterogeneity of the placenta is worthy of consideration. It is interesting to note that there are sampled and studied biopsies of the chorionic villi of the placenta that form the maternal-foetal interface. Further studies to examine whether methylation is homogenous across the placenta are required to understand the impact of environmental stressors, such as obesity, on specific tissue and cell types. Such studies would help further elucidate the mechanisms and potential clinical considerations associated with WJ-MSCs. The results of my study differed from those published by Nomura *et al.* (2014). My data did show significant differences in the methylation profiles between UC samples taken from both obese and non-obese

groups, irrespective of whether they were derived from specific regions of the UC (UC blood or WJ-MSCs).

Several environmental factors induce meta-inflammation, particularly certain nutrient stimuli that are associated with modern diets, even in the absence of obesity (Egger & Dixon, 2010). Other factors that induce a meta-inflammatory state include inactivity, sleep deficit, smoking and stress. Conversely, certain nutrients exhibit anti-inflammatory effects in the body, including nuts (Egger & Dixon, 2010) and various spices, including turmeric, which inhibits transcription factors associated with inflammation (Aggarwal & Sung, 2009). Additionally, in men, obesity-induced aberrant methylation patterns in sperm were abolished one week post-bariatric surgery, with methylation changes occurring in 1,500 genes during this short period (Donkin *et al.*, 2016).

Data from other studies indicate that the correlation between maternal obesity and alterations in DNA methylation may be tissue-specific, which could provide an explanation for the discrepancy between my data and results from comparable studies. This study is the first to investigate an association between maternal obesity and global DNA methylation in WJ-MSCs. Most other studies have analysed either UC blood or placental samples and have usually investigated methylation changes in particular genes. For example, Burris *et al.* (2015) found that the methylation rate of aryl-hydrocarbon receptor repressor *(AHRR)* was 2.1% higher in UC blood from the offspring of obese mothers than in that from the offspring of normal-weight mothers. In my cohort, four out of seven obese donors had a >20% higher methylation rate at one CpG site in *AHRR*, although there was no difference in the *AHRR* mRNA levels (Figure 41). *AHRR* is responsible for inhibiting aryl-hydrocarbon receptor (AHR) transcription, which mediates drug or xenobiotic metabolism, cell growth and differentiation. Another factor that is associated with *AHRR* methylation in children is maternal smoking,

supporting the hypothesis that obesity is an intrauterine stressor for the developing foetus, similar to environmental contaminants. Therefore, studies of both individual genes and global methylation in UC blood, WJ-MSCs, and other tissues provide a growing body of evidence to support the crucial role of *in utero* stressors in DNA methylation and infant phenotype determination. In addition, DNA methylation was also shown to positively correlate with gestational age, birth weight and obesity (Burris *et al.*, 2015). The health implications of *AHRR* methylation are unclear, but given the potential implications for drug metabolism and cell growth and differentiation, the results of my study should be considered alongside such gene-specific research when considering the therapeutic application of WJ-MSCs. Similarly, Lesseur *et al.* (2014) found that obesity during pregnancy affected the DNA methylation status of the leptin *(LEP)* promoter in placental tissue. *LEP* is an adipokine that regulates appetite and is important for energy homeostasis by signalling satiety. It is produced by the placenta and regulates foetal growth and nutrient exchange during pregnancy. *LEP* expression is negatively associated with promoter DNA methylation. It was concluded that because these effects alter DNA methylation within the placental tissue, they provide a potential mechanism by which metabolic dysregulation arises in the offspring and drives obesity-related conditions in the next generation (Lesseur *et al.*, 2014). Furthermore, Li *et al.* (2013) found that maternal obesity and diabetes in a mouse model were associated with extensive epigenetic changes, triggering altered expression of hepatic genes in male offspring. The offspring of obese mothers showed extensive changes in cytosine methylation related to developmental rather than metabolic pathways, suggesting that epigenetic changes may produce an altered response to a suboptimal intrauterine environment.

Another study investigating global methylation revealed that maternal GDM is associated with genome-wide DNA methylation changes in both the placenta and the

UC blood of the exposed offspring (Finer *et al.*, 2015), contradicting the notion of a tissue-specific association (Nomura *et al.*, 2014). A study by Finer *et al.* (2015) identified genome-wide DNA methylation changes in both the placenta and cord blood from infants born to healthy women and women suffering from GDM using methylation variable position (MVP) analysis. Pathways involved in endocytosis, mitogen-activated protein kinase (MAPK) signalling and extracellular triggers for intracellular metabolic processes were found to be enriched via KEGG pathway analysis, a bioinformatics tool used to elucidate the function of a biological system. The study also included considerations of cellular heterogeneity in cord blood with methylation analysis in different blood cell types. The correlation between methylation and GDM held for lymphocytes and monocytes but not for granulocytes. Comparative data for placental tissue were not evaluated in this study; therefore, placental cell results were not corrected for heterogeneity (Finer *et al.*, 2015). Differences in cord blood methylation according to cell type indicate that cellular heterogeneity in particular tissue types can lead to differing results in global methylation studies, which is relevant to this doctoral thesis.

Another consideration is that neighbouring CpG sites exhibit correlated methylation states. Further analysis is required to ensure that this type of co-methylation does not distort the results. Finer *et al.* (2015) found that allowing for a 5% β-value difference ensured that their results were valid and not a result of chance or technical variation. In addition, Finer *et al.* (2015) recruited a cohort from the South Asian population, which has a greater risk of type 2 diabetes at a population level. Asians are more likely to develop the disease even at lower BMIs, resulting in the development of diabetes in a disproportionately large percentage of the population. This risk is thought to be caused by the propensity to have less muscle and more abdominal fat, leading to insulin resistance (Finer *et al.*, 2015). This phenomenon is present at birth, with studies

showing that Indian newborns have higher levels of body fat and insulin than Caucasian babies, despite having a lower average birth weight (Yajnik *et al.*, 2002). Whether this phenomenon gives rise to differing methylation states in certain tissues is unclear, but a strong phenotypic trend with unknown molecular mechanisms in the recruited cohort group that is relevant to the area of study is noteworthy. Finer *et al.* (2015) also found that differences in DNA methylation were caused by genetic variation, although these differences were not dependent on SNP-associated methylation. However, this could account for the increased global methylation in both tissue types in their cohort. They concluded that SNP-associated methylation may be mechanistically important in the interaction of genes and the environment during early development.

Research on the differences in global DNA methylation between various ethnic or racial groups has been limited. Non-Caucasian head and neck cancer patients were reported to have increased methylation of leukocyte LINE-1 compared with Caucasians (Hsiung *et al.*, 2007). Another study by Zhang *et al.* (2011) demonstrated lower methylation of the same gene in non-Hispanic blacks and Hispanics than Caucasian study participants and concluded that the differing frequencies of the methylenetetrahydrofolate reductase *MTHFR*-C677T polymorphism found in distinct racial/ethnic groups could not explain the discrepancies in global DNA methylation between the groups. Other unknown influences, either environmental or genetic, could therefore be contributing factors to the differing levels of global DNA methylation between races that have been observed. Further research to explore the potential contribution of genetic polymorphisms along with global DNA methylation may help explain differences between ethnic groups (Zhang *et al.*, 2011). Regarding this thesis, the contribution of race/ethnicity effects to the observed differences in global DNA methylation cannot be determined because the impact of a small sample size cannot be eliminated. Future studies with a larger number of samples may help elucidate the

differences in global DNA methylation in obese donors according to race/ethnicity.

Another explanation for the different results in comparable studies is the use of different methodologies to analyse DNA methylation. For example, methylated DNA immunoprecipitation covers the entire genome but has limited resolution. Reduced representation bisulfite sequencing and Nimblegen MethSeq allow for single CpG resolution, but analysis is restricted to CpG islands and promoters (Walker *et al.*, 2015). It has also been shown that differences in the isolation and subculture protocols in different cell lines may result in differences in gene expression and pluripotency degree (La Rocca *et al.*, 2009). It has been hypothesized that isolation methods may alter the epigenetic profile of WJ-MSCs, which in turn alter their plasticity and potential for therapeutic application (Phinney & Prockop, 2007). These observations further demonstrate the bidirectional relationship between epigenetic changes and stemness and the importance of considering this relationship when interpreting results between tissue types and in terms of cell isolation procedures.

In this study, all fourteen UCs underwent the same treatment. Identical optimized conditions and sterile techniques were used for each sample from the time they were first collected until the very last stages of the experimental procedures. This was done to eliminate any technical errors and to minimize any variability among samples that could have impacted the outcome of the results. For the DNA methylation and gene expression array testing procedures, all sample reactions were processed in one batch to minimize variations that could result from any batch effects. This enabled the better evaluation of the potential biological relevance of the samples. Nevertheless, despite ensuring that bias attributed from technical variations was minimized, the results generated from some obese donors were shown to confound the data in some of the experiments. For these donors, I could not exclude the possibility that the changes seen in their results may have been caused by technical errors that were overlooked in

the study. Additionally, outlying results may have resulted from individual differences between the patients.

4.3 Role of obesity in *PNPLA7*

This study identified *PNPLA7* (Figure 42), which is also known as neuropathy target esterase-related 1 (NTE-R1) or NTE-related esterase (NRE). *PNPLA7* is a member of the *PNPLAs* family (Winrow *et al.*, 2003; Zhang *et al.*, 2016). The human genome expresses nine *PNPLAs (PNPLA1–9)* that have attracted attention, and this group plays crucial roles in various aspects of lipid metabolism and signalling (Kienesberger *et al.*, 2009). Mutations and gene polymorphisms in humans result in disease phenotypes that are associated with the disruption of energy homeostasis, neuronal integrity, and age-related bone morphology (Andrews *et al.*, 1988; Kienesberger *et al.*, 2009). *PNPLA7* has an important function in triglyceride hydrolysis, energy metabolism, lipid droplets, and adipocyte differentiation regulation (Kienesberger *et al.*, 2008; Wilson *et al.*, 2006; Zhang *et al.*, 2016). In obesity, excessively high levels of triacylglycerol in adipocytes (hypertrophy) accumulate due to an altered balance between lipogenic and/or lipolytic functions of the adipocytes (Ferry *et al.*, 2003). *PNPLA7* is an insulin-regulated and glucose-regulated lysophospholipase that plays a role in reducing cellular lysophosphatidic acid (LPA; 1-acyl-*sn*-glycerol-3-phosphate) under fasting conditions when lipid stores are mobilized for energy production (Kienesberger *et al.*, 2008; Kienesberger *et al.*, 2009; www.genecards.org). LPA is a bioactive phospholipid that regulates a broad range of responses at a cellular level (survival, proliferation, motility and secretion) via G-protein-coupled receptor activation (LPA1-receptor (R), LPA2-R, and LPA3-R). LPA is up-regulated with adipocyte differentiation and obesity (Chun *et al.*, 2002; Ferry *et al.*, 2003; Tigyi, 2001). Previous

studies have demonstrated that LPA is released from adipocytes *in vitro* and is found in the extracellular fluid of adipose tissue obtained through microdialysis *in vivo* (Ferry *et al.*, 2003).

Following findings from previous studies, it is not surprising that *PNPLA7* exhibits reduced expression in samples from obese pregnancies. In addition, it has been reported that DNA methylation regulates *PNPLA7* expression; it is down-regulated in hepatocellular carcinoma cell lines and tissue samples via the mechanism of transcriptional silencing by promoter hypermethylation. In cancer studies where there is a significant difference between tumour cells and normal cells with respect to their metabolic pathways, *PNPLA7* is a potential biomarker for diagnosis as a gene that affects energy metabolism (Zhang *et al.*, 2016).

Taken all data together, this pilot study suggested that if significant differences in the *PNPLA7* DNA methylation or expression could be correlated with onset of obesity in childhood, *PNPLA7* expression might be used as a potential biomarker. Although the number of analysed donors is limited, this data suggest that the abnormal metabolic environment related to excessive body weight might bear consequences on the WJ-MSCs and, if confirmed in future more extensive studies, might be considered as one of disqualifying criteria for allogeneic cellular therapy.

Summary

Global DNA methylation analyses and functional studies examining proliferation rate and immunomodulatory potential suggest that maternal obesity during pregnancy might have effects on WJ-MSCs isolated from UC explants. These studies concluded that

1. In general, cells from obese donor samples proliferate somewhat slower.
2. The differentiation potential into adipogenic, osteogenic and chondrogenic lineages is similar.
3. The WJ-MSCs from obese donors exhibited stronger inhibition of PHA-stimulated proliferation of PBMCs than their non-obese donor counterparts.
4. DNA methylation data showed 18 genes with significantly different CpG methylation sites between obese and non-obese groups. However, two genes, *DCAF6* and *ZNF714*, were found in segmentally duplicated regions.
5. Gene expression data showed that of the 16 genes with significantly different CpG methylation sites between the two groups, only *PNPLA7* showed significantly different levels of mRNA expression between the non-obese and obese groups, a finding that was confirmed independently by RT-PCR and Western blotting.

Taken together, the data of this pilot study suggested that *PNPLA7* expression might be a potential biomarker. To understand its significance, similar studies with a larger sample size are warranted. Regardless, the abnormal metabolic environment associated with excessive body weight might impact the use of WJ-MSCs in cellular therapy.

Future work

The work from this study has elucidated research topics for subsequent projects, including

- Expanding the study with a larger sample size to confer greater statistical power to the results and allow the study cohort to be divided into groups according to ethnic background.
- Investigating the potential of *PNPLA7* in other MSC cell type.
- Investigating the potential of *PNPLA7* in other tissues.
- *In vivo* comparative studies using WJ-MSCs from obese and non-obese donors for cellular therapy; this will determine whether the differences observed between obese and non-obese donors from the *in vitro* data are also relevant *in vivo* (e.g., GVHD mouse model).
- Investigating the potential of *PNPLA7* as a predictive biomarker for communal diseases in children from obese pregnancies (e.g., are *PNPLA7* levels at birth correlated with later BMI values?).

References

Ab Kadir, R., Zainal Ariffin, S. H., Megat Abdul Wahab, R., Kermani, S. and Senafi, S. (2012). Characterization of mononucleated human peripheral blood cells. *TheScientificWorldJournal* **2012**: 843843.

Aggarwal, B. B. and Sung, B. (2009). Pharmacological basis for the role of curcumin in chronic diseases: an age-old spice with modern targets. *Trends in pharmacological sciences* **30**(2): 85-94.

Aggarwal, S. and Pittenger, M. F. (2005). Human mesenchymal stem cells modulate allogeneic immune cell responses. *Blood* **105**(4): 1815-1822.

Akerman, F., Lei, Z. M. and Rao, C. V. (2002). Human umbilical cord and fetal membranes co-express leptin and its receptor genes. *Gynecological endocrinology : the official journal of the International Society of Gynecological Endocrinology* **16**(4): 299-306.

Ali, H., Al-Yatama, M. K., Abu-Farha, M., Behbehani, K. and Al Madhoun, A. (2015). Multi-lineage differentiation of human umbilical cord Wharton's Jelly Mesenchymal Stromal Cells mediates changes in the expression profile of stemness markers. *PloS one* **10**(4): e0122465.

Allickson, J. G., Sanchez, A., Yefimenko, N., Borlongan, C. V. and Sanberg, P. R. (2011). Recent studies assessing the proliferative capability of a novel adult stem cell identified in menstrual blood. *The open stem cell journal* **3**(2011): 4-10.

Altman, D. G. (1990). *Practical Statistics for Medical Research*.

Alvarez-Viejo, M., Menendez-Menendez, Y. and Otero-Hernandez, J. (2015). CD271 as a marker to identify mesenchymal stem cells from diverse sources before culture. *World journal of stem cells* **7**(2): 470-476.

Andrews, D. L., Beames, B., Summers, M. D. and Park, W. D. (1988). Characterization of the lipid acyl hydrolase activity of the major potato (Solanum tuberosum) tuber protein, patatin, by cloning and abundant expression in a baculovirus vector. *The Biochemical journal* **252**(1): 199-206.

Baccarelli, A. and Bollati, V. (2009). Epigenetics and environmental chemicals. *Current opinion in pediatrics* **21**(2): 243-251.

Badraiq, H., Devito, L. and Ilic, D. (2015). Isolation and expansion of mesenchymal stromal/stem cells from umbilical cord under chemically defined conditions. *Methods in molecular biology* **1283**: 65-71.

Baergen, R. N. (2011). *Manual of pathology of the human placenta*. 2nd Ed. New York, NY, Springer Science & Business Media.

Baksh, D., Song, L. and Tuan, R. S. (2004). Adult mesenchymal stem cells: characterization, differentiation, and application in cell and gene therapy. *Journal of cellular and molecular medicine* **8**(3): 301-316.

Baksh, D., Yao, R. and Tuan, R. S. (2007). Comparison of proliferative and multilineage differentiation potential of human mesenchymal stem cells derived from umbilical cord and bone marrow. *Stem cells* **25**(6): 1384-1392.

Bankowski, E., Sobolewski, K., Palka, J. and Jaworski, S. (2004). Decreased expression of the insulin-like growth factor-I-binding protein-1 (IGFBP-1) phosphoisoform in pre-eclamptic Wharton's jelly and its role in the regulation of collagen biosynthesis. *Clinical chemistry and laboratory medicine* **42**(2): 175-181.

Bankowski, E., Sobolewski, K., Romanowicz, L., Chyczewski, L. and Jaworski, S. (1996). Collagen and glycosaminoglycans of Wharton's jelly and their alterations in EPH-gestosis. *European journal of obstetrics, gynecology, and reproductive biology* **66**(2): 109-117.

Barfield, R. T., Kilaru, V., Smith, A. K. and Conneely, K. N. (2012). CpGassoc: an R function for analysis of DNA methylation microarray data. *Bioinformatics* **28**(9): 1280-1281.

Barker, D. J. (1998). *Mothers, babies, and health in later life*. 2nd Ed. Edinburgh, UK, Churchill Livingstone.

Barker, D. J. (2004). The developmental origins of adult disease. *Journal of the American College of Nutrition* **23**(6 Suppl): 588S-595S.

Barlow, S., Brooke, G., Chatterjee, K., Price, G., Pelekanos, R., Rossetti, T., Doody, M., Venter, D., Pain, S., Gilshenan, K. and Atkinson, K. (2008). Comparison of human placenta- and bone marrow-derived multipotent mesenchymal stem cells. *Stem Cells Dev* **17**(6): 1095-1107.

Barnes, P. J., Adcock, I. M. and Ito, K. (2005). Histone acetylation and deacetylation: importance in inflammatory lung diseases. *The European respiratory journal* **25**(3): 552-563.

Bartel, D. P. (2004). MicroRNAs: genomics, biogenesis, mechanism, and function. *Cell* **116**(2): 281-297.

Bartsch, G., Yoo, J. J., De Coppi, P., Siddiqui, M. M., Schuch, G., Pohl, H. G., Fuhr, J., Perin, L., Soker, S. and Atala, A. (2005). Propagation, expansion, and multilineage differentiation of human somatic stem cells from dermal progenitors. *Stem cells and development* **14**(3): 337-348.

Barua, S. and Junaid, M. A. (2015). Lifestyle, pregnancy and epigenetic effects. *Epigenomics* **7**(1): 85-102.

Batsali, A. K., Kastrinaki, M. C., Papadaki, H. A. and Pontikoglou, C. (2013). Mesenchymal stem cells derived from Wharton's Jelly of the umbilical cord: biological properties and emerging clinical applications. *Current stem cell research & therapy* **8**(2): 144-155.

Battula, V. L., Treml, S., Bareiss, P. M., Gieseke, F., Roelofs, H., de Zwart, P., Muller, I., Schewe, B., Skutella, T., Fibbe, W. E., Kanz, L. and Buhring, H. J. (2009). Isolation of functionally distinct mesenchymal stem cell subsets using antibodies against CD56, CD271, and mesenchymal stem cell antigen-1. *Haematologica* **94**(2): 173-184.

Baxter, M. A., Wynn, R. F., Jowitt, S. N., Wraith, J. E., Fairbairn, L. J. and Bellantuono, I. (2004). Study of telomere length reveals rapid aging of human marrow stromal cells following in vitro expansion. *Stem cells* **22**(5): 675-682.

Bentley, G. A., Lewit-Bentley, A., Finch, J. T., Podjarny, A. D. and Roth, M. (1984). Crystal structure of the nucleosome core particle at 16 A resolution. *Journal of molecular biology* **176**(1): 55-75.

Bernardo, M. E. and Fibbe, W. E. (2013). Mesenchymal stromal cells: sensors and switchers of inflammation. *Cell stem cell* **13**(4): 392-402.

Bestor, T. H. (2000). The DNA methyltransferases of mammals. *Human molecular genetics* **9**(16): 2395-2402.

Bianco, P., Riminucci, M., Gronthos, S. and Robey, P. G. (2001). Bone marrow stromal stem cells: nature, biology, and potential applications. *Stem cells* **19**(3): 180-192.

Bird, A. (2002). DNA methylation patterns and epigenetic memory. *Genes & development* **16**(1): 6-21.

Bland, J. M. and Altman, D. G. (1998). Survival probabilities (the Kaplan-Meier method). *Bmj*.

Bland, J. M. and Altman, D. G. (2015). Statistics Notes: Bootstrap resampling methods. *Bmj* **350**: h2622.

Bodger, M. P. (1987). Isolation of hemopoietic progenitor cells from human umbilical cord blood. *Experimental hematology* **15**(8): 869-876.

Bongso, A. and Fong, C. Y. (2013). The therapeutic potential, challenges and future clinical directions of stem cells from the Wharton's jelly of the human umbilical cord. *Stem cell reviews* **9**(2): 226-240.

Boyer, L. A., Lee, T. I., Cole, M. F., Johnstone, S. E., Levine, S. S., Zucker, J. P., Guenther, M. G., Kumar, R. M., Murray, H. L., Jenner, R. G., Gifford, D. K., Melton, D. A., Jaenisch, R. and Young, R. A. (2005). Core transcriptional regulatory circuitry in human embryonic stem cells. *Cell* **122**(6): 947-956.

Branch, M. J., Hashmani, K., Dhillon, P., Jones, D. R., Dua, H. S. and Hopkinson, A. (2012). Mesenchymal stem cells in the human corneal limbal stroma. *Investigative ophthalmology & visual science* **53**(9): 5109-5116.

Brooke, G., Rossetti, T., Pelekanos, R., Ilic, N., Murray, P., Hancock, S., Antonenas, V., Huang, G., Gottlieb, D., Bradstock, K. and Atkinson, K. (2009). Manufacturing of human placenta-derived mesenchymal stem cells for clinical trials. *Br J Haematol* **144**(4): 571-579.

Bruce, K. D. and Cagampang, F. R. (2011). Epigenetic priming of the metabolic syndrome. *Toxicology mechanisms and methods* **21**(4): 353-361.

Burdge, G. C. and Calder, P. C. (2006). Dietary alpha-linolenic acid and health-related outcomes: a metabolic perspective. *Nutrition research reviews* **19**(1): 26-52.

Burdge, G. C., Slater-Jefferies, J., Torrens, C., Phillips, E. S., Hanson, M. A. and Lillycrop, K. A. (2007). Dietary protein restriction of pregnant rats in the F0 generation induces altered methylation of hepatic gene promoters in the adult male offspring in the F1 and F2 generations. *The British journal of nutrition* **97**(3): 435-439.

Burris, H. H., Baccarelli, A. A., Byun, H. M., Cantoral, A., Just, A. C., Pantic, I., Solano-Gonzalez, M., Svensson, K., Tamayo y Ortiz, M., Zhao, Y., Wright, R. O. and Tellez-Rojo, M. M. (2015). Offspring DNA methylation of the aryl-hydrocarbon

receptor repressor gene is associated with maternal BMI, gestational age, and birth weight. *Epigenetics* **10**(10): 913-921.

Burton, A. and Torres-Padilla, M. E. (2010). Epigenetic reprogramming and development: a unique heterochromatin organization in the preimplantation mouse embryo. *Briefings in functional genomics* **9**(5-6): 444-454.

Busser, H., Najar, M., Raicevic, G., Pieters, K., Velez Pombo, R., Philippart, P., Meuleman, N., Bron, D. and Lagneaux, L. (2015). Isolation and characterization of human mesenchymal stromal cell subpopulations: Comparison of bone marrow and adipose tissue. *Stem cells and development* **24**(18): 2142-2157.

Campagnoli, C., Roberts, I. A., Kumar, S., Bennett, P. R., Bellantuono, I. and Fisk, N. M. (2001). Identification of mesenchymal stem/progenitor cells in human first-trimester fetal blood, liver, and bone marrow. *Blood* **98**(8): 2396-2402.

Can, A. and Karahuseyinoglu, S. (2007). Concise review: human umbilical cord stroma with regard to the source of fetus-derived stem cells. *Stem cells* **25**(11): 2886-2895.

Caplan, A. I. (1991). Mesenchymal stem cells. *Journal of orthopaedic research : official publication of the Orthopaedic Research Society* **9**(5): 641-650.

Caplan, A. I. (2007). Adult mesenchymal stem cells for tissue engineering versus regenerative medicine. *Journal of cellular physiology* **213**(2): 341-347.

Caplan, A. I. (2008). All MSCs are pericytes? *Cell stem cell* **3**(3): 229-230.

Caplan, A. I. (2015). Adult mesenchymal stem cells and women's health. *Menopause* **22**(2): 131-135.

Caplan, A. I. and Correa, D. (2011). PDGF in bone formation and regeneration: new insights into a novel mechanism involving MSCs. *J Orthop Res* **29**(12): 1795-1803.

Caplan, A. I. and Dennis, J. E. (2006). Mesenchymal stem cells as trophic mediators. *Journal of cellular biochemistry* **98**(5): 1076-1084.

Caplan, A. I. and Hariri, R. (2015). Body Management: Mesenchymal Stem Cells Control the Internal Regenerator. *Stem cells translational medicine* **4**(7): 695-701.

Carlin, R., Davis, D., Weiss, M., Schultz, B. and Troyer, D. (2006). Expression of early transcription factors Oct-4, Sox-2 and Nanog by porcine umbilical cord (PUC) matrix cells. *Reproductive biology and endocrinology : RB&E* **4**: 8.

Carty, D., Akehurst, C., Savage, R., Sungatullina, L., Robinson, S., McBride, M., McClure, J., Freeman, D. and Delles, C. (2014). Differential gene expression in obese pregnancy. *Pregnancy hypertension* **4**(3): 232-233.

Cash, H. L., McGarvey, S. T., Houseman, E. A., Marsit, C. J., Hawley, N. L., Lambert-Messerlian, G. M., Viali, S., Tuitele, J. and Kelsey, K. T. (2011). Cardiovascular disease risk factors and DNA methylation at the LINE-1 repeat region in peripheral blood from Samoan Islanders. *Epigenetics* **6**(10): 1257-1264.

Chambers, I., Colby, D., Robertson, M., Nichols, J., Lee, S., Tweedie, S. and Smith, A. (2003). Functional expression cloning of Nanog, a pluripotency sustaining factor in embryonic stem cells. *Cell* **113**(5): 643-655.

Chao, K. C., Chao, K. F., Fu, Y. S. and Liu, S. H. (2008). Islet-like clusters derived from mesenchymal stem cells in Wharton's Jelly of the human umbilical cord for transplantation to control type 1 diabetes. *PloS one* **3**(1): e1451.

Charbord, P., Livne, E., Gross, G., Haupl, T., Neves, N. M., Marie, P., Bianco, P. and Jorgensen, C. (2011). Human bone marrow mesenchymal stem cells: a systematic reappraisal via the genostem experience. *Stem Cell Rev* **7**(1): 32-42.

Chavez-Munoz, C., Nguyen, K. T., Xu, W., Hong, S. J., Mustoe, T. A. and Galiano, R. D. (2013). Transdifferentiation of adipose-derived stem cells into keratinocyte-like cells: engineering a stratified epidermis. *PloS one* **8**(12): e80587.

Chen, L., Tredget, E. E., Wu, P. Y. and Wu, Y. (2008). Paracrine factors of mesenchymal stem cells recruit macrophages and endothelial lineage cells and enhance wound healing. *PloS one* **3**(4): e1886.

Chen, L. B., Jiang, X. B. and Yang, L. (2004). Differentiation of rat marrow mesenchymal stem cells into pancreatic islet beta-cells. *World journal of gastroenterology* **10**(20): 3016-3020.

Chen, T. and Li, E. (2004). Structure and function of eukaryotic DNA methyltransferases. *Current topics in developmental biology* **60**: 55-89.

Chen, Y. A., Lemire, M., Choufani, S., Butcher, D. T., Grafodatskaya, D., Zanke, B. W., Gallinger, S., Hudson, T. J. and Weksberg, R. (2013). Discovery of cross-reactive probes and polymorphic CpGs in the Illumina Infinium HumanMethylation450 microarray. *Epigenetics* **8**(2): 203-209.

Cho, N. H., Park, Y. K., Kim, Y. T., Yang, H. and Kim, S. K. (2004). Lifetime expression of stem cell markers in the uterine endometrium. *Fertility and sterility* **81**(2): 403-407.

Chong, J. J., Chandrakanthan, V., Xaymardan, M., Asli, N. S., Li, J., Ahmed, I., Heffernan, C., Menon, M. K., Scarlett, C. J., Rashidianfar, A., Biben, C., Zoellner, H., Colvin, E. K., Pimanda, J. E., Biankin, A. V., Zhou, B., Pu, W. T., Prall, O. W. and Harvey, R. P. (2011). Adult cardiac-resident MSC-like stem cells with a proepicardial origin. *Cell stem cell* **9**(6): 527-540.

Chun, J., Goetzl, E. J., Hla, T., Igarashi, Y., Lynch, K. R., Moolenaar, W., Pyne, S. and Tigyi, G. (2002). International Union of Pharmacology. XXXIV. Lysophospholipid receptor nomenclature. *Pharmacological reviews* **54**(2): 265-269.

Cohnheim, J. (1867). Ueber entzündung und eiterung. *Virchows Archiv* **40**(1): 1-79.

Conconi, M. T., Di Liddo, R., Tommasini, M., Calore, C. and Parnigotto, P. P. (2011). Phenotype and differentiation potential of stromal populations obtained from

various zones of human umbilical cord: An overview. *Open Tissue Eng. Regen. Med. J.* **4**(1): 6-20.

Copland, I. B., Adamson, S. L., Post, M., Lye, S. J. and Caniggia, I. (2002). TGF-beta 3 expression during umbilical cord development and its alteration in pre-eclampsia. *Placenta* **23**(4): 311-321.

Crisan, M., Yap, S., Casteilla, L., Chen, C. W., Corselli, M., Park, T. S., Andriolo, G., Sun, B., Zheng, B., Zhang, L., Norotte, C., Teng, P. N., Traas, J., Schugar, R., Deasy, B. M., Badylak, S., Buhring, H. J., Giacobino, J. P., Lazzari, L., Huard, J. and Peault, B. (2008). A perivascular origin for mesenchymal stem cells in multiple human organs. *Cell stem cell* **3**(3): 301-313.

Crisostomo, P. R., Wang, Y., Markel, T. A., Wang, M., Lahm, T. and Meldrum, D. R. (2008). Human mesenchymal stem cells stimulated by TNF-alpha, LPS, or hypoxia produce growth factors by an NF kappa B- but not JNK-dependent mechanism. *American journal of physiology. Cell physiology* **294**(3): C675-682.

Cubas, P., Vincent, C. and Coen, E. (1999). An epigenetic mutation responsible for natural variation in floral symmetry. *Nature* **401**(6749): 157-161.

Curley, J. P., Jensen, C. L., Mashoodh, R. and Champagne, F. A. (2011). Social influences on neurobiology and behavior: epigenetic effects during development. *Psychoneuroendocrinology* **36**(3): 352-371.

Day, F. R. and Loos, R. J. (2011). Developments in obesity genetics in the era of genome-wide association studies. *Journal of nutrigenetics and nutrigenomics* **4**(4): 222-238.

De Bari, C., Dell'Accio, F., Tylzanowski, P. and Luyten, F. P. (2001). Multipotent mesenchymal stem cells from adult human synovial membrane. *Arthritis and rheumatism* **44**(8): 1928-1942.

De Bruyn, C., Najar, M., Raicevic, G., Meuleman, N., Pieters, K., Stamatopoulos, B., Delforge, A., Bron, D. and Lagneaux, L. (2011). A rapid, simple, and

reproducible method for the isolation of mesenchymal stromal cells from Wharton's jelly without enzymatic treatment. *Stem cells and development* **20**(3): 547-557.

Devito, L., Badraiq, H., Galleu, A., Taheem, D. K., Codognotto, S., Siow, R., Khalaf, Y., Briley, A., Shennan, A., Poston, L., McGrath, J., Gentleman, E., Dazzi, F. and Ilic, D. (2014). Wharton's jelly mesenchymal stromal/stem cells derived under chemically defined animal product-free low oxygen conditions are rich in MSCA-1(+) subpopulation. *Regenerative medicine* **9**(6): 723-732.

Di Naro, E., Ghezzi, F., Raio, L., Franchi, M. and D'Addario, V. (2001). Umbilical cord morphology and pregnancy outcome. *European journal of obstetrics, gynecology, and reproductive biology* **96**(2): 150-157.

Di Nicola, M., Carlo-Stella, C., Magni, M., Milanesi, M., Longoni, P. D., Matteucci, P., Grisanti, S. and Gianni, A. M. (2002). Human bone marrow stromal cells suppress T-lymphocyte proliferation induced by cellular or nonspecific mitogenic stimuli. *Blood* **99**(10): 3838-3843.

Diao, Y., Ma, Q., Cui, F. and Zhong, Y. (2009). Human umbilical cord mesenchymal stem cells: osteogenesis in vivo as seed cells for bone tissue engineering. *Journal of biomedical materials research. Part A* **91**(1): 123-131.

Ding, D. C., Chang, Y. H., Shyu, W. C. and Lin, S. Z. (2015). Human umbilical cord mesenchymal stem cells: a new era for stem cell therapy. *Cell transplantation* **24**(3): 339-347.

Ding, Y., Xu, D., Feng, G., Bushell, A., Muschel, R. J. and Wood, K. J. (2009). Mesenchymal stem cells prevent the rejection of fully allogenic islet grafts by the immunosuppressive activity of matrix metalloproteinase-2 and -9. *Diabetes* **58**(8): 1797-1806.

Dominici, M., Le Blanc, K., Mueller, I., Slaper-Cortenbach, I., Marini, F., Krause, D., Deans, R., Keating, A., Prockop, D. and Horwitz, E. (2006). Minimal criteria for

defining multipotent mesenchymal stromal cells. The International Society for Cellular Therapy position statement. *Cytotherapy* **8**(4): 315-317.

Donkin, I., Versteyhe, S., Ingerslev, L. R., Qian, K., Mechta, M., Nordkap, L., Mortensen, B., Appel, E. V., Jorgensen, N., Kristiansen, V. B., Hansen, T., Workman, C. T., Zierath, J. R. and Barres, R. (2016). Obesity and Bariatric Surgery Drive Epigenetic Variation of Spermatozoa in Humans. *Cell metabolism* **23**(2): 369-378.

Drake, A. J. and Liu, L. (2010). Intergenerational transmission of programmed effects: public health consequences. *Trends in endocrinology and metabolism: TEM* **21**(4): 206-213.

Drake, A. J., Walker, B. R. and Seckl, J. R. (2005). Intergenerational consequences of fetal programming by in utero exposure to glucocorticoids in rats. *American journal of physiology. Regulatory, integrative and comparative physiology* **288**(1): R34-38.

Dreyfuss, M. L., Msamanga, G. I., Spiegelman, D., Hunter, D. J., Urassa, E. J., Hertzmark, E. and Fawzi, W. W. (2001). Determinants of low birth weight among HIV-infected pregnant women in Tanzania. *The American journal of clinical nutrition* **74**(6): 814-826.

Du, P., Zhang, X., Huang, C. C., Jafari, N., Kibbe, W. A., Hou, L. and Lin, S. M. (2010). Comparison of Beta-value and M-value methods for quantifying methylation levels by microarray analysis. *BMC bioinformatics* **11**: 587.

Egger, G. and Dixon, J. (2010). Inflammatory effects of nutritional stimuli: further support for the need for a big picture approach to tackling obesity and chronic disease. *Obesity reviews : an official journal of the International Association for the Study of Obesity* **11**(2): 137-149.

Ehrlich, M., Gama-Sosa, M. A., Huang, L. H., Midgett, R. M., Kuo, K. C., McCune, R. A. and Gehrke, C. (1982). Amount and distribution of 5-methylcytosine in human

DNA from different types of tissues of cells. *Nucleic acids research* **10**(8): 2709-2721.

El Omar, R., Beroud, J., Stoltz, J. F., Menu, P., Velot, E. and Decot, V. (2014). Umbilical cord mesenchymal stem cells: the new gold standard for mesenchymal stem cell-based therapies? *Tissue engineering. Part B, Reviews* **20**(5): 523-544.

Erices, A., Conget, P. and Minguell, J. J. (2000). Mesenchymal progenitor cells in human umbilical cord blood. *British journal of haematology* **109**(1): 235-242.

Fan, C. G., Tang, F. W., Zhang, Q. J., Lu, S. H., Liu, H. Y., Zhao, Z. M., Liu, B., Han, Z. B. and Han, Z. C. (2005). Characterization and neural differentiation of fetal lung mesenchymal stem cells. *Cell transplantation* **14**(5): 311-321.

Fang, X., Neyrinck, A. P., Matthay, M. A. and Lee, J. W. (2010). Allogeneic human mesenchymal stem cells restore epithelial protein permeability in cultured human alveolar type II cells by secretion of angiopoietin-1. *The Journal of biological chemistry* **285**(34): 26211-26222.

Fatemi, M., Pao, M. M., Jeong, S., Gal-Yam, E. N., Egger, G., Weisenberger, D. J. and Jones, P. A. (2005). Footprinting of mammalian promoters: use of a CpG DNA methyltransferase revealing nucleosome positions at a single molecule level. *Nucleic acids research* **33**(20): e176.

Ferry, G., Tellier, E., Try, A., Gres, S., Naime, I., Simon, M. F., Rodriguez, M., Boucher, J., Tack, I., Gesta, S., Chomarat, P., Dieu, M., Raes, M., Galizzi, J. P., Valet, P., Boutin, J. A. and Saulnier-Blache, J. S. (2003). Autotaxin is released from adipocytes, catalyzes lysophosphatidic acid synthesis, and activates preadipocyte proliferation. Up-regulated expression with adipocyte differentiation and obesity. *J Biol Chem* **278**(20): 18162-18169.

Finer, S., Mathews, C., Lowe, R., Smart, M., Hillman, S., Foo, L., Sinha, A., Williams, D., Rakyan, V. K. and Hitman, G. A. (2015). Maternal gestational diabetes is

associated with genome-wide DNA methylation variation in placenta and cord blood of exposed offspring. *Human molecular genetics* **24**(11): 3021-3029.

Flegal, K. M., Graubard, B. I., Williamson, D. F. and Gail, M. H. (2005). Excess deaths associated with underweight, overweight, and obesity. *Jama* **293**(15): 1861-1867.

Fong, C. Y., Chak, L. L., Biswas, A., Tan, J. H., Gauthaman, K., Chan, W. K. and Bongso, A. (2011). Human Wharton's jelly stem cells have unique transcriptome profiles compared to human embryonic stem cells and other mesenchymal stem cells. *Stem cell reviews* **7**(1): 1-16.

Fong, C. Y., Richards, M., Manasi, N., Biswas, A. and Bongso, A. (2007). Comparative growth behaviour and characterization of stem cells from human Wharton's jelly. *Reproductive biomedicine online* **15**(6): 708-718.

Fong, C. Y., Subramanian, A., Biswas, A., Gauthaman, K., Srikanth, P., Hande, M. P. and Bongso, A. (2010). Derivation efficiency, cell proliferation, freeze-thaw survival, stem-cell properties and differentiation of human Wharton's jelly stem cells. *Reproductive biomedicine online* **21**(3): 391-401.

Foraker, J. E., Oh, J. Y., Ylostalo, J. H., Lee, R. H., Watanabe, J. and Prockop, D. J. (2011). Cross-talk between human mesenchymal stem/progenitor cells (MSCs) and rat hippocampal slices in LPS-stimulated cocultures: the MSCs are activated to secrete prostaglandin E2. *Journal of neurochemistry* **119**(5): 1052-1063.

Forte, A., Finicelli, M., Mattia, M., Berrino, L., Rossi, F., De Feo, M., Cotrufo, M., Cipollaro, M., Cascino, A. and Galderisi, U. (2008). Mesenchymal stem cells effectively reduce surgically induced stenosis in rat carotids. *Journal of cellular physiology* **217**(3): 789-799.

Fraga, M. F., Ballestar, E., Paz, M. F., Ropero, S., Setien, F., Ballestar, M. L., Heine-Suner, D., Cigudosa, J. C., Urioste, M., Benitez, J., Boix-Chornet, M., Sanchez-

Aguilera, A., Ling, C., Carlsson, E., Poulsen, P., Vaag, A., Stephan, Z., Spector, T. D., Wu, Y. Z., Plass, C. and Esteller, M. (2005). Epigenetic differences arise during the lifetime of monozygotic twins. *Proceedings of the National Academy of Sciences of the United States of America* **102**(30): 10604-10609.

Friedenstein, A. J., Chailakhjan, R. K. and Lalykina, K. S. (1970). The development of fibroblast colonies in monolayer cultures of guinea-pig bone marrow and spleen cells. *Cell and tissue kinetics* **3**(4): 393-403.

Friedenstein, A. J., Chailakhyan, R. K., Latsinik, N. V., Panasyuk, A. F. and Keiliss-Borok, I. V. (1974). Stromal cells responsible for transferring the microenvironment of the hemopoietic tissues. Cloning in vitro and retransplantation in vivo. *Transplantation* **17**(4): 331-340.

Friedenstein, A. J., Gorskaja, J. F. and Kulagina, N. N. (1976). Fibroblast precursors in normal and irradiated mouse hematopoietic organs. *Experimental hematology* **4**(5): 267-274.

Friedenstein, A. J., Piatetzky, S., II and Petrakova, K. V. (1966). Osteogenesis in transplants of bone marrow cells. *Journal of embryology and experimental morphology* **16**(3): 381-390.

Friedman, R., Betancur, M., Boissel, L., Tuncer, H., Cetrulo, C. and Klingemann, H. (2007). Umbilical cord mesenchymal stem cells: adjuvants for human cell transplantation. *Biology of blood and marrow transplantation : journal of the American Society for Blood and Marrow Transplantation* **13**(12): 1477-1486.

Fukuchi, Y., Nakajima, H., Sugiyama, D., Hirose, I., Kitamura, T. and Tsuji, K. (2004). Human placenta-derived cells have mesenchymal stem/progenitor cell potential. *Stem cells* **22**(5): 649-658.

Galderisi, U. and Giordano, A. (2014). The gap between the physiological and therapeutic roles of mesenchymal stem cells. *Medicinal research reviews* **34**(5): 1100-1126.

Galipeau, J. (2013). The mesenchymal stromal cells dilemma--does a negative phase III trial of random donor mesenchymal stromal cells in steroid-resistant graft-versus-host disease represent a death knell or a bump in the road? *Cytotherapy* **15**(1): 2-8.

Gama-Sosa, M. A., Midgett, R. M., Slagel, V. A., Githens, S., Kuo, K. C., Gehrke, C. W. and Ehrlich, M. (1983). Tissue-specific differences in DNA methylation in various mammals. *Biochimica et biophysica acta* **740**(2): 212-219.

Gardiner-Garden, M. and Frommer, M. (1987). CpG islands in vertebrate genomes. *Journal of molecular biology* **196**(2): 261-282.

Gardner, W., Mulvey, E. P. and Shaw, E. C. (1995). Regression analyses of counts and rates: Poisson, overdispersed Poisson, and negative binomial models. *Psychological bulletin* **118**(3): 392-404.

Ghannam, S., Pene, J., Moquet-Torcy, G., Jorgensen, C. and Yssel, H. (2010). Mesenchymal stem cells inhibit human Th17 cell differentiation and function and induce a T regulatory cell phenotype. *Journal of immunology* **185**(1): 302-312.

Girdlestone, J., Limbani, V. A., Cutler, A. J. and Navarrete, C. V. (2009). Efficient expansion of mesenchymal stromal cells from umbilical cord under low serum conditions. *Cytotherapy* **11**(6): 738-748.

Gluckman, P. D., Hanson, M. A., Cooper, C. and Thornburg, K. L. (2008). Effect of in utero and early-life conditions on adult health and disease. *The New England journal of medicine* **359**(1): 61-73.

Go, M. J., Takenaka, C. and Ohgushi, H. (2008). Forced expression of Sox2 or Nanog in human bone marrow derived mesenchymal stem cells maintains their expansion and differentiation capabilities. *Experimental cell research* **314**(5): 1147-1154.

Godfrey, K. M., Sheppard, A., Gluckman, P. D., Lillycrop, K. A., Burdge, G. C., McLean, C., Rodford, J., Slater-Jefferies, J. L., Garratt, E., Crozier, S. R., Emerald, B. S., Gale, C. R., Inskip, H. M., Cooper, C. and Hanson, M. A. (2011). Epigenetic gene promoter methylation at birth is associated with child's later adiposity. *Diabetes* **60**(5): 1528-1534.

Gonzalez, M. A., Gonzalez-Rey, E., Rico, L., Buscher, D. and Delgado, M. (2009). Treatment of experimental arthritis by inducing immune tolerance with human adipose-derived mesenchymal stem cells. *Arthritis and rheumatism* **60**(4): 1006-1019.

Gotherstrom, C., Ringden, O., Westgren, M., Tammik, C. and Le Blanc, K. (2003). Immunomodulatory effects of human foetal liver-derived mesenchymal stem cells. *Bone marrow transplantation* **32**(3): 265-272.

Gotherstrom, C., West, A., Liden, J., Uzunel, M., Lahesmaa, R. and Le Blanc, K. (2005). Difference in gene expression between human fetal liver and adult bone marrow mesenchymal stem cells. *Haematologica* **90**(8): 1017-1026.

Gregor, M. F. and Hotamisligil, G. S. (2011). Inflammatory mechanisms in obesity. *Annual review of immunology* **29**: 415-445.

Grewal, S. I. and Elgin, S. C. (2007). Transcription and RNA interference in the formation of heterochromatin. *Nature* **447**(7143): 399-406.

Gronthos, S., Mankani, M., Brahim, J., Robey, P. G. and Shi, S. (2000). Postnatal human dental pulp stem cells (DPSCs) in vitro and in vivo. *Proceedings of the National Academy of Sciences of the United States of America* **97**(25): 13625-13630.

Guerrero-Bosagna, C. and Skinner, M. K. (2012). Environmentally induced epigenetic transgenerational inheritance of phenotype and disease. *Molecular and cellular endocrinology* **354**(1-2): 3-8.

Guillot, P. V., Gotherstrom, C., Chan, J., Kurata, H. and Fisk, N. M. (2007). Human first-trimester fetal MSC express pluripotency markers and grow faster and have longer telomeres than adult MSC. *Stem cells* **25**(3): 646-654.

Gupta, N., Su, X., Popov, B., Lee, J. W., Serikov, V. and Matthay, M. A. (2007). Intrapulmonary delivery of bone marrow-derived mesenchymal stem cells improves survival and attenuates endotoxin-induced acute lung injury in mice. *Journal of immunology* **179**(3): 1855-1863.

Gupta, R., Nagarajan, A. and Wajapeyee, N. (2010). Advances in genome-wide DNA methylation analysis. *BioTechniques* **49**(4): iii-xi.

Hainer, V. and Aldhoon-Hainerova, I. (2013). Obesity paradox does exist. *Diabetes care* **36 Suppl 2**: S276-281.

Hajkova, P., Ancelin, K., Waldmann, T., Lacoste, N., Lange, U. C., Cesari, F., Lee, C., Almouzni, G., Schneider, R. and Surani, M. A. (2008). Chromatin dynamics during epigenetic reprogramming in the mouse germ line. *Nature* **452**(7189): 877-881.

Hajkova, P., Erhardt, S., Lane, N., Haaf, T., El-Maarri, O., Reik, W., Walter, J. and Surani, M. A. (2002). Epigenetic reprogramming in mouse primordial germ cells. *Mechanisms of development* **117**(1-2): 15-23.

Hake, S. B. and Allis, C. D. (2006). Histone H3 variants and their potential role in indexing mammalian genomes: the "H3 barcode hypothesis". *Proceedings of the National Academy of Sciences of the United States of America* **103**(17): 6428-6435.

Hales, C. N., Barker, D. J., Clark, P. M., Cox, L. J., Fall, C., Osmond, C. and Winter, P. D. (1991). Fetal and infant growth and impaired glucose tolerance at age 64. *Bmj* **303**(6809): 1019-1022.

Han, Y. F., Tao, R., Sun, T. J., Chai, J. K., Xu, G. and Liu, J. (2013). Optimization of human umbilical cord mesenchymal stem cell isolation and culture methods. *Cytotechnology* **65**(5): 819-827.

Han, Z., Jing, Y., Zhang, S., Liu, Y., Shi, Y. and Wei, L. (2012). The role of immunosuppression of mesenchymal stem cells in tissue repair and tumor growth. *Cell & bioscience* **2**(1): 8.

Handy, D. E., Castro, R. and Loscalzo, J. (2011). Epigenetic modifications: basic mechanisms and role in cardiovascular disease. *Circulation* **123**(19): 2145-2156.

Hebebrand, J., Bammann, K. and Hinney, A. (2010). [Genetic determinants of obesity. Current issues]. *Bundesgesundheitsblatt, Gesundheitsforschung, Gesundheitsschutz* **53**(7): 674-680.

Hennrick, K. T., Keeton, A. G., Nanua, S., Kijek, T. G., Goldsmith, A. M., Sajjan, U. S., Bentley, J. K., Lama, V. N., Moore, B. B., Schumacher, R. E., Thannickal, V. J. and Hershenson, M. B. (2007). Lung cells from neonates show a mesenchymal stem cell phenotype. *American journal of respiratory and critical care medicine* **175**(11): 1158-1164.

Heo, J. S., Choi, Y., Kim, H. S. and Kim, H. O. (2016). Comparison of molecular profiles of human mesenchymal stem cells derived from bone marrow, umbilical cord blood, placenta and adipose tissue. *International journal of molecular medicine* **37**(1): 115-125.

Hermann, A., Gowher, H. and Jeltsch, A. (2004). Biochemistry and biology of mammalian DNA methyltransferases. *Cellular and molecular life sciences : CMLS* **61**(19-20): 2571-2587.

Hogeveen, M., Blom, H. J. and den Heijer, M. (2012). Maternal homocysteine and small-for-gestational-age offspring: systematic review and meta-analysis. *The American journal of clinical nutrition* **95**(1): 130-136.

Hoile, S. P., Irvine, N. A., Kelsall, C. J., Sibbons, C., Feunteun, A., Collister, A., Torrens, C., Calder, P. C., Hanson, M. A., Lillycrop, K. A. and Burdge, G. C. (2013). Maternal fat intake in rats alters 20:4n-6 and 22:6n-3 status and the epigenetic regulation of Fads2 in offspring liver. *The Journal of nutritional biochemistry* **24**(7): 1213-1220.

Horwitz, E. M., Gordon, P. L., Koo, W. K., Marx, J. C., Neel, M. D., McNall, R. Y., Muul, L. and Hofmann, T. (2002). Isolated allogeneic bone marrow-derived mesenchymal cells engraft and stimulate growth in children with osteogenesis imperfecta: Implications for cell therapy of bone. *Proceedings of the National Academy of Sciences of the United States of America* **99**(13): 8932-8937.

Horwitz, E. M., Le Blanc, K., Dominici, M., Mueller, I., Slaper-Cortenbach, I., Marini, F. C., Deans, R. J., Krause, D. S., Keating, A. and International Society for Cellular Therapy (2005). Clarification of the nomenclature for MSC: The International Society for Cellular Therapy position statement. *Cytotherapy* **7**(5): 393-395.

Hou, T., Xu, J., Wu, X., Xie, Z., Luo, F., Zhang, Z. and Zeng, L. (2009). Umbilical cord Wharton's Jelly: a new potential cell source of mesenchymal stromal cells for bone tissue engineering. *Tissue engineering. Part A* **15**(9): 2325-2334.

Hsiung, D. T., Marsit, C. J., Houseman, E. A., Eddy, K., Furniss, C. S., McClean, M. D. and Kelsey, K. T. (2007). Global DNA methylation level in whole blood as a biomarker in head and neck squamous cell carcinoma. *Cancer epidemiology, biomarkers & prevention : a publication of the American Association for Cancer Research, cosponsored by the American Society of Preventive Oncology* **16**(1): 108-114.

Hu, F. B. (2008). *Measurements of adiposity and body composition*. In *Obesity epidemiology*. F. B. Hu. New York, Oxford University Press**:** 53-83.

Hua, J., Gong, J., Meng, H., Xu, B., Yao, L., Qian, M., He, Z., Zou, S., Zhou, B. and Song, Z. (2013). Comparison of different methods for the isolation of mesenchymal stem cells from umbilical cord matrix: proliferation and multilineage differentiation as compared to mesenchymal stem cells from umbilical cord blood and bone marrow. *Cell biology international* **38**(2): 198-210.

Huang, Y., Nayak, S., Jankowitz, R., Davidson, N. E. and Oesterreich, S. (2011). Epigenetics in breast cancer: what's new? *Breast cancer research : BCR* **13**(6): 225.

Hyslop, L., Stojkovic, M., Armstrong, L., Walter, T., Stojkovic, P., Przyborski, S., Herbert, M., Murdoch, A., Strachan, T. and Lako, M. (2005). Downregulation of NANOG induces differentiation of human embryonic stem cells to extraembryonic lineages. *Stem cells* **23**(8): 1035-1043.

Ilic, D. and Polak, J. M. (2011). Stem cells in regenerative medicine: introduction. *British medical bulletin* **98**: 117-126.

Illingworth, R. S. and Bird, A. P. (2009). CpG islands--'a rough guide'. *FEBS letters* **583**(11): 1713-1720.

In 't Anker, P. S., Scherjon, S. A., Kleijburg-van der Keur, C., Noort, W. A., Claas, F. H., Willemze, R., Fibbe, W. E. and Kanhai, H. H. (2003). Amniotic fluid as a novel source of mesenchymal stem cells for therapeutic transplantation. *Blood* **102**(4): 1548-1549.

Ishige, I., Nagamura-Inoue, T., Honda, M. J., Harnprasopwat, R., Kido, M., Sugimoto, M., Nakauchi, H. and Tojo, A. (2009). Comparison of mesenchymal stem cells derived from arterial, venous, and Wharton's jelly explants of human umbilical cord. *International journal of hematology* **90**(2): 261-269.

Jansson, T. and Powell, T. L. (2007). Role of the placenta in fetal programming: underlying mechanisms and potential interventional approaches. *Clinical science* **113**(1): 1-13.

Jenuwein, T. and Allis, C. D. (2001). Translating the histone code. *Science* **293**(5532): 1074-1080.

Jeon, Y. J., Kim, J., Cho, J. H., Chung, H. M. and Chae, J. I. (2016). Comparative Analysis of Human Mesenchymal Stem Cells Derived From Bone Marrow, Placenta, and Adipose Tissue as Sources of Cell Therapy. *J Cell Biochem* **117**(5): 1112-1125.

Jeschke, M. G., Gauglitz, G. G., Phan, T. T., Herndon, D. N. and Kita, K. (2011). Umbilical cord lining membrane and Wharton's jelly-derived mesenchymal stem cells: the similarities and differences. *Open Tissue Eng. Regen. Med. J.* **4**(1): 21-27.

Jiao, F., Wang, J., Dong, Z. L., Wu, M. J., Zhao, T. B., Li, D. D. and Wang, X. (2012). Human mesenchymal stem cells derived from limb bud can differentiate into all three embryonic germ layers lineages. *Cellular reprogramming* **14**(4): 324-333.

Jintaridth, P., Tungtrongchitr, R., Preutthipan, S. and Mutirangura, A. (2013). Hypomethylation of Alu elements in post-menopausal women with osteoporosis. *PloS one* **8**(8): e70386.

Johnstone, B., Hering, T. M., Caplan, A. I., Goldberg, V. M. and Yoo, J. U. (1998). In vitro chondrogenesis of bone marrow-derived mesenchymal progenitor cells. *Exp Cell Res* **238**(1): 265-272.

Jones, P. A. (2012). Functions of DNA methylation: islands, start sites, gene bodies and beyond. *Nature reviews. Genetics* **13**(7): 484-492.

Julious, S. A. (2005). Sample size of 12 per group rule of thumb for a pilot study. *PHARMACEUTICAL STATISTICS* **4**(4): 287–291.

Kadner, A., Hoerstrup, S. P., Tracy, J., Breymann, C., Maurus, C. F., Melnitchouk, S., Kadner, G., Zund, G. and Turina, M. (2002). Human umbilical cord cells: a new cell source for cardiovascular tissue engineering. *The Annals of thoracic surgery* **74**(4): S1422-1428.

Kadner, A., Zund, G., Maurus, C., Breymann, C., Yakarisik, S., Kadner, G., Turina, M. and Hoerstrup, S. P. (2004). Human umbilical cord cells for cardiovascular tissue engineering: a comparative study. *European journal of cardio-thoracic surgery : official journal of the European Association for Cardio-thoracic Surgery* **25**(4): 635-641.

Kalaszczynska, I. and Ferdyn, K. (2015). Wharton's jelly derived mesenchymal stem cells: future of regenerative medicine? Recent findings and clinical significance. *BioMed research international* **2015**: 430847.

Karahuseyinoglu, S., Cinar, O., Kilic, E., Kara, F., Akay, G. G., Demiralp, D. O., Tukun, A., Uckan, D. and Can, A. (2007). Biology of stem cells in human umbilical cord stroma: in situ and in vitro surveys. *Stem cells* **25**(2): 319-331.

Kassis, I., Zangi, L., Rivkin, R., Levdansky, L., Samuel, S., Marx, G. and Gorodetsky, R. (2006). Isolation of mesenchymal stem cells from G-CSF-mobilized human peripheral blood using fibrin microbeads. *Bone marrow transplantation* **37**(10): 967-976.

Kelsall, C. J., Hoile, S. P., Irvine, N. A., Masoodi, M., Torrens, C., Lillycrop, K. A., Calder, P. C., Clough, G. F., Hanson, M. A. and Burdge, G. C. (2012). Vascular dysfunction induced in offspring by maternal dietary fat involves altered arterial polyunsaturated fatty acid biosynthesis. *PloS one* **7**(4): e34492.

Kent, W. J., Sugnet, C. W., Furey, T. S., Roskin, K. M., Pringle, T. H., Zahler, A. M. and Haussler, D. (2002). The human genome browser at UCSC. *Genome research* **12**(6): 996-1006.

Kern, S., Eichler, H., Stoeve, J., Kluter, H. and Bieback, K. (2006). Comparative analysis of mesenchymal stem cells from bone marrow, umbilical cord blood, or adipose tissue. *Stem cells* **24**(5): 1294-1301.

Kienesberger, P. C., Lass, A., Preiss-Landl, K., Wolinski, H., Kohlwein, S. D., Zimmermann, R. and Zechner, R. (2008). Identification of an insulin-regulated

lysophospholipase with homology to neuropathy target esterase. *J Biol Chem* **283**(9): 5908-5917.

Kienesberger, P. C., Oberer, M., Lass, A. and Zechner, R. (2009). Mammalian patatin domain containing proteins: a family with diverse lipolytic activities involved in multiple biological functions. *Journal of lipid research* **50 Suppl**: S63-68.

Kilaru, V., Barfield, R. T., Schroeder, J. W., Smith, A. K. and Conneely, K. N. (2012). MethLAB: a graphical user interface package for the analysis of array-based DNA methylation data. *Epigenetics* **7**(3): 225-229.

Kim, D. W., Staples, M., Shinozuka, K., Pantcheva, P., Kang, S. D. and Borlongan, C. V. (2013). Wharton's jelly-derived mesenchymal stem cells: phenotypic characterization and optimizing their therapeutic potential for clinical applications. *International journal of molecular sciences* **14**(6): 11692-11712.

Kim, J. W., Kim, S. Y., Park, S. Y., Kim, Y. M., Kim, J. M., Lee, M. H. and Ryu, H. M. (2004). Mesenchymal progenitor cells in the human umbilical cord. *Annals of hematology* **83**(12): 733-738.

Kim, M., Long, T. I., Arakawa, K., Wang, R., Yu, M. C. and Laird, P. W. (2010). DNA methylation as a biomarker for cardiovascular disease risk. *PloS one* **5**(3): e9692.

Kim, Y., Kim, H., Cho, H., Bae, Y., Suh, K. and Jung, J. (2007). Direct comparison of human mesenchymal stem cells derived from adipose tissues and bone marrow in mediating neovascularization in response to vascular ischemia. *Cellular physiology and biochemistry : international journal of experimental cellular physiology, biochemistry, and pharmacology* **20**(6): 867-876.

Kinnaird, T., Stabile, E., Burnett, M. S., Lee, C. W., Barr, S., Fuchs, S. and Epstein, S. E. (2004). Marrow-derived stromal cells express genes encoding a broad spectrum of arteriogenic cytokines and promote in vitro and in vivo

arteriogenesis through paracrine mechanisms. *Circulation research* **94**(5): 678-685.

Klontzas, M. E., Kenanidis, E. I., Heliotis, M., Tsiridis, E. and Mantalaris, A. (2015). Bone and cartilage regeneration with the use of umbilical cord mesenchymal stem cells. *Expert opinion on biological therapy* **15**(11): 1541-1552.

Kobolak, J., Dinnyes, A., Memic, A., Khademhosseini, A. and Mobasheri, A. (2015). Mesenchymal stem cells: Identification, phenotypic characterization, biological properties and potential for regenerative medicine through biomaterial micro-engineering of their niche. *Methods* **[no volume]**([no issue]): [no pages].

Kopen, G. C., Prockop, D. J. and Phinney, D. G. (1999). Marrow stromal cells migrate throughout forebrain and cerebellum, and they differentiate into astrocytes after injection into neonatal mouse brains. *Proceedings of the National Academy of Sciences of the United States of America* **96**(19): 10711-10716.

Kotton, D. N., Ma, B. Y., Cardoso, W. V., Sanderson, E. A., Summer, R. S., Williams, M. C. and Fine, A. (2001). Bone marrow-derived cells as progenitors of lung alveolar epithelium. *Development* **128**(24): 5181-5188.

Kouzarides, T. (2007). Chromatin modifications and their function. *Cell* **128**(4): 693-705.

Krasnodembskaya, A., Song, Y., Fang, X., Gupta, N., Serikov, V., Lee, J. W. and Matthay, M. A. (2010). Antibacterial effect of human mesenchymal stem cells is mediated in part from secretion of the antimicrobial peptide LL-37. *Stem cells* **28**(12): 2229-2238.

Kucia, M., Reca, R., Jala, V. R., Dawn, B., Ratajczak, J. and Ratajczak, M. Z. (2005). Bone marrow as a home of heterogenous populations of nonhematopoietic stem cells. *Leukemia* **19**(7): 1118-1127.

Kuznetsov, S. A., Mankani, M. H., Gronthos, S., Satomura, K., Bianco, P. and Robey, P. G. (2001). Circulating skeletal stem cells. *The Journal of cell biology* **153**(5): 1133-1140.

La Rocca, G., Anzalone, R., Corrao, S., Magno, F., Loria, T., Lo Iacono, M., Di Stefano, A., Giannuzzi, P., Marasa, L., Cappello, F., Zummo, G. and Farina, F. (2009). Isolation and characterization of Oct-4+/HLA-G+ mesenchymal stem cells from human umbilical cord matrix: differentiation potential and detection of new markers. *Histochemistry and cell biology* **131**(2): 267-282.

Laird, P. W. and Jaenisch, R. (1996). The role of DNA methylation in cancer genetic and epigenetics. *Annual review of genetics* **30**: 441-464.

Lange, U. C. and Schneider, R. (2010). What an epigenome remembers. *BioEssays : news and reviews in molecular, cellular and developmental biology* **32**(8): 659-668.

Lazarus, H. M. (1995). Bone marrow transplantation in low-grade non-Hodgkin's lymphoma. *Leukemia & lymphoma* **17**(3-4): 199-210.

Le Blanc, K., Rasmusson, I., Sundberg, B., Gotherstrom, C., Hassan, M., Uzunel, M. and Ringden, O. (2004). Treatment of severe acute graft-versus-host disease with third party haploidentical mesenchymal stem cells. *Lancet* **363**(9419): 1439-1441.

Le Blanc, K. and Ringden, O. (2005). Immunobiology of human mesenchymal stem cells and future use in hematopoietic stem cell transplantation. *Biology of blood and marrow transplantation : journal of the American Society for Blood and Marrow Transplantation* **11**(5): 321-334.

Lee, J., Kim, H. K., Rho, J. Y., Han, Y. M. and Kim, J. (2006). The human OCT-4 isoforms differ in their ability to confer self-renewal. *The Journal of biological chemistry* **281**(44): 33554-33565.

Lee, J. W., Fang, X., Gupta, N., Serikov, V. and Matthay, M. A. (2009). Allogeneic human mesenchymal stem cells for treatment of E. coli endotoxin-induced acute lung injury in the ex vivo perfused human lung. *Proceedings of the*

National Academy of Sciences of the United States of America **106**(38): 16357-16362.

Lee, S. T., Jang, J. H., Cheong, J. W., Kim, J. S., Maemg, H. Y., Hahn, J. S., Ko, Y. W. and Min, Y. H. (2002). Treatment of high-risk acute myelogenous leukaemia by myeloablative chemoradiotherapy followed by co-infusion of T cell-depleted haematopoietic stem cells and culture-expanded marrow mesenchymal stem cells from a related donor with one fully mismatched human leucocyte antigen haplotype. *British journal of haematology* **118**(4): 1128-1131.

Lesseur, C., Armstrong, D. A., Paquette, A. G., Li, Z., Padbury, J. F. and Marsit, C. J. (2014). Maternal obesity and gestational diabetes are associated with placental leptin DNA methylation. *American journal of obstetrics and gynecology* **211**(6): 654 e651-659.

Li, C. C., Maloney, C. A., Cropley, J. E. and Suter, C. M. (2010). Epigenetic programming by maternal nutrition: shaping future generations. *Epigenomics* **2**(4): 539-549.

Li, C. C., Young, P. E., Maloney, C. A., Eaton, S. A., Cowley, M. J., Buckland, M. E., Preiss, T., Henstridge, D. C., Cooney, G. J., Febbraio, M. A., Martin, D. I., Cropley, J. E. and Suter, C. M. (2013). Maternal obesity and diabetes induces latent metabolic defects and widespread epigenetic changes in isogenic mice. *Epigenetics* **8**(6): 602-611.

Li, E., Bestor, T. H. and Jaenisch, R. (1992). Targeted mutation of the DNA methyltransferase gene results in embryonic lethality. *Cell* **69**(6): 915-926.

Li, K., Han, Q., Yan, X., Liao, L. and Zhao, R. C. (2010). Not a process of simple vicariousness, the differentiation of human adipose-derived mesenchymal stem cells to renal tubular epithelial cells plays an important role in acute kidney injury repairing. *Stem cells and development* **19**(8): 1267-1275.

Liechty, K. W., MacKenzie, T. C., Shaaban, A. F., Radu, A., Moseley, A. M., Deans, R., Marshak, D. R. and Flake, A. W. (2000). Human mesenchymal stem cells engraft and demonstrate site-specific differentiation after in utero transplantation in sheep. *Nature medicine* **6**(11): 1282-1286.

Lister, R., Pelizzola, M., Dowen, R. H., Hawkins, R. D., Hon, G., Tonti-Filippini, J., Nery, J. R., Lee, L., Ye, Z., Ngo, Q. M., Edsall, L., Antosiewicz-Bourget, J., Stewart, R., Ruotti, V., Millar, A. H., Thomson, J. A., Ren, B. and Ecker, J. R. (2009). Human DNA methylomes at base resolution show widespread epigenomic differences. *Nature* **462**(7271): 315-322.

Liu, T. M., Wu, Y. N., Guo, X. M., Hui, J. H., Lee, E. H. and Lim, B. (2009). Effects of ectopic Nanog and Oct4 overexpression on mesenchymal stem cells. *Stem cells and development* **18**(7): 1013-1022.

Lu, L. L., Liu, Y. J., Yang, S. G., Zhao, Q. J., Wang, X., Gong, W., Han, Z. B., Xu, Z. S., Lu, Y. X., Liu, D., Chen, Z. Z. and Han, Z. C. (2006). Isolation and characterization of human umbilical cord mesenchymal stem cells with hematopoiesis-supportive function and other potentials. *Haematologica* **91**(8): 1017-1026.

Mahmood, A., Lu, D., Lu, M. and Chopp, M. (2003). Treatment of traumatic brain injury in adult rats with intravenous administration of human bone marrow stromal cells. *Neurosurgery* **53**(3): 697-702; discussion 702-693.

Majore, I., Moretti, P., Stahl, F., Hass, R. and Kasper, C. (2011). Growth and differentiation properties of mesenchymal stromal cell populations derived from whole human umbilical cord. *Stem cell reviews* **7**(1): 17-31.

Makino, S., Fukuda, K., Miyoshi, S., Konishi, F., Kodama, H., Pan, J., Sano, M., Takahashi, T., Hori, S., Abe, H., Hata, J., Umezawa, A. and Ogawa, S. (1999). Cardiomyocytes can be generated from marrow stromal cells in vitro. *The Journal of clinical investigation* **103**(5): 697-705.

Malpas, P. and Symonds, E. M. (1966). Observations on the structure of the human umbilical cord. *Surgery, gynecology & obstetrics* **123**(4): 746-750.

Mantel, C., Guo, Y., Lee, M. R., Kim, M. K., Han, M. K., Shibayama, H., Fukuda, S., Yoder, M. C., Pelus, L. M., Kim, K. S. and Broxmeyer, H. E. (2007). Checkpoint-apoptosis uncoupling in human and mouse embryonic stem cells: a source of karyotpic instability. *Blood* **109**(10): 4518-4527.

Martin, D. I., Cropley, J. E. and Suter, C. M. (2011). Epigenetics in disease: leader or follower? *Epigenetics* **6**(7): 843-848.

Martinez-Frias, M. L. (2010). Can our understanding of epigenetics assist with primary prevention of congenital defects? *Journal of medical genetics* **47**(2): 73-80.

McElreavey, K. D., Irvine, A. I., Ennis, K. T. and McLean, W. H. (1991). Isolation, culture and characterisation of fibroblast-like cells derived from the Wharton's jelly portion of human umbilical cord. *Biochemical Society transactions* **19**(1): 29S.

McIntyre, H. D., Gibbons, K. S., Flenady, V. J. and Callaway, L. K. (2012). Overweight and obesity in Australian mothers: epidemic or endemic? *The Medical journal of Australia* **196**(3): 184-188.

Mei, Z., Grummer-Strawn, L. M., Pietrobelli, A., Goulding, A., Goran, M. I. and Dietz, W. H. (2002). Validity of body mass index compared with other body-composition screening indexes for the assessment of body fatness in children and adolescents. *The American journal of clinical nutrition* **75**(6): 978-985.

Mitchell, K. E., Weiss, M. L., Mitchell, B. M., Martin, P., Davis, D., Morales, L., Helwig, B., Beerenstrauch, M., Abou-Easa, K., Hildreth, T., Troyer, D. and Medicetty, S. (2003). Matrix cells from Wharton's jelly form neurons and glia. *Stem cells* **21**(1): 50-60.

Mitsui, K., Tokuzawa, Y., Itoh, H., Segawa, K., Murakami, M., Takahashi, K., Maruyama, M., Maeda, M. and Yamanaka, S. (2003). The homeoprotein Nanog

is required for maintenance of pluripotency in mouse epiblast and ES cells. *Cell* **113**(5): 631-642.

Mizoguchi, M., Suga, Y., Sanmano, B., Ikeda, S. and Ogawa, H. (2004). Organotypic culture and surface plantation using umbilical cord epithelial cells: morphogenesis and expression of differentiation markers mimicking cutaneous epidermis. *Journal of dermatological science* **35**(3): 199-206.

Morales Prieto, D. M. and Markert, U. R. (2011). MicroRNAs in pregnancy. *Journal of reproductive immunology* **88**(2): 106-111.

Morris, M. J. (2009). Early life influences on obesity risk: maternal overnutrition and programming of obesity. *Expert Rev. Endocronol. Metab.* **4**(6): 625-637.

Morris, T. J., Butcher, L. M., Feber, A., Teschendorff, A. E., Chakravarthy, A. R., Wojdacz, T. K. and Beck, S. (2014). ChAMP: 450k chip analysis methylation pipeline. *Bioinformatics* **30**(3): 428-430.

Moser, B. and Loetscher, P. (2001). Lymphocyte traffic control by chemokines. *Nature immunology* **2**(2): 123-128.

Munoz-Elias, G., Marcus, A. J., Coyne, T. M., Woodbury, D. and Black, I. B. (2004). Adult bone marrow stromal cells in the embryonic brain: engraftment, migration, differentiation, and long-term survival. *The Journal of neuroscience : the official journal of the Society for Neuroscience* **24**(19): 4585-4595.

Murphy, M. B., Moncivais, K. and Caplan, A. I. (2013). Mesenchymal stem cells: environmentally responsive therapeutics for regenerative medicine. *Experimental & molecular medicine* **45**: e54.

Murphy, S. K., Wylie, A. A., Coveler, K. J., Cotter, P. D., Papenhausen, P. R., Sutton, V. R., Shaffer, L. G. and Jirtle, R. L. (2003). Epigenetic detection of human chromosome 14 uniparental disomy. *Human mutation* **22**(1): 92-97.

Murray, I. R. and Peault, B. (2015). Q&A: Mesenchymal stem cells - where do they come from and is it important? *BMC biology* **13**(1): 99.

Nakagawa, H., Akita, S., Fukui, M., Fujii, T. and Akino, K. (2005). Human mesenchymal stem cells successfully improve skin-substitute wound healing. *The British journal of dermatology* **153**(1): 29-36.

Nakao, M. (2001). Epigenetics: interaction of DNA methylation and chromatin. *Gene* **278**(1-2): 25-31.

Nanaev, A. K., Kohnen, G., Milovanov, A. P., Domogatsky, S. P. and Kaufmann, P. (1997). Stromal differentiation and architecture of the human umbilical cord. *Placenta* **18**(1): 53-64.

National Marrow Donor Program. (2016). "*Be the match*." Available at: https://bethematch.org (Accessed: 15.02.2016]).

Nemeth, K., Leelahavanichkul, A., Yuen, P. S., Mayer, B., Parmelee, A., Doi, K., Robey, P. G., Leelahavanichkul, K., Koller, B. H., Brown, J. M., Hu, X., Jelinek, I., Star, R. A. and Mezey, E. (2009). Bone marrow stromal cells attenuate sepsis via prostaglandin E(2)-dependent reprogramming of host macrophages to increase their interleukin-10 production. *Nature medicine* **15**(1): 42-49.

Nemeth, K. and Mezey, E. (2015). Bone marrow stromal cells as immunomodulators. A primer for dermatologists. *J Dermatol Sci* **77**(1): 11-20.

Neuss, S., Becher, E., Woltje, M., Tietze, L. and Jahnen-Dechent, W. (2004). Functional expression of HGF and HGF receptor/c-met in adult human mesenchymal stem cells suggests a role in cell mobilization, tissue repair, and wound healing. *Stem cells* **22**(3): 405-414.

Ng, S. W., Zaghloul, S., Ali, H. I., Harrison, G. and Popkin, B. M. (2011). The prevalence and trends of overweight, obesity and nutrition-related non-communicable diseases in the Arabian Gulf States. *Obesity reviews : an official journal of the International Association for the Study of Obesity* **12**(1): 1-13.

NHS Blood and Transplant. (2016). "*The NHS cord blood bank*." Available at: http://www.nhsbt.nhs.uk/cordblood/ (Accessed: 15.02.2016]).

Niwa, H., Miyazaki, J. and Smith, A. G. (2000). Quantitative expression of Oct-3/4 defines differentiation, dedifferentiation or self-renewal of ES cells. *Nature genetics* **24**(4): 372-376.

Nombela-Arrieta, C., Ritz, J. and Silberstein, L. E. (2011). The elusive nature and function of mesenchymal stem cells. *Nature reviews. Molecular cell biology* **12**(2): 126-131.

Nomura, Y., Lambertini, L., Rialdi, A., Lee, M., Mystal, E. Y., Grabie, M., Manaster, I., Huynh, N., Finik, J., Davey, M., Davey, K., Ly, J., Stone, J., Loudon, H., Eglinton, G., Hurd, Y., Newcorn, J. H. and Chen, J. (2014). Global methylation in the placenta and umbilical cord blood from pregnancies with maternal gestational diabetes, preeclampsia, and obesity. *Reproductive sciences* **21**(1): 131-137.

Noort, W. A., Kruisselbrink, A. B., in't Anker, P. S., Kruger, M., van Bezooijen, R. L., de Paus, R. A., Heemskerk, M. H., Lowik, C. W., Falkenburg, J. H., Willemze, R. and Fibbe, W. E. (2002). Mesenchymal stem cells promote engraftment of human umbilical cord blood-derived CD34(+) cells in NOD/SCID mice. *Experimental hematology* **30**(8): 870-878.

Okano, M., Bell, D. W., Haber, D. A. and Li, E. (1999). DNA methyltransferases Dnmt3a and Dnmt3b are essential for de novo methylation and mammalian development. *Cell* **99**(3): 247-257.

Ortiz, L. A., Dutreil, M., Fattman, C., Pandey, A. C., Torres, G., Go, K. and Phinney, D. G. (2007). Interleukin 1 receptor antagonist mediates the antiinflammatory and antifibrotic effect of mesenchymal stem cells during lung injury. *Proceedings of the National Academy of Sciences of the United States of America* **104**(26): 11002-11007.

Ortiz, L. A., Gambelli, F., McBride, C., Gaupp, D., Baddoo, M., Kaminski, N. and Phinney, D. G. (2003). Mesenchymal stem cell engraftment in lung is enhanced

in response to bleomycin exposure and ameliorates its fibrotic effects. *Proceedings of the National Academy of Sciences of the United States of America* **100**(14): 8407-8411.

Owen, M. (1988). Marrow stromal stem cells. *Journal of cell science. Supplement* **10**: 63-76.

Palmieri, S. L., Peter, W., Hess, H. and Scholer, H. R. (1994). Oct-4 transcription factor is differentially expressed in the mouse embryo during establishment of the first two extraembryonic cell lineages involved in implantation. *Developmental biology* **166**(1): 259-267.

Panda, S. K. and Ravindran, B. (2013). In vitro culture of human PBMCs. *Bio-Protocol* **3**(3): e322.

Pansky, B. (1982). *The umbilical cord*. In *Review of medical embryology*. Chapter 35. London, Macmillan.

Pappa, K. I. and Anagnou, N. P. (2009). Novel sources of fetal stem cells: where do they fit on the developmental continuum? *Regenerative medicine* **4**(3): 423-433.

Peng, H. Q., Levitin-Smith, M., Rochelson, B. and Kahn, E. (2006). Umbilical cord stricture and overcoiling are common causes of fetal demise. *Pediatric and developmental pathology : the official journal of the Society for Pediatric Pathology and the Paediatric Pathology Society* **9**(1): 14-19.

Phinney, D. G. and Prockop, D. J. (2007). Concise review: mesenchymal stem/multipotent stromal cells: the state of transdifferentiation and modes of tissue repair--current views. *Stem cells* **25**(11): 2896-2902.

Pievani, A., Scagliotti, V., Russo, F. M., Azario, I., Rambaldi, B., Sacchetti, B., Marzorati, S., Erba, E., Giudici, G., Riminucci, M., Biondi, A., Vergani, P. and Serafini, M. (2014). Comparative analysis of multilineage properties of mesenchymal stromal cells derived from fetal sources shows an advantage of

mesenchymal stromal cells isolated from cord blood in chondrogenic differentiation potential. *Cytotherapy* **16**(7): 893-905.

Pittenger, M. F., Mackay, A. M., Beck, S. C., Jaiswal, R. K., Douglas, R., Mosca, J. D., Moorman, M. A., Simonetti, D. W., Craig, S. and Marshak, D. R. (1999). Multilineage potential of adult human mesenchymal stem cells. *Science* **284**(5411): 143-147.

Piyathilake, C. J., Badiga, S., Alvarez, R. D., Partridge, E. E. and Johanning, G. L. (2013). A lower degree of PBMC L1 methylation is associated with excess body weight and higher HOMA-IR in the presence of lower concentrations of plasma folate. *PloS one* **8**(1): e54544.

Popp, F. C., Eggenhofer, E., Renner, P., Slowik, P., Lang, S. A., Kaspar, H., Geissler, E. K., Piso, P., Schlitt, H. J. and Dahlke, M. H. (2008). Mesenchymal stem cells can induce long-term acceptance of solid organ allografts in synergy with low-dose mycophenolate. *Transplant immunology* **20**(1-2): 55-60.

Portela, A. and Esteller, M. (2010). Epigenetic modifications and human disease. *Nature biotechnology* **28**(10): 1057-1068.

Prentice, A. M. and Jebb, S. A. (2001). Beyond body mass index. *Obesity reviews : an official journal of the International Association for the Study of Obesity* **2**(3): 141-147.

Probst, A. V., Dunleavy, E. and Almouzni, G. (2009). Epigenetic inheritance during the cell cycle. *Nature reviews. Molecular cell biology* **10**(3): 192-206.

Pytlík, S., Stehlík and Matějkova (2011). Production of Clinical Grade Mesenchymal Stromal Cells. *Intechopen*.

Raio, L., Ghezzi, F., Di Naro, E., Gomez, R., Franchi, M., Mazor, M. and Bruhwiler, H. (1999). Sonographic measurement of the umbilical cord and fetal anthropometric parameters. *European journal of obstetrics, gynecology, and reproductive biology* **83**(2): 131-135.

Ramsahoye, B. H., Biniszkiewicz, D., Lyko, F., Clark, V., Bird, A. P. and Jaenisch, R. (2000). Non-CpG methylation is prevalent in embryonic stem cells and may be mediated by DNA methyltransferase 3a. *Proceedings of the National Academy of Sciences of the United States of America* **97**(10): 5237-5242.

Rao, M. S. (2006). Are there morally acceptable alternatives to blastocyst derived ESC? *Journal of cellular biochemistry* **98**(5): 1054-1061.

Ravelli, G. P., Stein, Z. A. and Susser, M. W. (1976). Obesity in young men after famine exposure in utero and early infancy. *The New England journal of medicine* **295**(7): 349-353.

Rebuzzini, P., Neri, T., Mazzini, G., Zuccotti, M., Redi, C. A. and Garagna, S. (2008). Karyotype analysis of the euploid cell population of a mouse embryonic stem cell line revealed a high incidence of chromosome abnormalities that varied during culture. *Cytogenetic and genome research* **121**(1): 18-24.

Reik, W. (2007). Stability and flexibility of epigenetic gene regulation in mammalian development. *Nature* **447**(7143): 425-432.

Reik, W., Dean, W. and Walter, J. (2001). Epigenetic reprogramming in mammalian development. *Science* **293**(5532): 1089-1093.

Reik, W. and Walter, J. (2001). Genomic imprinting: parental influence on the genome. *Nature reviews. Genetics* **2**(1): 21-32.

Reim, G. and Brand, M. (2002). Spiel-ohne-grenzen/pou2 mediates regional competence to respond to Fgf8 during zebrafish early neural development. *Development* **129**(4): 917-933.

Relton, C. L., Groom, A., St Pourcain, B., Sayers, A. E., Swan, D. C., Embleton, N. D., Pearce, M. S., Ring, S. M., Northstone, K., Tobias, J. H., Trakalo, J., Ness, A. R., Shaheen, S. O. and Davey Smith, G. (2012). DNA methylation patterns in cord blood DNA and body size in childhood. *PloS one* **7**(3): e31821.

Ren, G., Zhang, L., Zhao, X., Xu, G., Zhang, Y., Roberts, A. I., Zhao, R. C. and Shi, Y. (2008). Mesenchymal stem cell-mediated immunosuppression occurs via concerted action of chemokines and nitric oxide. *Cell stem cell* **2**(2): 141-150.

Ren, G., Zhao, X., Zhang, L., Zhang, J., L'Huillier, A., Ling, W., Roberts, A. I., Le, A. D., Shi, S., Shao, C. and Shi, Y. (2010). Inflammatory cytokine-induced intercellular adhesion molecule-1 and vascular cell adhesion molecule-1 in mesenchymal stem cells are critical for immunosuppression. *Journal of immunology* **184**(5): 2321-2328.

Riekstina, U., Muceniece, R., Cakstina, I., Muiznieks, I. and Ancans, J. (2008). Characterization of human skin-derived mesenchymal stem cell proliferation rate in different growth conditions. *Cytotechnology* **58**(3): 153-162.

Ries, C., Egea, V., Karow, M., Kolb, H., Jochum, M. and Neth, P. (2007). MMP-2, MT1-MMP, and TIMP-2 are essential for the invasive capacity of human mesenchymal stem cells: differential regulation by inflammatory cytokines. *Blood* **109**(9): 4055-4063.

Rojas, M., Xu, J., Woods, C. R., Mora, A. L., Spears, W., Roman, J. and Brigham, K. L. (2005). Bone marrow-derived mesenchymal stem cells in repair of the injured lung. *American journal of respiratory cell and molecular biology* **33**(2): 145-152.

Romanov, Y. A., Svintsitskaya, V. A. and Smirnov, V. N. (2003). Searching for alternative sources of postnatal human mesenchymal stem cells: candidate MSC-like cells from umbilical cord. *Stem cells* **21**(1): 105-110.

Rotter, N., Oder, J., Schlenke, P., Lindner, U., Bohrnsen, F., Kramer, J., Rohwedel, J., Huss, R., Brandau, S., Wollenberg, B. and Lang, S. (2008). Isolation and characterization of adult stem cells from human salivary glands. *Stem cells and development* **17**(3): 509-518.

Rui, Y. F., Lui, P. P., Li, G., Fu, S. C., Lee, Y. W. and Chan, K. M. (2010). Isolation and characterization of multipotent rat tendon-derived stem cells. *Tissue Eng Part A* **16**(5): 1549-1558.

Ruster, B., Gottig, S., Ludwig, R. J., Bistrian, R., Muller, S., Seifried, E., Gille, J. and Henschler, R. (2006). Mesenchymal stem cells display coordinated rolling and adhesion behavior on endothelial cells. *Blood* **108**(12): 3938-3944.

Ruthenburg, A. J., Li, H., Patel, D. J. and Allis, C. D. (2007). Multivalent engagement of chromatin modifications by linked binding modules. *Nature reviews. Molecular cell biology* **8**(12): 983-994.

Sadler, T. W. (1990). *Langman's medical embryology*. 6th Ed. Baltimore, MD, Williams & Wilkins.

Salehinejad, P., Alitheen, N. B., Ali, A. M., Omar, A. R., Mohit, M., Janzamin, E., Samani, F. S., Torshizi, Z. and Nematollahi-Mahani, S. N. (2012). Comparison of different methods for the isolation of mesenchymal stem cells from human umbilical cord Wharton's jelly. *In vitro cellular & developmental biology. Animal* **48**(2): 75-83.

Sandholt, C. H., Hansen, T. and Pedersen, O. (2012). Beyond the fourth wave of genome-wide obesity association studies. *Nutrition & diabetes* **2**: e37.

Sandoval, J., Heyn, H., Moran, S., Serra-Musach, J., Pujana, M. A., Bibikova, M. and Esteller, M. (2011). Validation of a DNA methylation microarray for 450,000 CpG sites in the human genome. *Epigenetics* **6**(6): 692-702.

Sarugaser, R., Lickorish, D., Baksh, D., Hosseini, M. M. and Davies, J. E. (2005). Human umbilical cord perivascular (HUCPV) cells: a source of mesenchymal progenitors. *Stem cells* **23**(2): 220-229.

Sasaki, A., de Vega, W. C. and McGowan, P. O. (2013). Biological embedding in mental health: an epigenomic perspective. *Biochemistry and cell biology = Biochimie et biologie cellulaire* **91**(1): 14-21.

Sasaki, H. and Matsui, Y. (2008). Epigenetic events in mammalian germ-cell development: reprogramming and beyond. *Nature reviews. Genetics* **9**(2): 129-140.

Sato, Y., Araki, H., Kato, J., Nakamura, K., Kawano, Y., Kobune, M., Sato, T., Miyanishi, K., Takayama, T., Takahashi, M., Takimoto, R., Iyama, S., Matsunaga, T., Ohtani, S., Matsuura, A., Hamada, H. and Niitsu, Y. (2005). Human mesenchymal stem cells xenografted directly to rat liver are differentiated into human hepatocytes without fusion. *Blood* **106**(2): 756-763.

Schmidt, A., Ladage, D., Steingen, C., Brixius, K., Schinkothe, T., Klinz, F. J., Schwinger, R. H., Mehlhorn, U. and Bloch, W. (2006). Mesenchymal stem cells transmigrate over the endothelial barrier. *European journal of cell biology* **85**(11): 1179-1188.

Schuring, A. N., Schulte, N., Kelsch, R., Ropke, A., Kiesel, L. and Gotte, M. (2011). Characterization of endometrial mesenchymal stem-like cells obtained by endometrial biopsy during routine diagnostics. *Fertility and sterility* **95**(1): 423-426.

Schwartz, R. E., Reyes, M., Koodie, L., Jiang, Y., Blackstad, M., Lund, T., Lenvik, T., Johnson, S., Hu, W. S. and Verfaillie, C. M. (2002). Multipotent adult progenitor cells from bone marrow differentiate into functional hepatocyte-like cells. *The Journal of clinical investigation* **109**(10): 1291-1302.

Sedgwick, P. (2012). Non-parametric statistical tests for independent groups: numerical data. *Bmj*.

Sedgwick, P. (2014). Non-parametric statistical tests for two independent groups: numerical data. *Bmj*.

Sedgwick, P. and Joekes, K. (2013). Kaplan-Meier survival curves: interpretation and communication of risk. *Bmj*.

Sharma, R. R., Pollock, K., Hubel, A. and McKenna, D. (2014). Mesenchymal stem or stromal cells: a review of clinical applications and manufacturing practices. *Transfusion* **54**(5): 1418-1437.

Shi, M., Li, J., Liao, L., Chen, B., Li, B., Chen, L., Jia, H. and Zhao, R. C. (2007). Regulation of CXCR4 expression in human mesenchymal stem cells by cytokine treatment: role in homing efficiency in NOD/SCID mice. *Haematologica* **92**(7): 897-904.

Sobolewski, K., Bankowski, E., Chyczewski, L. and Jaworski, S. (1997). Collagen and glycosaminoglycans of Wharton's jelly. *Biology of the neonate* **71**(1): 11-21.

Sohni, A. and Verfaillie, C. M. (2013). Mesenchymal stem cells migration homing and tracking. *Stem cells international* **2013**: 130763.

Son, B. R., Marquez-Curtis, L. A., Kucia, M., Wysoczynski, M., Turner, A. R., Ratajczak, J., Ratajczak, M. Z. and Janowska-Wieczorek, A. (2006). Migration of bone marrow and cord blood mesenchymal stem cells in vitro is regulated by stromal-derived factor-1-CXCR4 and hepatocyte growth factor-c-met axes and involves matrix metalloproteinases. *Stem cells* **24**(5): 1254-1264.

Spaeth, E., Klopp, A., Dembinski, J., Andreeff, M. and Marini, F. (2008). Inflammation and tumor microenvironments: defining the migratory itinerary of mesenchymal stem cells. *Gene therapy* **15**(10): 730-738.

Spraycar, M. (1995). *Stedman's medical dictionary*. 27th Ed. Baltimore, MD, Williams & Wilkins.

Squillaro, T., Peluso, G. and Galderisi, U. (2015). Clinical trials with mesenchymal stem cells: an update. *Cell transplantation*.

Srikanth, G. V., Tripathy, N. K. and Nityanand, S. (2013). Fetal cardiac mesenchymal stem cells express embryonal markers and exhibit differentiation into cells of all three germ layers. *World J Stem Cells* **5**(1): 26-33.

Storey, J. D. (2002). A direct approach to false discovery rates. *J. Roy. Stat. Soc. Series B Stat. Methodol.* **64**(3): 479-498.

Strahl, B. D. and Allis, C. D. (2000). The language of covalent histone modifications. *Nature* **403**(6765): 41-45.

Subramanian, A., Fong, C. Y., Biswas, A. and Bongso, A. (2015). Comparative characterization of cells from the various compartments of the human umbilical cord shows that the Wharton's jelly compartment provides the best source of clinically utilizable mesenchymal stem cells. *PloS one* **10**(6): e0127992.

Sukarieh, R., Joseph, R., Leow, S. C., Li, Y., Loffler, M., Aris, I. M., Tan, J. H., Teh, A. L., Chen, L., Holbrook, J. D., Ng, K. L., Lee, Y. S., Chong, Y. S., Summers, S. A., Gluckman, P. D. and Stunkel, W. (2014). Molecular pathways reflecting poor intrauterine growth are found in Wharton's jelly-derived mesenchymal stem cells. *Human reproduction* **29**(10): 2287-2301.

Sun, Q., van Dam, R. M., Spiegelman, D., Heymsfield, S. B., Willett, W. C. and Hu, F. B. (2010). Comparison of dual-energy x-ray absorptiometric and anthropometric measures of adiposity in relation to adiposity-related biologic factors. *American journal of epidemiology* **172**(12): 1442-1454.

Suzdal'tseva, Y. G., Burunova, V. V., Vakhrushev, I. V., Yarygin, V. N. and Yarygin, K. N. (2007). Capability of human mesenchymal cells isolated from different sources to differentiation into tissues of mesodermal origin. *Bulletin of experimental biology and medicine* **143**(1): 114-121.

Suzuki, M. M. and Bird, A. (2008). DNA methylation landscapes: provocative insights from epigenomics. *Nature reviews. Genetics* **9**(6): 465-476.

Taghizadeh, R. R., Cetrulo, K. J. and Cetrulo, C. L. (2011). Wharton's Jelly stem cells: future clinical applications. *Placenta* **32 Suppl 4**: S311-315.

Takahashi, M., Li, T. S., Suzuki, R., Kobayashi, T., Ito, H., Ikeda, Y., Matsuzaki, M. and Hamano, K. (2006). Cytokines produced by bone marrow cells can contribute to

functional improvement of the infarcted heart by protecting cardiomyocytes from ischemic injury. *American journal of physiology. Heart and circulatory physiology* **291**(2): H886-893.

Takai, D. and Jones, P. A. (2002). Comprehensive analysis of CpG islands in human chromosomes 21 and 22. *Proceedings of the National Academy of Sciences of the United States of America* **99**(6): 3740-3745.

Takechi, K., Kuwabara, Y. and Mizuno, M. (1993). Ultrastructural and immunohistochemical studies of Wharton's jelly umbilical cord cells. *Placenta* **14**(2): 235-245.

Takeda, J., Seino, S. and Bell, G. I. (1992). Human Oct3 gene family: cDNA sequences, alternative splicing, gene organization, chromosomal location, and expression at low levels in adult tissues. *Nucleic acids research* **20**(17): 4613-4620.

Tang, D. Q., Cao, L. Z., Burkhardt, B. R., Xia, C. Q., Litherland, S. A., Atkinson, M. A. and Yang, L. J. (2004). In vivo and in vitro characterization of insulin-producing cells obtained from murine bone marrow. *Diabetes* **53**(7): 1721-1732.

Tasso, R., Ilengo, C., Quarto, R., Cancedda, R., Caspi, R. R. and Pennesi, G. (2012). Mesenchymal stem cells induce functionally active T-regulatory lymphocytes in a paracrine fashion and ameliorate experimental autoimmune uveitis. *Investigative ophthalmology & visual science* **53**(2): 786-793.

Teschendorff, A. E., Marabita, F., Lechner, M., Bartlett, T., Tegner, J., Gomez-Cabrero, D. and Beck, S. (2013). A beta-mixture quantile normalization method for correcting probe design bias in Illumina Infinium 450 k DNA methylation data. *Bioinformatics* **29**(2): 189-196.

Tigyi, G. (2001). Physiological responses to lysophosphatidic acid and related glycero-phospholipids. *Prostaglandins & other lipid mediators* **64**(1-4): 47-62.

Tomari, Y. and Zamore, P. D. (2005). Perspective: machines for RNAi. *Genes & development* **19**(5): 517-529.

Tong, C. K., Vellasamy, S., Tan, B. C., Abdullah, M., Vidyadaran, S., Seow, H. F. and Ramasamy, R. (2011). Generation of mesenchymal stem cell from human umbilical cord tissue using a combination enzymatic and mechanical disassociation method. *Cell biology international* **35**(3): 221-226.

Tost, J. (2010). DNA methylation: an introduction to the biology and the disease-associated changes of a promising biomarker. *Molecular biotechnology* **44**(1): 71-81.

Toyserkani, N. M., Christensen, M. L., Sheikh, S. P. and Sorensen, J. A. (2015). Adipose-Derived Stem Cells: New Treatment for Wound Healing? *Annals of plastic surgery* **75**(1): 117-123.

Trevisanuto, D., Doglioni, N., Zanardo, V. and Chiarelli, S. (2007). Overcoiling of the umbilical cord. *The Journal of pediatrics* **150**(1): 112.

Troyer, D. L. and Weiss, M. L. (2008). Wharton's jelly-derived cells are a primitive stromal cell population. *Stem cells* **26**(3): 591-599.

Tsagias, N., Koliakos, I., Karagiannis, V., Eleftheriadou, M. and Koliakos, G. G. (2011). Isolation of mesenchymal stem cells using the total length of umbilical cord for transplantation purposes. *Transfusion medicine* **21**(4): 253-261.

Tsai, M. S., Lee, J. L., Chang, Y. J. and Hwang, S. M. (2004). Isolation of human multipotent mesenchymal stem cells from second-trimester amniotic fluid using a novel two-stage culture protocol. *Human reproduction* **19**(6): 1450-1456.

U.S. National Institute of Health. (2016). "*ClinicalTrials.gov*." Available at: http://clinicaltrials.gov (Accessed: 01.12.2016).

Uccelli, A., Moretta, L. and Pistoia, V. (2008). Mesenchymal stem cells in health and disease. *Nature reviews. Immunology* **8**(9): 726-736.

Ullah, I., Subbarao, R. B. and Rho, G. J. (2015). Human mesenchymal stem cells - current trends and future prospective. *Bioscience reports* **35**(2).

Ulrey, C. L., Liu, L., Andrews, L. G. and Tollefsbol, T. O. (2005). The impact of metabolism on DNA methylation. *Human molecular genetics* **14 Spec No 1**: R139-147.

Vaiserman, A. M. (2015). Epigenetic programming by early-life stress: Evidence from human populations. *Developmental dynamics : an official publication of the American Association of Anatomists* **244**(3): 254-265.

Vaissiere, T., Sawan, C. and Herceg, Z. (2008). Epigenetic interplay between histone modifications and DNA methylation in gene silencing. *Mutation research* **659**(1-2): 40-48.

van Poll, D., Parekkadan, B., Cho, C. H., Berthiaume, F., Nahmias, Y., Tilles, A. W. and Yarmush, M. L. (2008). Mesenchymal stem cell-derived molecules directly modulate hepatocellular death and regeneration in vitro and in vivo. *Hepatology* **47**(5): 1634-1643.

Waddington, C. H. (2012). The epigenotype. 1942. *International journal of epidemiology* **41**(1): 10-13.

Wagner, W., Wein, F., Seckinger, A., Frankhauser, M., Wirkner, U., Krause, U., Blake, J., Schwager, C., Eckstein, V., Ansorge, W. and Ho, A. D. (2005). Comparative characteristics of mesenchymal stem cells from human bone marrow, adipose tissue, and umbilical cord blood. *Experimental hematology* **33**(11): 1402-1416.

Wakitani, S., Saito, T. and Caplan, A. I. (1995). Myogenic cells derived from rat bone marrow mesenchymal stem cells exposed to 5-azacytidine. *Muscle & nerve* **18**(12): 1417-1426.

Walker, D. L., Bhagwate, A. V., Baheti, S., Smalley, R. L., Hilker, C. A., Sun, Z. and Cunningham, J. M. (2015). DNA methylation profiling: comparison of genome-

wide sequencing methods and the Infinium Human Methylation 450 Bead Chip. *Epigenomics* **7**(8): 1287-1302.

Wang, H. S., Hung, S. C., Peng, S. T., Huang, C. C., Wei, H. M., Guo, Y. J., Fu, Y. S., Lai, M. C. and Chen, C. C. (2004). Mesenchymal stem cells in the Wharton's jelly of the human umbilical cord. *Stem cells* **22**(7): 1330-1337.

Wang, J., Liao, L. and Tan, J. (2011). Mesenchymal-stem-cell-based experimental and clinical trials: current status and open questions. *Expert opinion on biological therapy* **11**(7): 893-909.

Wang, S., Qu, X. and Zhao, R. C. (2012). Clinical applications of mesenchymal stem cells. *Journal of hematology & oncology* **5**: 19.

Wang, X. Y., Lan, Y., He, W. Y., Zhang, L., Yao, H. Y., Hou, C. M., Tong, Y., Liu, Y. L., Yang, G., Liu, X. D., Yang, X., Liu, B. and Mao, N. (2008). Identification of mesenchymal stem cells in aorta-gonad-mesonephros and yolk sac of human embryos. *Blood* **111**(4): 2436-2443.

Waterland, R. A., Travisano, M., Tahiliani, K. G., Rached, M. T. and Mirza, S. (2008). Methyl donor supplementation prevents transgenerational amplification of obesity. *International journal of obesity* **32**(9): 1373-1379.

Wei, X., Yang, X., Han, Z. P., Qu, F. F., Shao, L. and Shi, Y. F. (2013). Mesenchymal stem cells: a new trend for cell therapy. *Acta pharmacologica Sinica* **34**(6): 747-754.

Weisenberger, D. J., Campan, M., Long, T. I., Kim, M., Woods, C., Fiala, E., Ehrlich, M. and Laird, P. W. (2005). Analysis of repetitive element DNA methylation by MethyLight. *Nucleic acids research* **33**(21): 6823-6836.

Weiss, M. L. and Troyer, D. L. (2006). Stem cells in the umbilical cord. *Stem cell reviews* **2**(2): 155-162.

Wharton, T. W. (1656). *Adenographia, Translated by Freer S. (1996)*. Oxford, UK, Oxford University Press.

Williams, J. T., Southerland, S. S., Souza, J., Calcutt, A. F. and Cartledge, R. G. (1999). Cells isolated from adult human skeletal muscle capable of differentiating into multiple mesodermal phenotypes. *The American surgeon* **65**(1): 22-26.

Wilson, P. A., Gardner, S. D., Lambie, N. M., Commans, S. A. and Crowther, D. J. (2006). Characterization of the human patatin-like phospholipase family. *Journal of lipid research* **47**(9): 1940-1949.

Winrow, C. J., Hemming, M. L., Allen, D. M., Quistad, G. B., Casida, J. E. and Barlow, C. (2003). Loss of neuropathy target esterase in mice links organophosphate exposure to hyperactivity. *Nat Genet* **33**(4): 477-485.

World Health Organization (2000). *Obesity: preventing and managing the global epidemic*. Geneva, World Health Organization.

World Health Organization (2011). *Non-communicable diseases Saudi Arabia profile*. Geneva, World Health Organization.

World Health Organization (2014). *Noncommunicable diseases. Risk factors—overweight and obesity*. Geneva, World Health Organization.

World Health Organization (2015). *Overweight and obesity*.

Wu, C. and Morris, J. R. (2001). Genes, genetics, and epigenetics: a correspondence. *Science* **293**(5532): 1103-1105.

Wu, C. L., Diekman, B. O., Jain, D. and Guilak, F. (2013). Diet-induced obesity alters the differentiation potential of stem cells isolated from bone marrow, adipose tissue and infrapatellar fat pad: the effects of free fatty acids. *International journal of obesity* **37**(8): 1079-1087.

http://www.genecards.org. (Available at: http://www.genecards.org/cgi-bin/carddisp.pl?gene=PNPLA7 (Accessed: 30.11.2016

).

Wynn, R. F., Hart, C. A., Corradi-Perini, C., O'Neill, L., Evans, C. A., Wraith, J. E., Fairbairn, L. J. and Bellantuono, I. (2004). A small proportion of mesenchymal stem cells strongly expresses functionally active CXCR4 receptor capable of promoting migration to bone marrow. *Blood* **104**(9): 2643-2645.

Xu, J., Liao, W., Gu, D., Liang, L., Liu, M., Du, W., Liu, P., Zhang, L., Lu, S., Dong, C., Zhou, B. and Han, Z. (2009). Neural ganglioside GD2 identifies a subpopulation of mesenchymal stem cells in umbilical cord. *Cellular physiology and biochemistry : international journal of experimental cellular physiology, biochemistry, and pharmacology* **23**(4-6): 415-424.

Yajnik, C. S., Lubree, H. G., Rege, S. S., Naik, S. S., Deshpande, J. A., Deshpande, S. S., Joglekar, C. V. and Yudkin, J. S. (2002). Adiposity and hyperinsulinemia in Indians are present at birth. *The Journal of clinical endocrinology and metabolism* **87**(12): 5575-5580.

Yang, S. E., Ha, C. W., Jung, M., Jin, H. J., Lee, M., Song, H., Choi, S., Oh, W. and Yang, Y. S. (2004). Mesenchymal stem/progenitor cells developed in cultures from UC blood. *Cytotherapy* **6**(5): 476-486.

Yen, B. L., Huang, H. I., Chien, C. C., Jui, H. Y., Ko, B. S., Yao, M., Shun, C. T., Yen, M. L., Lee, M. C. and Chen, Y. C. (2005). Isolation of multipotent cells from human term placenta. *Stem cells* **23**(1): 3-9.

Yeung, M. L., Bennasser, Y., Le, S. Y. and Jeang, K. T. (2005). siRNA, miRNA and HIV: promises and challenges. *Cell research* **15**(11-12): 935-946.

Yoshimura, H., Muneta, T., Nimura, A., Yokoyama, A., Koga, H. and Sekiya, I. (2007). Comparison of rat mesenchymal stem cells derived from bone marrow, synovium, periosteum, adipose tissue, and muscle. *Cell and tissue research* **327**(3): 449-462.

Young, R. G., Butler, D. L., Weber, W., Caplan, A. I., Gordon, S. L. and Fink, D. J. (1998). Use of mesenchymal stem cells in a collagen matrix for Achilles tendon

repair. *Journal of orthopaedic research : official publication of the Orthopaedic Research Society* **16**(4): 406-413.

Zhang, F. F., Cardarelli, R., Carroll, J., Fulda, K. G., Kaur, M., Gonzalez, K., Vishwanatha, J. K., Santella, R. M. and Morabia, A. (2011). Significant differences in global genomic DNA methylation by gender and race/ethnicity in peripheral blood. *Epigenetics* **6**(5): 623-629.

Zhang, X., Yang, M., Lin, L., Chen, P., Ma, K. T., Zhou, C. Y. and Ao, Y. F. (2006). Runx2 overexpression enhances osteoblastic differentiation and mineralization in adipose--derived stem cells in vitro and in vivo. *Calcified tissue international* **79**(3): 169-178.

Zhang, X., Zhang, J., Wang, R., Guo, S., Zhang, H., Ma, Y., Liu, Q., Chu, H., Xu, X., Zhang, Y., Yang, D., Wang, J. and Liu, J. (2016). Hypermethylation reduces the expression of PNPLA7 in hepatocellular carcinoma. *Oncology letters* **12**(1): 670-674.

Zhao, K., Lou, R., Huang, F., Peng, Y., Jiang, Z., Huang, K., Wu, X., Zhang, Y., Fan, Z., Zhou, H., Liu, C., Xiao, Y., Sun, J., Li, Y., Xiang, P. and Liu, Q. (2015). Immunomodulation effects of mesenchymal stromal cells on acute graft-versus-host disease after hematopoietic stem cell transplantation. *Biology of blood and marrow transplantation : journal of the American Society for Blood and Marrow Transplantation* **21**(1): 97-104.

Zhao, R. and Daley, G. Q. (2008). From fibroblasts to iPS cells: induced pluripotency by defined factors. *Journal of cellular biochemistry* **105**(4): 949-955.

Zuk, P. A., Zhu, M., Mizuno, H., Huang, J., Futrell, J. W., Katz, A. J., Benhaim, P., Lorenz, H. P. and Hedrick, M. H. (2001). Multilineage cells from human adipose tissue: implications for cell-based therapies. *Tissue engineering* **7**(2): 211-228.

Zvaifler, N. J., Marinova-Mutafchieva, L., Adams, G., Edwards, C. J., Moss, J., Burger, J. A. and Maini, R. N. (2000). Mesenchymal precursor cells in the blood of normal individuals. *Arthritis research* **2**(6): 477-488.